

**REPORT ON REGIONAL SURVEY
FOR
MINERAL RESOURCES
IN
THE NORTHWEST AREA
THE ARGENTINE REPUBLIC
FINAL REPORT**

MARCH 2003

METAL MINING AGENCY OF JAPAN
JAPAN INTERNATIONAL COOPERATION AGENCY

MPN
JR
03-065

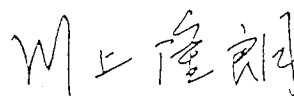
PREFACE

In responding to the request of the Government of the Argentine Republic, the Government of Japan decided to conduct a regional survey for mineral resources in the Northwest area, Argentine republic, and entrusted the survey to the Japan International Cooperation Agency (JICA). JICA, considering the technical nature of geology and mineral resources, entrusted the survey to the Metal Mining Agency of Japan (MMAJ).

JICA and MMAJ agreed on the Scope of Work (S/W) with the Servicio Geologico Minero Argentino, Subsecretaria de Minería, Secretaria de Industria, Comercio y Minería of the Government of the Argentine Republic after discussing the survey program, on July 12, 2001. The survey had been carried out a period of two years commencing from 2001. MMAJ dispatched a survey team consisting of four members to Argentina from October 9 to December 9, 2002. The survey in Argentina was carried out successfully with close cooperation of the Argentine government authorities. This report summarizes the results of the survey carried out in the first year and second year, and it also constitutes a part of the final report.

We would like to express our sincere appreciation to the officials concerned of the Argentine government, and we also grateful to the officials concerned of the Ministry of Foreign Affairs of Japan, the Ministry of Economy, Trade and Industry of Japan, and the Japanese Embassy in Argentina for their helpful supports to conduct the survey.

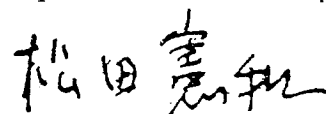
March 2003



Takao Kawakami

President

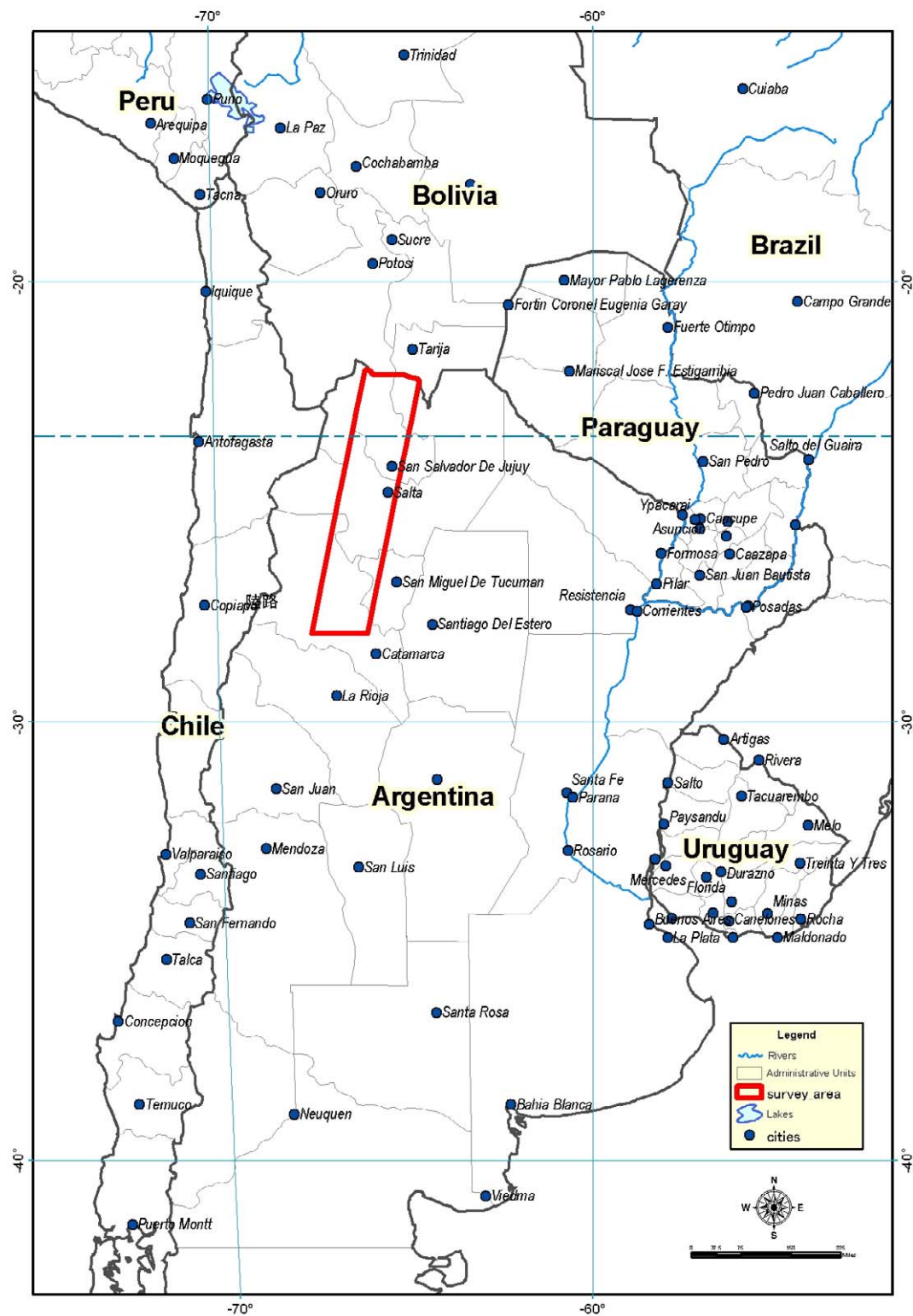
Japan International Cooperation Agency



Norikazu Matsuda

President

Metal Mining Agency of Japan



Location map of the North West Area, the Argentine Republic.

Summary

This survey is conducted, under the scope of work in the agreement dated July 12, 2001, between the Japanese government and the Argentine government, over a time span of two years for the investigation of nonferrous metallic mineral resources in the Northwestern area of the Argentine republic. The objective is to assess mineral resources potential and to select promising areas over the entire survey area.

In the first year of this project (Phase I), the analysis of existing data, satellite images, airborne geophysics data, stream sediments, and ground truth were implemented. In the existing data analysis, collected information was summarized in order to concentrate on potential area for minerals. For airborne geophysical data analysis, magnetic and radiometric data provided by the Argentine side were processed to find relations between regional geology and mineral deposits. In geochemical analysis, stream sediment samples collected by Argentine side in the past were analyzed. In the satellite image analysis, ASTER images were used to discriminate alteration zones and to classify the alteration minerals.

In consideration of the possibility of future mining development, this survey focused on porphyry copper and copper/gold deposits, epithermal gold/silver deposits, SEDEX-type lead/zinc deposit and volcanogenic massive sulfide deposits. The analysis shows that the SEDEX/sulfide deposits and volcanogenic massive sulfide deposits are mainly controlled by the distribution of Ordovician sediments in passive margin or magmatic arc in the north of survey area. Meanwhile, porphyry copper and copper/gold deposits, and the epithermal gold/silver deposits are mainly restricted to the four elongated area ("volcanic rock zone") that Tertiary volcanic rocks are widely distributed in the NW-SE direction from the Chilean border and restricted also to the area of intrusive rocks between the four elongated volcanic zone extensions. Finally, 24 areas were selected as a promising area, and then ground truth was conducted in 40 mineral showings and alteration zones outlined from the satellite images.

Consequently, it was found that the litho-geochemical exploration with using mudstone was especially effective in order to the discriminate ore horizon associated with the SEDEX-type lead/zinc deposits. Further, it was verified that the potential for the SEDEX-type lead/zinc deposit is high in the north-south trending zone from the Mina Aguilar deposit to the Pumahuasi deposit, meanwhile the potential for the volcanogenic massive sulfide deposits is particularly high in the area that volcanic rocks are distributed in Ordovician sediments in the western part of survey area. Detailed survey will be recommended to these areas in the future.

It was further shown that porphyry copper and copper/gold deposits develop in Farallon Negro area in a volcanic rock zone with relatively advanced erosion and in Inca Viejo area located in margin of intrusive rocks between volcanic rock zones, and in the west of Tucuman located in an volcanic

zone extension. On the other hand, the alteration zone related to the epithermal gold/silver deposit has a tendency to distribute in eroded area, such as Agua Caliente caldera.

In the analysis of ASTER images, the known porphyry copper and copper/gold deposits, and their related alteration zones were well discriminated and effectiveness of ASTER was verified.

In the second year (Phase II), prior to the field survey, an analysis of the existing (revising mineral showing data base), satellite image analysis using 22 scene of ASTER (alteration minerals identification and detailed topographical map making, etc.), and data analysis of stream sediment samples have been carried out.

A field survey was conducted of the following eight zones in total: they are four zones (Aguilar mine, Pumahuasi, Santa Victoria ranges, and La Colorada) for the exploration of the SEDEX/VMS deposits, and four zones for the exploration of porphyry copper and the epithermal deposits (Pancho Arias, Rachaite, Cerro Galan, El Pago).

In the four areas for exploration of SEDEX/VMS deposits, field survey and sample collections were made for conducting various laboratory tests for fossil identification and chemical analysis. To clear the petrological, paleontologic, geochemical features of the ore horizon of SEDEX/VMS deposits and their hanging/foot walls and to discover similar horizon to the already-known SEDEX deposit horizon.

The principal components were analyzed by using the analytical data of the 197 pieces of samples in total collected from the ground surface rock in the four zones. In the Aguilar mine area and La Colorada area, in addition, a discriminant analysis and principal component analysis were carried out by using the analytical data of the drilling cores from the Esperanza ore bodies as SEDEX type deposit and La Colorada ore bodies assumed to be VMS type, respectively.

As results, it was clarified that geochemical feature can identified the SEDEX and VMS ore horizon with using geochemical method such as principal component analysis, and the possibility of tracing similar horizon of SEDEX/VMS deposits is increased. Based on these results, the detailed study of sedimentary basin related to ore genesis from the regional scale of view, will be made progress if geochemical feature is identified for all lower Ordovician sediments area. It will be very important base for SEDEX/VMS exploration, which has no enough effective exploration standard.

In the four areas for exploration of porphyry copper and the epithermal type deposits, field survey and sample collections were made for conducting various laboratory tests in order to clear alteration mineral distribution (alteration zone mapping) and geochemical features.

As a results, this survey cleared that there is no enough economical mineralization for advanced stage development so far for these four zones. However the survey also found that El Pago has typical porphyry copper type mineralization and alteration zone, and there is cluster of similar type alteration zone with NNE-SSW in direction from El Pago area to extending to Agua Rica, Filo Colorado which

are very important mineral showing porphyry copper type in NOA. El Pago and the cluster of alterations will be important candidate for future exploration depending on its condition. Meanwhile, other three area (Pancho Arias, Rachaite, Cerro Galan) also have large scale of alteration zone which are considered to be very shallow part of epithermal system, therefore this survey do not deny possibility to have high potential zone in deeper level from the surface.

CONTENTS

Preface	
Location map of the survey area	
Summary	
Contents	
List of figures and tables	

PART I: GENERAL DISCUSSIONS

Chapter 1 Introduction

1-1 Background of the survey	1
1-2 Outline of the survey	2
1-2-1 Objectives of the survey	2
1-2-2 Survey area	2
1-2-3 Survey method	2
1-2-4 Survey team	3
1-2-5 Period and volume of the survey	4

Chapter 2 Geography of the survey area

2-1 Location and accessibility	5
2-2 Topography and drainage system	5
2-3 Climate and vegetation	5

Chapter 3 General geology and recent mining activities

3-1 General geology	8
3-1-1 Outline of geology in Argentina and locations of the survey area	8
3-1-2 Geology and mineral deposits in the survey area	16
3-2 Mining activity	28
3-2-1 Mining policies	28
3-2-2 Mining production	28
3-2-3 Mining legislation system	28
3-2-4 Recent trends of exploration and development	30

Chapter 4 Outline of survey results in Phase I

4-1 Outline of survey	33
4-2 Survey contents and results	33

4-3 Summary	39
-------------------	----

Chapter 5 Outline of survey results in Phase II

5-1 Analysis of the existing data	45
5-2 Stream sediments geochemistry	45
5-3 Satellite image analysis	48
5-4 Ground truth	49
5-5 Summary	49

PART II: DETAILED DISCUSSIONS

Chapter 1 Existing data analysis

1-1 Collecting existing data	55
1-2 Database	55
1-3 Distribution of known mineral deposits and mineral showings	55
1-4 Compilation and analysis of existing data	55

Chapter 2 Stream sediments geochemistry

2-1 Circumstances	59
2-2 Samples	59
2-3 Method, elements and detection limit for geochemical analysis	59
2-4 Analysis	61
2-5 Evaluation	61

Chapter 3 Satellite image analysis

3-1 Data processing of the image	73
3-1-1 Outline of analysis	73
3-1-2 Data used	74
3-1-3 Pseudo reflectance conversion	76
3-1-4 Removing vegetation effects	77
3-1-5 Processing of false color images and the band ratioing composites	86

3-1-6 Identification of alteration minerals	87
3-1-7 SiO ₂ content map	89
3-1-8 DEM(Digital Elevation Model)	91
3-1-9 Task for the future	91
3-2 Interpretation and analysis of image	93
3-2-1 Method of interpretation and analysis	93
3-2-2 Result of interpretation and analysis	113
3-3 Discussion	168
3-4 Summary	169

Chapter 4 Ground truth

4-1 Selection of survey zones	175
4-2 Survey results for each district	177
4-2-1 SEDEX/VMS type deposits	177
4-2-2 Porphyry copper and epithermal type deposits	236
4-3 Discussion of survey results	288
4-3-1 SEDEX/VMS type deposits	288
4-3-2 Porphyry copper and epithermal type deposits	317

Chapter 5 Discussion

5-1 Mineralization and potentiality of existing mineral deposits	329
5-2 SEDEX/VMS type deposits	329
5-3 Porphyry copper and epithermal type deposits	331

PART III: CONCLUSION AND RECOMMENDATION

Chapter 1 Conclusions	335
------------------------------------	-----

Chapter 2 Recommendation for future survey	338
---------------------------------------------------------	-----

References	340
------------------	-----

Appendixes	
------------	--

List of figures and tables

Figures

Part-I

Fig.I-3-1-1-1	Accretionary terrane in the southern region of South America (taken from Zappettini, 1998)	9
Fig.I-3-1-1-2	Major segments of Southern Central Andes related to the Nazca Plate segmentation (taken from Ramos, 2000).	15
Fig.I-3-1-1-3	Topographic units in Argentina (taken from Ramos, 1999b).	17
Fig.I-3-1-2-1	Geological map of the survey area (compiled from mapa geologico de la provincia de “Jujuy”, “Salta”, “Tucuman” and “Catamarca”).	20
Fig.I-3-1-2-2	Geological structure map of the survey area (compiled from JICA and MMAJ,1998 and Riller et al., 2001).	21
Fig.I-3-1-2-3	Distribution of mineral deposits in the survey area (taken from Zappettini, 1998).	23
Fig.I-3-2-1-1	Idealized trends in mining sector reform in the 1990s and mineral activities in some selected successful countries (taken from Naito and Remy, 2001).	29
Fig.I-4-2-1	Location of Mineralized zones in the Project area and survey points.	34
Fig.I-4-2-2	Total Magnetic Intensity(Reduced to the Pole:RTP).	36
Fig.I-4-2-3	Geochemical anomaly map (Cu).	37
Fig.I-4-2-4	Image analysis (ASTER BGR=147)	38
Fig.I-4-3-1	SEDEX type deposits and promising zone.	43
Fig.I-4-3-2	Porphyry copper type and epithermal type deposits and promising zone.	44
Fig.I-5-1-1	Location of mineral showings and deposits, and cluster of them listed on the Appendix.	47
Fig.I-5-4-1	Area of ground truth survey, year 2002.	52

Part-II

Fig.II-2-2-1	Location of samples for stream sediment geochemistry	60
Fig.II-2-5-1	Geochemical anomaly map (Au)	62
Fig.II-2-5-2	Geochemical anomaly map (Ag)	63
Fig.II-2-5-3	Geochemical anomaly map (Cu)	64
Fig.II-2-5-4	Geochemical anomaly map (Pb)	65
Fig.II-2-5-5	Geochemical anomaly map (Zn)	66
Fig.II-2-5-6	PC1 high score distribution map	69
Fig.II-2-5-7	PC2 high score distribution map	70
Fig.II-2-5-8	PC7 high score distribution map	71
Fig.II-2-5-9	PC10 high score distribution map	72
Fig.II-3-1-2-1	Index map of analyzed ASTER data	75
Fig.II-3-1-4-1	Vegetation situation in semi-arid area and their spectral reflectance	78
Fig.II-3-1-4-2	Synthesized spectral reflectance of soil and vegetation	79

Fig.II-3-1-4-3	Reflectance versus SAVI with change in soil brightness and vegetation coverage ratio	80
Fig.II-3-1-4-4	Reflectance versus PSAVI with change in soil brightness and vegetation coverage ratio	81
Fig.II-3-1-4-5	PSAVI versus pseudo reflectance for different pathes	83
Fig.II-3-1-4-6	Effect of removing influence of vegetation in semi-arid area	84
Fig.II-3-1-4-7	Mis-identification caused by changing the composition ratio of vegetation types	85
Fig.II-3-2-1-1	BGR=147 (False color image)	95
Fig.II-3-2-1-2a	BGR=4/5, 4/6, 4/7 (Ratio image)	97
Fig.II-3-2-1-2b	BGR=4/5, 4/6, 4/7 (Emphasized ratio image)	99
Fig.II-3-2-1-3	BGR=Sericite, Kaolinite, Alunite (Mineral identification)	101
Fig.II-3-2-1-4	BGR=Chlorite, Sericite, Alunite+Kaolinite (Mineral identification)	103
Fig.II-3-2-1-5	BGR=Calcite, Sericite, Chlorite (Mineral identification)	105
Fig.II-3-2-1-6	BGR=Hematite, Goethite, Jarosite (Mineral identification)	107
Fig.II-3-2-1-7	SiO ₂ content	109
Fig.II-3-2-1-8	Alteration zone outlined by ASTER data analysis	111
Fig.II-3-2-2-1	False color image of scene A10 (BGR=147)	114
Fig.II-3-2-2-2	False color image of scene A11 (BGR=147)	116
Fig.II-3-2-2-3	False color image of scene B02 (BGR=147)	118
Fig.II-3-2-2-4	False color image of scene B03 (BGR=147)	120
Fig.II-3-2-2-5	False color image of scene B09 (BGR=147)	122
Fig.II-3-2-2-6	False color image of scene B10 (BGR=147)	124
Fig.II-3-2-2-7	False color image of scene B11 (BGR=147)	126
Fig.II-3-2-2-8	False color image of scene B12 (BGR=147)	130
Fig.II-3-2-2-9	False color image of scene C01 (BGR=147)	132
Fig.II-3-2-2-10	False color image of scene C02 (BGR=147)	136
Fig.II-3-2-2-11	False color image of scene C03 (BGR=147)	140
Fig.II-3-2-2-12	False color image of scene C04 (BGR=147)	144
Fig.II-3-2-2-13	False color image of scene C05 (BGR=147)	146
Fig.II-3-2-2-14	False color image of scene C06 (BGR=147)	150
Fig.II-3-2-2-15	False color image of scene C07 (BGR=147)	152
Fig.II-3-2-2-16	False color image of scene C08 (BGR=147)	154
Fig.II-3-2-2-17	False color image of scene C09 (BGR=147)	156
Fig.II-3-2-2-18	False color image of scene C10 (BGR=147)	158
Fig.II-3-2-2-19	False color image of scene C11 (BGR=147)	160
Fig.II-3-2-2-20	False color image of scene C12 (BGR=147)	162
Fig.II-3-2-2-21	False color image of scene D03 (BGR=147)	164
Fig.II-3-2-2-22	False color image of scene D04 (BGR=147)	166
Fig.II-3-3-1	Interested area extracted from satellite data analysis	171
Fig.II-3-3-2	Alteration zone, major tectonic line, Tertiary volcanic rock s	173

Fig.II-4-2-1-1	Location map of samples collected in the Aguilar range area	178
Fig.II-4-2-1-2	Geological map of the Aguilar range area	
Fig.II-4-2-1-3	Location map of the mineral occurrences in the Aguilar range area	182
Fig.II-4-2-1-4	Location and photos of the Esperanza outcrop in the Aguilar range area	183
Fig.II-4-2-1-5	Location and photos of the Rincon mineral showing in the Aguilar range area	185
Fig.II-4-2-1-6	Location and photos of the Oriental mineral showing in the Aguilar range area	187
Fig.II-4-2-1-7	Photos of the Tapada mineral showing in the Aguilar range area	188
Fig.II-4-2-1-8	Photos of the Despensa mineral showing in the Aguilar range area	189
Fig.II-4-2-1-9	Predicted horizons by geochemical discriminant analysis, Aguilar range area	194
Fig.II-4-2-1-10	Principal component loadings for the drill core 72 samples, Aguilar range area	200
Fig.II-4-2-1-11	Variation diagrams of PC scores for the drill core 72 samples, Aguilar range area	204
Fig.II-4-2-1-12	Sample location and geological map of Pumahuasi area	207
Fig.II-4-2-1-13	Predicted horizons by geochemical discriminant analysis, Pumahuasi area	210
Fig.II-4-2-1-14	Sample location and geological map of Santa Victoria mountains area	213
Fig.II-4-2-1-15	Conodont fossil collected in the Santa Victoria mountains area	215
Fig.II-4-2-1-16	Predicted horizons by geochemical discriminant analysis, Santa Victoria mountains area	218
Fig.II-4-2-1-17	Photos of bedded sandstone and shale outcrops, Santa Victoria mountains area	219
Fig.II-4-2-1-18	Sample locations on the columns of the five holes, La Colorada area	221
Fig.II-4-2-1-19	Sample location and geological map of La Colorada area	222
Fig.II-4-2-1-20	Predicted horizons by geochemical discriminant analysis, La Colorada area	235
Fig.II-4-2-2-1-1	Location map of the Pancho Arias area	237
Fig.II-4-2-2-1-2	Status of mining concessions in the Pancho Arias area	238
Fig.II-4-2-2-1-3	Geological map of the Pancho Arias area	240
Fig.II-4-2-2-1-4	ASTER image analysis of alteration zones in the Pancho Arias area	243
Fig.II-4-2-2-1-5	Results of the survey in the Mina Pancho Arias	247
Fig.II-4-2-2-1-6	Results of the survey in the Prospecto Lass Burras	251
Fig.II-4-2-2-1-7	Results of the survey in the Prospecto Incahuasi	253
Fig.II-4-2-2-2-1	Location map of the El Pago area	256
Fig.II-4-2-2-2-2	Geological map of the El Pago area	257
Fig.II-4-2-2-2-3	ASTER image analysis of alteration zones in the El Pago area	259
Fig.II-4-2-2-2-4	Results of the survey in the El Pago area	265
Fig.II-4-2-2-3-1	Location map of the Rachaite area	268
Fig.II-4-2-2-3-2	Status of mining concessions in the Rachaite area	269
Fig.II-4-2-2-3-3	Geological map of the Rachaite area	271
Fig.II-4-2-2-3-4	ASTER image analysis of alteration zones in the Rachaite area	274
Fig.II-4-2-2-3-5	Results of the survey in the Rachaite area	277
Fig.II-4-2-2-4-1	Location map of the Cerro Galán area	280
Fig.II-4-2-2-4-2	Status of mining concessions in the Cerro Galán area	281

Fig.II-4-2-2-4-3	Geological map of the Cerro Galán area ······	283
Fig.II-4-2-2-4-4	ASTER image analysis of alteration zones in the Cerro Galán area ······	284
Fig.II-4-2-2-4-5	Results of the survey in the Cerro Galán area ······	285
Fig.II-4-3-1-1	Diagrams of principal component loadings for the 197 geochemical samples ······	297
Fig.II-4-3-1-2	Histograms of PC scores for 197 geochemical samples ······	299
Fig.II-4-3-1-3	PC1 score distribution map ······	300
Fig.II-4-3-1-4	PC2 score distribution map ······	305
Fig.II-4-3-1-5	PC3 score distribution map ······	310
Fig.II-4-3-2-3-1	Distribution of Neogene Tertiary volcanic rocks in the NOA region ······	324
Fig.II-4-3-2-3-2	Regional Geological structure of the NOA region ······	325

Tables

Part-I

Table I-2-3-1	Climate table of La Quiaca. and Salta	7
Table I-3-1-2-1	Simplified stratigraphy of the survey area.	18
Table I-3-1-2-2	Deposit type and mineral deposits in the survey area.	24
Table I-3-2-2-1	Investment of mining development in the Argentine Republic.	29
Table I-3-2-4-1	Recent mineral exploration around the survey area.	32
Table I-4-2-1	Record of the ground truth. 2001.	40
Table I-4-2-2	Outline of survey results 2001.	41
Table I-5-1-1	List of mineralized zones in the survey area	46
Table I-5-4-1	Record of ground truth 2002	50
Table I-5-4-2	Outline of survey results 2002	51

Part-II

Table II-1-1-4-1	Detailed survey plan for 2002	57
Table II-2-3-1	List of elements and detection limits	61
Table II-2-5-1	Principal component loading matrix after varimax rotation	68
Table II-3-1-1	ASTER data analyzed in F.Y.2002	74
Table II-4-2-1-1	Chemical analysis results of the drill core 72 samples	191
Table II-4-2-1-2	Result of DA (discriminant analysis) for the drill core 72 samples, Aguilar range area	192
Table II-4-2-1-3	Horizons predicted by using the discriminant functions, Aguilar range area	193
Table II-4-2-1-4	Statistics of the drill core 72 samples, Aguilar range area	197
Table II-4-2-1-5	Correlation coefficient matrix of 29 elements for the drill core 72 samples, Aguilar range area	197
Table II-4-2-1-6	PC (principal component) loading matrix after varimax rotation for the drill core 72 samples, Aguilar range area	199
Table II-4-2-1-7	PC scores and descriptions for the drill core 72 samples, Aguilar range area	202
Table II-4-2-1-8	The main principal components with related elements and their characteristics	203
Table II-4-2-1-9	Horizons predicted by using the discriminant functions, Pumahuasi area	209
Table II-4-2-1-10	Horizons predicted by using the discriminant functions, Santa Victoria mountains area	216
Table II-4-2-1-11	X-ray diffractive analysis result of the drill core samples, La Colorada area	226
Table II-4-2-1-12	Geology of the drill core samples, La Colorada area	228
Table II-4-2-1-13	Analytical results of the drill core samples, La Colorada area	229
Table II-4-2-1-14	Result of DA for the drill core 35 samples, La Colorada area	230
Table II-4-2-1-15	PC loading matrix after varimax rotation for the drill core 35 samples, La Colorada area	231
Table II-4-2-1-16	Relative situations and PC scores of the drill core 35 samples, La Colorada area	232
Table II-4-2-1-17	The main principal components with related elements and their characteristics, La Colorada drill core Samples	233

Table II-4-2-1-18	Horizons predicted by using the discriminant functions, La Colorada area ·····	234
Table II-4-3-1-1	Analytical results of the 197 samples for the SEDEX/VMS exploration ·····	289
Table II-4-3-1-2	Statistics of the 197 samples for the SEDEX/VMS exploration ·····	293
Table II-4-3-1-3	Correlation coefficient matrix of 29 elements for the 197 geochemical samples ·····	293
Table II-4-3-1-4	Principal component loading matrix after varimax rotation for the 197 geochemical samples ·····	295
Table II-4-3-1-5	Principal component scores and sample descriptions for the 197 geochemical samples ·····	296

Appendix

Table A-1	List of samples and laboratory test
Table A-2	Result of the laboratory test (microscopic observation of rock and ore samples)
Table A-3	Result of the laboratory test (X-ray diffraction)
Table A-4	Result of the laboratory test (geochemical analysis)
Table A-5	List of mineral occurrence in the survey area
Table A-6	List of mega fossil (a, b)
Table A-7	List of collected printed data
Document. A-1	Study of 5 conodont samples
Document. A-2	Palynological study of 19 samples
CD-ROM	

PART I: GENERAL DISCUSSIONS

PART I: GENERAL DISCUSSIONS

Chapter 1 Introduction

1-1 Background of the survey

Technical cooperation by the Japanese Government in the field of nonferrous mineral resources in the Argentine Republic was started in 1977. The main object of these surveys was to assess potentials of mineral resources in mining concession areas held by organizations related to the Argentine Government and to discover mineral deposits. The Argentine Government started a reform of mining policies in the early 1990s. Laws related to mining (the Mining Investment Law, the Mining Reorganization Law and Federal Mining agreement Law) were revised in 1993, and separation of the roles of the public sector and private sector was clearly shown. At the same time, policies for promotion of foreign investment were set out. The role of the government was allotted to improvement and provision of basic information. Accompanying this, the regarding assistance of Japanese Government, priority was given to basic surveys to promote mining investment, and, therefore, regional geological survey program have been carried out since 1997.

The following are the projects carried out in the Argentine Republic so far.

Name of the area	Scheme	Period (Japanese fiscal year*)
Northern area	Geological Survey	1977-1980
Famatina area	Regional Development Planning	1980
Patagonia area	Geological Survey	1981-1983
Alto de la Blenda area	Geological Survey	1986-1989
Farallon Negro area	Regional Development Planning	1990-1991
Western area	Geological Survey	1992-1994
Eastern Andes area	Regional Geological Survey	1997-1998
Southern Andes area	Regional Geological Survey	1999-2000

* From April to next March

Under such situation, Secretaria de Industria, Comercio y Minería highly appreciated the results of the project carried out so far and requested to the Japanese government to execute a geological survey in the northwestern area of the country which has high potentialities for the existence of copper, gold and lead/zinc deposits by Official Letter F No. 408 on November 7, 2000. Considering the high potential of mineral resources in the country and the importance of contribution to resource policies of the country, the Japanese Government determined to execute a regional geological survey over two years, from the 2001 fiscal year.

1-2 Outline of the survey

1-2-1 Objectives of the survey

The objectives of the survey is to efficiently extract promising areas with potential for the presence of deposits from the wide area by carrying out analysis of the existing data (including analysis of data of airborne magnetic surveys and radioactive exploration, and interpretation of results of geochemical exploration), analysis of satellite images, and ground truth, and then by comprehensively analyzing the obtained results. It is also aimed at promoting technical transfer to organizations of the counterpart country.

1-2-2 Survey area

The survey area covers about 100,000 km² located in the northwestern part of the Argentine Republic and is framed in by four corner of Long. 64.5°W. Lat. 22°S, Long. 66°W. Lat. 22°S, Long. 67.5°W. Lat. 28°S, and Long. 66°W, Lat. 28°S. Administrative districts covered by the survey extend over Jujuy, Salta, Tucuman and Catamarca provinces.

1-2-3 Survey method

1) Analysis of the existing data

A database was made after collecting publications by organizations related to Government of the Argentine Republic and state governments such as SEGEMAR, research paper and internal materials of mining companies. Database are used as part of reference material for the selection of promising area of porphyry copper and copper/gold deposits, epithermal gold deposits, SEDEX lead/zinc deposits and volcanogenic massive sulfide deposits, as deposit types which are thought to be having high economic values in the survey area.

2) Analysis of airborne magnetics and radioactive data (Phase I only)

There was provision of digital data obtained by the SEGEMAR in 1998. A total magnetic map (reduced to pole) and a vertical derivative analysis map etc. were processed from magnetic data, and Th, U and K map etc. were prepared from radiometric data. Then, geological interpretation was implemented.

3) Analysis of stream sediment geochemical data

Geochemical analysis of stream sediments for 10,000 samples with 48 elements and interpretation were also implemented. Samples were previously taken by Argentine side and provided to this project.

4) Analysis of satellite images

Analysis of satellite images was carried out by the ASTER image whose data service was started in 2001. Using 37 scenes of clouds free data, alteration zones and lineaments were mapped out from false color images and color-ratio composites and the iso-grain model method. For the area not covered by the ASTER image, analysis was made with results of analysis of the LANDSAT TM image (JICA and MMAJ, 1998).

5) Ground truth

In Phase I, based on analyses by the above-mentioned four methods, 28 zones of a cluster of deposits and places of mineral showings were selected. Among representative places of mineral showings and alteration zones of them, considering records of investigations carried out so far and accessibility, 36 mineral showings and 4 alteration zones inferred by satellite image analysis were selected as ground truth areas. The survey was carried out in these representative places of mineral showings and alteration zones. The object of the survey was to grasp the geological structure, alteration and mineralization. Samples for laboratory tests were also collected and used for analysis.

In Phase II, 8-target area as promising zone was selected base on the results of Phase I, and ground truth checking and laboratory tests were carried out.

1-2-4 Survey team

(1) Japanese side

(Phase I)

Leader	Ken Nakayama	Japan Mining Engineering Center
	Ikuhiro Hayashi	Japan Mining Engineering Center
	Takashi Ooka	Japan Mining Engineering Center
	Ryu-ta Ookubo	Japan Mining Engineering Center

(Phase II)

Leader	Takashi Ooka	Japan Mining Engineering Center
	Kouhei Iida	Japan Mining Engineering Center
	Ikuhiro Hayashi	Japan Mining Engineering Center
	Kenichi Kurihara	Japan Mining Engineering Center

(2) Argentine side

(Phase I)

Leader	Jorge Guillou	Servicio Geologico Minero Argentino, Salta
	Osvaldo Gonzalez	Servicio Geologico Minero Argentino, Tucuman
	Eulogio Ramallo	Servicio Geologico Minero Argentino, Salta
	Raul Seggiaro	Servicio Geologico Minero Argentino, Salta

Raul Becchio	Servicio Geologico Minero Argentino, Salta
(Phase II)	
Leader Jorge Guillou	Servicio Geologico Minero Argentino, Salta
Osvaldo Gonzalez	Servicio Geologico Minero Argentino, Tucuman
Eulogio Ramallo	Servicio Geologico Minero Argentino, Salta
Raul Seggiaro	Servicio Geologico Minero Argentino, Salta
Raul Becchio	Servicio Geologico Minero Argentino, Salta

(3) Project supervisor

(Phase I)

NoboruFujii Metal Mining Agency of Japan

(Phase II)

Masaomi Kurihara Metal Mining Agency of Japan

1-2-5 Period and volume of the survey

1) Period of the survey

(Phase I)

From August 21, 2001, to March 15, 2002 (Ground truth: September 20, 2001-November 17, 2001.)

(Phase II)

From October 9, 2002, to March 15, 2003 (Ground truth: September 20, 2001-November 17, 2001.)

2) Quantity of the survey

(Phase I)

Existing data analysis: 12 days

Data analysis of airborne magnetics and radioactive exploration: 67,000 km²

Analysis of stream sediments: 5,000 samples

Analysis of satellite images: 15 scenes of the ASTER image

Ground truth: 36 days

(Phase II)

Existing data analysis: 12 days

Analysis of stream sediments: 4,319 samples

Analysis of satellite images: 22 scenes of the ASTER image

Ground truth: 39 days

Chapter 2 Geography of the survey area

2-1 Location and accessibility

This survey area is located in the northwestern part of the Argentine Republic and covers over four administrative provinces. The capital of province such as Jujuy and Salta exists in the area. Regular flights from Buenos Aires are operated. Although out of the area, there are the capital of province such as Tucuman, Catamarca and La Rioja where regular flights are also operated; therefore, access to the survey area is good. On the eastern side of the area, paved national and provincial roads are well developed, including National Road 9, and transportation from the north to south direction is convenient. In Puna region to the western side, the main road is National Road 40 running north and south. It is not paved, but the condition of maintenance is not bad. The road network is limited in the east to west direction. Bolivia is reached through La Quiaca, a town at the northernmost end. On the other hand, Antofagasta in Chile is reached through San Antonio de los Cobres.

2-2 Topography and drainage system

The topography of the survey area reflects its geology well. According to Ramos (1999), the northern part of the area is divided into four topographical zones; Puna, Cordillera Oriental, Sierras Subandinas and Sierras Pampeanas westward from the east. Puna is highlands about 3,500 m above sea level, located in the extension of Altiplano, Bolivia. Because of an inland basin, development of the drainage system is poor, and there are many salt lakes. Cordillera Oriental is also a mountainous district 4,000 to 5,000 m above sea level, extending south and north direction from Bolivia, and the south-to-north tending drainage system develops. Access is poor, and the population is also very sparse. Sierras Pampeanas comprises an alluvial basin and a mountainous district 1,500 to 5,000 m above sea level, and a south-to-north tending system develops.

2-3 Climate and vegetation

Climate and vegetation in the survey area are controlled largely by topography. Puna, the northern part of Sierras Pampeanas and Cordillera Oriental 3,500 to 5,000 m above sea level have an inland dry climate and little vegetation. In La Quiaca located on the border with Bolivia, the average daily difference in temperature is as high as 19°C, annual precipitation is 322 mm and average humidity is 50%. Particularly in the winter season from May to September, average monthly precipitation is 1.2 mm, which is an extremely small amount (Table I-2-3-1A). On the other hand, in the eastern border part of Cordillera Oriental covering Jujuy, Salta and Tucuman cities, a jungle zone around 2,000 m above sea level develops, and it is humid. Salta is relatively humid, the

average annual precipitation is approximately 670 mm and average humidity reaches 70% (Table I-2-3-1B). The best period for field surveys is the early summer, i.e., October and November.

Table I-2-3-1 Climate table of La Quiaca and Salta

(A) La Quiaca

Latitude 22°06'S, longitude 65°36'W, elevation 3,459 m

Month	Mean sta. press. (mbar)	Temperature(°C)				Mean vapor press. (mbar)	Precipitation (mm)		Relat. humid. (%)	Number of days with			Mean cloud- iness (tenths)	Mean daily sun- shine	Wind		Clear days	Cloudy days	Mean evap. (mm)
		daily mean	daily range	extreme max.	extreme min.		mean	max in 24 h		precip. (>1mm)	thunder storm	fog			prevail. direct.	mean speed			
Jan.	672.2	12.4	14.3	27.1	-1.2	8.9	89	45	62	15	10	0	5.7	8.6	NE	3.6	0.7	16.7	184
Feb.	672.3	12.4	14.4	27	-1.2	9.2	77	35	64	12	9	<1	5.4	8.5	NE	3.3	0.3	13.2	158
Mar.	672.5	12.2	15.9	27.8	-3.1	8.2			58	8	7	<1	4.2	9.3	NE	3.1	3.2	8	182
Apr.	672.8	10.3	19.4	25.8	-8.7	5.6	5	35	45	2	2	<1	3	9.7	NE	2.8	8.7	4.2	150
May	672.8	6.6	21.7	25	-12.7	3.5	1		36	<1	<1	<1	2	9.8	S	2.8	15.2	2.9	121
June	672.8	3.9	23.3	22	-15.8	2.8	2	25	35	<1	0	<1	1.9	9.4	S	3.3	16.7	2.5	102
July	672.7	4	23.5	21.1	-15.2	2.9	1	5	36	<1	<1	<1	1.6	9.6	S	3.1	16.4	1.7	99
Aug.	672.4	6.4	23.4	22.8	-14.6	3.2	0	15	38	<1	<1	<1	2	9.8	S	3.6	15.5	2.1	132
Sept.	671.9	9.2	21.7	25.8	-12.2	4.4	2	5	38	1	1	<1	2.6	9.6	S	4.2	9.9	3.5	177
Oct.	671.5	11.1	20.2	27.4	-10.7	5.8	9	25	44	2	3	0	3.4	10	NE	4.4	6.5	5.8	212
Nov.	671.2	12.3	18.1	28.4	-4.7	7.3	31	25	51	6	9	<1	4.3	10.1	NE	4.4	2.2	6.1	208
Dec.	671.6	12.6	15.8	28.3	-1.2	8.4	63	25	57	12	12	<1	5.2	9.4	NE	4.2	0.5	12.5	196
Annual	672.3	9.5	19.1	28.4	-15.8	5.9	322	45	50	59	54	2	3.4	9.5	NE	3.6	95.8	79.2	1,921

(B) Salta

Latitude 24°51'S, longitude 65°29'W, elevation 1,226 m

Month	Mean sta. press. (mbar)	Temperature (°C)				Mean vapor press. (mbar)	Precipitation(mm)		Relat. humid. (%)	Number of days with			Mean cloud- iness (tenths)	Mean daily sun- shine	Wind		Clear days	Cloudy days
		daily mean	daily range	extreme max.	extreme min.		mean	max in 24 h		precip. (>1mm)	thunder- storm	fog			prevail. direct.	mean speed		
Jan.	875.7	21.4	12.7	38.4	6.1	18.9	176	95	78	14	7	1	5.6	6.3	NE	1.4	0.3	15.2
Feb.	876.3	20.5	11.6	39.3	7.7	18.9	149	115	82	13	4	<1	5.8	5.3	NE	1.1	0.9	14.8
Mar.	877	19.2	11.7	34.7	2.6	17.7	94	75	80	12	3	2	5.4	4.4	NE	0.8	1.2	17
Apr.	878.1	16.5	13	33.6	-1.2	14.1	25	55	75	6	<1	3	5.3	4.8	NE	1.1	3	13.9
May	878.3	13.5	15.1	33.9	-4.6	11.5	6	35	74	3	<1	2	4.5	5.1	N	1.1	6.1	11.6
June	878.2	11.1	16.6	33.1	-9.5	9.8	3	15	74	1	0	2	4.1	4.6	N	1.1	7.4	9.7
July	878.6	10.6	18.3	35	-9.9	8.4	2	5	66	1	0	1	3.2	6	N	1.4	9.3	8.1
Aug.	878.5	12.4	19.4	36.3	-6.6	8.3	4		58	1	<1	<1	3	7	NE	1.4	12	7.4
Sept.	877.7	15.9	17.7	38	-3.6	9.6	5	15	53	3	<1	<1	3.5	5.9	NE	1.4	6.4	8.8
Oct.	876.6	18.4	15.6	38.8	-2.2	12.3	25	45	58	6	1	<1	4.5	5.3	NE	1.7	5.1	10.2
Nov.	875.7	20.7	14.4	39	1.8	14.8	61	45	61	8	4	<1	4.4	5.9	NE	1.7	2.1	11
Dec.	875.4	21.5	13.7	39.5	3.9	17.2	121	95	67	12	6	<1	4.5	6	NE	1.7	1.1	10.6
Annual	877.1	16.8	15	39.5	-9.9	13.4	671	115	69	80	26	12	4.5	5.6	NE	1.3	54.9	138.3

Chapter 3 General geology and recent mining activities

3-1 General geology

3-1-1 Outline of geology in Argentina and locations of the survey area

3-1-1-1 Tectonic classification in Argentina

It was shown in the paper written by Ramos et al. (in 1986) and the paper written by Ramos (in 1988) that the land of Argentina was formed in the tectonic stratigraphical way by collisions and additions of allochthonous terranes which originally had been independent (Fig. I-3-1-1-1). The land of Argentina is roughly divided into five parts; Rio de la Plata Craton, Pampia Terrane, Cuyania Terrane, Chilenia Terrane and Patagonia Terrane.

Rio de la Plata Craton is further subdivided into several small terranes, which were added around 2300 to 1900 Ma. It is considered that these small terranes were fused and concreted by Trans-Amazonic (or Tandillia) orogenic movements by the lower Proterozoic.

Pampia Terrane is basically composed of carbonate rock basements accompanied by crystalline schist and gneiss. These were a metamorphosed sequence that had been accumulated in the stable marginal sea in the period around 1000 to 900 Ma and collided with and added to Rio de la Plata Craton in about 750 Ma (the upper Proterozoic). Calc-alkali magmatic arcs prior to the suture with Rio de la Plata Craton are distributed as tonalite and orthogneiss in Cordoba Province. Suture lines are shown by ophiolite or basic-ultrabasic rock zones and, probably, the largest one corresponds to the addition of Famatina in the lower Paleozoic.

In the northwestern border side of Pampia Terrane, Arequipa - Antofalla Terrane is added and forms the basement of Puna (a plateau 3,500 - 4,000 m above sea level, which extends over Puna de Atacama, Bolivia, Chile and Argentina). The present locational relationship was formed in the upper Proterozoic. Arequipa in the north side was formed in the lower to middle Proterozoic, and Antofalla in the south side was formed the upper Proterozoic to the early Paleozoic; they stretch from the north-west end to Chile, Bolivia and Peru. Arequipa-Antofalla Terrane separated from Pampia Terrane in the lower Paleozoic through the lifting process, and a marginal sea was formed between them. After that, these terranes collided again by Ocoyic orogenic movements and re-constructed suture lines. The volcanic rock belt in the western part of Puna is considered to represent magmatic arcs before the suture.

Cuyania Terrane is also called Cuyania-Precordillera Terrane; it is composed of metamorphic rocks of high- to low-metamorphic grades that were metamorphosed from 900 to 1,100 Ma, and of sedimentary rocks in the early Paleozoic. It is considered from the sedimentary sequence and the age of metamorphism of the basement that these have their origin in Grenville Zone in the east part of Laurentia. Suture lines that seem to show the addition of Cuyania and

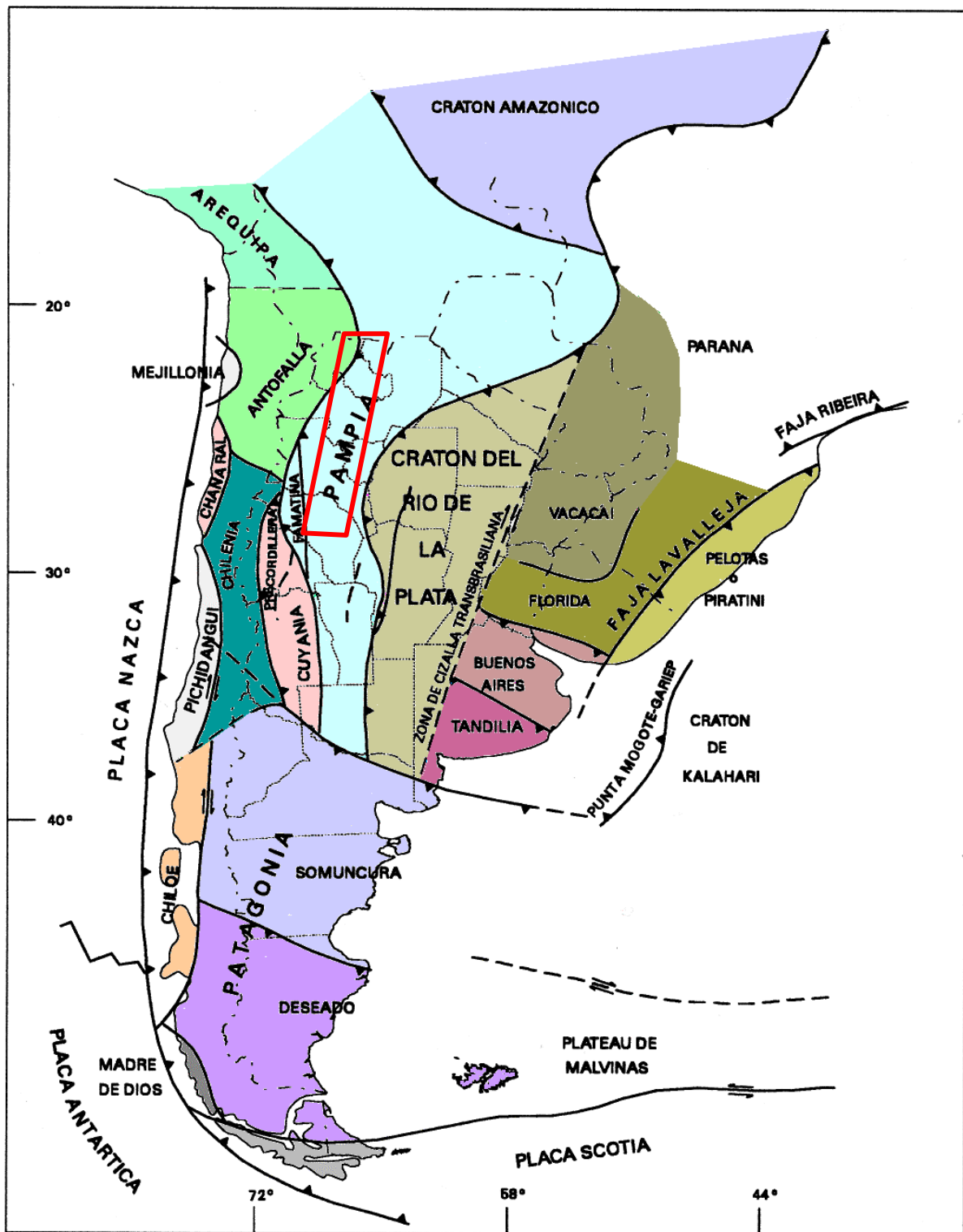


Fig. I-3-1-1-1 Accretionary terranes in the southern region of South America(taken from Zappettini, 1998)

Precordillera in the Proterozoic appear on the west slope of the Pie de Palo mountains. It is deemed that Cuyania Terrane was added to Pampia Terrane around the end of the Ordovician.

One of characteristics of the basement of Chilenia Terrane is that it was covered with magmatic activities and metamorphism in the upper Paleozoic. There are evidences of deformation and metamorphism from 500 to 415 Ma in some part of the basement, which are covered with Silurian deposits. Chilenia Terrane was added to Cuyania Terrane in the upper Devonian. Those suture lines are shown by many fragmentary ophiolite rocks. Plutonic rocks and andesitic volcanic rocks forming Cordillera Frontal represent magmatic arcs prior to the suture.

Patagonia Terrane is composed of two terranes, Somuncura and Deseado. These collided in the period of Famatina orogenic movements in the lower Paleozoic, before which magmatic arcs related to subduction of Deseado crustal block had been formed. Patagonia Terrane was added to the Argentine main body in the upper Paleozoic. Activities of plutonic rocks of the Somun Cura group of the Permian System correspond to magmatic arcs prior to the suture.

3-1-1-2 History of tectogenesis in Argentina

According to Ramos (1999a), the following roughly seven orogenic movements cycles are recognized in Argentina.

Cycle	Age (Ma)	Mountains
Andes	45 - 0	Andes
Patagonia	98 - 75	Fueguina
Gondwana	290 - 250	Ventania and Cordillera Frontal
Famatina	465 - 385	Precordillera and Pampeanas western mountains
Pampia	600 - 520	Pampeanas eastern mountains
Grenville	1,100 - 1,050	Proto-Pie de Palo
Tandillia	2,000 - 1,800	Tandillia

There were two ages in the Mesozoic when numerous lifted sedimentary basins were formed by tensile movements over a very wide area. These are called the Gondwana tensile cycle (from the Triassic to the Jurassic) and the Patagonia tensile cycle (in the Cretaceous).

Precambrian (Tandillia cycle - Grenville cycle - Pampia cycle)

The oldest rocks in Argentina correspond to the Tandillia cycle in the lower Proterozoic and are exposed in the middle-southern part of Buenos Aires Province and on the Martin Garcia Island scatteringly. The main types of composing rocks are granite to tonalitic gneiss, migmatite and amphibolite, accompanied by crystalline schist, marble and acid to basic dykes. A distinctive feature

is development of a mylonite zone that has been highly deformed and is considered to have been formed when Tandilia Terrane collided with Buenos Aires Terrane.

It is seemed that the Grenville cycle is a cycle that formed the basement of Cuyania Terrane, and is confirmed as metamorphic basement rocks of the Pie de Palo mountains at the west end of Pampeanas mountains in San Juan Province. This basement is composed of the young crust formed by addition of island arcs in the period between 1,050 Ma and 950 Ma.

It is considered that the Pampia cycle is related to the collision of Pampia Terrane with Rio de la Plata Terrane in the upper Proterozoic. It is made up of sedimentary rocks that received diverse deformation and metamorphism, metamorphic rocks, granite rocks and volcanic rocks. Judging from granite rocks concerning subduction, the age of this cycle corresponds to the period from the upper Proterozoic to the early Cambrian. These rocks compose the basements of Puna Zone, Cordillera Oriental Zone and Sierras Pampeanas Zone. Representative rocks in the survey area are turbidite metasediments in the Santa Victoria mountains (Cordillera Oriental) and Puncoviscana layer distributed in Puna and corresponding layers. Metasediments and gneiss of the same age are also distributed in the southern part and the eastern part of Farallon Negro Region. Puncoviscana layer received folding from the lower Proterozoic to the early Cambrian; it was slightly metamorphosed and intruded by granite rocks of Cañani and La Quesera. Angular unconformity is observed between Puncoviscana layer and Cambrian sedimentary rocks above it; this is called the Tilcaric deformation event.

Paleozoic (Famatina cycle - Gondwana cycle)

The Famatina cycle corresponds to a cycle that influenced the north and middle parts of Argentina from the middle Ordovician to the middle Devonian. It is composed of two crustal deformation events, Ocoyic orogenic movements of the middle to lower Ordovician and Chanic orogenic movements of the lower to middle Devonian.

In the northwestern region in Argentina, Arequipa-Antofalla Terrane collided with the Gondwana Continent in the early Cambrian but was cut off again by lifting in the period from the upper Cambrian to the lower Ordovician. On this lifted sedimentary basin, siliceous sandstone of Meson Formations of the middle to upper Cambrian and pelite of Santa Victoria group of the lower to middle Ordovician accumulated. In the upper part of Santa Victoria group in Cordillera Oriental, there is an insertion of volcanic rocks and volcanic pyroclastic rocks of the Arenig-Llanvirn series of 476 to 467 Ma, which were generated by bimodal magmatic activities of dacite and basalt. Near surface intrusive rock is also seen. These magmatic activities are recognized as the Eastern La Puna Effusion Zone (Faja Eruptiva Oriental). After these activities, the sedimentary basin was closed over in the middle to upper Ordovician, and Arequipa Antofalla Terrane and Pampia Terrane were combined again. Together with the combination, the clastic rock sequence and the igneous rocks and

the volcanoclastic material sequence were deformed hard by orogenic movements with west-facing vergence, which are called Ocloyic deformation movements.

In the Precordillera - Pampeanas mountains, rocks of the Famatina cycle, are distributed in Precordillera and the Pampeanas western mountains. They now compose Cuyania Terrane. It is said that Cuyania Terrane was separated from the Laurentian Continent in the lower Cambrian and collided with Pampeia Terrane around the period between 460 and 470 Ma. In Pampeanas western mountains, granite rocks and volcanic rocks related to subduction are recognized in the period between 510 and 470 Ma, and ceased in about 465 Ma. After that, Ocloyic deformation movements, which brought about intrusion activities of granite and severe deformation actions at the time of collision, started. The collision and combination of Chilenia in and after the early Devonian caused both development of foreland sedimentary basins and deformation and uplift of the basement of Precordillera. Episodes of deformation actions that took place in the Devonian are grouped as Chanic movements, which are a cause of unconformity between sediments of the Devonian system and the lime system.

The Gondwana cycle represents orogenic movements of the Andes type that developed widely along the western edge of the Gondwana Continent in the Permian. Magmatic activities are distinctive, and large-scale episodes of volcanic rocks and plutonic rocks are contained. As volcanic rocks of this cycle, those of Choiyoi group are representative. The base of Choiyoi group begins with a basic sequence related to tholeiitic magmatic arcs, the middle part has andesite and dacite, and rhyolitic volcanic rocks and volcanoclastic material are seen widely in the top. The rhyolite sequence in the top indicates that there were important tensile events after deformation actions of the Gondwana cycle. Rocks ranging from rhyolite to dacite of Choiyoi group are related to near surface intrusive rocks with similar composition, which are composed of syenitic to monzonitic granite. Granite rocks of the late orogenic period from the Permian to the Triassic spread from the south of Catamarca Province to the western part of La Rioja Province, from which part to Cordillera Frontal in San Juan and Mendoza Provinces these rocks are widely observed. In Neuquén Province, these granite rocks are distributed in the Viento mountains and Cerro Granito.

Mesozoic (Gondwana tensional cycle - Patagonia tensional cycle - Patagonia cycle)

In the age of the Gondwana tensional cycle (from the Triassic to the Jurassic), a wide region of the basement of the Andes and adjoining areas was put in remarkable tensional condition. Several lifted sedimentary basins appeared in the Las Malvinas plateau, the San Julian basin, the Cuyo basin, Neuquen basin and Patagonia. These lifted systems began as Triassic terrestrial sedimentary basins, and many of them became marine sedimentary basins successively in the Jurassic.

In the age of the Patagonia tensional cycle (the Cretaceous), accompanying the development of the subduction zone of the Mariana type, the back arc area was controlled by the wide tensional process along magmatic arcs. This tensional system is related to opening of the South Pacific following the Gondwana lifting system. The Patagonian lifting system developed several lifted sedimentary basins extending north and south in the middle northern part of Argentina. Several lifted sub-sedimentary basins represented by Salta group belong to this cycle. In the eastern part of Puna and in Cordillera Oriental, these tensile events are related to intrusion of granite rocks and small-scale intrusion of carbonatite in the plate.

Rocks associated with the Patagonia orogenic movement cycle (in the upper Cretaceous) are observed in the Fueguina mountains in Patagonia and in the insular region in the southern side of the Fuego Island. In these places, turbidite received deformation actions, and the ophiolite composite rock that was split accompanying them is seen.

Cenozoic (Andes cycle)

The Andes cycle is an orogenic movement cycle that took place along the Andes and has continued from the late Mesozoic to the present time. This cycle is characterized by 1) fault movements accompanying uplift, folding structure and diagonal subduction of the Andes, 2) volcanic and intrusive rocks widely distributed and 3) many hydrothermal deposits. This cycle is roughly divided into two subcycles, that of the Paleogene and that of the Neogene. Both cycles are controlled by change in relative convergence speed between the Nasca plate and the South American plate.

The Paleogene subcycle is represented by volcanic rocks of the Eocene to the early Pliocene distributed west of the Arizaro salt lake in Puna, Salta Province. In connection with this, sedimentary basins subsided around Arizaro, and several thick sedimentary basins between mountains developed. In relation to this subcycle, what is known in the southern part of Mendoza Province and the western part of Neuquén Province is a series of several sediments at the time of orogenic movements of the Eocene, several volcanos and a center of intrusive rocks. Magmatic arcs of this subcycle are distributed on the Chilean side, enter into the Argentine side from the place around the northwestern part of Neuquén Province, and reach the middle western part of Chubuto Province through Balneario in Rio Negro. Although andesite is dominant in the volcanic rock sequence, basalt is dominant in Mendoza and Santa Cruz Provinces. In the period of the Paleogene subcycle, the plate convergence speed of the South American plate and the Nasca plate was relatively slow, and constituents of diagonal subduction were contained. In Chile, this resulted in sideslips of the Domyko fault system extending south and north, and, along them, there is distribution of many deposits of porphyry copper, copper and gold and epithermal deposits. On the other hand, on the Argentine side, numerous lineaments extending northwest and southeast

developed. Among them, El Toro - Olacapato Lineament became a factor that let granite rocks such as those in El Acay intrude.

The Neogene subcycle has continued since the Miocene up to now, and shows orogenic movements and magmatic activities, whose forms differ according to latitude (Fig. I-3-1-1-2).

The northern area (at 22° to 27° S Lat.) almost corresponds to the range of Puna. Volcanic activities started around 26 Ma in the Andes on the Chilean side. After that, the accompanying dip of subduction of the Nasca plate became gentle, and magmatic arcs expanded east to the Argentine side from 17 to 12 Ma. This expansion occurred along selective structural corridors (corredores preferenciales), along which lineaments controlling stratovolcanos, volcanic domes, calderas, volcanic cone, subvolcanic rock and others were determined. Stratovolcanos are composed of andesite to dacite lava and volcanoclastic flow, while volcanic domes are made up of dacitic to rhyodacitic rocks. The expansion of magmatic arcs was accompanied by movement of the landslide front and formation of foreland sedimentary basins following it. This movement continued toward Puna, Cordillera Oriental and the Subandinas mountains from the lower Miocene to the Quaternary. In Cordillera Oriental and the Subandinas mountains, both of which are at 24° to 25° S Lat., the basement received deformation actions by inversion tectonics of Cretaceous normal faults that had formed the Salta group. On and after 12 Ma, the accompanying dip of the subduction plate became steep again, and the main magmatic activities moved to the west and flowed out to the ground surface as large-scale ignimbrite flow. Magmatic arcs in this latitude zone have been located on the Chilean side since the lower Pliocene up to now.

The central area (at 27° to 33° S Lat.) includes the highest part of the Andes in La Rioja, San Juan and Mendoza Provinces. It is characterized by a lack of volcanic activities from the late Miocene to the present time. This is related to the fact that the dip of subduction in this area became gentle in and after 18 Ma, and the crust came to have a thick formation. In this area, there were no volcanic activities in the Oligocene, but the volcanic activities restarted on the Chilean side from 26 Ma. Volcanic activities expanded to the Argentine side in Cordillera Principal around 15 to 16 Ma, then further expanded to Precordillera and reached the Pampeanas mountains in the middle to upper Miocene. At the same time, the orogenic front characterized by fold and thrust also moved to the east. These magmatic activities associated with subduction ceased later in the east places than in the west places; they ceased in Cordillera Principal and Precordillera in the period 6 Ma, and in the Pampeanas mountains in the period between 4.9 and 1.9 Ma.

In the southern area (at 33° to 46° S Lat.), the subduction speed of the plate increased in the Miocene, and a compression place was formed. This compression place is remarkable in places north of 36° S Lat., insignificant at 36° to 40° S Lat., and is not recognized in the area south of this latitude zone. Magmatic arcs of the upper Cenozoic show two different characteristics; andesite to dacite is dominant at 33° to 37° S Lat., and basalt is dominant at 37° to 46° S Lat. The dip of

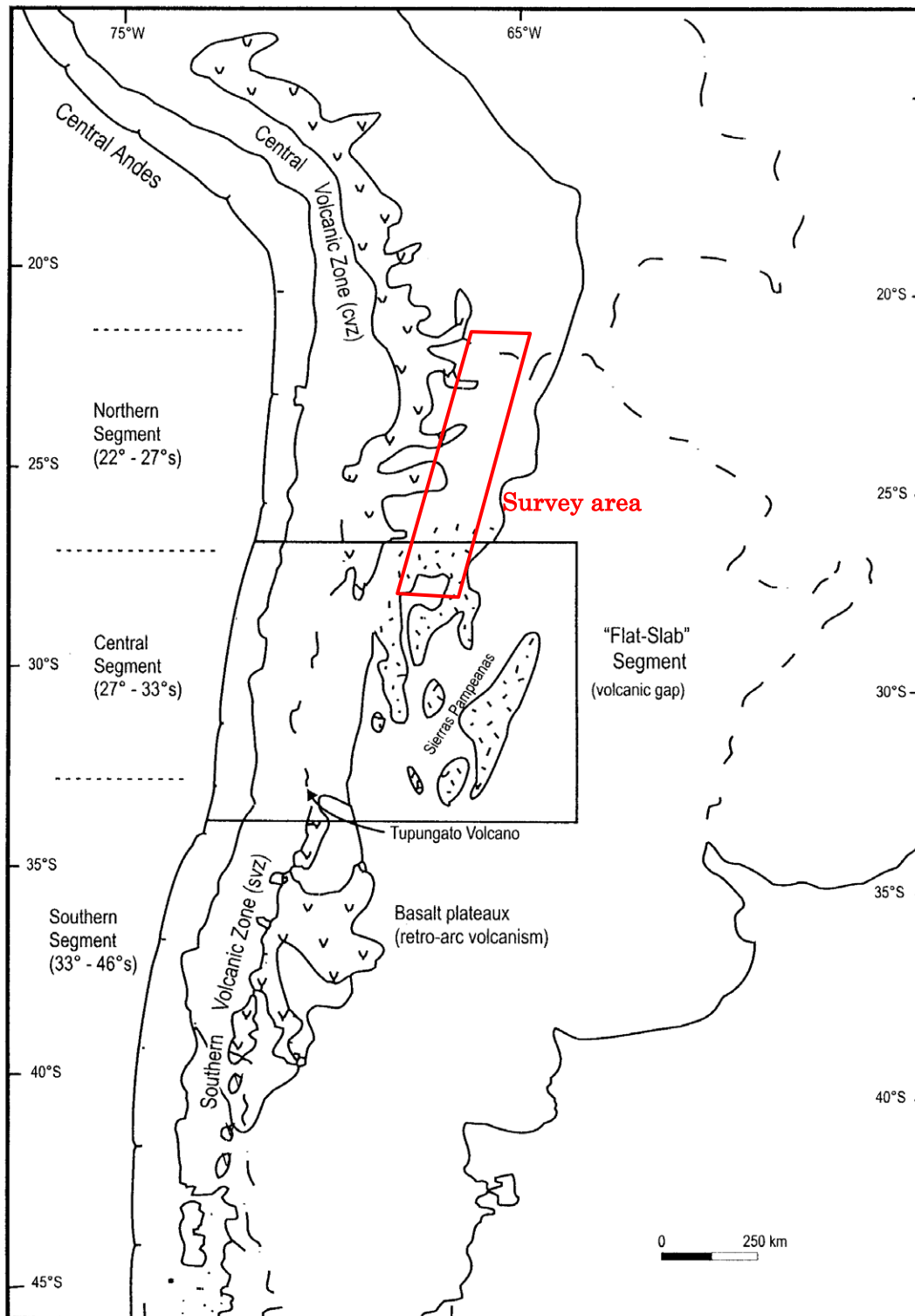


Fig. I-3-1-1-2 Major segments of Southern Central Andes related to the Nazca Plate segmentation (taken from Ramos, 2000).

subduction in this area is about 30 degrees, while the dip in places around 35° to 36° S Lat. is about 40 degrees. North of 36° S Lat., Neogene foreland sedimentary basins have developed well, and thick sediment during orogenic movements are distributed.

3-1-1-3 Location of the survey area

In the terrane division, the most part of the area covered by this survey is included in Pampia Terrane, and a part of the northwest area is included in Arequipa-Antofalla Terrane (Fig. I-3-1-1-1). According to geographical structure division, a part of the northwest to west area belongs to the Puna area, the north to middle part belongs to the Cordillera Oriental area, the south part to Pampeanas mountains area, the northeast part to the Subandinas mountains area and the east part to the area of the Santa Barbara system (Fig. I-3-1-1-3).

According to three latitude zones divided according to the dip of plate subduction in the Neogene subcycle, almost the whole survey area is included in the northern part, and only part of the southern side belongs to the central area (Fig. I-3-1-1-2). In the Andes on the Chilean side west of this survey area, Paleogene magmatic arcs are distributed, and many large-scale porphyry copper deposits (such as El Abra, Chuquicamata, Zaldivar, Escondida and El Salvador) exist, while porphyry gold deposits (represented by Maricunga Belt) exist in the Miocene magmatic arcs.

3-1-2 Geology and mineral deposits in the survey area

3-1-2-1 Geology of the survey area

Table I-3-1-2-1 shows the outline of geological stratigraphy of this survey area. The stratigraphy is shown by dividing the survey area into Puna area, Cordillera Oriental area and Pampeanas Mountains area. The schematic diagram of geology in this survey area is shown in Fig. I-3-1-2-1 and Fig. I-3-1-2-2. Although the survey area includes Subandinas Mountains area and Santa Barbara System area, these areas are not put in the stratigraphy table because they are part of the northeast to east part and do not have important places of ore indications. The summary of geology in the survey area is explained below, based on Table I-3-1-2-1.

The basement of the survey area is sedimentary rocks and metamorphic rocks of the late Proterozoic to the early Cambrian, and is Puncoviscana multiple seam and corresponding layers that are distributed in the Cordillera Oriental mountains (the Santa Victoria mountains), the Cachi mountains, the Quilmes mountains and the Aconquija mountains. The distribution is relatively wide in Cordillera Oriental area and the Pampeanas mountains and little in Puna area. The type of composing rocks include non-metamorphic to weak-metamorphic sedimentary rocks, gneiss (tonalite and granite), crystalline schist, migmatite, marble, felsite and metamorphic basic rock.

In the early Cambrian, these basement rocks received intrusion of granite rocks represented by trondhemitic distributed west of Cachi. These granite rocks are called Cachi, Canani, Tipayoc,

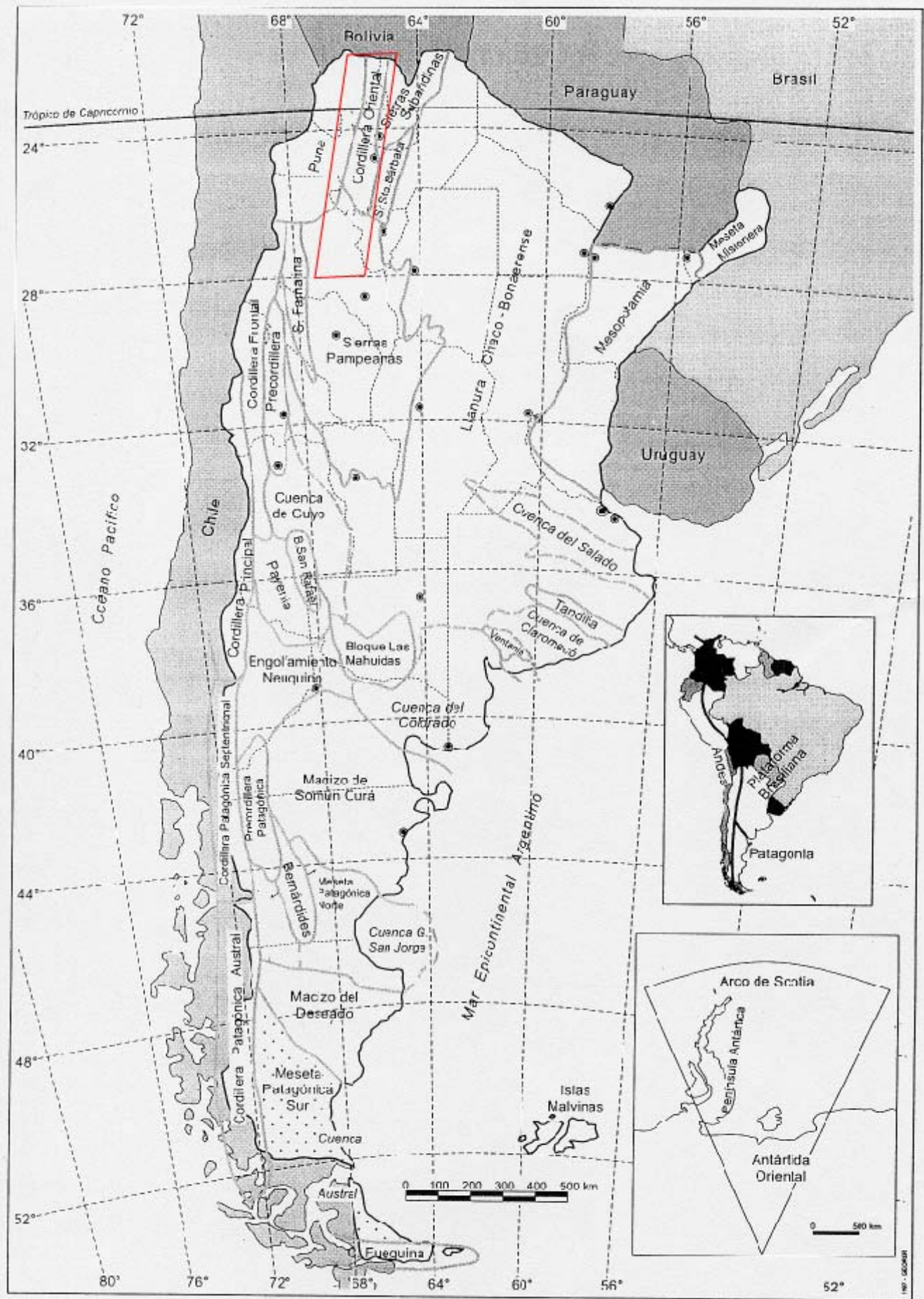


Fig. I-3-1-1-3 Topographic units in Argentina in Argentina (taken from Ramos,1999b)

Table I-3-1-2-1 Simplified stratigraphy of the survey area.

	Puna Region		Cordillera Oriental Region		Sierras Pampeanas Region		Tectonic Cycles
	Stratigraphy	Intrusive	Stratigraphy	Intrusive	Stratigraphy	Intrusive	
Quaternary	Modern detrital accumulation, evaporite of salt, modern volcanic center (basalt)		Modern detrital accumulation, modern volcanic center (basalt)	Tuzile effusive complex (dacite, rhyodacite, andesite porphyry, rhyodacitic tuff)	Modern detrital accumulation, evaporite deposits, monogenetic center (andesite, basalt)		
Neogene	Pliocene	Fm.Rumbola (andesite, basalt)	Fm.Uquia, Fm.Mamara				Neogene subcycle
	Miocene	Clastic and volcanoclastic sequences: (dacite-rhyolitic ignimbrite, andesite - dacite lava, tuff, breccia)					Andes cycle
Paleogene	Oligocene						
	Eocene						
	Paleocene						
Cretaceous		Gr.Salta (continental conglomerate, pelite, arenite, limestone), Subgr.Santa Barbara, Subgr.Balbuena, Subgr.Pirgua					
Jurassic							
Silurian							
Ordovician							
Cambrian							
Precambrian							

and Quesera multiple seams and are mainly distributed in Cordillera Oriental area. The type of composing rocks include trondheimite, granite, tonalite and granodiorite.

Dip unconformity is observed between strata of the Precambrian system and the Cambrian system, and is associated with Tilcaric deformation movements in the Pampia cycle. The Cambrian system in Cordillera Oriental area includes marine siliceous sandstone, shale and slate, which are collectively called Meson group. Meson group covers the upper part of the plutonic rock body of Canani multiple seam in unconformity. In Pampeanas Mountains area, gneiss, slate and crystalline schist of the same age are distributed in the Penon, the Laguna Blanca and the Altohuasi mountains located in the southwest end of the survey area.

Strata of the lower Ordovician are composed of marine shale, slate and siliceous sandstone, which are represented by Santa Victoria group in Cordillera Oriental area and cover the upper part of Meson group partially in conformity (Fig. I-3-1-2-1). Santa Victoria group has many vein-type lead/zinc deposits including El Aguilar Deposit, which is a SEDEX-type zinc and lead deposit. In the upper part (Acoite Formation) of Santa Victoria group, volcanic to semi-plutonic rocks called Faja Eruptiva (Oriental) exist and intrude widely. These rocks are volcanic rocks and volcanoclastic rocks of the Arenig-Llanvirn series generated by bimodal magmatic activities of dacite to rhyolite and basalt, and are accompanied by near surface intrusive rocks with similar composition. These sedimentary rocks and volcanic/volcanoclastic rocks received compressed deformation by Ocloyic deformation movements of the Famatina cycle and were subjected to fold/fault movements. As a result, primitive Puna uplifted and formed unconformity with the Silurian sediments, its upper strata.

The range of distribution of Silurian to Jurassic strata is limited, and shallow-marine to terrestrial sedimentary strata are distributed only locally in the eastern part of the Cordillera Oriental mountains and in the Subandinas mountains. These strata do not have a relationship with deposits.

The eastern part of Puna and Cordillera Oriental area adjoining it received intrusion of granite rocks related to the Patagonia tensile cycle from the end of the Jurassic to the lower Cretaceous. Representative of these rocks are Aguilar granite rocks distributed along the Aguilar mountains, which are composed of biotite tourmaline granite, monzonitic granite, granite-porphyry, muscovitic granite and hornblende granite. Aguilar granite rocks exerted contact metamorphism upon the SEDEX deposit of El Aguilar Mine.

Lifted sedimentary basins extending south and north created by the Patagonia tensile cycle were formed in various places, such as Cordillera Oriental area and the southern part of Salta City, from the lower Cretaceous to the Eocene. In these terrestrial sedimentary basins, conglomerate, mudstone, sandstone and limestone are deposited.

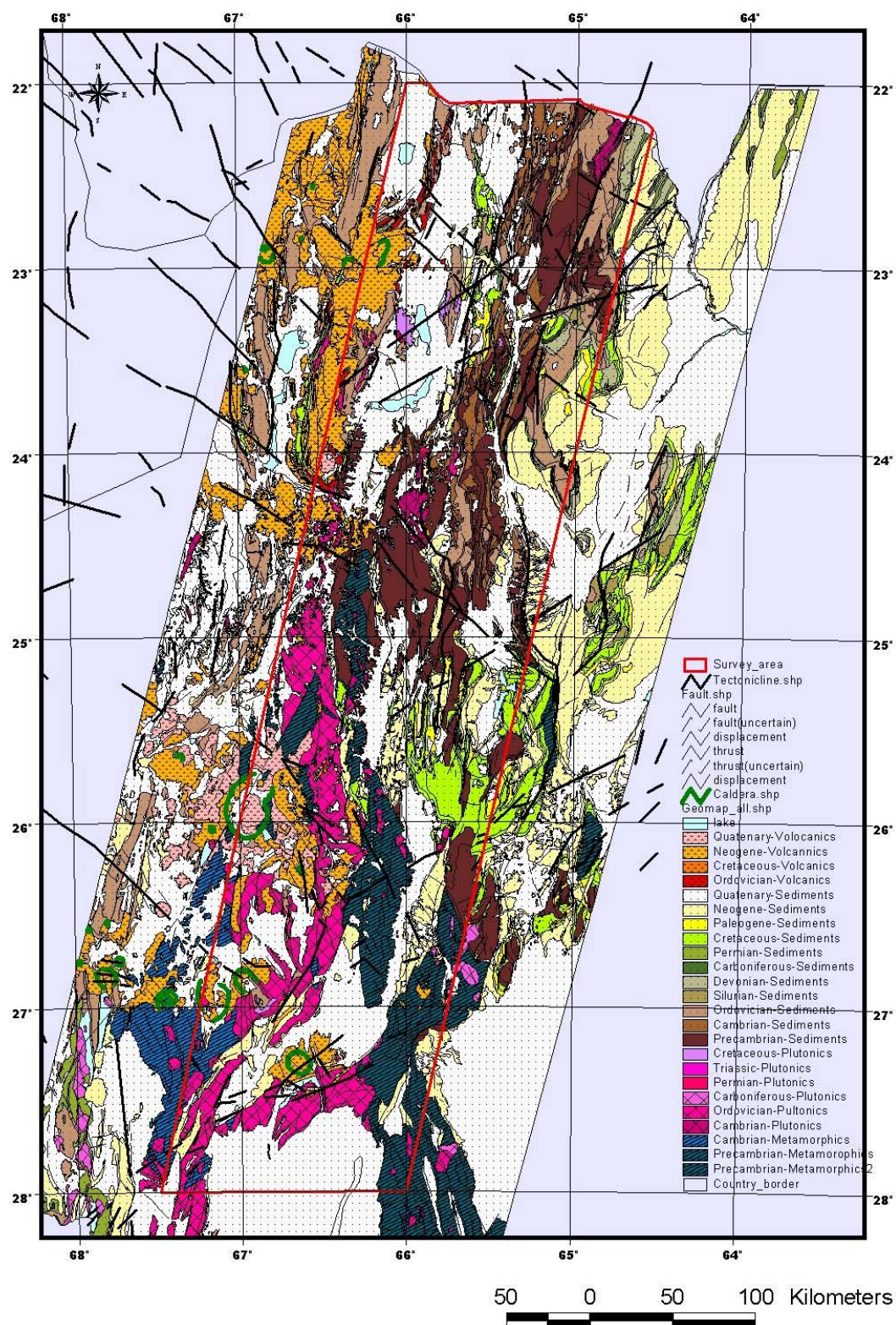


Fig. I-3-1-2-1 Geological map of the survey area (compiled from mapa geológico de la provincia de “Jujuy”, “Salta”, “Tucuman” and “Catamarca”)

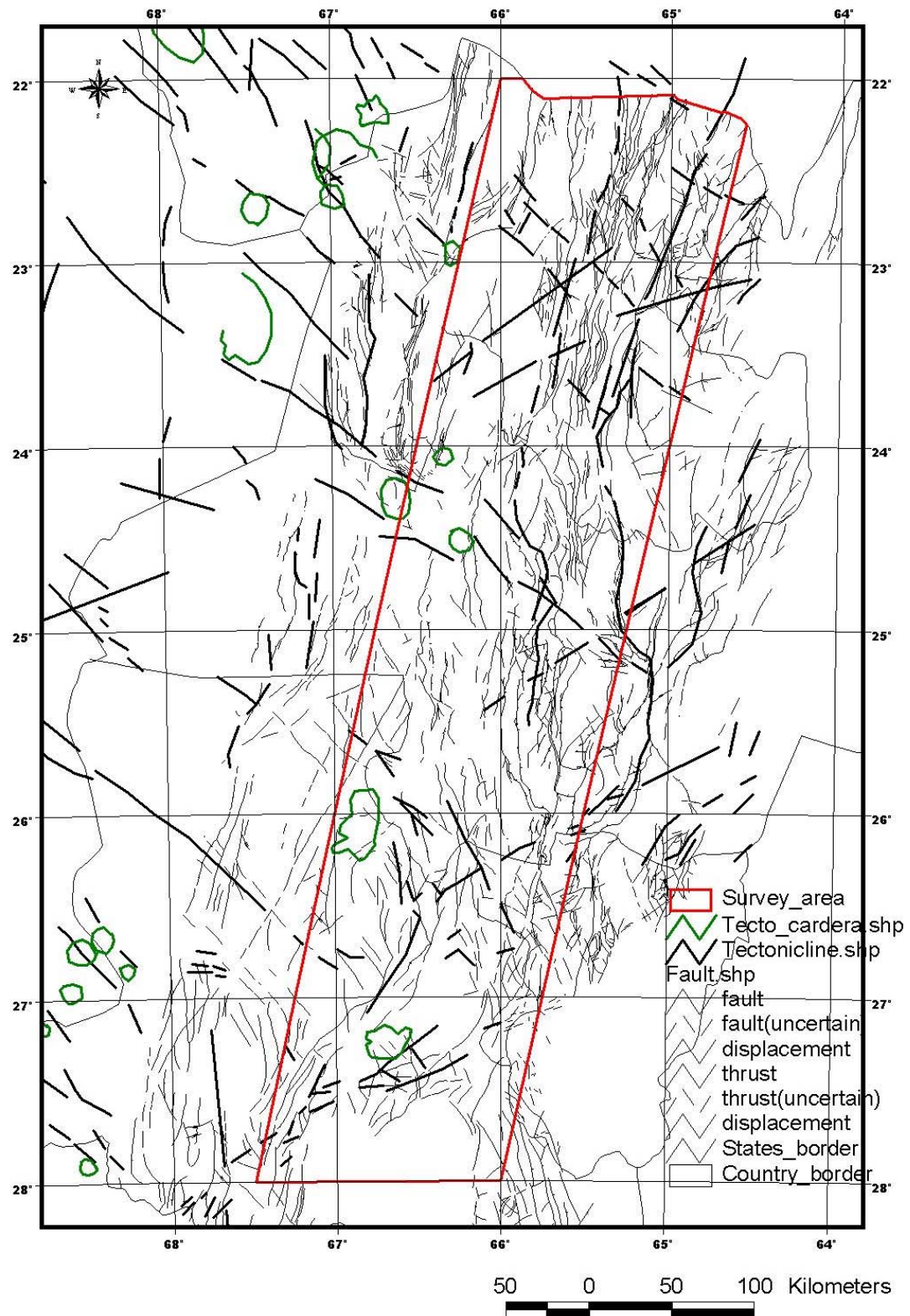


Fig. I-3-1-2-2 Geological structure map of the survey area (compiled from JICA and MMAJ,1998 and Riller et al., 2001)

In the age of the Andes cycle, local foreland sedimentary basins accompanying the Andes orogenic movements were formed in various places, and the formation continues still while the center of sediment is being moved to the east.

In the Oligocene, there was formation of several northwest-southeast lineaments in the area ranging from Chile to Argentina, such as El Toro-Olacapato Lineament, which is related to diagonal subduction of the plate from the Andes cycle to the Paleogene subcycle. Acay granite rocks (granite and monzonite) intruding the top of Mount Acay (5,716 m) are located in this El Toro-Olacapato Lineament.

In the Miocene, the accompanying dip of the subducting plate became gentle, and magmatic arcs expanded to inland of Argentina and formed a sequence of volcanic rocks - volcanoclastic rocks - intrusive rocks mainly composed of andesite, dacite and rhyolite. These arcs did not expand uniformly but in a beltlike form extending northwest and southeast, and four belts of this kind are observed in the survey area (Fig. I-3-1-2-1). The southernmost one of these four belts includes Farallon Negro Volcanic Complex and has many porphyry copper/gold deposits and epithermal deposits. In other belts, the existence of similar deposits has been confirmed.

From the upper Miocene to the Quaternary, scaling down on the Chilean side, the main magmatic arcs locally formed andesite, basaltic lava, dacite and rhyolitic ignimbrite. The cause of this is considered to be calc-alkali magmatic activities inside the plate that are related to the fact that the plate subduction angle became deep again.

3-1-2-2 Mineral deposits in the survey area

The distribution of the main known places of ore indications in the survey area is shown in Fig. I-3-1-2-3. The main ones of these known places of ore indications are shown in Table I-3-1-2-2. In the survey area, various types of nonferrous metal deposits and places of these ore indications are known, including porphyry copper/gold deposits, epithermal gold/silver deposits, mesothermal gold deposits, SEDEX lead/zinc deposits, volcanic massive sulfide deposits, polymetallic vein deposits, skarn deposits, pegmatite deposits, and sedimentary copper/uranium deposits. The number of these deposits and places is five hundred or more. Those which are important from an economic point of view are porphyry copper/gold deposits, epithermal gold/silver deposits, SEDEX lead/zinc deposits and polymetallic vein deposits. Porphyry copper/gold deposits and epithermal gold deposits were formed by Neogene magmatic activities, while SEDEX lead/zinc deposits are syngenetic deposits held by Santa Victoria group of the Ordovician system. Although polymetallic vein deposits were formed in each age, there were more formations in the Precambrian, the Ordovician and the Neogene. The main deposit types are outlined below.

Vein deposits with wall rock of the Precambrian group

Table I-3-1-2-2 Deposit type and main deposits in the survey area

Deposit type	Province	Zone	Name of mine	Elements	Type	Age	Lithology
Precambrian vein	SALTA	Z-12	Esperanza (Esther)	Cu-Pb-Zn-Ag-U-Co	Polymetallic vein	Precambrian, Cambrian	Schists, slates and quartzites
	JUJUY	Z-23	9 de julio	Pb-Ag-Zn	Polymetallic vein	Precambrian	Schists, slates, greynwackes, phyllites
	JUJUY	Z-24	Coiruro	Sb-Au	Epithermal	Precambrian	Schists, slates and greynwackes, rhyolitic dikes
	JUJUY	Z-24	Chorrillos	Cu-Ag-Sb-Pb	Vein and brecciated vein	Precambrian	Schists, slates, limestones, phyllites
	SALTA	Z-34	Brealito	Cu	Unknown	Precambrian, Cretaceous	Metasediments, Porphyritic body
Ordovician SEDEX (VMS)	JUJUY	Z-15	Esperanza	Pb-Ag-Zn	SEDEX	Ordovician	Shale
	JUJUY	Z-15	El Aguilar	Pb-Ag-Zn	SEDEX	Ordovician-Cretaceous	Quartzites, granite
	SALTA	Z-18	La Colorada	Cu-Pb-Zn-Fe	SEDEX? (VMS)	Ordovician	Quartzitic sandstones, greynwackes, shales and granites
	JUJUY	Z-01	La Gateada	Pb	Vein	Ordovician	Sandstones, shales
	JUJUY	Z-02	Pumahuasi	Pb-Zn	Vein	Ordovician	Sandstones and shales
Ordovician polymetallic vein	JUJUY	Z-02	Sol de Mayo	Pb-Zn	Vein	Ordovician	Sandstones and shales
	JUJUY	Z-02	La Bélgica	Pb-Zn	Vein	Ordovician	Sandstones and shales
	SALTA	Z-03	La Niquelina	Ni-Pb-Zn-(Co-As-Cu-U)	Polymetallic vein	Cambrian, Ordovician	Quartzite, shale and sandstone
	SALTA	Z-05	La Ciénaga	Pb-Cu-Ag-Zn-Barite	Polymetallic vein	Ordovician	Shales and sandstones
	SALTA	Z-05	Vizcachani	Pb-Ba-Ag-Cu	Polymetallic vein	Ordovician	Shales and sandstones
Miocene porphyry Cu-Au-Mo	JUJUY	Z-11	La Purísima (Rumicruz)	Cu-Pb-Barite	Polymetallic vein	Ordovician	Sandstones, shales and siltstones
	SALTA	Z-27	Organullo	Au	Porphyry Au	Tertiary	Dacitic and andesitic flows. Dioritic stock
	SALTA	Z-28	Pancho Arias	Mo-Cu-Au	Porphyry Mo-Cu	Precambrian, Miocene	Leptometamorphic rocks, Dacitic porphyry dikes swarm and intrusive and hydrothermal breccias
	SALTA	Z-31	Inca Viejo	Au-(Cu-Mo)	Porphyry Au	Tertiary (Miocene)	Monzonitic and dacitic porphyries, intrusive and collapse
	SALTA	Z-31	Diablillos	Au-Cu	Porphyry Au-Cu	Miocene	tourmaline-bearing breccias
	CATAMARCA	Z-43	Bajo de la Alumbra	Cu, Au	Porphyry Cu-Au	Upper Miocene	Granitic intrusive, intrusive breccia
	CATAMARCA	Z-43	Bajo de Agua Tapada	Cu-Au	Porphyry Cu-Au	Upper Miocene	Andesitic breccia, Andesitic tuff, Andesitic dikes and sills. Quartz andesitic stock and dikes
	CATAMARCA	Z-43	Agua Rica	Cu, Mo, Au	Porphyry Cu	Upper Miocene	Dacitic porphyry stock, andesitic breccia, qz-andesite
	CATAMARCA	Z-43	Filo Colorado	Cu, Au, Mo	Porphyry Cu	Ordovician, Upper Miocene	Syenodiorite, porphyries
	TUCUMAN	Z-46	El Alisar	Cu-Au	Porphyry Cu-Au	Miocene	Granite, Dolerite and Dacites
Miocene epithermal vein	TUCUMAN		El Pago	Cu-Au-Pb-Zn	Porphyry Cu-Au	Precambrian upper, miocene?	Andesitic porphyry, andesites and intrusive and hidrotemal breccias
	SALTA	Z-26	Incachule	Sb	Epithermal vein	Tertiary (Miocene)	Gneiss/Migmatite
	SALTA	Z-31	Diablillos	Au-Cu	High sulfidation epithermal	Miocene	Dacite
	CATAMARCA	Z-43	Agua Tapada	Au-Ag	Low sulfidation epithermal	Upper Miocene	Granitic intrusive, intrusive breccia
	CATAMARCA	Z-43	Farallon Negro (Alto de la Blenda)	Au, Ag, Mn	Low sulfidation epithermal	Upper Miocene	Andesitic breccias and Quartz andesites
	CATAMARCA	Z-43	Mina Capillitas	Cu-Au-Pb-Zn-Ag	Disseminated, veinlets, filling, massive, chimney and vein (High sulfidation)	Upper Miocene	Andesitic breccias and Monzonite
	CATAMARCA	Z-43	Agua Rica	Cu, Mo, Pb, Zn, Ag, Au	High sulfidation epithermal	Upper Miocene	Volcanic breccia/Rhyolite/Tuff
	JUJUY	Z-07	Pan de Azúcar-Potosí-España	Pb-Ag-Zn-Sb	Epithermal polymetallic	Middle Miocene	Igneous breccia, hydrothermal breccias
	JUJUY	Z-09	Rachaite	Pb-Zn-Ag-Mn	Epithermal polymetallic	Miocene superior	Dacites and andesites
	SALTA	Z-26	Concordia	Pb-Ag-Zn	Epithermal polymetallic	Cretaceous, Miocene-Pliocene	Dacites, andesites, tuffs, breccias
Miocene polymetallic vein	SALTA	Z-26	La Poma	Pb-Ag-Zn	Epithermal polymetallic	Tertiary	Conglomerates, dacites and dacitic breccias
	SALTA	Z-27	Organullo	Au-Bi-Cu-Pb-Zn	Epithermal polymetallic	Tertiary, Precambria	Dacites and dacitic tuffs
	SALTA	Z-27	El Acay	Fe-Cu-Pb-Zn	Skarn and vein	Cretaceous, Oligocene	Slates and schists
	CATAMARCA	Z-39	Languna del Salitre	Pb, Zn, Ag, Au	Epithermal polymetallic	Miocene	Gametiferous skarn, limestone, calcareous sandstone, marl, granite
	SALTA	Z-38	Vallecito	Cu	Impregnation, disseminated (stratabound)	Miocene	Monzodiorite
Cretaceous Stratabound Cu	SALTA	Z-39	Margarita, Zorriquín	Cu	Stratabound Cu	Ordovician (Cretaceous)	Migmatites, granites (conglomerates, sandstones)
	SALTA		Custodio, San Martín, Salamanca	Cu	Stratabound Cu	Cretaceous	Sandstones and conglomerates
	SALTA		Doña Inés	Cu-Fe	Stratabound, impregnation, vein	Cretaceous	Conglomerates and arcose sandstones
	SALTA		Elba, María, León	Cu-Pb	Stratabound Cu	Cretaceous	Conglomerates and sandstones
	SALTA	Z-04	Pueblo de Minas	Au	Alluvial gold	Pleistocene, Holocene	Calcareous sandstone, oolitic limestone, sandy limestone
Alluvial placer Au	SALTA	Z-04	Santa Cruz	Au	Alluvial gold	Pleistocene, Holocene	Alluvial-colluvial deposits
	SALTA	Z-04	Pucará	Au	Alluvial gold	Pleistocene, Holocene	Alluvial plane deposit
	SALTA	Z-04	Santa Rosita, Pucará, Cerros Bravos	Au	Alluvial gold	Pleistocene, Holocene	Alluvial plane deposit
	SALTA	Z-04	Cerros Bravos	Au	Alluvial gold	Pleistocene-Holocene	Alluvial plane deposit

Mineral deposits belonging to this type include Esperanza (in the Esther area, Pb-Ag-Zn-U) in Zone 12, 9 de Julio (Pb-Ag-Zn) in Zone 23, Pueblo Viejo (Au) in Zone 19, Coiruro (Sb-Au) and Chorrillos (Cu-Ag-Sb-Pb) in Zone 24 and Brealito (Cu) in Zone 34. These deposits are considered to have vein deposits with various origins, and all are held in rocks of the Precambrian system. There is the possibility that the age of deposit generation is much more younger.

Ordovician SEDEX lead/zinc deposits (or VMS deposits)

Deposits of this type are El Aguilar and Esperanza in Zone 15 and La Colorada in Zone 18 only. It is said that these are massive sulfide deposits existing in the Ordovician system. El Aguilar and Esperanza are SEDEX deposits and produce lead, zinc and silver at present. Although La Colorada is classified as SEDEX in many materials, it is considered from materials and drilling core samples collected this time that it is classified as a volcanic massive sulfide deposit.

Polymetallic vein deposits with Ordovician wall rock

More deposits of this type exist in the northern part of the survey area than in other parts, and there are many deposits of this type including La Gateada (Pb-Ag-Zn) in Zone 1, Pumahuasi, La Belgica, Sol de Mayo (Pb-Zn) in Zone 2, La Niquelina (Ni-Pb-Zn) in Zone 3, Vizcachani (Pb-Ba-Ag-Cu) and La Cienaga (Pb-Cu-Ag-Zn-Ba) in Zone 5 and Rumicruz (La Purisima, Cu-Pb-Ba) in Zone 11. Among these vein deposits, there are many mines where small-scale mining was carried out. Because of the small scale, however, it is considered to be difficult to execute development targeting base metal such as copper, lead and zinc at present. There is the possibility that these vein deposits are relevant to SEDEX deposits, and they may become important as a guide to investigation of the SEDEX type.

Miocene Porphyry (Cu-Au-Mo) deposits

Deposits of this type are distributed in the southern part and the middle part of the survey area and include Organullo (Au-Bi-Cu-Pb-Zn) in Zone 27, Pancho Arias (Cu-Mo) in Zone 28, Inca Viejo (Cu-Mo) and Diablillos (Au-Cu) in Zone 31, Bajo de la Alumbrera, Bajo de Agua Tapada (Cu-Au), Agua Rica (Cu-Mo-Au) and Filo Colorado (Cu-Au-Mo) in Zone 43, El Alisal (Cu-Au) in Zone 46, and El Pago (Cu-Au-Pb-Zn) in Zone 47. In Bajo de la Alumbrera, open-pit mining is being carried out now, and copper concentrates of 215,000 tons were produced in 1999. These porphyry deposits are distributed along Miocene magmatic arcs stretching out from the Chilean side together with the next Miocene epithermal deposits. In the survey area, four such magmatic arcs extend northwest and southeast on the whole in a beltlike form.

Miocene epithermal deposits and polymetallic vein deposits

Accompanying Miocene porphyry deposits, epithermal deposits are distributed mainly in the southern part and the middle part of the survey area. Many polymetallic vein deposits exist and are distributed in all of the southern part, the middle part and the northern part. Representative epithermal deposits include Incachule (epithermal Sb) in Zone 26, Diablillos (gold and silver of the high sulfidation system) in Zone 31, Agua Tapada (gold and silver of the low sulfide system), Farellon Negro (Alto de la Blenda, low-sulfidation system gold and silver Mn), Agua Rica (gold and silver of the high sulfidation system) and Capillitas (Cu-Au-Pb-Zn-Ag of the high sulfide system) in Zone 43. As representative polymetallic vein deposits, many deposits are widely distributed, including Pan de Azucar-Potosi-España (Pb-Ag-Zn-Sb) in Zone 7, Rachaite (Pb-Zn-Ag-Mn) in Zone 9, Concordia (Pb-Ag-Zn) and La Poma (Pb-Ag-Zn) in Zone 26, Organullo (Au-Cu-Bi-Pb-Zn) and El Acay (skarn, dike, slate, Cu-Pb-Zn) in Zone 27, Laguna del Salitre (Pb-Zn-Cu) in Zone 39.

Cretaceous sedimentary copper deposits

Deposits of this type exist in Salta group from the Cretaceous system to the Paleogene system in the middle part of the survey area. They include Vallecito in Zone 38, Margarita (Zorriquin) in Zone 39, and Custodio (San Martin, Salamanca), Dona Ines and Elba (Maria, Leon) of which have not been zoned at this time. The importance of these deposits seems to be low.

Quaternary placer gold deposits

Many deposits of this type are distributed along the Santa Cruz river in Zone 4 in the northern part of the survey area. There are a lot of deposits with past production records, such as Santa Cruz, Pucara, Santa Rosita, Pueblo de Minas and Cerros Bravos. Although the economic importance of placer gold seems to be low, vein gold deposits as a supplying source may be significant.

Quaternary evaporate deposits

Deposits of this type are evaporation deposits and exist in salt lake sediments of this age. Although they are not included in minerals covered by this survey, many mines producing boron/rock salt now exist in Zones 21, 29 and 30. Outside the survey area, Salar del Hombre Muerto, a lithium mine, exists west of the middle part of the survey area.

Regarding the summary of the geology of and deposits in Andes Region stated above, although there is a lot of general literature, the materials listed below were mainly referred to.

- Zappettini, E.O. (Ed.), Mapa metalogenético de la República Argentina, Version Preliminar (CD-ROM): SEGEMAR, 1998.

- Zappettini, E.O., 1999, Evolución geotectónica y metalogénesis de Argentina: Recursos Minerales de la Republica Argentina Vol.1 (Ed. E.O.Zappettini), SEGEMAR, Anales 35, pp.51-73.
- Ramos, V.A., 1999a, Ciclos orogénicos y evolución tectónica: Recursos Minerales de la Republica Argentina Vol.1 (Ed. E.O.Sappettini), SEGEMAR, Anales 35, pp.29-49.
- Ramos V.A., 1999b, Las provincias geológicas del territorio Argentino: Geología Argentina (Ed. R.Caminos), SEGEMAR, Anales no,29, pp.41-96.
- Ramos, V.A., 2000, The southern central Andes: Tectonic evolution of South America (Ed. Cordani,U.G., Milani,E.J., Thomaz,F.A., Campos,D.A), pp561-604, Rio de Janeiro,2000.

For regional geology, provincial geological maps and 1/250,000 geological maps of Jujuy, Salta, Tucuman and Catamarca Provinces were also referred to.

- Mapa Geológico de la Provincia de Catamarca, 1:500,000, SEGEMAR,1995.
- Mapa Geológico de la Provincia de Tucuman, 1:500,000, SEGEMAR,1994.
- Mapa Geológico de la Provincia de Salta, 1:500,000, SEGEMAR,1998.
- Mapa Geológico de la Provincia de Jujuy, 1:500,000, SEGEMAR,1996.
- Hoja Geológica 2566-I, San Antonio de los Cobres, Dirección Nacional del Servicio Geológico,1996.
- Hoja Geológica 2766-II, San Miguel de Tucumán, Dirección Nacional del Servicio Geológico,1999.
- Hoja Geológica 2366-II y 2166-IV, La Quiaca, Dirección Nacional del Servicio Geológico,1999.
- Hoja Geológica 2566-III, Cachi, Dirección Nacional del Servicio Geológico,1998.

3-2 Mining activity

3-2-1 Mining policies

With support from the World Bank, the Argentine Republic launched a radical economic reform program in the beginning of the 1990s. As a result of this mining policy reform, a legislation system meeting the international standard was completed and an environment for mining investment was improved. The object is to complete the legal system necessary for mining development and to create a competitive market for the reduction of private investment risk and for advantageous investment. In the analysis by the MMAJ and the World Bank (2001), the Argentine Republic was classified as a country developing reform (Fig. I-3-2-1-1). Countries completing the reform are Chile, Peru, Mexico and Indonesia. In these countries, mining production has increased by leaps and bounds.

3-2-2 Mining production

The effect of the mining policy reform was truly shown in mining production activities, and there was remarkable increase in the amount of investments, amount of production and amount of exports in the mining sector after 1993 (Table I-3-2-2-1). In particular, the increase in the amount of production and the amount of export was largely attributed to the start of production at three international-scale mines; Bajo de la Alumbrera, Cerro Vanguardia and Salar del Hombre Muerto.

3-2-3 Mining legislation system

As mentioned above, the Government of the Argentine Republic carried out improvement and completion of the legislation system to promote mining investment in the 1990s. At present, there are the following laws related to mining:

- Mining Code: enacted in 1886, revised in 1997
- Mining Investment Law No. 24,196: established in 1993

Stable tax system, exemption from property tax, exemption/reduction of the import tax and placing the highest limit of royalties at 3%.

- Mining Reorganization Law No. 24,224: established in 1993

Preparation of geological maps, establishment of COGEMIN, and expansion of mining and exploitation areas.

- Federal Mining Agreement Law No. 24,228: established in 1993

Association of mining producer for each province, open bids of large scale exploration projects, auction of mines, and promotion of update of mining registration.

- Mining Updating Law No. 24,498: established in 1995

Exploration in exclusive areas, and deletion of mines with nullified license from registration.

- Environmental Protection for Mining Industry Law No. 24,585: established in 1995

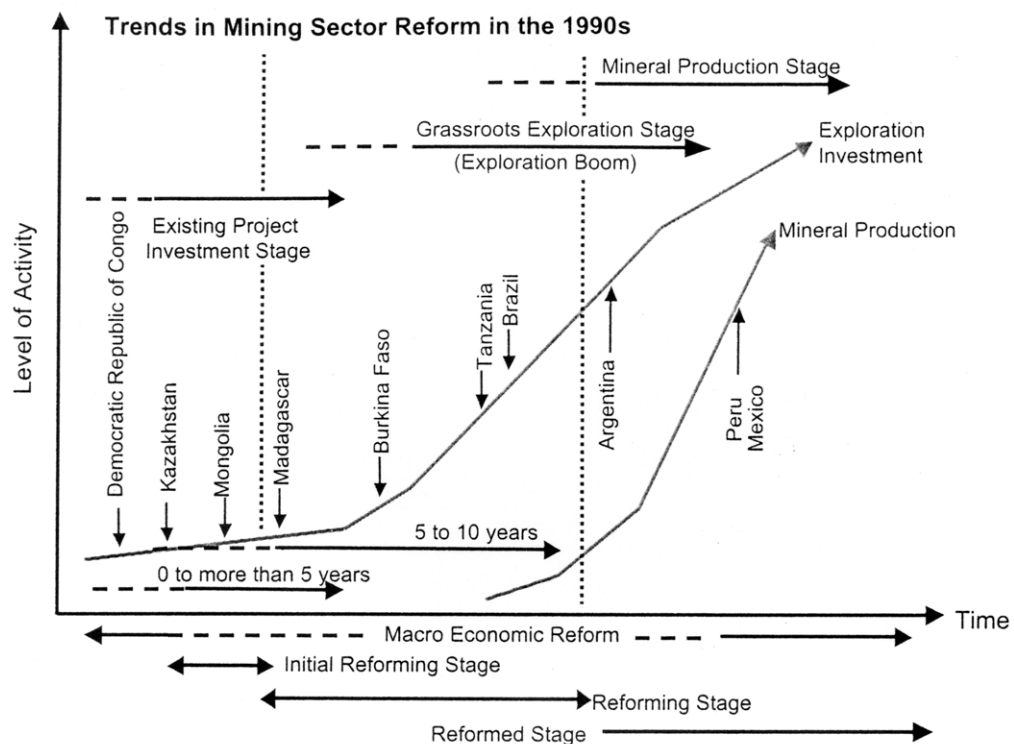


Fig. I-3-2-1-1 Idealized trends in mining sector reform in the 1990s and mining activities in some selected successful countries (taken from Naito and Remy (2001))

Table I-3-2-2-1 Investment of mining development in Argentine Republic (MMUS\$)

year	1993	1994	1995	1996	1997	1998	1999
Mining Investment	-	23	101	708	658	249	156
Mining Production	481	468	513	543	665	1151	1329
Export of Mineral Products	16	24	30	36	113	565	791

(Source: Secretaria de Energia y Minería)

Promotion of environmentally sustainable production, and promotion of environmental protection mechanism

Although the details of these laws related to mining are omitted, importance is attached to promotion and guarantee of mining investment from inside and outside of the country, based on the following basic concepts.

- Ownership of minerals shall belong to the state or province to which land where minerals are produced.
- The state or province shall grant the private sector the right to execute prospecting, development and/or mining.
- The mining right shall be an independent right that is separate and different from land ownership.
- Mine development shall be put into the private sector, including foreign capital.

That is to say, tax incentives are employed for the following purposes: neutrality of foreign capital, legal guarantee of mining rights obtained, leadership of the private sector regarding the development of natural resources, opening of state mining concession, expansion of exploration and mining areas, and reduction of environmental protection and prospecting costs and business and operation costs.

3-2-4 Recent trends of exploration and development

In the 1990s, South America was a region where mining investment expanded most widely. The background was, of course, the high potential of mineral resources in South America, but improvement of the environment for mining investment realized by the mining policy reform of countries holding resources contributed largely to this. Although being behind Chile, which established the Mining Law in 1983, Argentina established three laws - the Mining Investment Law, the Mining Reorganization Law and the Federal Mining Agreement Law - in 1993, which allowed an environment for private investment to become in place. As a result, the amount of this country's prospecting investment increased by leaps and bounds, from 70 million dollars in 1992 to 790 million dollars in 1997. This led to the development of large-scale mines, such as Bajo de la Alumbrera Mine (in Catamarca Province; porphyry type copper/gold deposits), Cerro Vanguardia Mine (in Santa Cruz Province; epithermal gold deposits), and Salar de Hombre Muerto Mine (in Catamarca Province; lithium deposits in salt lake). In particular, from 1996 to 1998, foreign capital rushed to the country, which brought about a prospecting boom. In and after 1999, however, due to saturation of prospecting, the worsened world economy and sluggish metal market conditions, foreign prospecting companies have tended to pull out. In such a situation, the three mines mentioned above were developed after the mining policy reform and continue production satisfactorily.

Deposits whose development is suspended due to sluggish metal market conditions and for financial reasons are El Pachon (in San Juan Province; porphyry type copper/molybdenum deposits; Cambior (50%) and Campania Minera San Jose (50%)), Agua Rica (in Catamarca Province; porphyry type copper deposits; BHP Biliton (70%) and Northern Orion (30%)), San Jorge (in Mendoza Province; porphyry type copper/gold deposits; Northern Orion (100%)), Del Carmen (in San Juan Province; epithermal gold and silver deposits; Barrick and Homestake), Manantial Espejo (in Santa Cruz Province; epithermal gold and silver deposits; Silver Black Hawk (80%) and Barrick (20%)), and Pirquitas (in Jujuy Province; polymetallic vein type silver, zinc and tin deposits; Sunshine Argentina (100%)).

Deposits that can be mentioned as those in preparation for development now are Veladero (in San Juan Province; epithermal gold and silver deposits; Barrick (40%) and Argentina Gold (60%)), Pascua-Lama (in San Juan Province; epithermal gold and silver deposits; Barrick (100%)) and Esquel (in Chubut Province; epithermal gold and silver deposits; Brancote (74%) and others (26%)).

Similarly, in places surrounding the survey area, exploration activities were carried out from 1996 to 1998, but most of them are slowed down now. Table I-3-2-4-1 shows the exploration during the above-mentioned period. The main target of exploration was porphyry type copper and copper/gold deposits and epithermal gold deposits.

Table I-3-2-4-1 Recent exploration around the survey area

Name of Project	Province	Company	Deposit type	Duration	Methodology	Status
Agua Caliente	Jujuy	MIM Argentina Exploration S. A.	Epithermal (Au, Ag)	1998	GS, GC, DR	abandon
Centenario North	Salta	Aranlee Resources (USA)	Epithermal (Au, Ag)	1999	GC, GP, TR, DR	abandon
Centenario South	Salta	Lapacha Mineral SRL	Porphyry (Cu, Au)	2001	GS, GC, DR	?
Cerro Gordo	Salta	Mansfield Minera S. A. and RTZ	Epithermal (Au, Ag)	1997	GC, TR, DR	?
Cerro Juncal	Salta	Mansfield Minera S. A.	Epithermal (Au, Ag)	1999		
Cerro Samenta	Salta	Mansfield Minera S. A.	Porphyry (Cu, Au)	1996-2001		abandon
Chincillas	Jujuy	Aranlee Resources (USA)	Porphyry (Cu, Au)	1996-1997	GA, GC, TR, DR	abandon
Condor Yacu	Salta	Cardero Resource Corp. (USA)	Epithermal (Au, Ag)	2001	DR	under exploration
Diablillos	Salta	Pacific Rim (Canada) and Barrick Exploration Argentina (Canada)	Epithermal (Au, Ag)	1989-2001	GS, GC, GP, TR, DR	start development from 2002 ?
El Acay	Salta	Aranlee Resources (USA), RTZ	Epithermal (Au, Ag)	1996-1997		abandon
El Alisar	Tucuman		Porphyry (Cu, Au)		GC	?
El Oculito	Jujuy	Aranlee Resources (USA)	Epithermal (Au, Ag)	1996	Dr	abandon
Inca Viejo	Salta	High American Gold	Porphyry (Cu, Au)	1997-1999	DR	?
La Colorada	Salta	Pacific Rim (Canada)	VMSD	1993-1998	GS, GC, GP, TR, DR	abandon
Mina Concordia	Salta	Mansfield Minera S. A. and RTZ	Epithermal (Au, Ag)	1995-1998	GS, GC, GP, TR, DR ?	
Organullo	Salta	Triton Mining (Canada)	Epithermal (Au, Ag)			
Pancho Arias	Salta	Aranlee Resources (USA)	Porphyry (Cu, Mo)	1995		abandon
Socompa	Salta	RTZ	Porphyry (Cu, Au)	1997-1998		abandon
TacaTaca Bajo	Salta	Corrientes Resources and RTZ	Porphyry (Cu, Au)			
TacaTaca Sur	Salta	Mansfield Minera S. A. and Teck Corporation	Epithermal (Au, Ag) ?	1998 ?		abandon

GS: Geological survey

GC: Geochemical exploration

GP: Geophysical exploration

TR: Trenching

DR: Drilling

Chapter 4 Outline of survey results in Phase I

4-1 Outline of survey

In order to extract promising areas with potential for the presence of deposits from the wide area efficiently and to promote technical transfer to organizations of the counterpart country, this survey carried out analysis of the existing data (including analysis of data of airborne magnetic surveys and radioactive exploration, and interpretation of results of geochemical exploration), analysis of satellite images, and ground truth, and then by comprehensively analyzing the obtained results.

4-2 Survey contents and results

(1) Analysis of the existing data

The database includes information about metal elements such as Au, Ag, Cu, Pb, Zn, rare metals and industrial material such as rare earth, perite, limestone, borax, phosphate minerals, salt, mica, Kaolinite, and rhodochrosite, topaz etc with geo-code. In order to help better and easy understanding the relation between geology and mineral distribution, the database information are added to GIS system for visualization, and finally mineral deposits and mineral showings were grouped as 44 mineral potential area (Fig.I-4-2-1). Through the database compilation, the following results especially regarding to distribution of minerals were summarized.

-Potential area of porphyry copper and copper/gold deposits, epithermal gold deposits

The high possibility area having these type deposits overlap the area of Tertiary volcanic rocks such as Zone-07, Zone-09, Zone-24, Zone-26, Zone-27, Zone-28, Zone-39, Zone-42, Zone-43, Zone-46:

-Potential area of SEDEX lead/zinc deposits and volcanic massive sulfide

Known SEDEX type deposits are El Aguilar mine and Esperanza in Z-15, Aguilar range. The high possibility area having these type deposits such as Zone-15, Zone-01, Zone-02, Zone-08, Zone-10, Zone-11, Zone-12, Zone-15, Zone-17, Zone-22, Zone-03, Zone-05, Zone-18.

(2) Data analysis of airborne geophysics

In order to select highly potential area for mineral deposits and regional geological structures, airborne geophysical data (magnetics and radioactivity) provided by SEGEMAR are processed. The area spreads over Jujuy, Salta and Catamarca States, covering the west part of the survey area with total approximately 67,000 km².

Characteristics of the whole survey area were compared from the viewpoint of regional scale for these magnetic and radioactive data. As a result, in the magnetic data analysis, the area with

NOA, Argentine

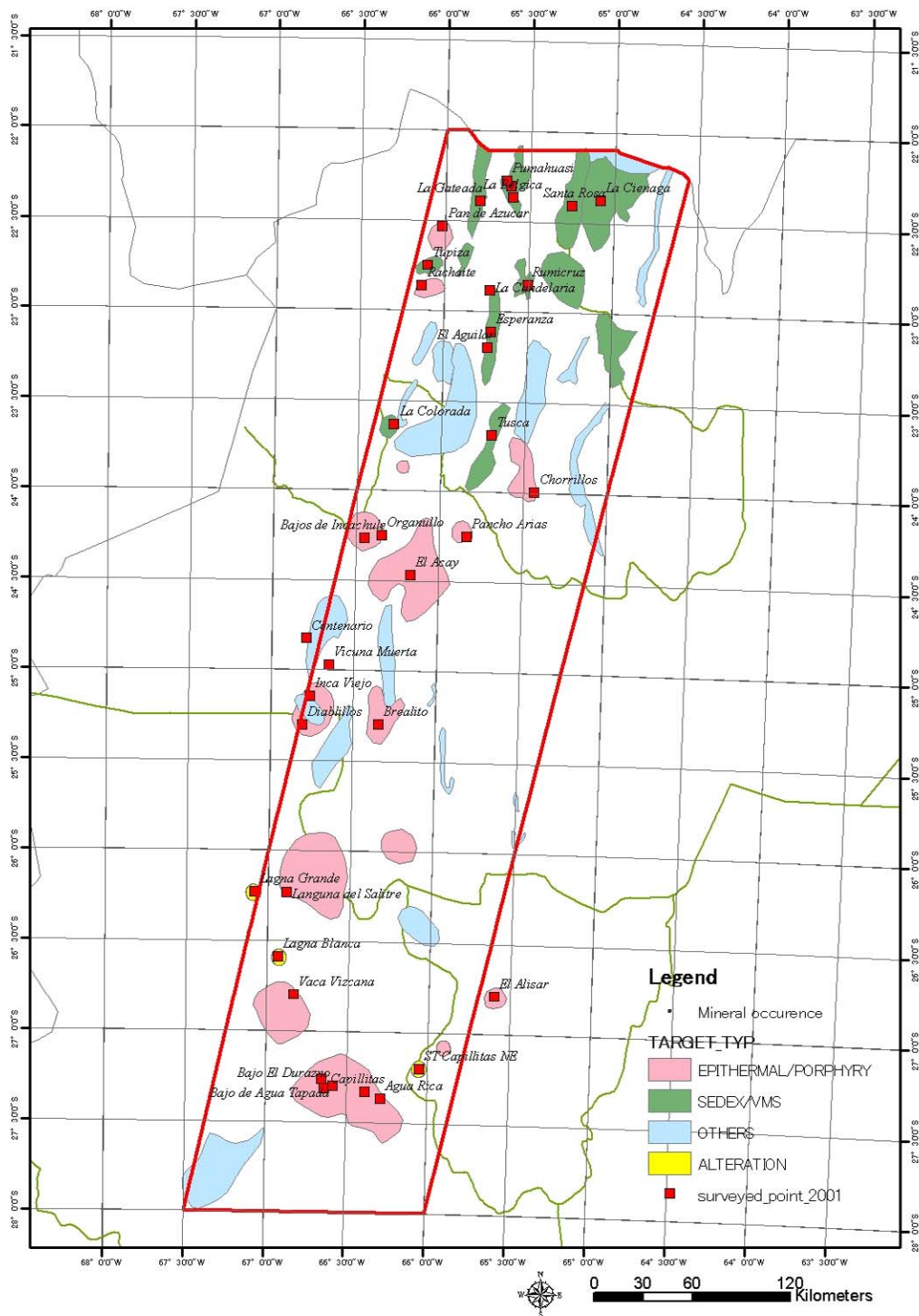


Fig.I-4-2-1 Location of Mineralized zones in the Project area and survey points.

distribution of Tertiary volcanic rocks is clearly shown as an area with short wavelength in the magnetic data. In the survey area, epithermal deposits and porphyry-type deposits are consistent with the area with distribution of these volcanic rocks well (Fig. I-4-2-2).

By radioactive data, the distribution of volcanic rocks in particular could be clearly shown, and, therefore, it seems possible to use this data for presumption of rock types. The ratio of potassium to potassium plus thorium plus uranium in order to assume the presence of epithermal deposits, etc were calculated. The results show that places where this ratio is high correspond to the area with deposits distribution from the viewpoint of the wide area. On the other hand, from the viewpoint of the local area, there is a tendency that deposits concentrate near places with a high ratio of potassium to thorium.

As a future subject, it is necessary to minutely compare geology, tectonics, radiometric data, etc. of specified areas extracted as highly potential areas in order to specify areas with deposits distribution from the more minute point of view.

(3) Stream sediments geochemistry

In Phase I, the 48 elements analysis was made for the stream sediment samples of about 5000 that had collected by SEGEMAR in the past geological survey.

The analysis results show the distributions of copper, lead, zinc and silver in Northwest area. A copper anomaly corresponds to the distribution of known porphyry copper deposits, especially the high anomaly value is seen around Agua Rica mineral showings (Fig. I-4-2-3). Lead anomaly is mainly distributing over known SEDEX deposits, and partly seen around porphyry copper deposits. Zinc anomaly also distributes the SEDEX deposits. Silver anomaly is seen in the wide area in the southern part of surveyed area. The distribution corresponds well to the distribution of Ordovician granites in Southern part of the area.

(4) Satellite image analysis

In order to identify alteration minerals accompanying deposits with ASTER data, false color image (Fig I-4-2-4), ratio image and mineral identification image were processed. Then, to check these results, ground truth was carried out. For identification and semi-quantitative analysis of alteration minerals, the iso-grain model, for which consideration was given to reflection and absorption among mineral particles, was used. After comparing with iso-grain model image and false color image and ratio image, the distribution of alteration minerals was defined.

As a result of the field verification, it was found that 1) ASTER improve the ability to discriminated alteration minerals spectacularly compare to Landsat TM, 2) almost all of the known deposits, mineral showings and very weak clay alteration zone with fault system were detected by ASTER analysis, 3) alteration minerals could be mapped out even there is vegetation of 30.

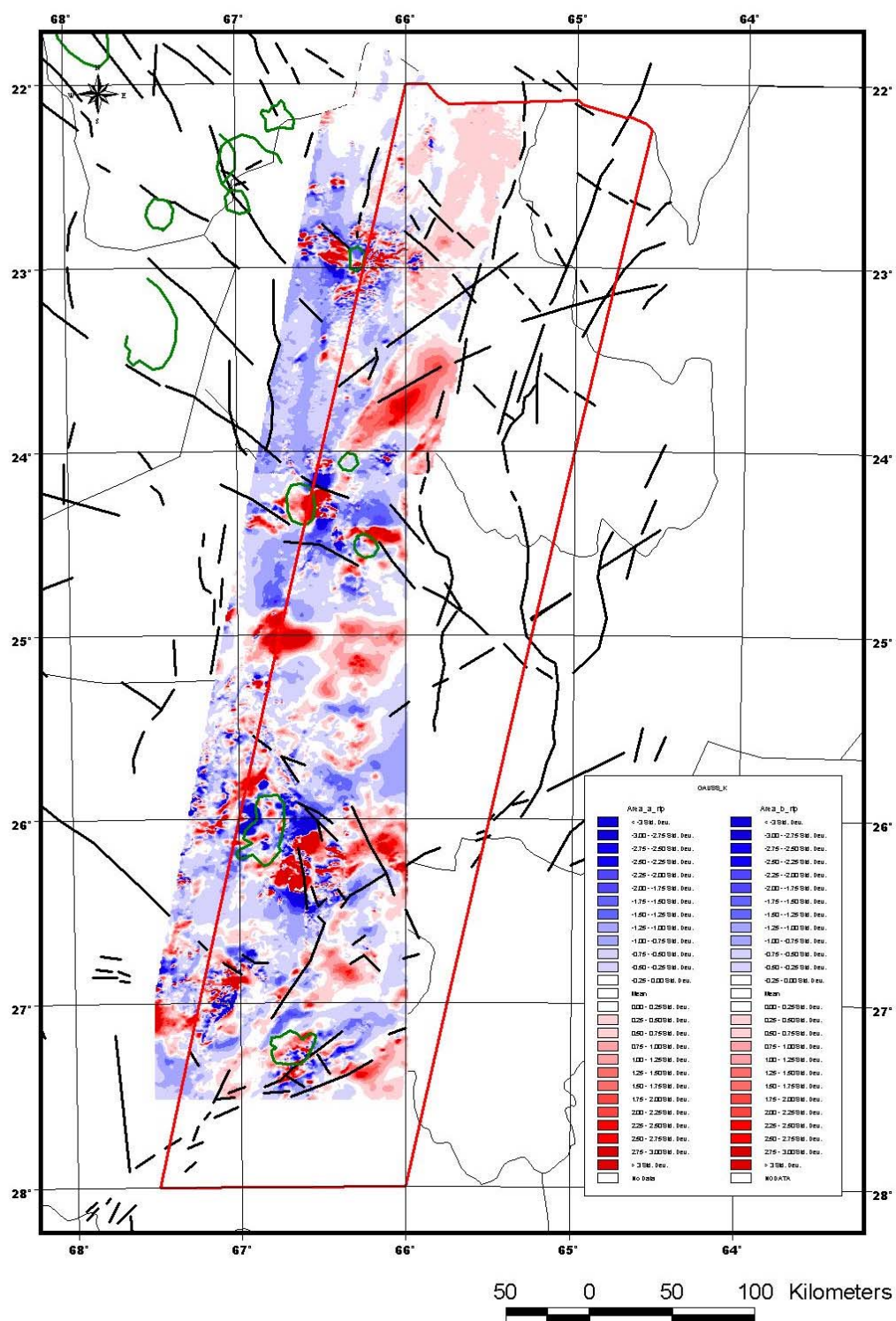


Fig.I-4-2-2 Total Magnetic Intensity (Reduced to the Pole:RTP)

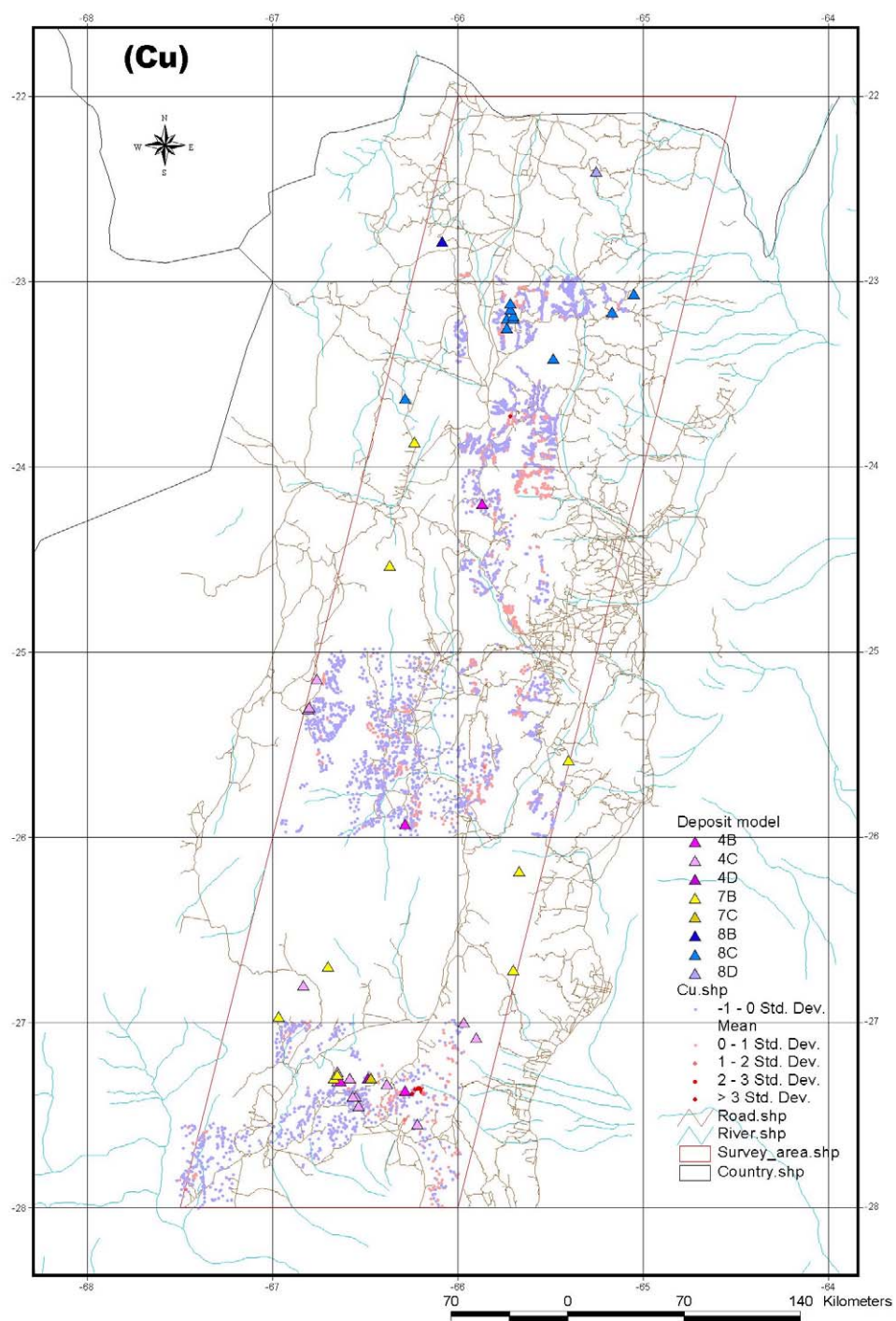


Fig.I-4-2-3 Geochemical anomaly map (Cu).

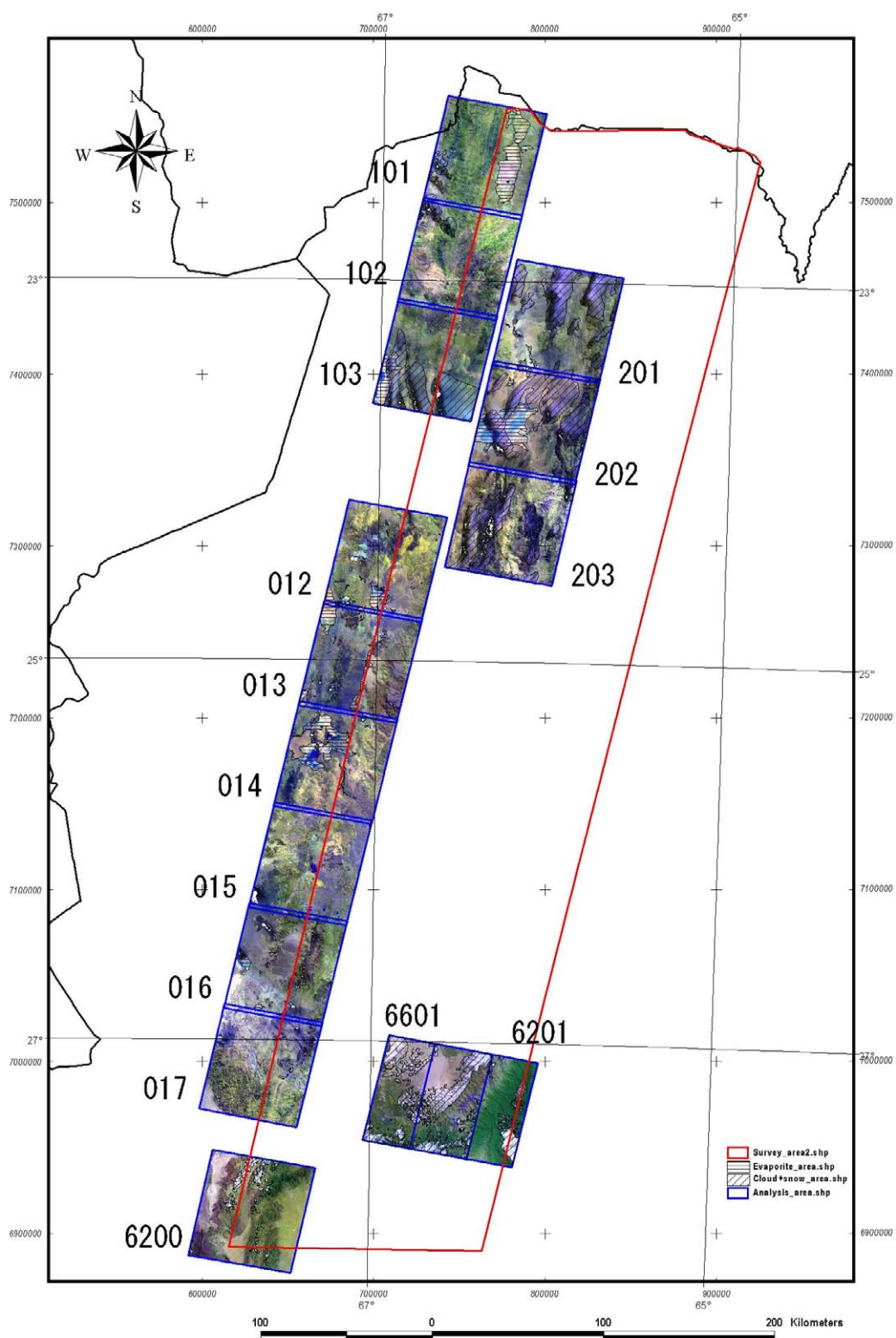


Fig.I-4-2-4 Image analysis (ASTER BGR=147)

Furthermore, SiO₂ contents image with TIR bands and DEM (Digital Elevation Model) image were processed for ground truth survey.

(5) Ground truth

Based on above survey methods, 24-survey zone were selected as potential area of mineral deposits. Then 36 mineral showings and 4-alteration zone were selected among the zone from viewpoint of exploration history and accessibility to carry out field survey. Major proposes of the survey were to make the features of geological structure, alteration, mineralization clear and to collect samples for geochemical analysis. Fig.I-4-2-1 shows the location of field survey conducted and Table I-4-2-2 shows summary of result.

4-3 Summary

(1) Structure and Control factors of mineralization

The geology of northwestern Argentina is characterized by Cordillera type orogeny caused by the accretion and collision of micro continents to the Gondwana continent at its southwestern periphery in the times of the upper Precambrian to the lower Paleozoic, and also by the easterly oceanic plate subduction from the upper Paleozoic to the present.

From Precambrian to Quaternary mineralization is closely related with geological development of the area. Above all, in the Ordovician system, there is high potentiality of existing SEDEX type lead and zinc deposits and volcanogenic massive sulfide deposits and in the Neogene system there is high potentiality of existing porphyry type copper and copper/gold deposits and epithermal gold deposits.

The El Aguilar deposit classified as SEDEX type lead and zinc deposits exists in the lower Ordovician Santa Victoria group which is passive margin deposits to the east of the north of the survey area. The La Colorada deposit classified as volcanogenic massive sulfide deposit occurred in the Ordovician magmatic arc to the west of the north of the survey area (Fig. I-4-3-1).

The porphyry type copper and copper/gold deposits and the epithermal gold and silver deposit are limited to the areas of four Neogene volcanic rock extending like an armed shape (volcanic rock zone) in a SE direction from the Chilean border, in the neighborhood of intrusive rocks between the zone, and on the zone extensions (Fig. I-4-3-2). The porphyry type copper and copper/gold deposits develop around Farallon Negro, which is one of the volcanic rock arm of relatively advanced erosion, in the neighborhood of Inca Viejo, which is on the periphery of intrusive rock area between the arms, and to the west of Tucuman, which is the volcanic rock zone extension. On the other hand, the alteration zones related to the epithermal gold and silver deposit tend to exist at a less eroded area, such as those near the Agua Caliente caldera.

Table I-4-2-1 Record of ground truth 2001

Date	October																									November									
Mineral showings	6	7	8	9	10	11	12	13	14	15	16	17	18	19	20	21	22	23	24	25	26	27	28	29	30	31	1	2	3	4	5	6	7		
Farallon Negro																																			
Agua Tapada																																			
Bajo de la Alumbra																																			
Bajo El Durazno																																			
Agua Rica																																			
Capillitas																																			
Capillitas NE																																			
Vaca Vizcana																																			
Laguna Blanca																																			
Laguna del Salitre																																			
Laguna Grande																																			
El Alisar																																			
Brealito																																			
El Acay																																			
Incachule																																			
Organullo																																			
Vicuña Muerta																																			
Inca Viejo																																			
Diablillos																																			
Condor Yacu																																			
Centenario																																			
Pancho Arias																																			
Mina El Aguilar																																			
Esperanza																																			
Río Grande																																			
Bélgica																																			
Pumahuasi																																			
Sol de Mayo																																			
La Ciénaga																																			
Santa Rosa																																			
La Geteada																																			
Pan de Azucar																																			
Tupiza																																			
La Purísima																																			
Rumicruz																																			
La Candelaria																																			
Rachalte																																			
La Colorada																																			
Limeca																																			
Tusca																																			
Coiruro																																			

Table I-4-2-2 Outline of survey results 2001

No.	Mineral occurrences surveyed	Zone No.	Element / Material	Type	Alteration extracted by ASTER image	Survey results	Project status	Activity status	Holding of mining right	Evaluation
1	La Gateada	Zone-01	Pb	Vein	-	A quartz vein with Cu-Pb-Zn was observed.	AP	ABD	-	×
2	La Bélgica	Zone-02	Pb-Zn	Vein	-	Some barite vein with Pb were observed.	AP	ABD	-	×
3	La Pumahuasi	Zone-02	Pb-Zn	Vein	-	Barite with Pb was observed in waste dumps.	AP	ABD	-	×
4	Sol de Mayo	Zone-02	Pb-Zn	Vein	-	Barite with Pb was observed in a stock pile.	AP	ABD	-	×
5	Santa Rosa	Zone-03	Barite	Vein	-	Barite with Pb was observed in a stock pile.	AP	ABD	-	×
6	La Ciénaga	Zone-05	Pb -Cu-Barite	Vein	-	Some barite vein with malachite was observed at the entrance of a gallery and Pb-Zn-Cu ore were found in a stock pile.	AP	ABD	-	×
7	Pan de Azucar	Zone-07	Pb-Ag-Zn -Sb	Vein	○		AP	ABD	-	
8	Tupiza	Zone-08	Pb-Ag-Zn-Cu	Vein	-		AP	ABD	-	×
9	Rachaité	Zone-09	Pb-Zn-Ag-Mn	Vein and Dissemination	○		BS	NOA	?	○
10	La Candelaria	Zone-15	Pb	Vein	×	Some small barite veins with Pb were observed.	AP	ABD	-	×
11	La Purísima - Rumicruz	Zone-11	Cu-Pb-Barite-Ni-Co-Zn-Ag-Au	Vein	×		AP	ABD	-	×
12	El Aguilar	Zone-15	Pb-Ag-Zn	SEDEX	×	Active mine of SEDEX	PR	ACT	Compania Minera Aguilar S. A	○
13	Rio Grande	Zone-15		SEDEX	×	Some massive pyrrhotite beds were found.	BS	HLD	Compania Minera Aguilar S. A	○
14	La Colorada	Zone-18	Cu-Pb-Zn-Fe	SEDEX or VMS	×	Thick massive sulphide ore with a high Fe-S content was found in the drill cores which were collected by a private	RD	ABD	-	○
15	Limeca	Zone-18			×	The existence of SEDEX horizon is reported.	BS	ABD		○
16	Tusca	Zone-22	Barite	Vein	○?	Barite veins have been mined out on the surface.	AP	ABD	-	×
17	Coiruro	Zone-24	Sb-Au	Vein	-	Old adits and pits are found on the steep slope.	AP	ABD	-	×
18	Incachule	Out of			○		RD	HLD?		○
19	Organullo	Zone-27	Cu-Pb-Bi / Cu-Au	Vein and Dissemination	○	In the Organullo north, drillings were carried out for porphyry Cu by a private company.	RD	HLD?		○
20	El Acay	Zone-27	Fe-Cu-Pb-Zn	Vein and Dissemination	-		BS	HLD?		○
21	Pancho Arias	Zone-28	Mo-Cu-Au	Dissemination and Porphyry	○	It has been drilled for porphyry Cu by a private company.	RD	HLD?		○
22	Centenario	Alteration	-	-	○		RD	HLD?		○
23	Vicuña Muerta	Zone-31	-	-	○	The topography shows an interesting circular	BS			×
24	Inca Viejo	Zone-31	Au-(Cu-Mo)	Dissemination and Vein	○	It has been drilled for porphyry Cu by a private company.	RD	HLD?		○
25	Diablillos	Zone-31	Au-Cu		○	It has been drilled for porphyry Cu by private companies	FS	HLD	Pacific Rim	○
26	Condor Yacu	Zone-31	Au-Cu		○	Explorations including drillings are being carried out by a private company	RD	HLD		○
27	Brealito	Zone-34	Cu		×		RD	?		×
28	Laguna Grande	Alteration	-	-	○		-	-		×
29	Laguna del Salitre	Zone-39	Pb-Zn	Vein and Stratabound	×		AP	-		×
30	Laguna Blanca	Alteration	-	-	○		-	-		×
31	Vaca Vizcana	Zone-42	Cu-Au	Porphyry Cu	-		AP	-		×
32	El Alisar	Zone-46	Cu-Au	Porphyry Cu	-	Porphyry Cu-Au hosted by the Ordovician Mala Mala granodiorite and the intruding Miocene andesitic rocks.	BS	HLD		○
33	El Pago	Zone-47	Cu-Au-Pb-Zn	Dissemination	○		BS	HLD		○
34	Alto de la Blenda (Laboreo, Nudo, Esperanza)	Zone-43	Au-Ag-Mn	Epithermal, low sulfidation	○		PR	ACT	YMAD	○
35	Agua Tapada	Zone-43	Au		○		RD?	HLD?		
36	Bajo de la Alumbreira	Zone-43	Cu-Au	Porphyry Cu-Au	○		PR	ACT	YMAD	○
37	Bajo El Durazo	Zone-43	Cu-Au	Porphyry Cu-Au	○		RD?	HLD?		
38	Agua Rica	Zone-43	Cu-Mo-Pb-Zn-Ag-Au	Porphyry Cu	○		FS	ACT	BHP	○
39	Capillitas	Zone-43	Cu-Au-Pb-Zn-Ag	Vein and Dissemination	○		AP	HLD		×
40	Capillitas NE Alteration	Alteration	-	-	○		-	-		×

(2) Potentiality of known mineral deposits and selection of promising areas

As described above, a new deposit is expected to be discovered for the SEDEX type lead/zinc deposit, a stratabound type deposit, in the Santa Victoria group extending from El Aguilar to Pumahuasi among all the Ordovician system, and for the volcanogenic massive sulfide deposit in the magmatic arc (Fig. I-4-3-1). For porphyry type copper and copper/gold deposits throughout this area, there is a possibility to find the deposits in the extension of the volcanic rock zones (Fig. I-4-3-2). While detailed surveys have already been carried out on the epithermal gold and silver deposit, detailed surveys are desired at the hydrothermally altered zones around the calderas of less eroded area, such as Garan, Agua Calenie, Coranzuli, etc. In particular, since the area around the Coranzuli caldera overlaps the tin zone, which continues from the Bolivian side, this area is expected simultaneously to carry polymetallic deposits.

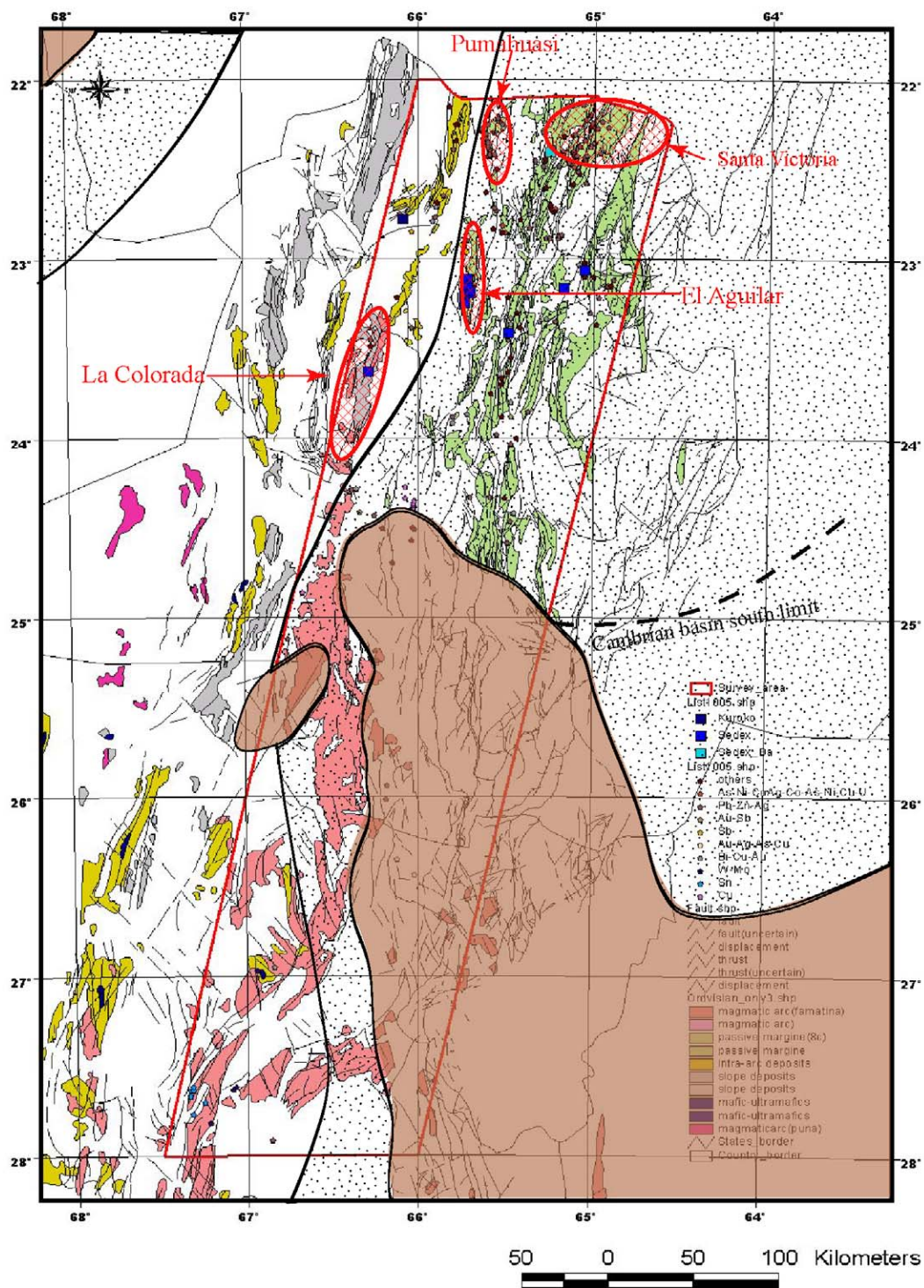


Fig.I-4-3-1 SEDEX type deposits and promising zone.

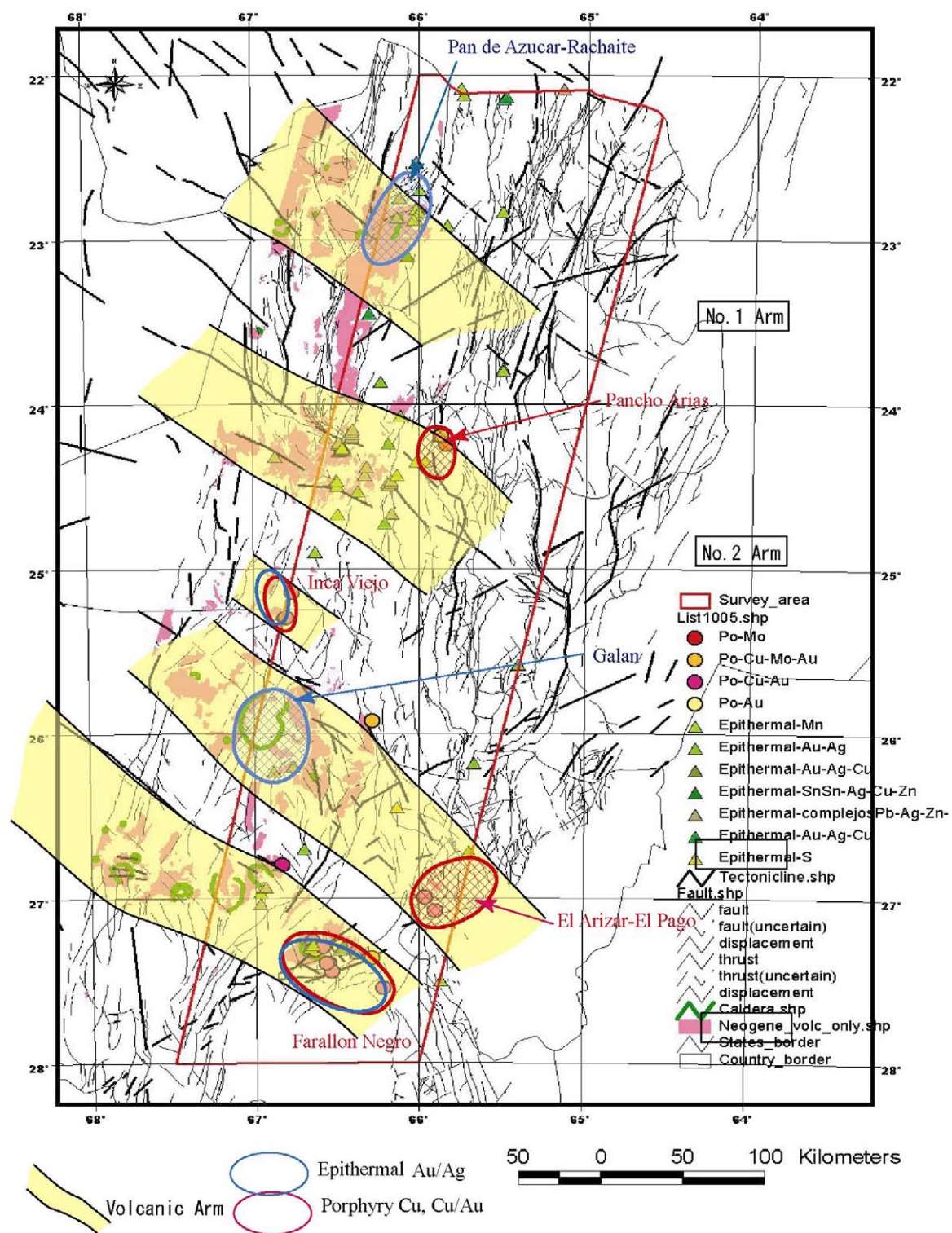


Fig.I-4-3-2 Porphyry copper type and epithermal type deposits and promising zone.

Chapter 5 Outline of survey results in Phase II

5-1 Analysis of the existing data

The database includes information about metal elements such as Au, Ag, Cu, Pb, Zn, rare metals and industrial material such as rare earth, perite, limestone, borax, phosphate minerals, salt, mica, Kaolinite, and rhodochrosite, topaz etc with geo-code. In order to help better and easy understanding the relation between geology and mineral distribution, the database information are added to GIS system for visualization, and finally mineral deposits and mineral showings were grouped as 44 mineral potential areas (Fig. I-5-1-1, Table I-5-1-1). Through the database compilation, the following results especially regarding to distribution of minerals were summarized.

-Potential area of porphyry copper and copper/gold deposits, epithermal gold deposits

The high possibility area having these type deposits overlap the area of Tertiary volcanic rocks such as Zone-07, Zone-09, Zone-24, Zone-26, Zone-27, Zone-28, Zone-39, Zone-42, Zone-43, Zone-46:

-Potential area of SEDEX lead/zinc deposits and volcanic massive sulfide

Known SEDEX type deposits are El Aguilar mine and Esperanza in Z-15, Aguilar range. The high possibility area having these type deposits such as Zone-15, Zone-01, Zone-02, Zone-08, Zone-10, Zone-11, Zone-12, Zone-15, Zone-17, Zone-22, Zone-03, Zone-05, Zone-18.

5-2 Stream sediments geochemistry

Using with stream sediment samples, which were stored in SEGEMAR, geochemical analysis of 48 elements was carried out. Threshold classification and principal component analysis were applied to 4,100 samples of Phase II and 5,123 samples of Phase I (total 9,491 samples) for geochemical analysis (Due to the lack of coordination data, 7,632 samples were used for principal component analysis). Results are shown as follows.

Significant gold anomaly is seen at the center of the survey area. El Acay and other several prospects are existed near to the anomaly. Anomalies are also seen around the Aguilar mine area. Silver anomaly is seen widely in the southern part of surveyed area and the distribution corresponds well to the distribution of Ordovician granites in Southern part of the area. In addition, anomalous values are seen at the central western part where porphyry copper-gold deposits, Diablillos deposit etc., are located. Copper anomaly corresponds to the distribution of known porphyry copper deposits, especially the high anomaly value is seen around Agua Rica mineral showings. Lead anomaly is mainly distributing over known SEDEX deposits, and partly seen around porphyry copper deposits. Zinc anomaly also distributes around the SEDEX deposits

Principal Component Analysis shows that the distribution of PC1 plot corresponds well

Table I-5-1-1 List of mineralized zones in the survey area

Zone No	Province	Element / Material	Type	Age of Host Rock	Location and Access	Topography and Vegetation	Geology	Mineralization	Geological structure	Aero-magnetic anomaly	Alteration extracted by ASTER image	Area (km ²)	Number of mineral occurrences	Mineral occurrence surveyed	Evaluation
Zone-01	JUJUY	Cu (Pb)	Vein	Ordovician	It covers Cordón de Escaya and a northern part of Sierra Cochinea and is located about 10km to the northern end of the zone from La Quiaca and about 20km to the southern end from Abra Pampa. Two Roads crossing the zone exist northern and central parts of the zone.	Mountains with altitudes of 3,500-4,500m and a few scattered shrubs.	Dacite porphyry, sandstone and shale of the Ordovician Cochinea-Escaya Complex	It includes three occurrences of Cu and one occurrence of Pb vein type mineralization hosted by the Cochinea-Escaya Complex.	N-S trending faults and volcanics distributions	A low magnetic anomalous area exists trending N-S with a weak to medium grade and is associated with a small magnetic semi-circular structure with 5km in a diameter to the west.	A small alteration zone with an area of 1km ² is extracted along the western fault in the north area.	400	5	La Gualada	
Zone-02	JUJUY	Pb-Zn (Ag-Cu)	Vein	Ordovician	It occupies a wide area including the Pumahuasi mining district to the south of La Quiaca.	Hilly regions with altitudes of 3,500-4,000m and a few vegetation.	Sandstone and shale of the Ordovician Acote Formation	It includes 19 occurrences composed mainly of Pb-Zn vein type mineralization hosted by the Acote Formation.	N-S trending faults and folding axes	A weak high magnetic anomalous area exists trending N-S.	-	340	24	La Bélgica La Pumahuasi Sol de Mayo	
Zone-03	SALTA	Barite-Pb (Cu-Zn)	Vein	Ordovician, Cambrian	It covers the main part of Sierra Santa Victoria located about 40km to the east of La Quiaca.	Mountains with altitudes of 4,000-5,000m and a few vegetation.	Cambrian Mesón Group and Ordovician Santa Rostia Formation	Ten in a total of 17 occurrences are barite and/or Pb vein type mineralizations, and the other 7 occurrences are Cu-associated vein type mineralizations. Most of the mineralizations are hosted by shale and sandstone of the Santa Rostia Formation. Only La Niquelina mineralization is unique. It contains Ni and hosted by the Upper Cambrian Chahualmayoc and the Santa Rostia formations.	-	-	-	1000	16	Santa Rosa	
Zone-04	SALTA	Au	Placer	Pleistocene - Holocene	It is located about 60km to the east of La Quiaca and covers the Santa Cruz river and its tributaries. The northern side of the zone is limited by the border of Bolivia.	Mountains with altitudes of 2,000-4,000m and woody vegetation.	-	Placer gold in the alluvial plain deposits	-	-	-	350	11		Out of the survey target
Zone-05	SALTA	Barite-Pb (Cu-Zn)	Vein	Precambrian, Ordovician, Silurian	It covers an eastern wide foot area of Sierra Santa Victoria. Santa Victoria town is located within the zone.	Mountains with altitudes of 3,500-4,500m and woody vegetation.	Precambrian Puncoviscana Formation, Cambrian Mesón Group and Ordovician Santa Rostia Formation	The 26 occurrences in a total of 30 occurrences are mainly of Pb-barite vein type mineralization hosted by shale and sandstone of the Ordovician Santa Rostia Formation. Nine in the 26 occurrences contain Cu, and Churquipampa, El Quinsallal and Río Blanco occurrences more contain U.	Faults and folding axes show NNW-SSE to NNE-SSW trends	-	-	1100	30	La Cienega	
Zone-06	SALTA	P ₂ O ₅	Stratiform	Ordovician, Silurian	It is located about 30km to the east of Santa Victoria town and covers a narrow area with a width of about 10km and a length of about 80km, trending NNE-SSW.	Mountains with altitudes of 1,000-2,000m and woody vegetation.	Ordovician Labrado and Centinela formations, and Silurian Lipetons Formation	Stratiform biocarbonate phosphates beds intercalated with quartzite, sandstone and shale of the Ordovician Labrado and Centinela formations, and stratiform oolitic iron beds in siltstone and greywacke of the overlying Silurian Lipetons Formation.	Approximate N-S trending structure (strike of bedding)	-	-	450	10		Out of the survey target
Zone-07	JUJUY	Pb-Ag-Zn (Sb)	Vein	Middle Miocene	It is an area including Pan de Azúcar mine located about 40km to Abra Pampa.	Hills with altitudes of 3,700-4,200m and a few vegetation.	Middle Miocene Laguna de Pozuelos Volcanic Complex	It includes occurrences of Pb-Ag-Zn (Sb) veins hosted by dacite and andesite of Middle Miocene Laguna de Pozuelos Volcanic Complex. A mineralized zone of Pan de Azúcar-Potosí-España has a reserve of 59,000t with 4.62%Pb, 6.58%Zn, 0.224g/tAg and 0.88%Sb.	NE-SW trending fault zone and NNW-SSE trending faults	A small area exists with a striped pattern of high and low magnetic anomalies.	The small alteration zone extracted by TM is observed as similar location and size in the southern part.	200	1	Pan de Azúcar	
Zone-08	JUJUY	Pb-Zn-Cu-Ag-Au-Sb)	Vein	Ordovician	It is located about 30km from Abra Pampa. Road condition is not good within the zone.	Mountains with altitudes of 3,500-4,500m and scattered shrubs.	Lutite and sandstone of the Ordovician Acote Formation, and sandstone, shale and rhyodacite porphyry of the Ordovician Cochinea-Escaya Complex	It includes two occurrences composed mainly Pb-Zn mineralization and some Sb and Au.	NE-SW and N-S trending faults and NE-SW trending volcanics distributions	The zone is located in a low magnetic anomalous area with a medium grade.	No alteration zone is extracted.	110	3	Topiza	
Zone-09	JUJUY	Sb-Au) / Pb-Zn-Ag	Vein and Dissemination	Neogene tertiary	It is an area to the south of Rachaita village located about 50km to the WSW of Abra Pampa.	Mountains with altitudes of 3,500-5,000m and a few vegetation.	Neogene Tertiary (Miocene)	It includes two occurrences of Sb-Au vein type mineralization in the eastern part and one occurrence of Pb-Zn-Ag stockwork and vein type mineralization in the western part. All of them are hosted by dacite, andesite and tuff of Neogene Tertiary.	A large fault trending E-W to NE-SW in the north and a semi-circular structure with about 15km of the major axis and about 5km of minor axis in the southwestern part of the zone.	An area with a striped pattern of intense high and low magnetic anomalies exists trending E-W, semi-circular structure in the southwestern part.	Some alteration zones with a total area of 3km ² are extracted in the semi-circular structure in the southwestern part.	150	4	Rachaita	
Zone-10	JUJUY	Barite-Pb (Cu)	Vein	Ordovician	It is located at southern part of the Sierra Cochinea and includes Cochinea village of about 20km from Abra Pampa.	Mountains with altitudes of 3,500-4,500m and scattered shrubs.	Ordovician Acote Formation and Cochinea-Escaya Complex	Four in a total of 5 occurrences are barite and/or Pb mineralization of vein type. Only Barcosonte occurrence is composed of Cu mineralization.	Faults, folding axes and distribution of volcanics, all trend approximately N-S.	A low magnetic anomalous area exists with a weak grade.	No alteration zone is extracted.	100	5		
Zone-11	JUJUY	Barite-Pb (Cu-Zn-Ag)	Vein and Dissemination	Ordovician	It is located about 15km from Abra Pampa. Road condition is not good within the zone.	Mountains with altitudes of 3,700-4,100m and scattered shrubs.	Ordovician Santa Victoria Group surrounded by post-Cretaceous formations	Five in a total of eight occurrences are mineralization mainly of Cu vein type, other two are Pb-barite vein type mineralization. Four occurrences in the Rumicruz district are characterized by Ni association.	Either faults or folding axes trend approximately N-S.	A set of high and low magnetic anomalies with a weak grade exists trending NE-SW in the southern half of the zone.	-	130	8	La Prieta - Rumicruz	

NOA, Argentine

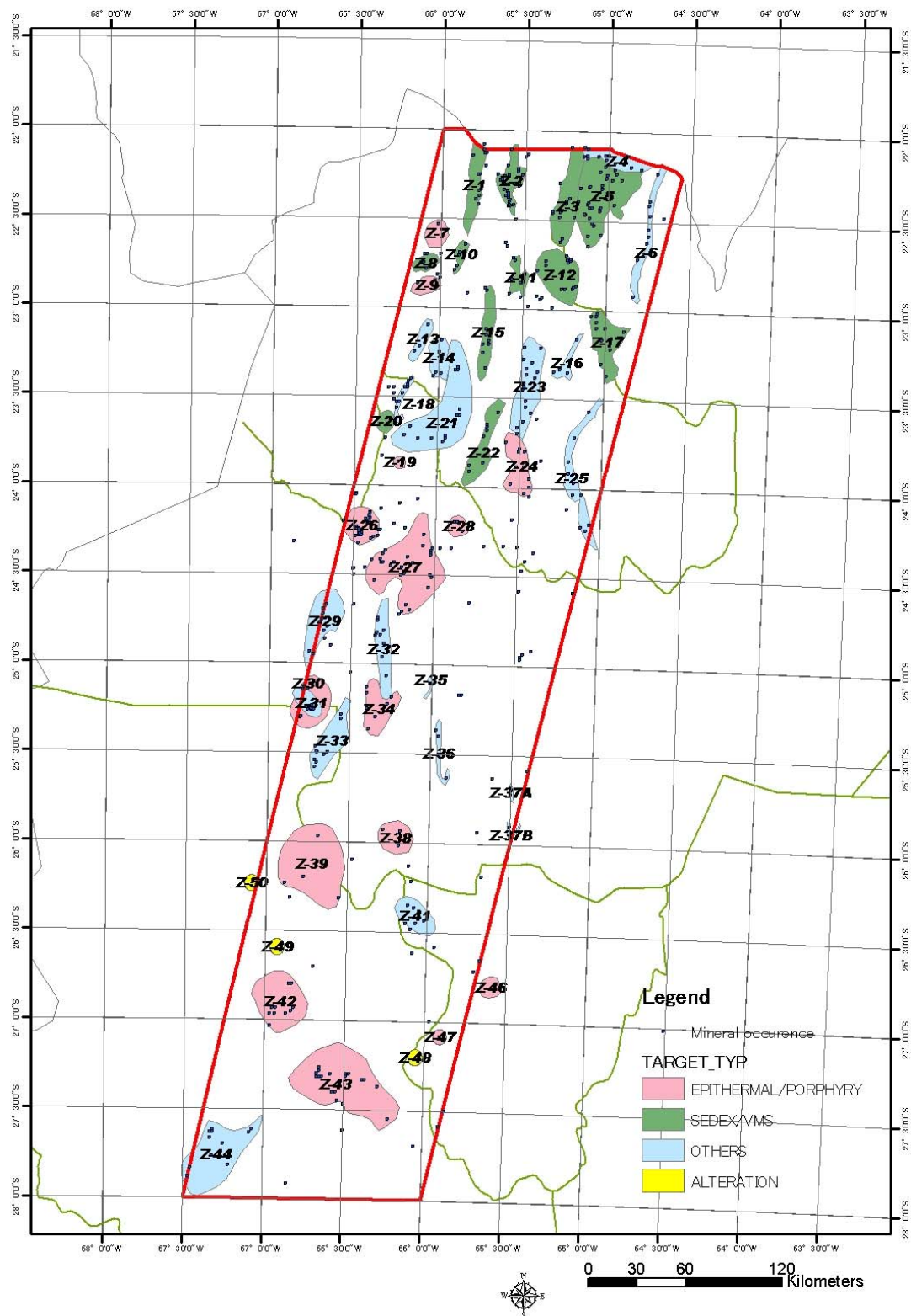


Fig. I-5-1-1 Location of mineral showings and deposits, and cluster of them listed on the Appendix.

to the distribution of Pre-Cambrian and Cambrian sedimentary and metamorphic rocks in southern part of the survey area. The distribution of PC2 is corresponds well to the distribution of Cretaceous sedimentary rocks in the central and northern part, and of Cambrian metamorphic rocks in the southern part. In spite of many of the elements related to mineralization have higher correlation to PC2, no significant relation have seen with known mineral occurrence. Lead and cadmium have higher correlation with PC7 and its distribution is corresponds to the distribution of sedimentary rocks in the northern part and of granites in the southern part. PC10 includes gold, mercury and indium as high correlation elements. The plot of PC10 tends to locate around known mineralization and also granites distribution.(Fig.II-2-5-6~9)

5-3 Satellite image analysis

This analysis was carried out to identify the altered minerals in the alteration zones that are accompanied by ore deposit by using actual ASTER data that is able to use satellite data effectively for the metal deposit survey. The target area is located in rock exposing area and the climate of this area is semi-arid. The following pre-processing was carried out before the analysis.

- Conversion to pseudo-reflectance by using pseudo-reflectance conversion coefficients (Ministry of Economy, Trade and Industry, 2002)

- Removal of reflection spectrum from vegetation by using PSVI (Pseudo Soil Adjust Vegetation Index)

The iso-grain Model that is considered the reflection and absorption among the particles of minerals were used in the identification of alteration minerals and the semi-quantitative analysis. In this analysis, using the iso-grain Model made the database of spectral reflectivity. Mixing of the selected 10 popular minerals made the Model. Then mineral identification on the surface and the semi-quantitative analysis were carried out to make the mineral mapping.

The atmospheric correction, and the separation of the temperature and emissivity of the data of thermal band that is one of the characteristics of ASTER. Then, the mapping of SiO₂ contents was carried out. The mapping was carried out by using the conversion equation that had been proposed in the data analysis of Earth Resources Satellite (Ministry of Economy, Trade and Industry, 2000).

541 alteration zones were extracted by using the visible and short wavelength of infrared Bands, and iso-grain model. Within the extracted zone, there are the places that have no relation to ore showing. Based on the analysis, the establishment of recognition method (or standard) of alteration zone with ore showing is the subject for the future. Based on the field verification, the areas that are desirable to make further prospecting from the result of satellite image analysis are as follows:

- ①The area where the alteration developed and acid altered minerals such as alunite and

kaolinite were sampled

: B11 – No.55, C11 – No.56

②The area where the alteration is weak, and chlorite was (ring-shaped) extracted

:C05 – C and 40 (Fig.II-3-3-1)

5-4 Ground truth

For the selection of survey zones in Phase I, among 44 zones those are dense with mineral deposits as shown in Table I-5-1-1, the 20 zones that had little relationship with porphyry copper or copper/gold deposits, epithermal gold deposits, polymetallic vein deposits or SEDEX lead/zinc deposits, all of which had been selected as the targets for the reasons mentioned above, were excluded from the survey. From the remaining 24 zones, 21 zones, or a total of 36 places (of mineral showings), were selected as zones to be covered by the field survey of Phase I.

In Phase II, the 8 areas (SEDEX/VMS; El Aguilar area, Pumahuasi, Santa Victoria area, La Colorada area. Porphyry copper and epithermal type deposits; Pancho Arias area, El Pago area, Rachaite area, Galan area) were selected. Because these area are thought to have high potential for the existence of deposits but have been surveyed insufficiently, and future survey are expected to lead to the discovery of new deposits, among potential zones extracted in the evaluation of Phase I (Fig. I-5-4-1, Table I-5-4-1, Table I-5-4-2).

5-5 Summary

In the second year (Phase II), prior to the field survey, an analysis of the existing (revising mineral showing data base), satellite image analysis using 22 scene of ASTER (alteration minerals identification and detailed topographical map making, etc.), and data analysis of stream sediment samples have been carried out.

A field survey was conducted of the following eight zones in total: they are four zones (Aguilar mine, Pumahuasi, Santa Victoria ranges, and La Colorada) for the exploration of the SEDEX/VMS deposits, and four zones for the exploration of porphyry copper and the epithermal deposits (Pancho Arias, Rachaite, Cerro Galan, El Pago).

In the four areas for exploration of SEDEX/VMS deposits, field survey and sample collections were made for conducting various laboratory tests for fossil identification and chemical analysis. To clear the petrological, paleontologic, geochemical features of the ore horizon of SEDEX/VMS deposits and their hanging/foot walls and to discover similar horizon to the already-known SEDEX deposit horizon.

The principal components were analyzed by using the analytical data of the 197 pieces of samples in total collected from the ground surface rock in the four zones. In the Aguilar mine area and La Colorada area, in addition, a discriminant analysis and principal component analysis were

Table I-5-4-1 Record of ground truth 2002

Date	October															November																																	
	16	17	18	19	20	21	22	23	24	25	26	27	28	29	30	31	1	2	3	4	5	6	7	8	9	10	11	12	13	14	15	16	17	18	19	20	21	22	23	24	25	26	27	28	29	30			
Mineral showings																																																	
Pancho Arias																																																	
Mina El Aguilar																																																	
Punahuasi																																																	
Santa Victoria																																																	
Rachaita																																																	
La Colorada/Limeca																																																	
Cerro Galan																																																	
El Pago																																																	

Table I-5-4-2 Outline of survey results 2002

No.	Mineral occurrences surveyed	Zone No.	Element / Material	Type	Alteration extracted by ASTER image	Survey results	Project status	Activity status	Holding of mining right	Evaluation
1	Pancho Arias	Zone-28	Mo-Cu-Au	Dissemination and Porphyry	○	It has been drilled for porphyry Cu by a private company.	RD	HLD	Lapacha Minera SRL, Minera Argentina Gold SA	○
2	Mina El Aguilar	Zone-15	Pb-Ag-Zn	SEDEX	○	Active mine of SEDEX	PR	ACT	Compania Minera Aguilar S. A	○
3	Pumahuasi	Zone-02	Pb-Zn	Vein	○	Barite with Pb was observed in waste dumps.	AP	ABD	-	-
4	Santa Victoria	Zone-03/05	Pb-Zn	SEDEX	○	Barite with Pb was observed in a stock pile.	AP	NOA	-	-
5	Rachaita	Zone-09	Pb-Zn-Ag-Mn	Vein and Dissemination	○		BS	HLD	Opawica Min. Ar. SA RTZ Min. Exp. Ltd etc.	○
6	La Colorada/Limeca	Zone-18	Cu-Pb-Zn-Fe	SEDEX or VMS	○	Thick massive sulphide ore with a high Fe-S content was found in the drill cores which were collected by a private company.	RD	ABD	-	○
7	Cerro Galan	Zone-39	Pb-Ag-Zn-Sb	Vein	○		AP	HLD	Catamarca provincial govt	-
8	El Pago	Zone-47	-	-	○		AP	HLD?	Private?	○

NOA, Argentina

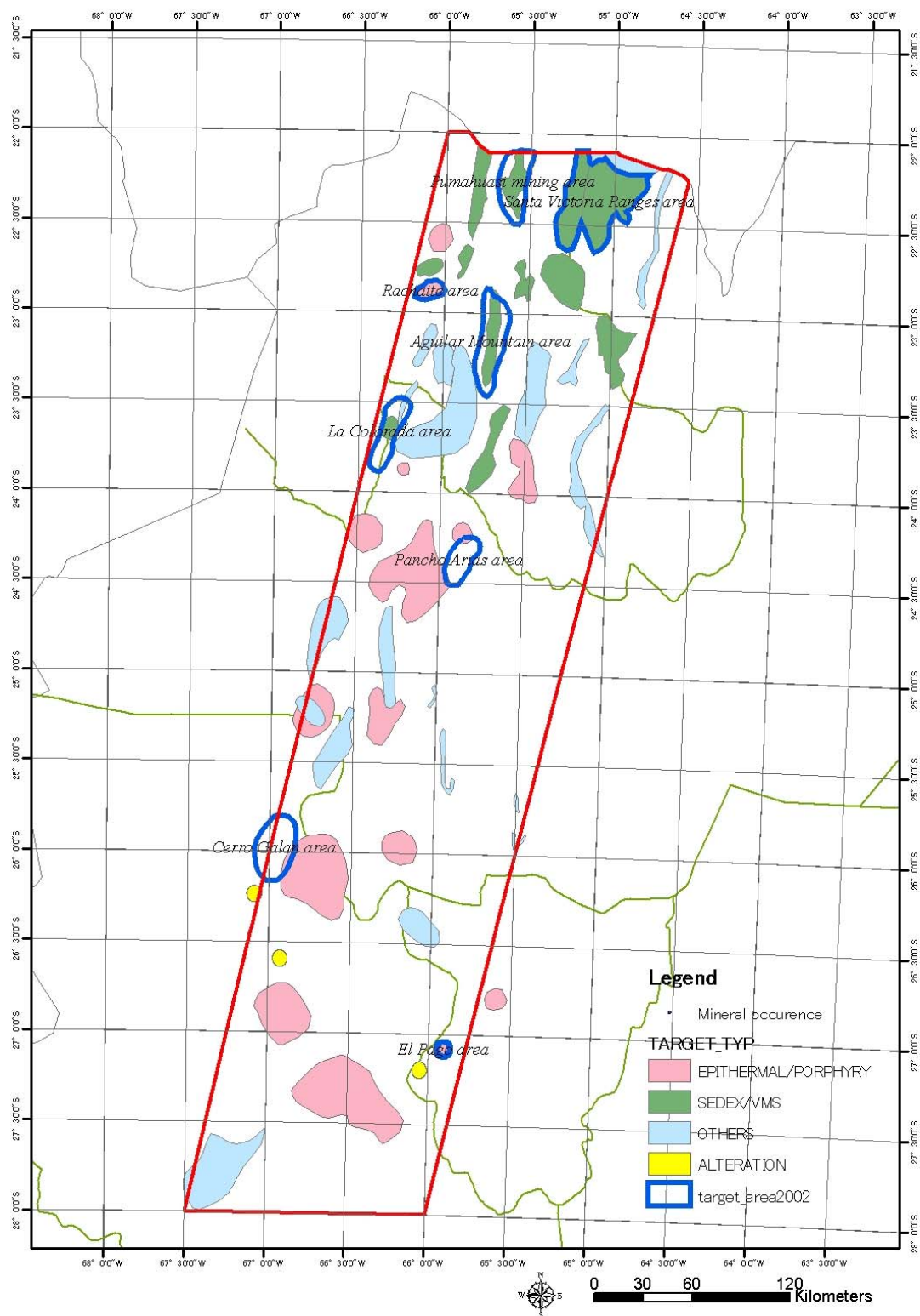


Fig.I-5-4-1 Area of ground truth survey, year 2002.

carried out by using the analytical data of the drilling cores from the Esperanza ore bodies as SEDEX type deposit and La Colorada ore bodies assumed to be VMS type, respectively.

As results, it was clarified that geochemical feature can identified the SEDEX and VMS ore horizon with using geochemical method such as principal component analysis, and the possibility of tracing similar horizon of SEDEX/VMS deposits is increased. Based on these results, the detailed study of sedimentary basin related to ore genesis from the regional scale of view, will be made progress if geochemical feature is identified for all lower Ordovician sediments area. It will be very important base for SEDEX/VMS exploration, which has no enough effective exploration standard.

In the four areas for exploration of porphyry copper and the epithermal type deposits, field survey and sample collections were made for conducting various laboratory tests in order to clear alteration mineral distribution (alteration zone mapping) and geochemical features.

As a results, this survey cleared that there is no enough economical mineralization for advanced stage development so far for these four zones. However the survey also found that El Pago has typical porphyry copper type mineralization and alteration zone, and there is cluster of similar type alteration zone with NNE-SSW in direction from El Pago area to extending to Agua Rica, Filo Colorado which are very important mineral showing porphyry copper type in NOA. El Pago and the cluster of alterations will be important candidate for future exploration depending on its condition. Meanwhile, other three area (Pancho Arias, Rachaite, Cerro Galan) also have large scale of alteration zone which are considered to be very shallow part of epithermal system, therefore this survey do not deny possibility to have high potential zone in deeper level from the surface.

PART II: DETAILED DISCUSSIONS

PART II: DETAILED DISCUSSIONS

Chapter 1 Existing data analysis

1-1 Collecting existing data

In order to concentrate on mineral potential area, information about geology, explorations, concessions etc., were collected and summarized from publications of organizations related to Government of the Argentine Republic and state governments, such as the Bureau of Geology and Mineral Resources (SEGEMAR), academy publications and internal materials of mining companies.

1-2 Database

A new database of mineral deposit and mineral showings (total 512 point, Appendix CD-ROM) was created in this analysis from compiling existing database of SSM, SEGEMAR y IGRM, (1999), database of Zappettini, (1999, CD-ROM) and geological maps published in Argentine (1:250,000) etc., with cooperation of SEGEMAR experts.

1-3 Distribution of known mineral deposits and mineral showings

The database includes information about metal elements such as Au, Ag, Cu, Pb, Zn, rare metals and industrial material such as rare earth, perite, limestone, borax, phosphate minerals, salt, mica, Kaolinite, and rhodochrosite, topaz etc with geo-code. In order to help better and easy understanding the relation between geology and mineral distribution, the database information are added to GIS system for visualization, and finally mineral deposits and mineral showings were grouped as 44 mineral potential area (Fig.I-5-1-1, Table I-5-1-1).

1-4 Compilation and analysis of existing data

Through the database compilation, the following results especially regarding to distribution of minerals were summarized.

-Potential area of known porphyry copper deposit

Zone-43: Miocene porphyry copper and gold deposit in Andalgala, Catamarca states (Bajo de la Alumbreira, Agua Rica etc.)

-Potential area of porphyry copper and copper/gold deposits, epithermal gold deposits

The high possibility area having these type deposits overlap the area of Tertiary volcanic rocks such as Zone-07, Zone-09, Zone-24, Zone-26, Zone-27, Zone-28, Zone-39, Zone-42, Zone-43, Zone-46: Tertiary volcanic area in north side of survey area.

-Potential area of SEDEX lead/zinc deposits and volcanic massive sulfide

Known SEDEX type deposits are El Aguilar mine and Esperanza in Z-15, Aguilar range. The high possibility area having these type deposits such as Zone-15: SEDEXtype (El Aguilar, Esperanza), Zone-01, Zone-02, Zone-08, Zone-10, Zone-11, Zone-12, Zone-15, Zone-17, Zone-22, Zone-03, Zone-05, Zone-18.

In Phase II, 8 area as promising area was selected based on the results of Phase I. Table II-1-1-4-1 shows the outline of 8 area.

Table II-1-1-4-1 Detailed survey plan for 2002

Target Deposits	Objectives	Survey Area	Location & Access	Aaccommodation	Outline of the Survey 2001	References	Survey Methods 2002	Days for Field Survey
SEDEX-type Pb-Zn deposit	To clarify the petrographical, paleontological and geochemical characteristics of mineralized horizon, the hangingwall and footwall, and the Padrioc-Lampazar Formation. To trace the mineralized horizon and the Padrioc-Lampazar Formation and extract the promising area with the SEDEX-type mineralization from Zone-15, 3 and 5.	Zone-15 Aguilar Mountain area	El Aguilar mine is located approximately 60 km south of Abra Pampa town and accessed by driving 1.5 hours from the town.	Abra Pampa and Aguilar	Reconnaissance surveys were carried out in the open pit of El Aguilar mine, Esperanza mine and Rio Grande prospect and geochemical study was done using core samples from the exploration holes around the Esperanza mine.	No.34, No.35, No.53	Detailed observation and sampling will be done on the mineralization outcrops such as El Aguilar, Oriental, Pirta, Esperanza and Rio Grande, in order to clarify the petrographical, paleontological and geochemical characteristics of mineralized horizon, the hangingwall and footwall.	1 day
							Detailed observation and sampling will be carried out on the outcrops of the Padrioc-Lampazar Formation in the lower part of the Santa Victoria Group, in order to find a zone with similar characteristics to the SEDEX mineralized horizon.	2 days
							Observation of the ASTER images will be carried out, in order to clarify the characteristics of the Padrioc and Lampazar formations accompanying with mineralized horizon and to trace the horizon.	
		Zone-2 Pumahuasi Mining area	Pumahuasi mine abandoned is located about 16 km south of La Quiaca town and accessed by driving about 30 minutes from the town.	La Quiaca	Reconnaissance surveys were carried out in the abandoned mines of La Belgica, Pumahuasi and Sol de Mayo.	No.14, No.35, No.36, No.45, No.57	There is few possibility of the SEDEX horizon crop out because the area is covered by the Acoite Formation, the upper part of the Santa Victoria Group, according to the known informations. A few samples will be collected for only reference.	1 day
		Zone-3 & 5 Santa Victoria Ranges area	It takes one hour by car from La Quiaca to Agua Chilca, a colony at the western foot of the Santa Victoria Range, through the Provincial Route 5, an un-paved road along Casti valley and the Provincial Route 69.	La Quiaca	Reconnaissance survey were carried out in the abandoned mines Santa Rosa and La Cienaga.	No.35	Geological observation and sampling will be carried out on the outcrops of the Santa Rosita Formation, that is, the lower part of the Santa Victoria Group, along the Provincial Route 5 - 7 and Route 69.	3 days
VMS-type Cu-Pb-Zn deposit	To clarify the petrographical, paleontological, mineralogical and geochemical characteristics of mineralized horizon in La Colorada deposit, the hangingwall and footwall. To extract the promising area with the VMS-type mineralization such as La Colorada deposit from the Zone-18.	Zone-18 La Colorada area	La Colorada mine abandoned is located approximately 65 km north of San Antonio de los Cobres and it takes 1.5 hours by car from the town.	San Antonio de los Cobres	Reconnaissance survey was carried out in La Colorada abandoned mine and laboratory tests were done for some of the drill core samples stored in Salta.		Detailed observation and sampling will be done for the drill core stored in Salta, in order to clarify the petrographical, paleontological and geochemical characteristics of the massive sulphide ore horizon, the hangingwall and footwall in La Colorada mine.	2 days
						No.35, No.63	Geological observation and sampling will be carried out on the outcrops along some cross sections of the mineralized zones in La Colorada mine.	1 day
		Zone-18 La Colorada area (Limeca)	Limeca prospect is located about 5 km southeast of La Colorada.	San Antonio de los Cobres	Reconnaissance survey was carried out around the Limeca, but mineral showings are not found yet.	No.62	Geological observation and sampling will be carried out on the outcrops along the valleys in the prospect area shown by Mendez y Mendez (2001) and the SEDEX-type mineralization shown by them must be found out.	1 day
								1 day
Porphyry Copper-Gold	①Investigate the geology, geologic structure and mineralization, and evaluate the potential of porphyry copper-gold deposit in the NW Argentina. ②Define the promising area. ③Recommend for the further exploration program.	Pancho Arias	Cordinates: (24°16' S, 65°51' W). Approx. 3,500 m above sea level. It is located 75 km NW of Salta. Jurisdictionally belongs to Departamento de Rosario de Lerma, Provincia de Salta. Access: From Salta via Route 51 (to San Antonio de los Cobres), turn at Puerta Tastil into a river truck along Rio Rosario, then go up to north for 35 km until the prospect (4WD car is necessary).	Campo Quijano	[Outline]Part of the Pancho Arias mineral showings was surveyed. Hydrothermal alteration zone was defined mainly in Miocene decite porphyry (1,300 m×800 m). The alteration was concentrically zoned, potassic core, intermediate phyllic-argillic, and outer propylitic alteration. Sulfide mineralization mainly comprizing pyrite-chalcopyrite-molybdenite occurs in these alteration zones. Drilling was carried out in 1970's (10 holes totalling 1,716 m). A Canadian exploration company surveyed in the prospect recently (1990's) [Samples collected] 12 [Comments] This is a typical porphyry-type deposit accompanying the primary copper-molybdenum sulfides. Detailed survey is recommended in the second phase.	•Direccion General de Fabricaciones Militares, 1975, Informe Final — Area de Reserva No. 14 – Viscacheral (Provincia de Salta, Dept. Rosario de Lerma): 72p. •Americas Mining News July 9, 1997: www2.cdn-news.com/newsnet/1998/12/30/1230029n.htm •Aranlee Resources web-site:www.infomine.com/press_releases/arb •Sureda, R. J., 2002, Metalogenia Andina subvolcanica neo'gena: Novedades de la exploracio' n minera auri' fera en sistemas porfi' ricos y depo'sitos epithermales del NOA: Argentina Mining 2002, August 28th – 30th, 2002, Mendoza.	(1) Geological survey (mainly on alteration and mineralization) and rock-chip geochemical sampling at the known mineral showings in the Pancho Arias prospect. (2) Study of DGMF's drill cores stored in the Secretary of Mining, Salta. (3) Also field survey at some potential alteration/mineralization zones in the surrounding area which are extracted by the ASTER image analysis. (Many significant alteration zones were delineated in and around the Panch Arias prospect by the ASTER image analysis. The biggest one, which is correlated to the Pancho Arias mineral showings, exhibits a concentric alteration mineral zoning. It is approx. 2 km in diameter. Two other smaller alteration zones occur to the NW of the biggest one. The occurrence of several other alteration zones were recognized 10 to 20 km south of Pancho Arias prospect. Some of them may correspond to the prospects of Mansfield Minerals explored in 1997 – 1999 (Incahuasi and Las Burras).	4 days
		El Pago	Cordinates: (27°06' S, 65°55' W). Altitude: 3,000 – 4,300 m. Jurisdictionally belongs to Departamento de Monteros, Provincia de Tucuma'n. It is situated in the mountain area of Sierra del Aconquija, at upstream of Rio de la Horqueta. There is no access road to the prospect. Only horse truck is available from Tafi del Valle (probably takes 2 days by horse each way).	Camp	[Outline]No field survey in the 1st phase. Only laboratory study on some rock samples provided by SEGEMAR (10 X-ray diffraction analyses). Several preliminary geochemical samplings were made since 1970's, and some anomalies of Au, Cu, Mo were found in the prospect. Two old workings for prospecting auriferous quartz veins exist, and Au assays up to 12.6 g/t were obtained (Mina Rica). [Comments]It is difficult to evaluate the prospt by only some laboratory works. It is recommended to make field survey in the next phase even under the difficulty for the accessibility.	•Sureda, R. J., 2002, Metalogenia Andina subvolcanica neo'gena: Novedades de la exploracio' n minera auri' fera en sistemas porfi' ricos y depo'sitos epithermales del NOA: Argentina Mining 2002, August 28th – 30th, 2002, Mendoza. •Morello, C. H., 2001, Mina Rica – Prospecto porfidico de cobre y oro, Departamento Monteros, Provincia de Tucuma'n (personal memo).	(1) Detailed study on the existing geological data (A significant silicified-argillaceous alteration zone of 3.5 km by 1.5 km was delineated by the past geological & geochemical works). (2) Field survey consisting of geology, mineralization/alteration, and rock-geochemistry on the alteration zone (approx. 2 km in diameter) obtained by the ASTER image analysis. (According to the ASTER analysis, the alteration zone occurs in a "Bajo" structure of 2 km by 3 km probably produced by weathering and erosion on the hydrothermally altered ground.)	3 days
Epithermal Gold-Silver	①Investigate the geology, geologic structure and mineralization, and evaluate the potential of epithermal gold-silver deposit in the NW Argentina. ②Define the promising area. ③Recommend for the further exploration program.	Rachaite	Cordinates: (22° 52' S, 66° 08' W). Altitude: 3,600 – 4,000 m. It is located approx. 60 km west of Abra Pampa, and 45 km south of Rinconada. Jurisdictionally belongs to Departamento de Rinconada, Provincia de Jujuy. Access: From Abra Pampa via Route 74 to the east of Rachaite village, then turn down to south along Quebrada Liviara for 4 km until the prospect (total 58 km and about 1 hour and 30 minutes by 4WD vehicle).	Abra Pampa	[Outline]Part of the Rachaite prospect was surveyed. Several old workings (1950's) exist. Quartz veins/veinlets containing Ag, Pb, Zn minerals, and hydrothermal alteration zones (sericite-montmorillonite, 3km×0.7km) were observed. [Samples collected] 25. [Comments] The alteration zones are neutral ones formed by the volcanic hydrothermal system of Coranzuri composite caldera. They are located on the wall of the caldera structure, and it is assumed that hydrothermal activities occurred along the caldera wall. In the alteration zone on the west side, kaolin minerals are observed characteristically and are considered to be those overprinted on neutral alteration. As opaline quartz is observed, it is assumed that this zone represents the shallow part of the hydrothermal system. As silica sinter has been confirmed, although it was not confirmed in this survey, we may see the ground surface part of hydrothermal activities. Regarding the degree of alteration, neutral altered minerals are smectite, smectite and sericite mixed-layer minerals, and acid mineral is kaolin. Considering together with this, it is assumed that the shallow part of a low-sulfide hydrothermal system is presented. With gold deposits as a target, it is presumed that the level of precipitation of gold is somewhat deep. It is desired to assume places where gold precipitates by grasping the hydrothermal system from the detailed characteristics of alteration zones.	•Coira, B. L., 1999, Potencialidad minera de sistemas megacaldericos Miocenos en Puna Norte: In Zappettini, E. O. (ed.) Recursos Minerales de la Republica Argetina, SEGEMAR, No. 35, 1557-1567. •Coira, B., Chayle, W., Barber, E., Solis, N., Brodtkorb, M., Camacho, M. y Daiz, A., 1990, Paleosistema geothermal del Terciario Superior y su mineralizacion de metales basicos (Pb, Zn, Ag), Rachaite, Jujuy, Argentina: Decimo Primer Congreso Geologico Argentino, San Juan, 1990, Actas I, 303-306. •Loma Sur S. A., 19** : (Internal Exploration Report of the Rachaite Prospect) . •Informe Preliminar, 19**: Area Minerazada de Rachaite, Mina Chocaya. •SEGEMAR, 2000: Carta Geologica de la Republica Argentina, Escala 1:250,000, Mina Pirquitas.	(1) Check the possibility of epithermal gold mineralization by the ASTER image analysis combined with the existing geologic data. (2) Geochemical data analysis. (3) Field survey in and around the known mineral showings.	1 day
		Cerro Gala'n	Cordinates: (26° 52' S, 67° 02' W). Approx. 5,000 m above sea level. 40 km NE of Antofagasta de la Sierra, and 18 km north of Laguna Diamante. Jurisdictionally belongs to Departamento de San Carlos, Provincia de Salta. Access: Approx. 80 km from El Peñon. Camping is required depending on the conditions.	Camp/El Peñon	[Outline] The Laguna del Salitre mineral showings located to the south of Co. Gala'n was surveyed in the 1st phase. [Samples collected] One sample in Laguna del Salitre. [Comments] The Laguna del Salitre mineral showings seem to be not significant due to the weak alteration which was associated with the Tertiary volcanic activity. In the vicinity of Co. Gala'n volcano, epithermal mineralization is expected to be accompanied by the volcanic activity. Among the aleration zones delineiated by the ASTER image analysis, some zones which occur near the caldera wall must be surveyed because they have a possibility of epithermal mineralization. (In addition to Laguna del Salitre, two other alteration zones which were extracted by the image analysis (Laguna Grande and Laguna Blanca) were surveyed in the 1st phase. Both zones were identified to be weathered granitic ground. The ASTER image analysis covered only the western half of the whole Co. Gala'n area in the 1st phase.)	•Gonzalez, O., 1981, Estudio geologico economico area de investigacion geologico minera No. 34 "Laguna del Salitre", Departamento Belen, Provincia Catamarca: Servicio Minero Nacional, Exploracion Minera de la Region Noreste, Noa Geologico Minero, 43p. •Garcia, L. N. F., 19** , Area de reserva "Laguna del Salitre": Mosaicos 19-A1-B1. Ministerio de Industria y Minera, Subsecretaria de Minera, NOA 1. •Ministerio de Industria y Minera, 19** , Area de reserva No. 34 "Laguna del Salitre" 2p. •Sparks, R. S. J., Francis, P. W., Pankhurst, R. D. Gallagher, Thorpe, R. S. and Page, R., 1985, Ignimbrite of the Cero Gala'n Caldera, NW Argentina: Jour. Volcanol. Geotherm. Res., 24, 295-248.	(1) Definition of target deposit type (Study of the possibility of epithermal Au-Ag mineralization in this are by means of the ASTER image analysis combined with the existing geological data). (2) Geochemical data analysis. (3) Field survey (on alteration and rock-geochemistry) in the alteration zones extracted by the ASTER image analysis. (The following results are obtained through the ASTER image analysis: The most significant alteration zone which has a dimension of 4 km in diameter occurs just inside the caldera wall. The geology is mainly composed of Pliocene dacite lava dome. A set of lineaments of WNW-ESE and ENE-WSW systems crosscut the center of the alteration zone. All these evidences indicate that the alteration was controlled by the caldron subsidence. Several smaller alteration zones occur 500 m south of this zone arranging along the caldera wall.)	4 days

Chapter 2 Stream sediments geochemistry

2-1 Circumstances

The regional survey of the mineral resources had carried out in the area along the Andes, in the project of Plan Cordillerano in 1960's. In the survey, stream sediment samples were collected at that time and were analyzed about major elements such as copper/lead/zinc. However, the elements as mineralization indicator such as arsenic/antimony mercury and gold/silver/molybdenum etc were not yet analyzed. Since the detection level of geochemical analysis in that time is not sufficient, SEGEMAR stored the remainder specimen for future detailed analysis.

2-2 Samples

Stream sediment samples were collected from the northwestern part of Argentina. Removing those that could not analyzed due to insufficient quantity and those that lacked coordinate information, 4,100 samples were analyzed this year. Additional 5,123 samples for which analyzed last year and 268 samples for which SEGEMAR had been published were added to these. Finally analysis was carried out for 9,491 samples in total. Location of samples are shown in Fig.II-2-2-1.

2-3 Method, elements and detection limit for geochemical analysis

Geochemical analysis method of the package of INAA law and ICP-AES was adopted by the request of Argentina side, since the methods can applied even for small volume of sample, and has quick and low cost advantage for the analysis of the base metal, precious metals, rare earth metals. The analysis company are the XRAL Laboratories, A Division of SGS Canada Inc. which analyzed the samples of previous regional survey studies, eastern and southern area of Andes, Argentine. Analyzed elements and their detection limits are shown in Table II-2-3-1.

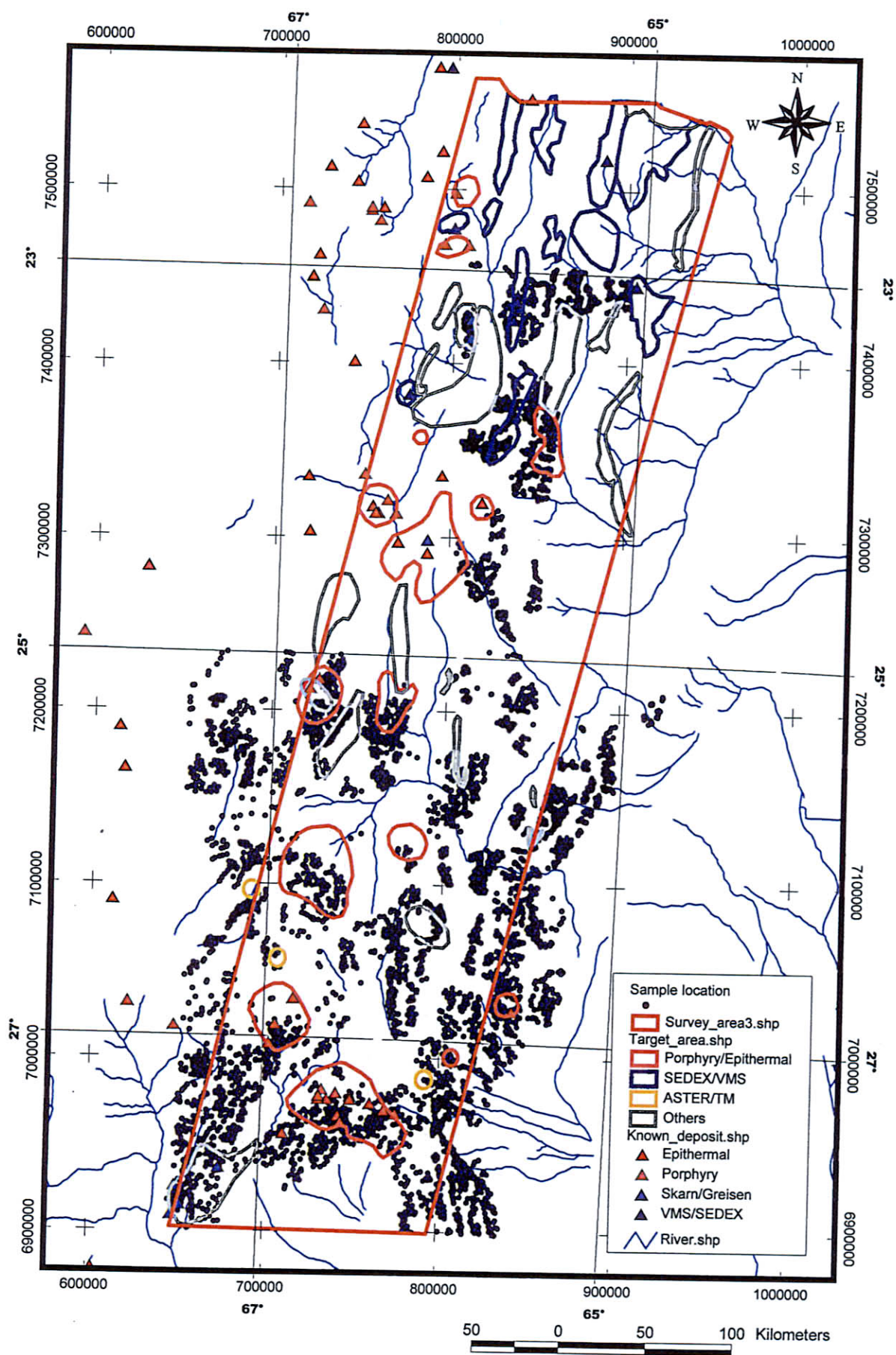


Fig.II-2-2-1 Location of samples for stream sediment geochemistry

Table II-2-3-1 List of elements and detection limits

(upper:INAA Metod, lower:ICP-AES Method)

Element	D.L.	Element	D.L.	Element	D.L.
As	0.5ppm	Au	2ppb	Br	0.5ppm
Ce	3ppm	Cr	5ppm	Cs	1ppm
Eu	0.2ppm	Hf	1ppm	Hg	1ppm
Ir	5ppb	Lu	0.05ppm	Nd	5ppm
Rb	5ppm	Sb	0.1ppm	Se	3ppm
Sm	0.1ppm	Ta	0.5ppm	Tb	0.5ppm
Th	0.2ppm	U	0.5ppm	W	1ppm
Yb	0.2ppm				
Ag	0.2ppm	Al	0.01%	Ba	1ppm
Be	1ppm	Bi	5ppm	Ca	0.01%
Cd	0.5ppm	Co	2ppm	Cu	0.5ppm
Fe	0.02%	K	0.01%	La	2ppm
Mg	0.01%	Mn	1ppm	Mo	1ppm
Na	0.005%	Ni	1ppm	P	0.001%
Pb	2ppm	Sc	2ppm	Sn	10ppm
Sr	0.5ppm	Ti	0.01%	V	2ppm
Y	0.5ppm	Zn	0.5ppm		

2-4 Analysis

Threshold classification and principal component analysis has done with using the results of the geochemical analysis in this year. For thresholds classification, standard deviation classification was applied with the Arc View. For principal component analysis, 7,632 samples of which all of the elements (48) have analyzed were selected. Since values except for Al, K, Mg, Na, Ti, V showed logarithmic distribution, those values were converted into log form prior to calculation.

Analysis result that was below a minimum detection limit adopted the half of the detection limit value and the result that was over a highest detection limit adopted the twice of the maximum detection limit value. When two or more minimum/maximum detection limits exist, worst (largest/smallest) value was used for adopting.

Since this data set is composed of several different data group and corrections on minimum/maximum detection limit have done on the point of calculation, it is required to be careful for interpreting the result. The analysis results are stored in CD-ROM of Appendix.

2-5 Evaluation

Fig.II-2-5-1~5 show the distributions of gold, silver, copper, lead and zinc anomaly in the northwestern area.

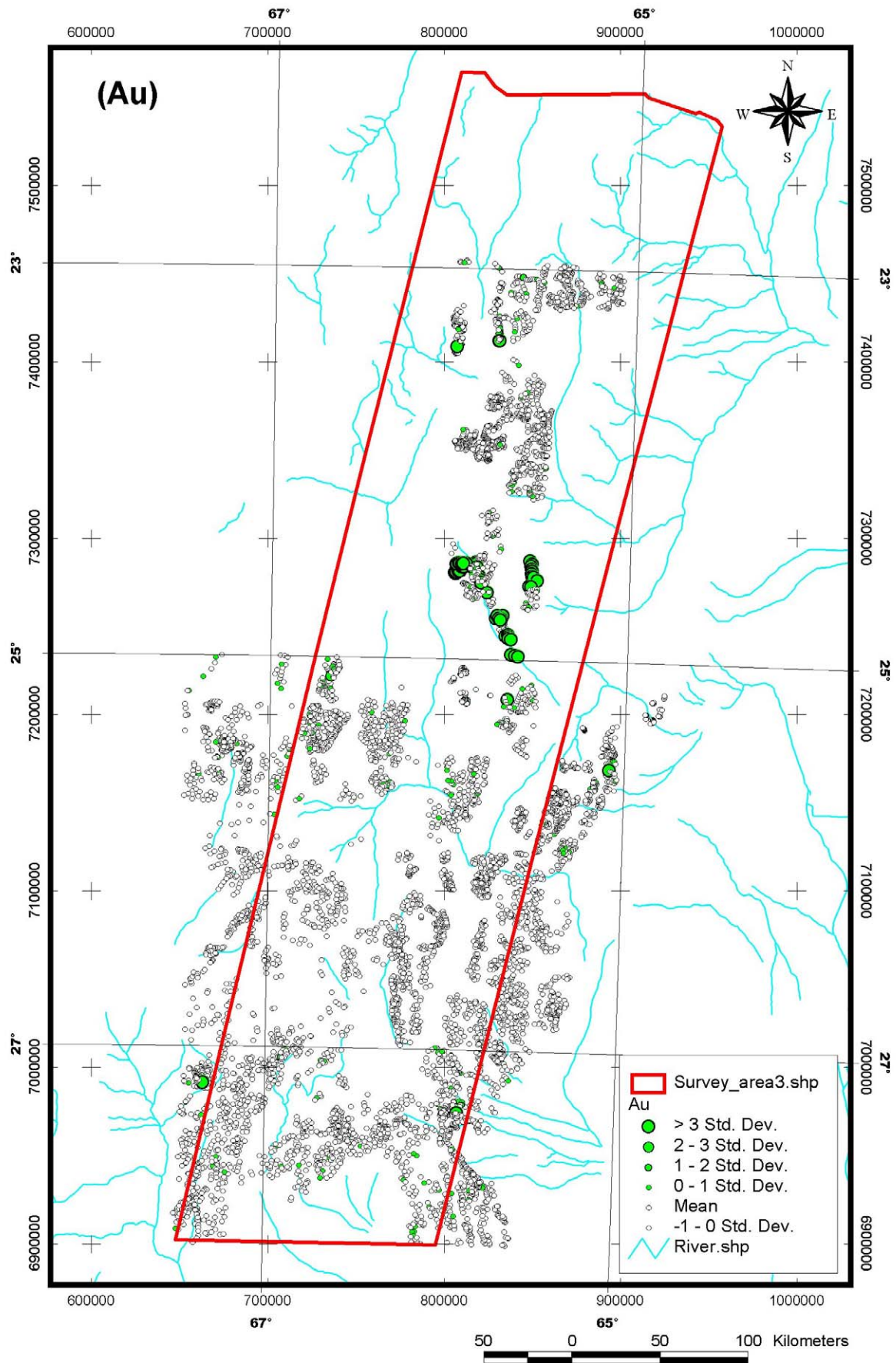


Fig.II-2-5-1 Geochemical anomaly map (Au)

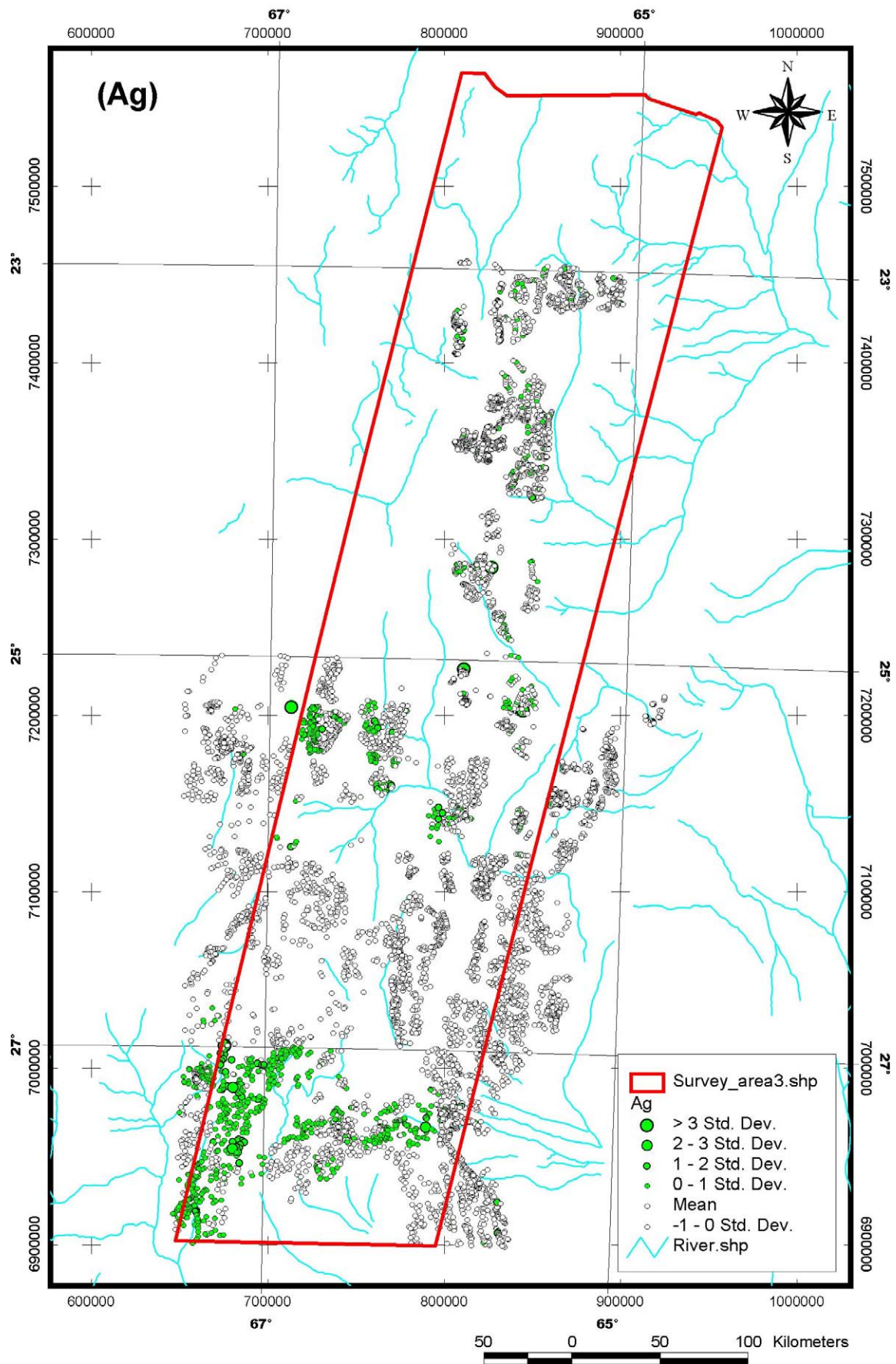


Fig.II-2-5-2 Geochemical anomaly map (Ag)

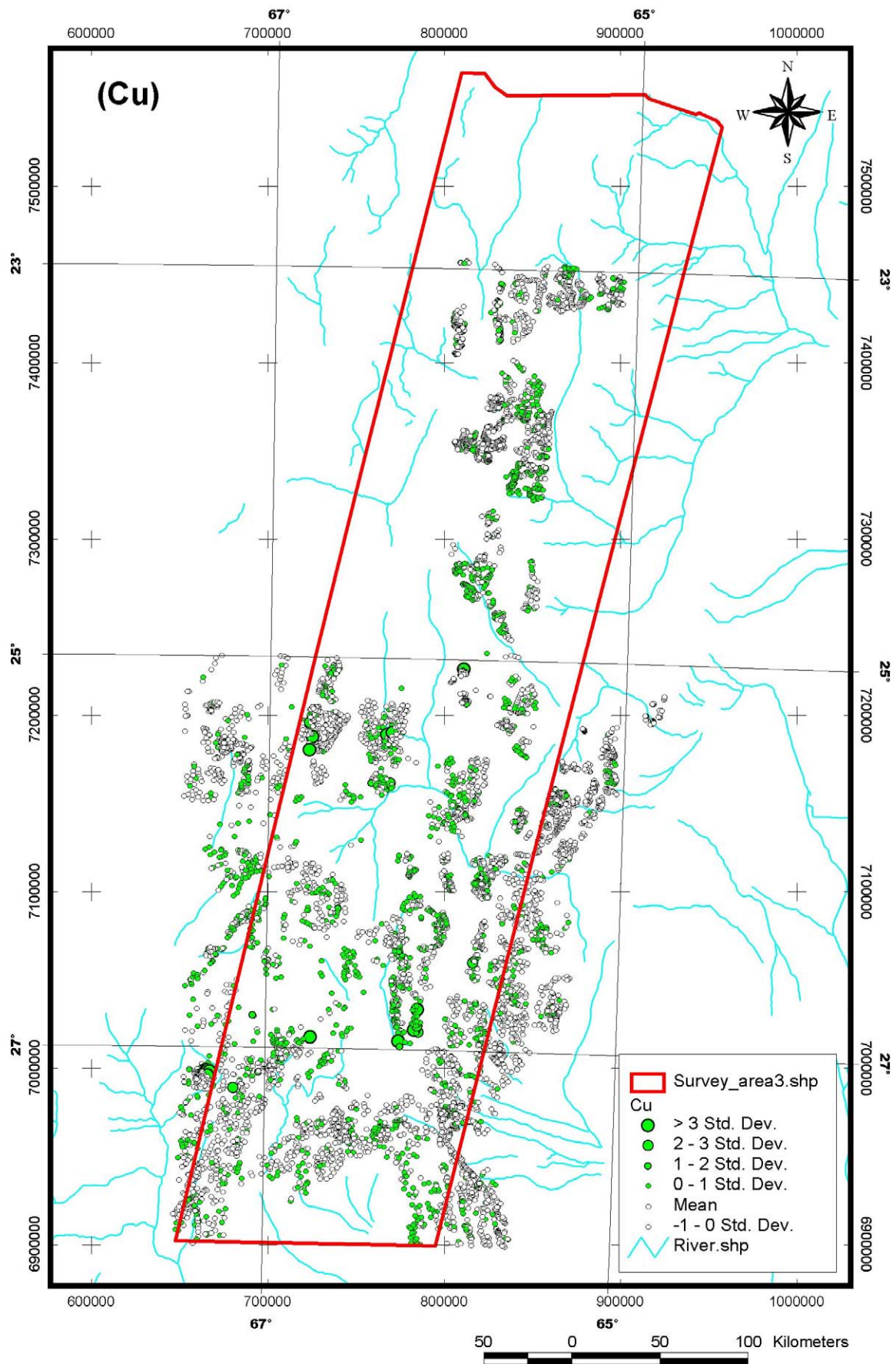


Fig.II-2-5-3 Geochemical anomaly map (Cu)

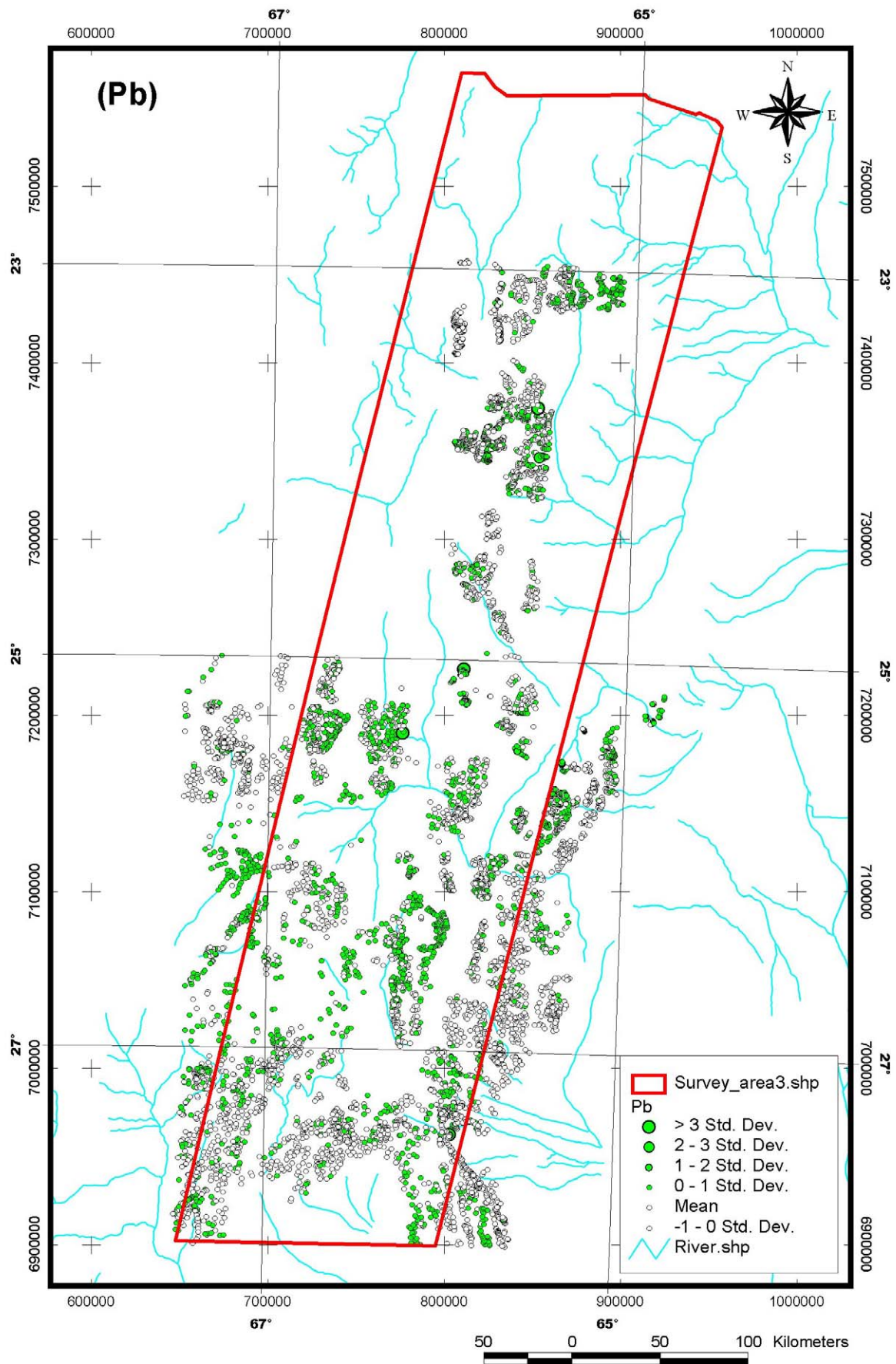


Fig.II-2-5-4 Geochemical anomaly map (Pb)

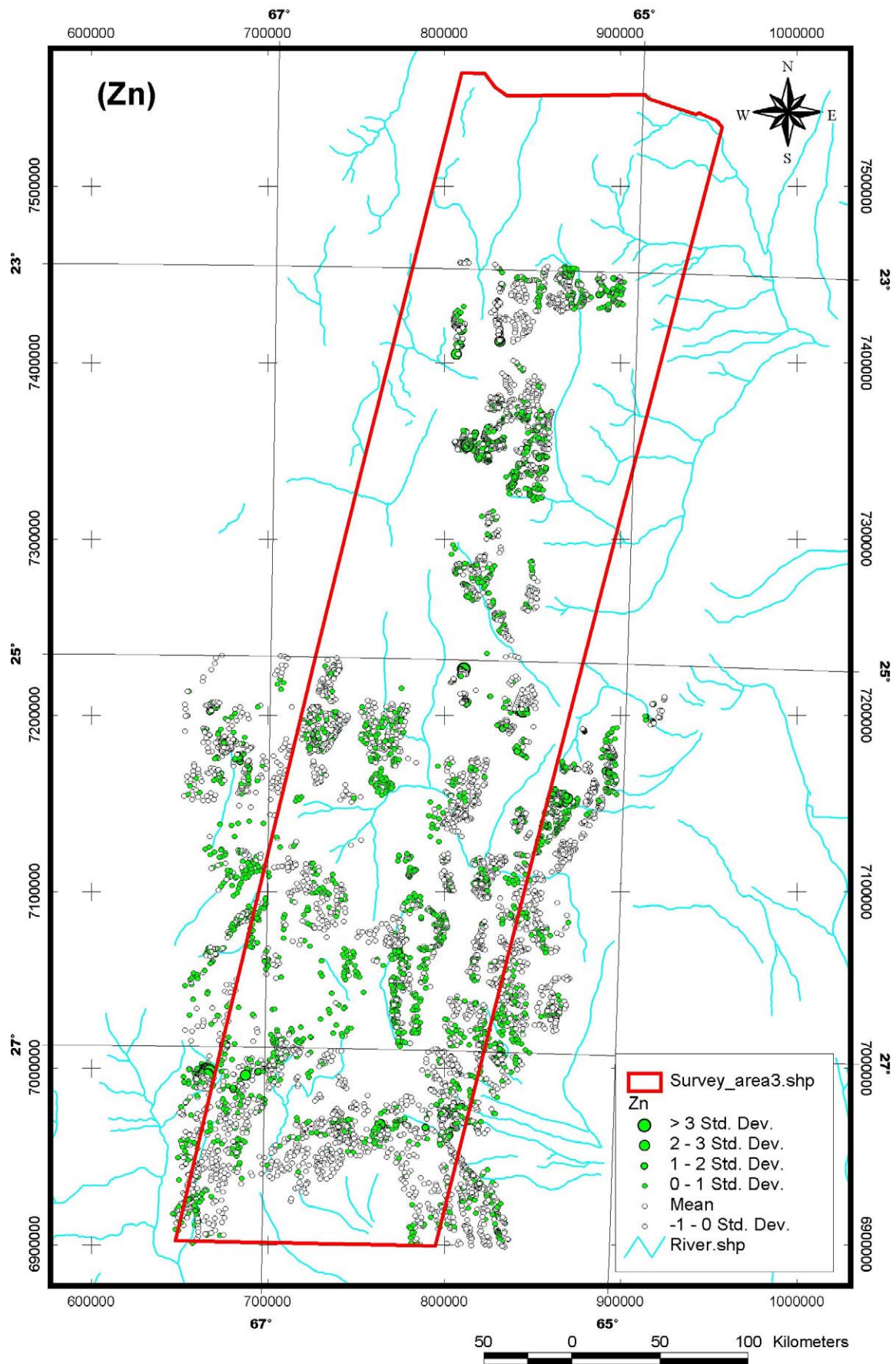


Fig.II-2-5-5 Geochemical anomaly map (Zn)

Significant gold anomaly is seen at the center of the survey area. El Acay and other several prospects are existed near to the anomaly. Anomalous values are also seen around the Aguilar mine. Silver anomaly is seen in the wide area in the southern part of surveyed area. The distribution corresponds well to the distribution of Ordovician granites in Southern part of the area. In addition, anomalous values are seen at the central western part where porphyry copper-gold deposits, Diablillos deposit etc., are distributed. Copper anomaly corresponds to the distribution of known porphyry copper deposits, especially the high anomaly value is seen around Agua Rica mineral showings. Lead anomaly is mainly distributing over known SEDEX deposits, and partly seen around porphyry copper deposits. Zinc anomaly also distributes around the SEDEX deposits

Results of the Principal Component Analysis are shown in Fig.II-2-5-6~9. Detail of methodology of the Principal Component Analysis used here is described in "(II-)4-2-1SEDEX/VMS type deposit". In this analysis, 190 samples (2.5% of all samples) of which have larger absolute values of principal component loading matrix were extracted and plotted. Principal component loading matrix of each element is shown in Table II-2-5-1.

The distribution of PC1 plot corresponds well to the distribution of Pre-Cambrian and Cambrian sedimentary and metamorphic rocks in southern part of the survey area. The distribution of PC2 is corresponds well to the distribution of Cretaceous sedimentary rocks in the central and northern part, and of Cambrian metamorphic rocks in the southern part. In spite of many of the elements related to mineralization have higher correlation to PC2, no significant relation have seen with known mineral occurrence. Lead and cadmium have higher correlation with PC7 and its distribution is corresponds to the distribution of sedimentary rocks in the northern part and of granites in the southern part. PC10 includes gold, mercury and indium as high correlation elements. The plots of PC10 tend to locate around known mineralization and also granites distribution.

Table II-2-5-1 Principal component loading matrix after varimax rotation

	PC1	PC2	PC3	PC4	PC5	PC6	PC7	PC8	PC9	PC10	Contribution ratio
log Ag	-0.242	-0.202	-0.286	0.079	0.179	-0.268	-0.001	-0.165	-0.433	0.284	0.587
Al	0.083	-0.383	-0.714	0.332	0.047	0.159	-0.073	0.136	0.093	0.010	0.834
log Ba	0.093	-0.212	0.044	0.074	-0.286	0.717	-0.097	-0.012	-0.017	0.036	0.668
log Be	0.119	-0.069	-0.777	0.118	-0.022	-0.109	-0.019	-0.069	0.075	-0.064	0.663
log Bi	0.000	-0.118	-0.085	0.236	-0.073	-0.005	0.148	-0.778	0.030	-0.078	0.717
log Ca	0.039	-0.072	0.081	0.871	0.055	0.050	-0.020	-0.097	-0.124	-0.004	0.803
log Cd	0.047	0.030	0.122	-0.013	0.033	0.093	-0.615	-0.070	-0.164	-0.211	0.482
log Co	0.151	-0.936	-0.069	0.037	-0.053	0.107	-0.050	0.022	-0.018	0.000	0.923
log Cu	0.080	-0.583	-0.166	-0.247	0.124	0.331	-0.395	0.024	-0.159	-0.052	0.744
log Fe	0.271	-0.877	-0.021	0.129	-0.168	-0.063	-0.034	-0.143	0.091	-0.042	0.923
K	0.003	-0.032	-0.858	-0.112	0.074	0.074	-0.017	-0.106	0.052	0.027	0.776
log La	0.886	-0.205	-0.046	0.112	-0.077	-0.033	-0.087	0.023	0.140	-0.021	0.877
Mg	-0.057	-0.848	-0.067	0.110	0.176	0.095	0.068	0.025	-0.090	0.018	0.793
log Mn	0.235	-0.718	-0.262	0.187	0.141	-0.155	-0.142	-0.229	-0.084	0.032	0.798
log Mo	0.033	-0.324	-0.030	0.165	-0.277	-0.173	-0.486	0.241	0.015	-0.049	0.538
Na	-0.016	0.022	-0.360	0.684	0.206	-0.253	0.077	0.036	0.123	0.050	0.729
log Ni	0.056	-0.894	-0.083	-0.139	0.041	0.096	-0.002	0.149	-0.068	0.026	0.867
log P	0.516	-0.339	-0.238	0.164	0.429	0.084	-0.040	-0.077	-0.147	0.038	0.687
log Pb	0.131	-0.026	-0.264	-0.051	-0.083	0.003	-0.653	0.008	0.147	0.115	0.558
log Sc	0.194	-0.837	-0.333	0.070	-0.002	0.155	0.009	0.000	0.005	-0.010	0.878
log Sn	-0.038	0.005	-0.009	-0.055	0.045	0.026	-0.305	-0.386	0.111	0.152	0.285
log Sr	-0.091	-0.233	-0.083	0.891	-0.125	0.078	0.016	-0.064	-0.026	-0.001	0.891
Ti	0.315	-0.707	0.098	0.335	-0.175	-0.218	0.059	-0.208	0.123	-0.014	0.861
V	0.186	-0.697	0.279	0.265	-0.274	-0.215	0.027	-0.212	0.157	-0.035	0.862
log Y	0.724	-0.273	-0.273	0.221	0.271	-0.031	-0.091	-0.127	-0.055	0.014	0.824
log Zn	0.178	-0.800	-0.256	0.088	-0.137	-0.032	-0.220	-0.168	0.056	-0.028	0.845
log As	-0.133	-0.195	-0.022	0.158	-0.774	0.170	-0.103	-0.015	-0.140	-0.095	0.749
log Au	-0.002	-0.006	0.043	-0.079	-0.042	0.091	-0.133	0.059	0.080	-0.582	0.384
log Br	0.040	0.003	-0.354	0.093	-0.118	-0.134	-0.096	0.056	-0.548	-0.085	0.488
log Ce	0.911	-0.173	-0.045	0.093	-0.085	-0.121	-0.074	0.082	0.089	0.002	0.912
log Cr	0.196	-0.809	0.097	-0.092	-0.113	-0.063	0.092	0.134	-0.048	0.025	0.757
log Cs	0.027	-0.191	-0.655	0.207	-0.383	-0.124	-0.027	0.004	-0.145	-0.019	0.693
log Eu	0.782	-0.307	-0.023	0.085	-0.029	0.225	-0.037	0.078	0.078	-0.058	0.783
log Hf	0.813	-0.108	0.269	-0.147	-0.147	-0.107	0.004	-0.058	0.087	-0.009	0.810
log Hg	0.029	0.015	-0.036	0.050	-0.110	0.054	-0.016	-0.043	0.141	-0.514	0.306
log Ir	-0.002	-0.031	-0.005	0.010	0.001	-0.086	0.084	-0.024	-0.096	-0.611	0.398
log Lu	0.721	0.000	0.013	-0.255	0.236	0.097	0.036	-0.143	-0.135	-0.025	0.691
log Nd	0.625	-0.086	-0.023	0.069	-0.081	-0.014	-0.042	0.114	0.023	-0.021	0.426
log Rb	0.022	-0.035	-0.776	-0.088	0.086	-0.099	-0.008	-0.017	-0.124	0.040	0.645
log Sb	-0.126	-0.012	-0.014	-0.234	-0.714	0.158	-0.006	-0.087	0.019	-0.144	0.634
log Se	-0.007	-0.005	-0.119	0.018	0.029	-0.046	-0.049	-0.073	0.592	-0.130	0.392
log Sm	0.956	-0.154	-0.059	-0.004	0.028	0.001	-0.053	0.016	0.012	-0.022	0.944
log Ta	0.306	-0.252	-0.426	0.057	-0.015	-0.544	-0.020	-0.048	-0.153	0.222	0.713
log Tb	0.704	-0.080	-0.071	-0.169	0.258	0.016	0.043	-0.036	-0.152	0.026	0.630
log Th	0.805	-0.067	-0.305	0.131	-0.044	-0.342	-0.047	-0.031	0.041	0.044	0.889
log U	0.294	-0.022	-0.452	0.123	0.124	-0.479	-0.073	-0.018	-0.221	0.134	0.624
log W	0.160	-0.037	-0.320	-0.156	-0.140	-0.141	-0.137	-0.326	-0.002	-0.173	0.349
log Yb	0.791	0.001	-0.066	-0.226	0.280	0.042	0.027	-0.128	-0.141	-0.015	0.799
Sum of loading square	8.040	7.969	4.532	3.090	2.341	1.907	1.530	1.349	1.341	1.326	
Contribution ratio	16.751	16.603	9.441	6.438	4.877	3.974	3.187	2.810	2.794	2.763	
Cumulative Contribution ratio	16.751	33.354	42.795	49.232	54.110	58.083	61.271	64.080	66.875	69.638	

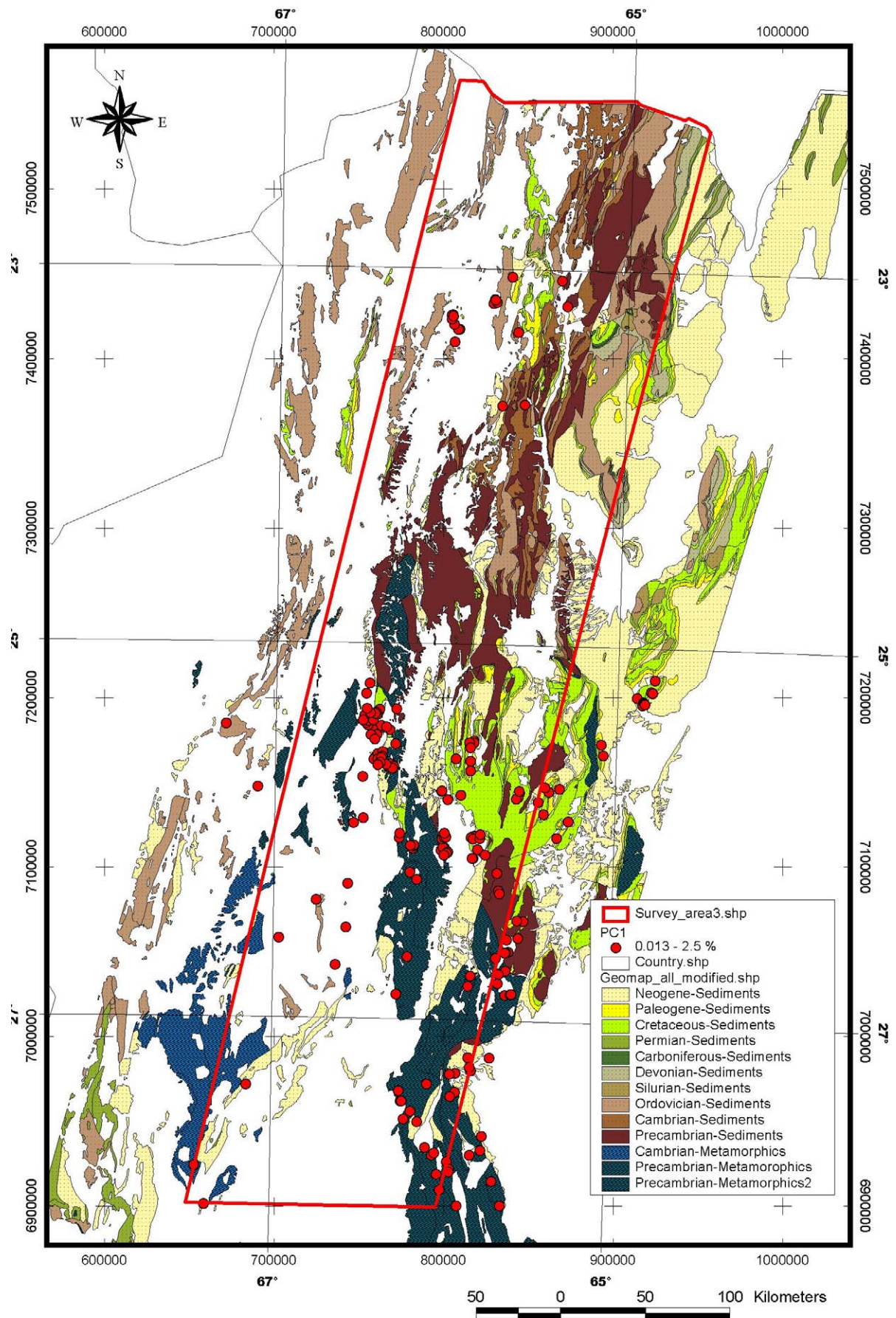


Fig.II-2-5-6 PC1 high score distribution map

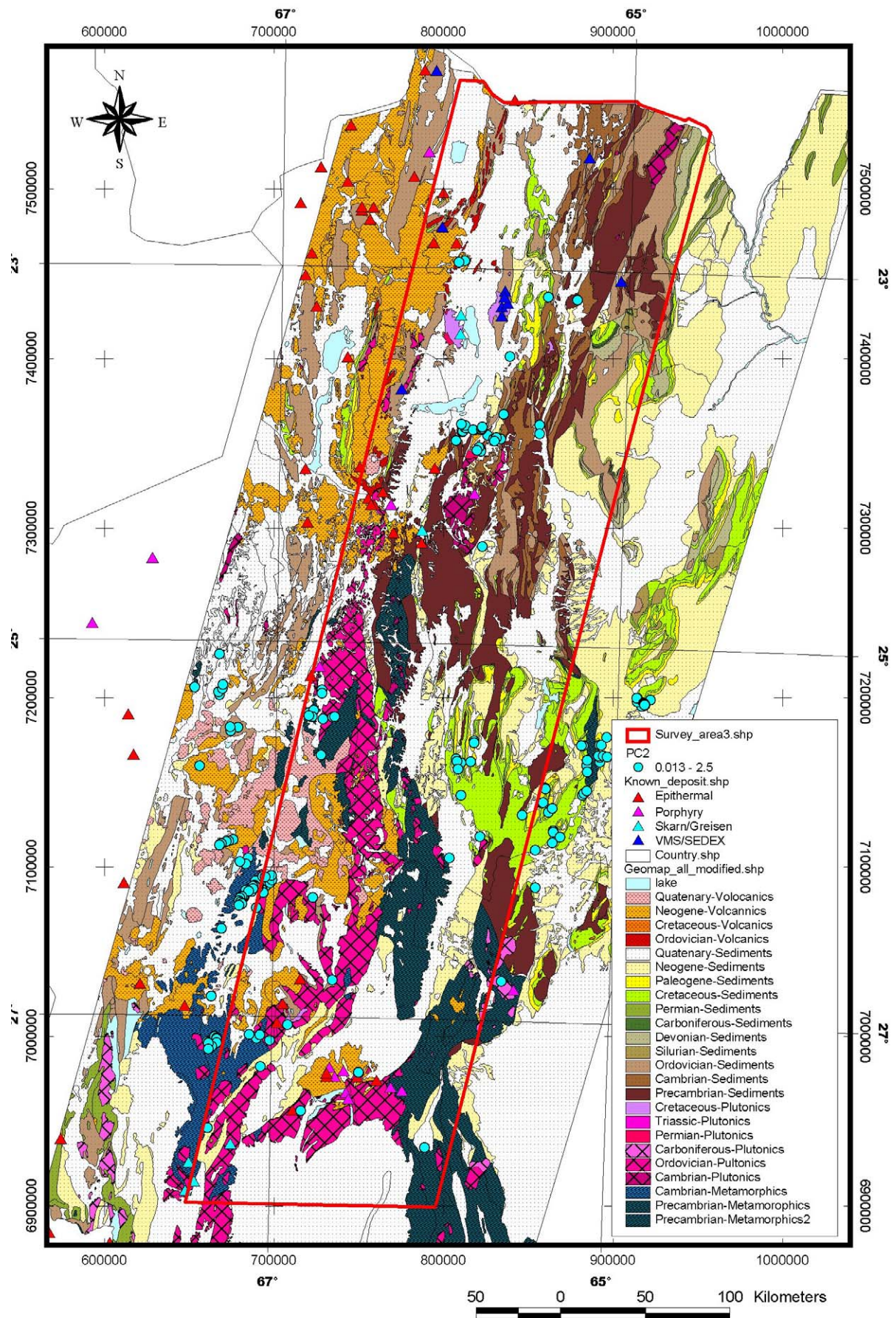


Fig.II-2-5-7 PC2 high score distribution map

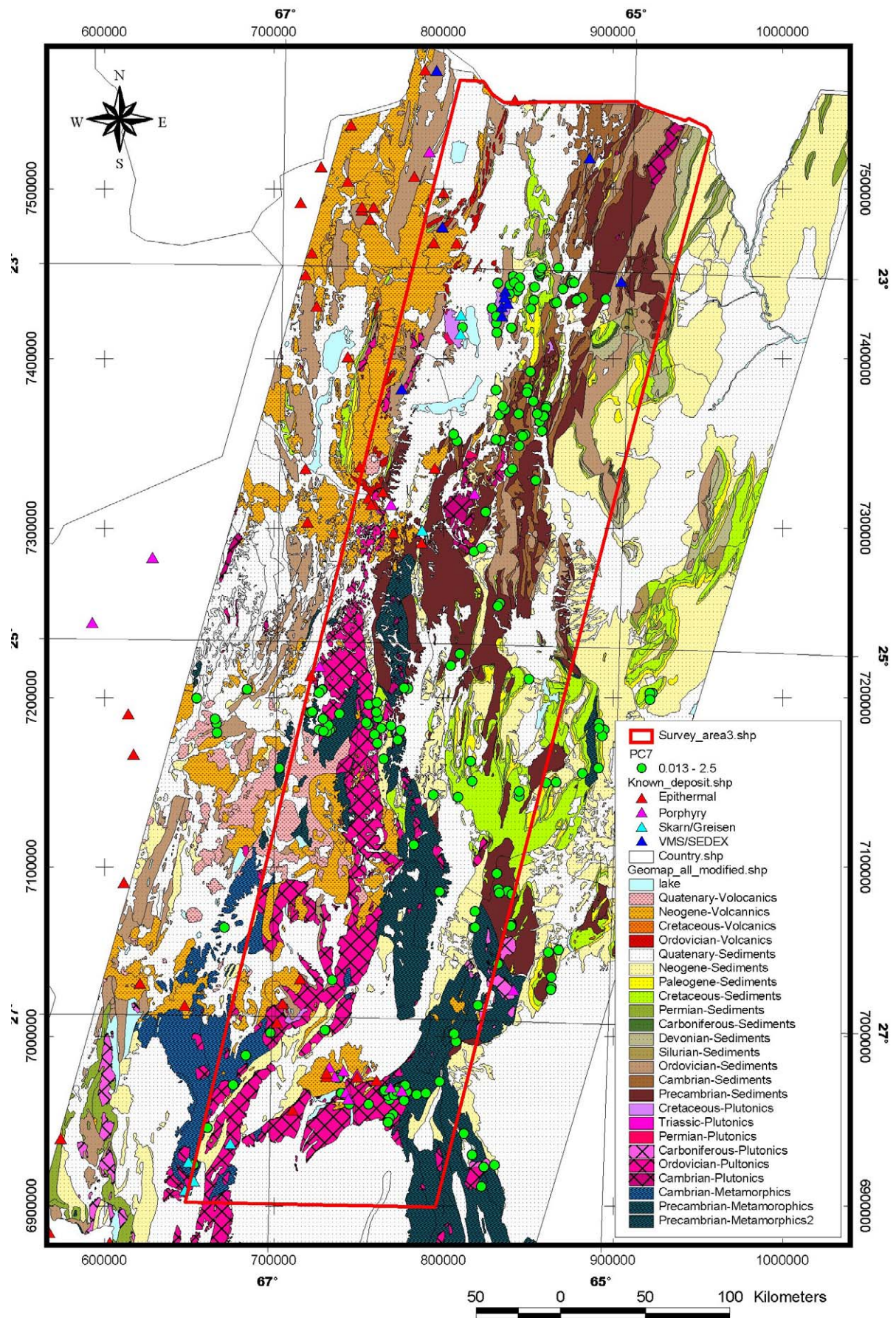


Fig.II-2-5-8 PC7 high score distribution map

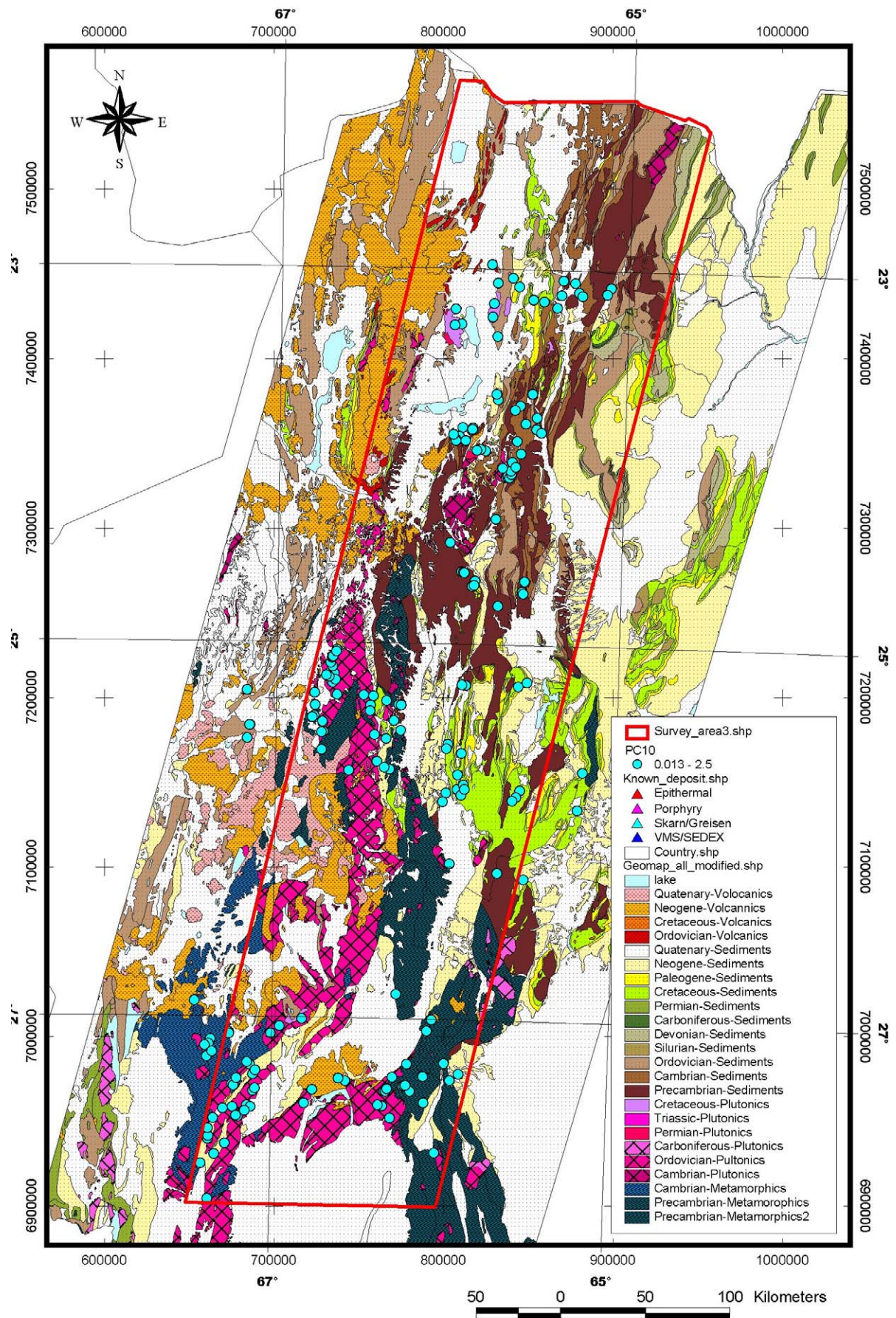


Fig.II-2-5-9 PC10 high score distribution map

Chapter 3 Satellite image analysis

3-1 Data processing of the image

3-1-1 Outline of analysis

The purpose of this analysis covering arid areas is to identify alteration minerals with the ASTER, which was designed for effective mineral exploration. Prior to the analysis, pseudo reflectance conversion was applied for 22 scenes. The conversion were calculated based on characteristics of spectral reflectance of Pampa distributed in the survey area, because the fact that the ratio between bands of surface materials of Pampa is almost constant regardless of areas, and this is the first trial to use this method for practical filed survey. Pseudo reflectance conversion coefficient were based on METI (2002(planed)). Minerals identification is the main object of this analysis, and characteristics of spectral reflectance are used for this identification. Therefore, it can be said that accuracy of pseudo reflectance conversion is an important correction that determines the accuracy of analysis.

The survey area is nearly non-vegetated, but sparse vegetation is recognized in the mountainous zone on the east side of the survey area. In zones where vegetation grow sparsely on soils, reflectance spectra are affected by the reflectance spectra of plants. If minerals are identified by reflectance spectra mixed with vegetation, a large amount of alunite and kaolinite will be detected. A spectral reflectance mixed with vegetation can be represented by a composite sum corresponding to the area ratio between reflectance spectra of bare rock/soil and the reflectance spectra of plants. In the analysis of last year, the spectrum from vegetation was removed by using SAVI (Solid Adjust Vegetation Index), the coverage index of vegetation. In the analysis of this year, a new attempt of reflection spectrum removal from vegetation was made to correct the effect caused by the soil brightness by using SAVI calculated from pseudo-reflectance (PSAVI: Pseudo Soil Adjust Vegetation Index). As the result, generally satisfied result could be obtained for the area with the vegetation coverage up to 40%.

For identification and semi-quantitative analysis of alteration minerals, a iso-grain model is used. The weathered ground surface generally consists of a mixture of several or more kinds of minerals. Therefore, with the iso-grain model, for which reflection and absorption among mineral grains are taken into consideration, it is possible to explain changes of reflectance spectra of this mixture theoretically. In this analysis, 10 minerals widely observed were selected, and a database of spectral reflection with a mixture of these minerals was created with the iso-grain model. Next, comparing image data and spectral reflectance per one pixel, minerals are identified and mapped. In addition, mineral identification using 12 minerals was carried out for specific area to distinguish the alteration type.

SiO₂ content mapping was carried out using the conversion method proposed in METI(2000), after radiometric correction(remove atmospheric effects) and temperature-emissivity

separation were applied for thermal bands data that are characteristic of the ASTER.

Since the above image processing method and imaging method of the result were used the same method of last year's analysis except the removal of vegetation, only the outline of the methods is described in this report. The details are described in the Annual Report of JICA/MMAJ (2001).

The following parameters were used in the projection of the images.

Projection : Transverse Mercator (UTM)

Spheroid : International 1909

Central Meridian : -69

False easting : 500000

False northing : 10000000

3-1-2 Data used

The 22 scenes of data used are shown below (Table II-3-1-1). Data was retrieved by the image retrieval system (ASTER GDS) of the Earth Remote Sensing Data Analysis Center (ERSDAC). The best images with lesser amounts of clouds at that time (August 2002) were selected, and given by ERSDAC. ERSDAC started providing higher level product in this year. In this analysis 3A01 product, which is composed of orthorectified image and DEM (Digital Elevation Model) was used for analysis. Index map is shown in Fig.II-3-1-2-1.

Table II-3-1-1 ASTER data analyzed in F.Y.2002

Area No.	Granule ID	Product	Lat. Center	Lon. Center	Aquisition Date	Cloud Cov.(%)
A01	ASTL1A 010811144430108221106	3A01	-26.48°	-65.20°	2001/08/11	11
A02	ASTL1A 0108111444520108221107	3A01	-27.20°	-65.27°	2001/08/11	4
B02	ASTL1A 0112011439500112160323	3A01	-22.27°	-64.55°	2001/12/01	17
B03	ASTL1A 0112011439590112160324	3A01	-22.59°	-65.03°	2001/12/01	16
B09	ASTL1A 0101311448490111020448	3A01	-26.11°	-65.48°	2001/01/31	5
B10	ASTL1A 0101311448580111020449	3A01	-26.43°	-65.56°	2001/01/31	9
B11	ASTL1A 0101311449070111020450	3A01	-27.15°	-66.04°	2001/01/31	15
B12	ASTL1A 0101311449160111020451	3A01	-27.47°	-66.12°	2001/01/31	5
C01	ASTL1A 0110211447140111010599	3A01	-22.03°	-65.20°	2001/10/21	6
C02	ASTL1A 0110211447230111010600	3A01	-22.35°	-65.28°	2001/10/21	6
C03	ASTL1A 0110211447320111010601	3A01	-23.07°	-65.35°	2001/10/21	4
C04	ASTL1A 0110211447400111010602	3A01	-23.40°	-65.42°	2001/10/21	10
C05	ASTL1A 0110211447490111010603	3A01	-24.12°	-65.50°	2001/10/21	18
C06	ASTL1A 0105231445530106010410	3A01	-24.32°	-65.47°	2001/05/23	13
C07	ASTL1A 0105231446020106010411	3A01	-25.04°	-65.55°	2001/05/23	6
C08	ASTL1A 0105231446110106010412	3A01	-25.36°	-66.03°	2001/05/23	3
C09	ASTL1A 0105231446200106010413	3A01	-26.08°	-66.11°	2001/05/23	9
C10	ASTL1A 0105231446290106010414	3A01	-26.40°	-66.19°	2001/05/23	10
C11	ASTL1A 0105231446370106010415	3A01	-27.12°	-66.27°	2001/05/23	6
C12	ASTL1A 0105231446460106010416	3A01	-27.43°	-66.35°	2001/05/23	3
D03	ASTL1A 0103041447160201010247	3A01	-23.22°	-66.09°	2001/03/04	16
D04	ASTL1A 0103041447250201010248	3A01	-23.54°	-66.17°	2001/03/04	23

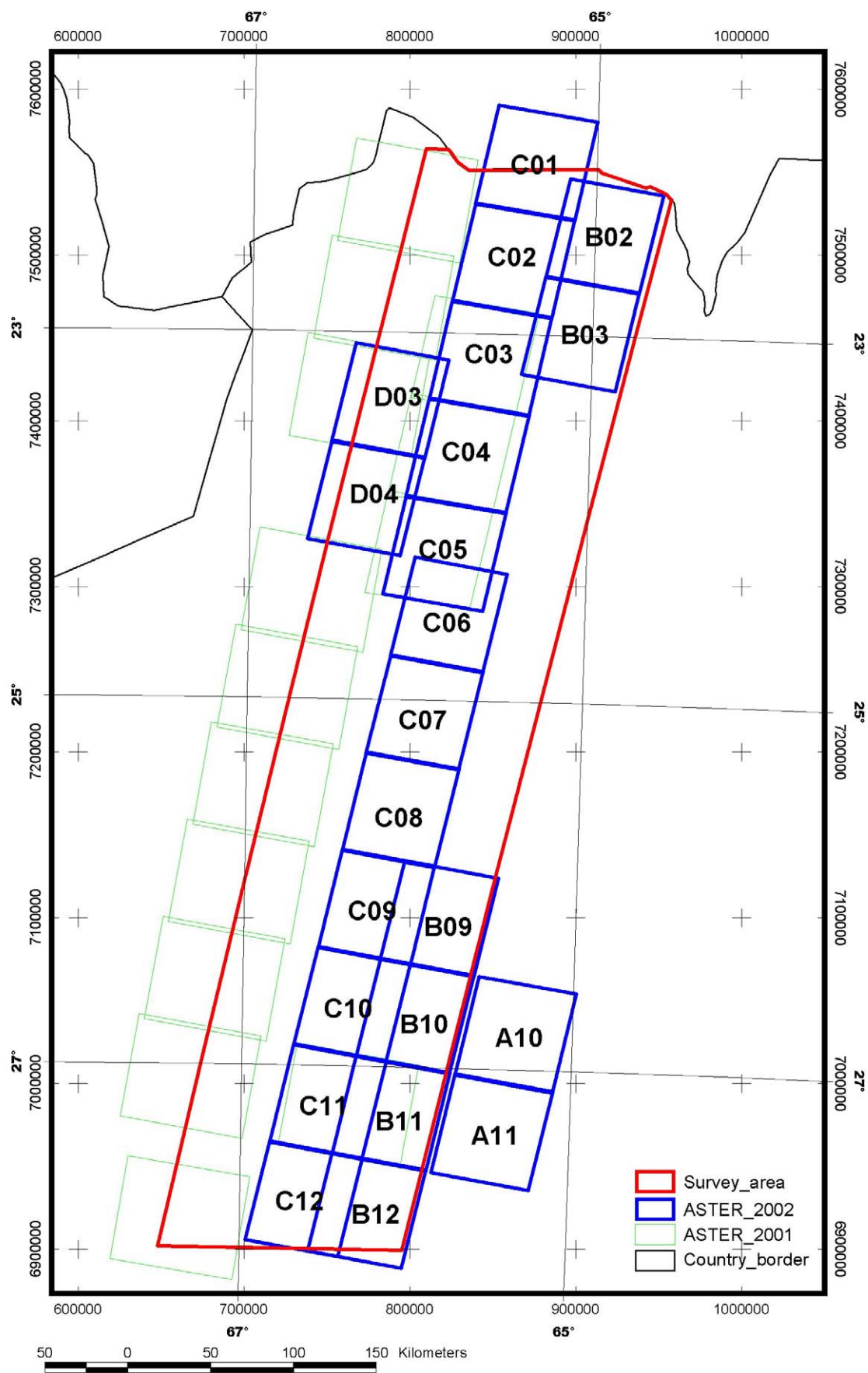


Fig.II-3-1-2-1 Index map of analyzed ASTER data

Data A10 ~ 11 are the images that consists of mountainous region that is covered by thick vegetation and city area. The images are generally hazy and the image looks pale white. The useful analysis result was not obtained due to the haze.

Data B02 ~ 03 are images with high quality in spite of the partly existence of cloud. The images were taken in December that is the summer season in this area and in this season the sun angle is high. The images are proper to analyze. There are several places that are not possible to analyze, because of thick vegetation coverage.

Data B09 ~ 12 are images with high quality in spite of partly existence of the cloud. These images were taken in January. The images are proper to analyze as same as the Data B02 ~ 03. There are several places covered by thick vegetation.

Data C01 ~ 05 are images with high quality. The small vegetation areas are observed along the streams.

Data C06 ~ 12 were taken in May. Since May is the winter in this area, the sun angle and the brightness are low. By the reason, S/N ratio is low. Therefore, the reliability of analysis is generally low compared to the other scenes, the reliability is particularly low in the shadow side of mountains due to its low brightness.

Data D03 ~ 04 are the images that the clouds are scattered all over the image like islands. The places that covered by the clouds and the shadow parts of the clouds are not possible to analyze.

3-1-3 Pseudo reflectance conversion

Radiance value in ASTER data is a digital number of 256 gradations of digital values quantified by applying gain and bias independently per band. This value expresses an intensity ratio of relative reflectance in a band, but comparison of the values is nonsense. Therefore, if identification of minerals is carried out in the patterns of Bands 1 to 9, it is necessary to convert radiance values among bands to comparable numeric values by some manner. This is pseudo reflectance conversion and with this conversion, minerals can be identified from absorption patterns of the band.

METI(2000) carried out pseudo reflectance conversion by measuring indoors reflectance of gravel of Pampa sampled on the site, and then fitting to this reflectance. This is a pseudo reflectance conversion method that does not require atmospheric correction. The greatest disadvantage is, however, that a sample is required. In areas without any samples, like this case, this method cannot be used. For this reason, we developed a method of conversion into pseudo reflectance for this analysis, using optical properties of the surface materials of Pampa. This method is as follows:

- ① Identification of materials without characteristic reflectance spectra, mainly at Pampa.
- ② Calculation of intensity ratios between bands of detected materials
- ③ Identification of materials without characteristic spectral reflectance in areas with known

pseudo reflectance (mainly at Pampa)

- ④ Calculation of the intensity ratio among bands of materials detected in ③.
- ⑤ Calculation of a conversion coefficient to make consistent the intensity ratios obtained in ② and ④.

By the operation mentioned above, radiance ratios between bands in the analysis area can be corrected to be radiance ratios between bands in the areas where the pseudo reflectance conversion coefficient has already been found. As the coefficient is known in the area of ③, data of the analysis area can be converted to pseudo reflectance by multiplying by this value.

As this method requires data with known pseudo reflectance conversion coefficients, the results of analysis by the METI (2002(planned)) were used. Accordingly, if the pseudo reflectance conversion coefficients in this data are wrong, this analysis is also wrong. But because these results are good, it is considered that our correction coefficient is right on the whole.

3-1-4 Removing vegetation effects

Although most of the analyzed area in this year is composed of non-vegetated area, small amount of vegetation could be observed in such a semi-arid area (Fig.II-3-1-4-1). In these areas, at first the reflection spectrum from vegetation must be removed from the brightness within each pixel as the vegetation correction to make the mineral identification. The spectral data from the part that is composed of several minerals closely exist is affected by the reflection from each mineral and mutual absorption among minerals. Therefore, the spectral data do not shift in linear to the mixing ratio of minerals. On the other hand, since there is enough distance between soil and vegetation, the effect of the mutual reflection and absorption is considered to be extremely small. So, the reflection spectrum from the part with small coverage of vegetation is spectrum mixed from soil and vegetation. The spectral data is considered to shift in linear with correlation to the vegetation coverage area.

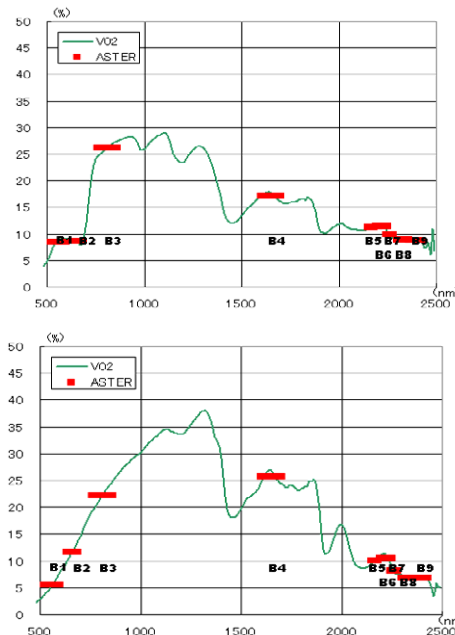


Fig.II-3-1-4-1 Vegetation situation in semi-arid area and their spectral reflectance

The reflection spectrum from the surface that is observed in the air is estimated to be the weighting mean of the spectrum from vegetation and soil with correlating to each coverage as shown in Fig.II-3-1-4-2. Therefore, the removal of vegetation information from the satellite data is to estimate the reflection spectrum from soil by the reverse processing of the above method.

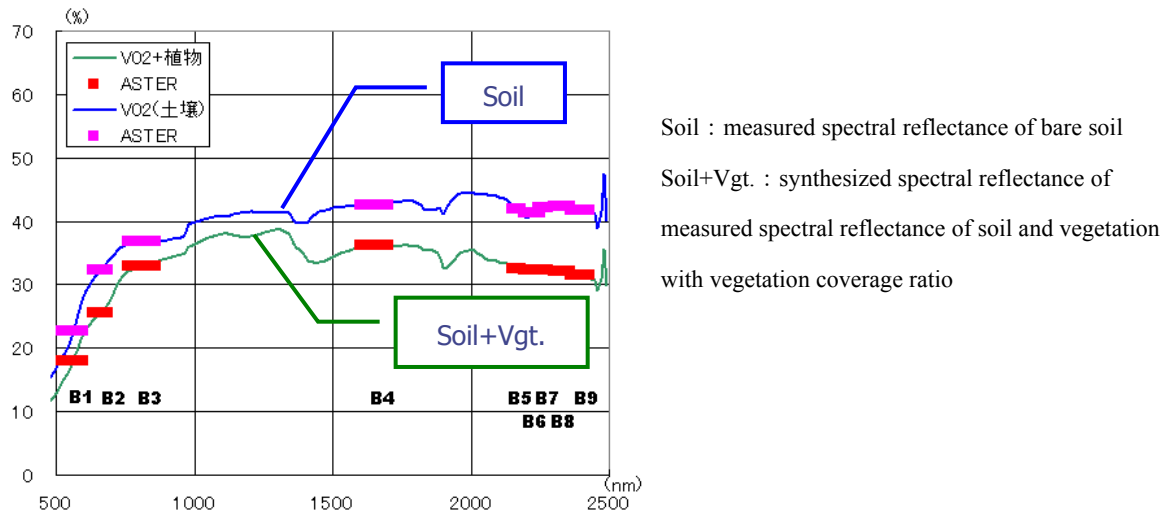


Fig.II-3-1-4-2 Synthesized spectral reflectance of soil and vegetation

(1) Model of vegetation information removal by SAVI and the failure

To remove the vegetation information, the degree of influence by vegetation, that is, the estimation of vegetation coverage in the satellite data is necessary. To estimate the vegetation coverage in the satellite data, vegetation index that is calculated by using the data of specific Band or Bands that includes the absorption and reflection by plants. Vegetation Index is calculated by using the above specific Bands (Vegetation Index is generally used as index not as the coverage of vegetation). NDVI (Normalized Differential Vegetation Index) and SAVI (Soil Adjusted Vegetation Index) are the representative Vegetation Indexes. The former is calculated by using Band 3 and Band 4 data of LANDSAT TM and is mainly applied to the dense vegetation area. The latter is mainly applied to the scarce vegetation in the semi-arid area. Since SAVI is the index considering to the effect of the soil brightness, the adjustment of correction term is necessary. In this analysis, 0.5 is substituted for the term.

Calculations were carried out to observe the reflection spectrum change according to the vegetation coverage change as model cases assuming the constant reflection spectrum from vegetation in two different cases. In these cases, the psuedo-reflection spectrum from soil is constant and only the brightness changes as the assumption. The reason of the assumption is to reflect the characteristics to the reflection spectrum from the standard material that mentioned in the previous clause.

The composite reflection spectral change according to the vegetation coverage is shown in Fig.II-3-1-4-3a. The black line means the reflection of soil. The left Figure is the case of bright soil and the right is of dark soil. The reflection spectrum from the standard material that was calculated in the previous section is applied as the reflection spectrum from soil. At that time the brightness assumed 5 times. The change of the reflectivity from soil in each Band according to the vegetation

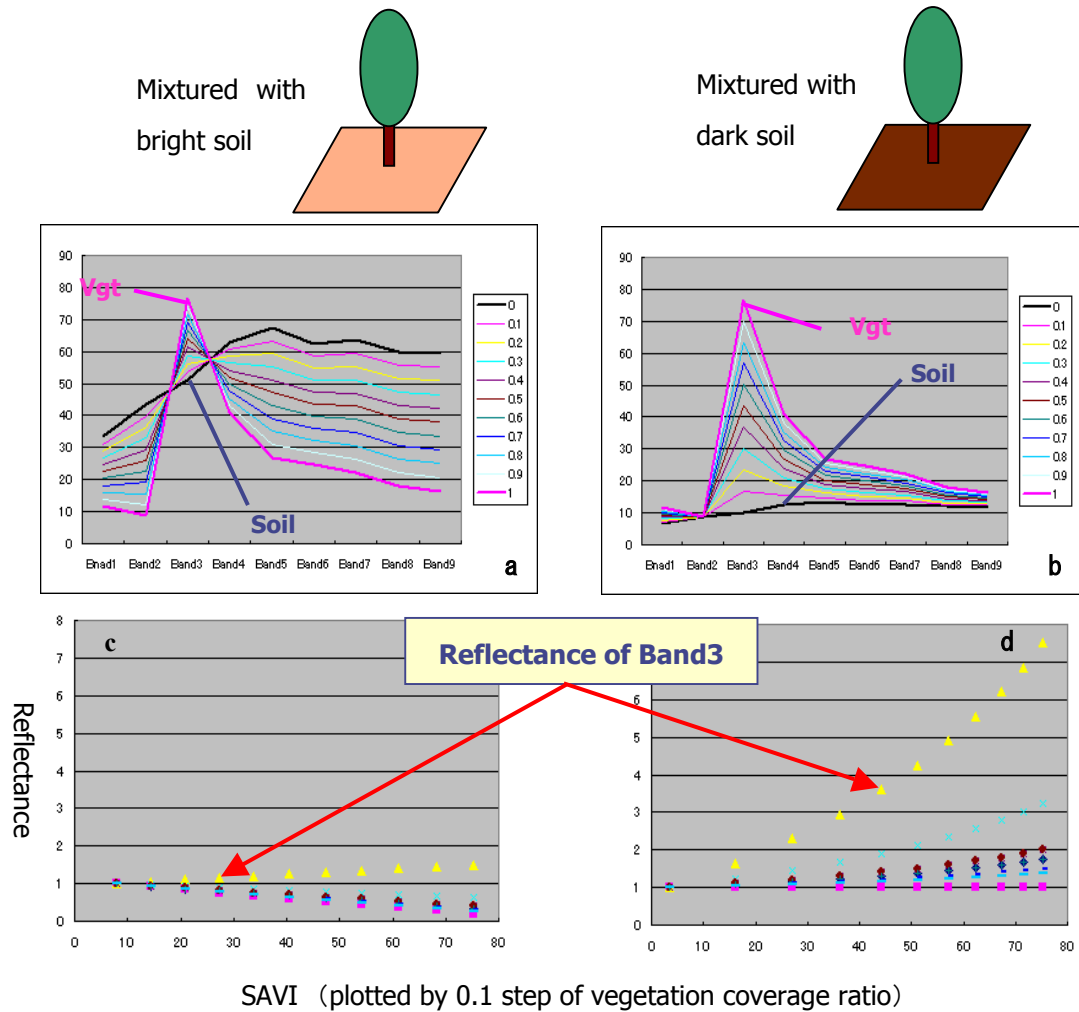


Fig.II-3-1-4-3 Reflectance versus SAVI with change on soil brightness and vegetation coverage ratio

coverage is shown in the lower graph of Fig.II-3-1-4-3. In this case, the reflectivity with no vegetation coverage assumes 1. The horizontal axis shows SAVI that calculated from the reflectivity, and the vertical axis shows the change of reflectivity. The calculation results are plotted at interval 0.1 of the vegetation coverage.

The calculated SAVI shows approximate 0.75 in 1.0 of the vegetation coverage in case of bright soil. The SAVI that was calculated at interval 0.1 of the vegetation coverage shows nearly the same interval. In the above case, the reflectivity change of Band 3 (yellow ▲) shows small change corresponding to the vegetation coverage because of the high soil brightness for composition. The change shows approximate 1.5 times in 1.0 of the vegetation coverage.

SAVI that was calculated by using dark soil is 0.1 that is the same value of the bright soil case. SAVI that is calculated at interval 0.1 of the vegetation coverage is plotted with relatively wide interval in the low vegetation coverage area, and is plotted with narrow interval in the high vegetation coverage area. The biggest difference is in the change of reflectivity. Comparing to the vegetation coverage 0 in Band 3, the reflectivity becomes 7.5 times in 1.0 of the vegetation coverage.

The above result means that the reflection spectrum in the vegetation coverage can be assumed by SAVI with specified soil brightness. The shape of graph corresponding to SAVI of each Band is markedly influenced by the soil brightness. Therefore, in case that the soil brightness is not correctly specified, the removal of vegetation information includes the big error. In this case, although the reflection spectrum from 100% of vegetation coverage was assumed, the assumption is difficult in semi-arid area. The error becomes bigger after correction by using this way. At first, the satisfactory result of vegetation correction could not be obtained by this method.

(2) Model of Vegetation Information Removal by using PSAVI

Noticing the characteristic of pseudo-reflectance, the above calculation was carried out as a model after obtaining SAVI by using pseudo-reflectance. Though the assuming condition is the same of the above case, the difference is that the reflection spectrum after mixing of soil and vegetation is replaced by pseudo-reflectance.

The soil that was used in the model only differs in the brightness; so, the shape of the psuedo-reflection spectrum becomes the same in the previous trial. Therefore, the change of the reflection spectrum of mixed soil and vegetation with the optional rate changes only the inside of the end members. The pseudo-reflectance of composed reflection spectrum became as the graph that is shown in Fig.II-3-1-4-4. In this report, the SAVI that is obtained by the calculation by using pseudo-reflectance is called PSAVI.

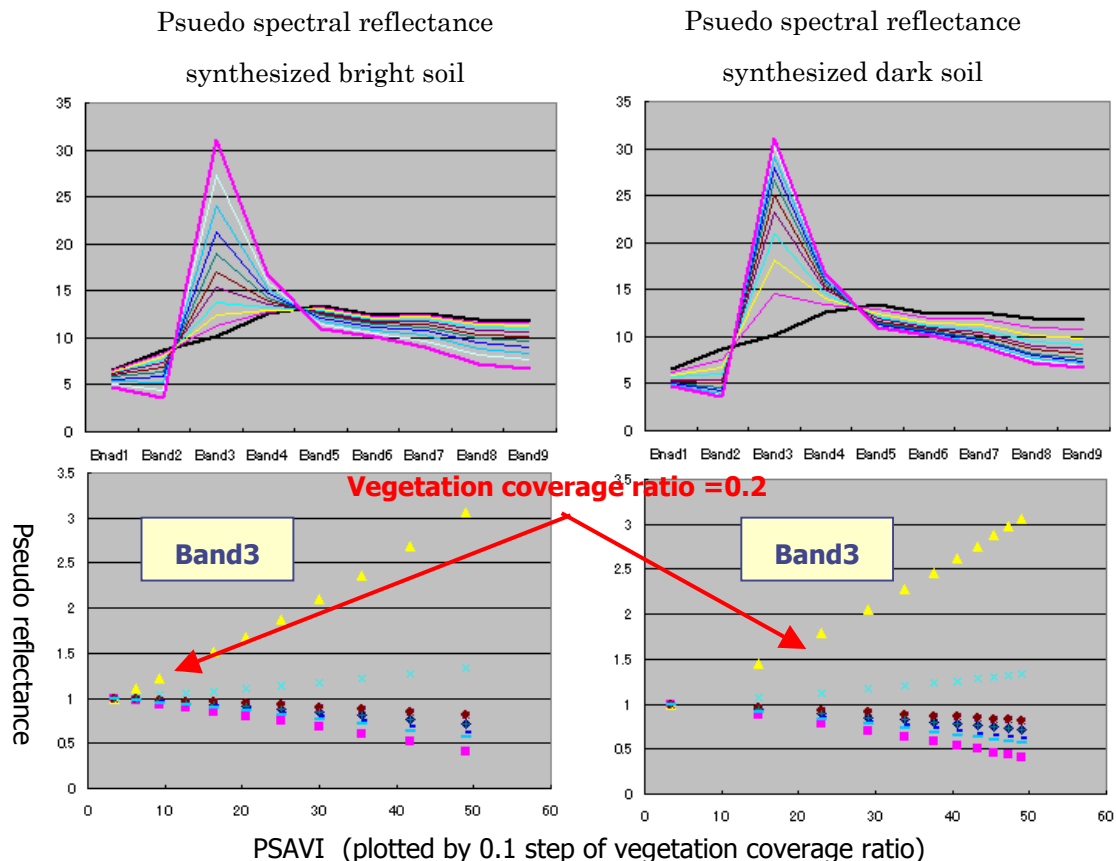


Fig.II-3-1-4-4 Reflectance versus PSAVI with change on soil brightness and vegetation coverage ratio

Assuming the pseudo-reflectance of each Band is 1 at the vegetation coverage 0, the change of pseudo-reflectance of each Band is shown as the graph in the lower of Fig.II-3-1-4-4. The change of the reflectivity was markedly influenced by the soil brightness in SAVI that was calculated by using the reflection spectrum. On the other hand, in PSAVI, the shape of the graph is constant in spite of the soil brightness change. The change of pseudo-reflectance is not influenced by the soil brightness, it is necessary to specify the one correction equation to remove the vegetation information.

The reason that it is enough to specify one correction equation is that PSAVI includes the information of soil brightness. On the contrary, since PSAVI includes the information of soil brightness, PSAVI is not the Index of the vegetation coverage. For example, PSAVI is 9 at the vegetation coverage 0.2 in the bright soil. On the other hand, PSAVI in the dark soil shows bigger value more than 20 in the same vegetation coverage condition.

As mentioned above, the assumed equation for removal of the vegetation information is calculated to make the graph that is shown in the lower of Fig.II-3-1-4-4 in each target scene. In this method, it is not necessary to estimate the reflection spectrum in the vegetation coverage 1.0 that is difficult to estimate in the semi-arid area, and at the same time, the estimation of the soil brightness is not necessary. Moreover, in the model by using the reflectivity (Section (1)), because the observation brightness differs from the surface topography in spite of the soil with the same reflection spectrum. At the same time, SAVI changes corresponding to the change of the observation brightness. The above phenomena occur by the different quantity of incidence light per the unit area according to the slope angles. On the contrary, by using pseudo-reflectance, PSAVI is not influenced by the up and down of topography, because the correction of the quantity of incident light was already carried out.

(3) Checking of Model of Vegetation Information Removal by PSAVI

The usability of the Model by using PSAVI was explained in the previous section. Using real satellite data carried out the verification of the usability of the above model. The verification is as follows; the neighboring three series of data (5 scenes/one series) observed in the different date were selected. The original data was converted to pseudo-reflectivity by atmospheric correction method, and PSAVI was calculated, then the average pseudo-reflectivity at interval of 0.5 was calculated in each PSAVI. The calculated average pseudo-reflectivity is shown in Fig.II-3-1-4-5.

The series A data consists the scenes that the highland of the elevation 4,000 ~ 5,000 meters is widely distributed. The series B data consists the scenes that the highland of the elevation 2,000 ~ 4,000 meters occupies the greater part of the whole area. The series C data consists the scenes that the area with scares vegetation with the elevation less than 2,000 meters.

As the result, almost all the same result shown in Fig.II-3-1-4-3 was obtained, and the correction equation was also obtained to remove the vegetation information. Since the correction

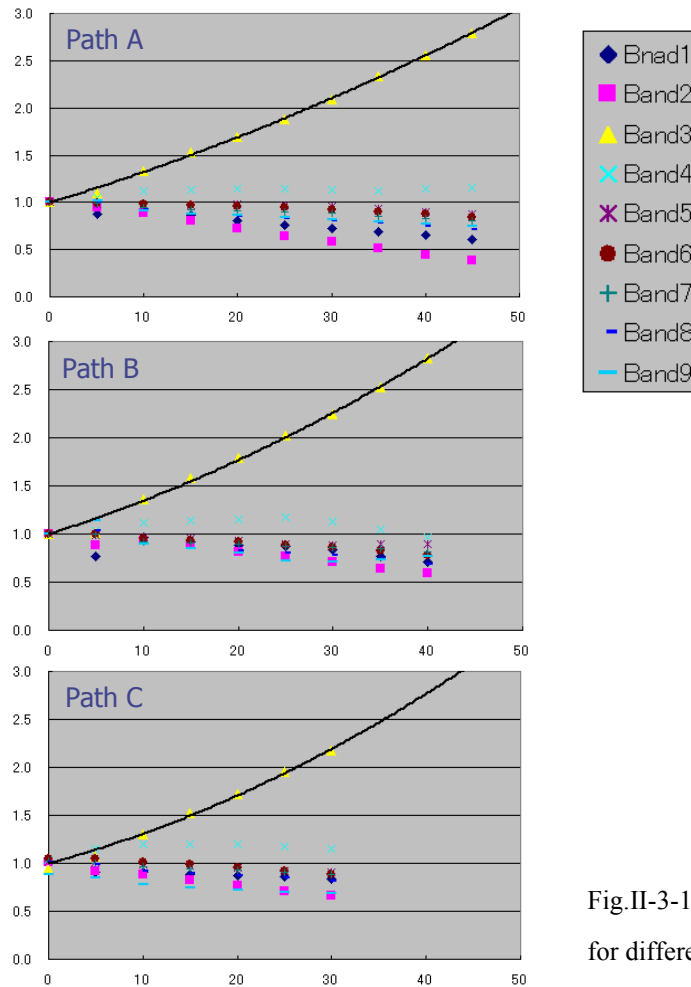


Fig.II-3-1-4-5 PSAVI versus pseudo reflectance for different pathes

equation is obtained by using the statistic information of the image, the specification of the reflection spectrum from the vegetation coverage of 100% that is difficult to estimate in the semi-arid area is not necessary. Moreover, this method is considered to be possibility of more correct correction because of the possibility of application of vegetation information corresponding to the target area.

(4) The Difference of Mineral Identification by the Removal of Vegetation Information

The above method was tested in the area where is covered with thick vegetation to confirm the effect of the vegetation information removal. The test area is shown in Fig.II-3-1-4-6a. In this scene, BGR were corresponded to Band 1, Band 4 and Band 7, respectively. The green color in image shows the area where vegetation grows thick. Fig.II-3-1-4-6b is the image without removal of the vegetation information. By using this image, alunite (red) and kaolinite (green) are widely distributed in the vegetation area, and the alteration zone that is already known is not identified. On the other hand, the image after the removal of the vegetation information is shown in Fig.II-3-1-4-6c. In this image, alunite and kaolinite are detected in the alteration zone that is already known. This means the removal of the vegetation information is effective to identify the minerals. The black part

is the area with the PSAVI less than 4.0 that is the area of analyzing limit in the present.

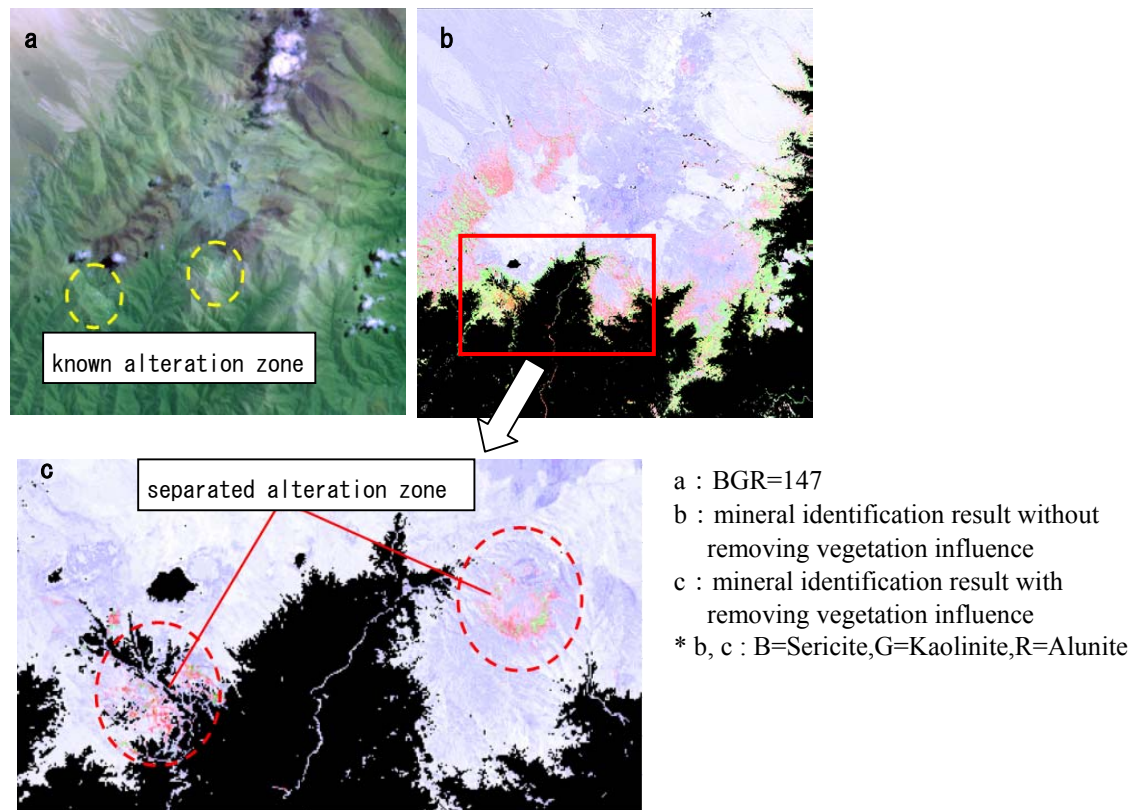


Fig.II-3-1-4-6 Effect of removing influence of vegetation in semi-vegetated area

(5) Problem of Vegetation Information Removal by PSAVI

As mentioned above, PSAVI is the method to estimate the pseudo-reflectance change by statistics and to correct the reflection spectrum from soil by using the statistics. The advantage is as follows; 1) not influenced by the soil brightness, 2) not necessary to estimate the reflection spectrum from the vegetation, and the correction equation can be obtained from the statistics corresponding to the vegetation of the target area, 3) not necessary to correct the quantity of the incident light, 4) can be applied by one correction equation.

The vegetation in the dried area is often composed of green plants and brown plants as dry grass. Although the reflection spectra from the green plants and the brown plants have the similar characteristics in the longer wavelength area of Band 4 (SWIR area), the spectrum in VNIR area shows different properties in Band 2 and Band 3 of ASTER by the effect of chlorophyll. In the case that the plants with different spectrum coexist, it is necessary to change the correction equation corresponding to the mixing rate. But, there are regrettably not the counter-measures in the present. Considering to the above spectrum change, it is necessary to introduce the parameters to evaluate the dry grass except Band 2 and 3, and to assume the correction equation with the parameters and the properties of Band 2 and 3. But, since the property of the reflection spectrum is similar to that of iron oxide minerals, the correction of this method is also considered to be difficult.

The influence of the vegetation information removal in the case that the change of quantity ratio of coexisting plants with different spectrum appears in the result of mineral identification. The mineral distribution is shown in Fig.II-3-1-4-7b after the mineral identification. In the Figure, BGR is corresponds to dolomite, chlorite + epidote and calcite, respectively. In this Figure, the extremely small quantity of chlorite is identified in the area T-11 that is dry grass largely occupied area. On the other hand, the small quantity of dolomite is identified in the outskirt to mountainside (T12 ~ 15) that the area in the little high ratio of the green plants. The observed reflection spectrum in these areas is almost constant, however, the spectrum change recognized in the Mineral Identification Map was not detected. The mineral change is estimated the mis-identification by the rate change of coexisting two kinds of plants. The fact remains as the subject in the future.

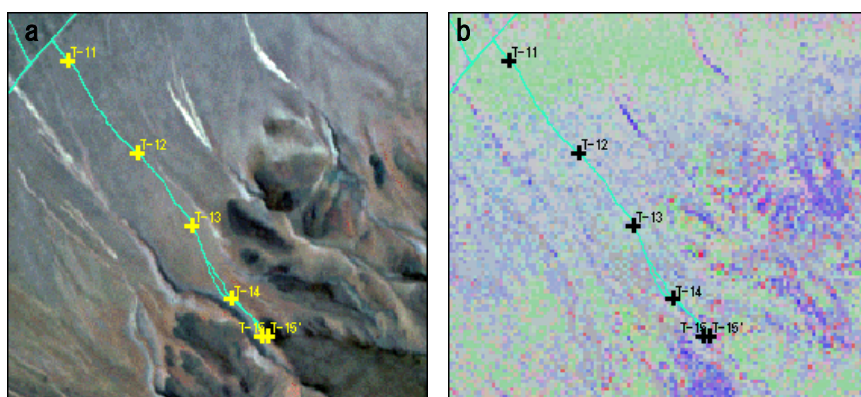


Fig.II-3-1-4-7 Mis-identification caused by change the composition ratio of vegetation types
a : BGR=123, b : BGR= Dolomite, Chlorite+Epidote, Calcite

3-1-5 Processing of false color images and the band ratioing composites

(1) False color images

ASTER data consists of three VNIR bands (excluding backward-view images), six SWIR bands and five TIR bands. False color images are prepared by selecting three kinds of appropriate combination of bands from these bands according to the purpose of analysis. In this work, the following two false color images were prepared.

① BGR = 123

② BGR = 147

Those of ① are false color images with three VNIR bands used, and their characteristic is high resolution (15 m/pixel). Therefore, these images can be used as a map to replace a geological map of the field survey. Particularly in areas where the geological map is not renewed frequently, there may be roads that do not show on the geological map, and/or locations of roads may be very different from their actual locations even if they are shown on the map in some cases. On these false color images, bare rocks and deserts are expressed with a brownish color tone, which is not suitable for geological analysis such as the identification of rock.

② is a false color image made by combining one VNIR band and two SWIR bands, and is effective for geological mapping and analysis including those of alteration zones. Alteration zones are composed of alteration minerals such as quartz, sericite, alunite, kaolinite and chlorite. Among these, sericite, alunite and kaolinite show characteristic absorption in the SWIR region and show large absorption particularly in SWIR Band 7. As sericite, kaolinite and alunite generally show high reflectance in Band 5, the decrease in reflectance is remarkable from Band 5 to Band 7. Therefore, it is possible to express alteration zones in a color tone clearly different from that of the vicinity on the false color image with Bands 5 and 7 used. When the purpose is not detection of alteration zones but identification of rocks, the false color image of non-correlation stretches, etc. is used in some cases.

(2) Band ratioing

For discriminating of alteration zones by band ratioing, band ratioing of BGR = 3/1, 5/4 and 5/7 is relatively frequently used for LANDSAT TM. With this calculation used, as alteration minerals show absorption around 2 μ m and 5/7 of the band ratioing value shows a large value in alteration zones, alteration zones are expressed as slightly reddish white. Because LANDSAT TM has a sensor with only one band (Band 7) around the wavelength of 2 μ m, alteration minerals cannot be subdivided. However, the ASTER sensor has five bands, Bands 5 to 9, around the wavelength of 2 μ m, and, therefore, alteration minerals can be identified more minutely from their characteristics of absorption.

The band ratioing places the minimum digital value as the atmospheric path radiance, obtains the value by deducting the minimum value from the digital value of each band, and obtains the ratio between the bands of these values. The ratio between the bands (value of band ratioing) is

usually in a range of 0 to 10, but density conversion is necessary to express the ratio between bands in the image, similar to the false color image. For density conversion, standard deviation and an average value of band ratioing values were calculated, and bias and gain were calculated so that the average of the band ratioing values would be 128 and 3σ would have 128 graduations of digital values.

In this work, two kinds of band ratioing were carried out; one is a method whose purpose is detection of alteration zones, and the other is emphasized band ratioing where the difference of alteration minerals in alteration zones is expressed as a difference in the color tone. Both have the same combination of band ratioing, and 4/5, 4/6 and 4/7 were used as BGR.

As the object of the former was detection of alteration zones, band ratioing values were calculated from the whole of one scene, and, after calculation of their average value and standard deviation, gain to be used for density conversion was determined. In the latter method, band ratioing values were calculated only from data of regions detected as alteration zones (regions where more similar rocks are distributed) and gain to be used for density conversion was determined. Therefore, the latter was given a larger gain than the former. If band ratioing is carried out targeting only regions containing alteration zones, it is possible to prepare an image where a difference of dominant kinds of alteration minerals is expressed by a difference in the color tone

3-1-6 Identification of alteration minerals

According to the operations described in the preceding sections, conversion into pseudo reflectance and correction of vegetation effect were carried out. Next, sensitive identification of minerals with iso-grain model was executed based on this pseudo reflectance data.

(1) Iso-grain model

Weathered material is generally made up of two or more minerals, and the reflectance spectra of weathered materials are composed of what is summed up with reflectance spectra peculiar to the minerals comprising the material. A reflectance spectrum of each mineral and that of weathered material have a non-linear relationship. In iso-grain model, when surface reflectance and absorption rate per wavelength are given for each mineral, and particle size is assumed, a synthetic spectrum allowed to be calculated with the mixture ratio of two or more components given.

(2) Identification minerals and the database of simulation

Nine minerals were identified in the analysis of last year. In the analysis of this year, the database with 10 minerals to add jarosite of iron oxide mineral to the last year's identification minerals, and mineral identification was carried out. The identified minerals are as follows:

- ①Alunite (Aln) ②Kaolinite (Kao) ③Gypsum (Gyp) ④Sericite (Ser) ⑤Hematite (Hem)
⑥Calcite (Cal) ⑦Chlorite (Chl) ⑧Quartz (Qtz) ⑨Goethite (Goe) ⑩Jarosite (Jar)

In addition, mineral identification was carried out with twelve minerals, epidote (epi) and pyrophyrite (pyr) was added to the above mentioned ten minerals, on the scene of B11 and C05 of which include El Pago area and Pancho Arias area to distinguish alteration types. For the result of this analysis, see Chapter4.

The database of mixing reflectance of minerals was prepared with multiple components in units of 10% (all mixing patterns where total percentage of minerals is 100% were considered. For example, Aln 20%, Kao 20%, Ser 30%, Goe 20% and Qtz 10%).

(3) Identification of minerals

A database that calculates pseudo reflectance of the combinations of minerals mixed by various volume ratios was prepared in advance, and identification of kinds of minerals was carried out by comparing this index with pseudo reflectance of each pixel. For the identification, pseudo reflectance calculated from the image is compared with pseudo reflectance of a synthetic reflectance spectrum made with the database, one by one, and the solution is a synthetic reflectance spectrum that has the smallest sum of squares of error in each band. In the actual work, the standard error from data that are the most consistent is only a little different than the standard error from the second data and the third data. Identification of minerals does not have an accuracy with which such a small difference between standard errors can be identified due to the present accuracy of conversion of pseudo reflectance, the assumption of grain of the kind of minerals and the assumption that an identification mineral is represented by one spectral reflectance. Therefore, the top three were considered as the solution, and the average value of mineral contents of the top three was determined to be the output value here

Although an index was made with mineral mixture ratios in units of 10%, processing of one scene took one week, even though the program was made to work at high speed. Therefore, processing time was shortened (about 1/50 of the previous processing time) by the use of an index in units of 20% this time.

(4) Results of analysis

The results of the analysis were output as contents of ten components. If one component in these output data is expressed with a concentration, a concentration distribution map can be prepared. When any three components are expressed as BGR values, a distribution diagram of three components can be prepared. Alunite and kaolinite are summed up to be dealt with as one component and are expressed as "BGR = Chl, Ser, Aln+Kao" and a distribution map of porphyritic, phyllic and advanced argillic alteration zones can then be prepared. In this analysis, three components, hematite, goethite, and jarosite, were taken; therefore, a distribution map of iron oxide can be prepared.

In this case, the following four kinds of alteration mineral distribution maps were prepared:

- ① BGR = Ser, Kao, Aln

- ② BGR = Chl, Ser, Aln+Kao
- ③ BGR = Chl, Ser, Cal
- ④ BGR = Hem, Goe, Jar

On the images used for this analysis, lots of clouds, shadows of clouds and salt lake sediments are distributed. In the regions of clouds, the alteration minerals are wrongly identified according to the density of clouds in some cases. In the portions of shadows, because of a very low luminance value, the influence of noise is received, and a wrong result is similarly output in some cases. As there is a distribution of rock salt, which is not included in the identification minerals, in salt lake sediments, alunite and kaolinite are identified together with gypsum. These regions could be identified wrongly were distinguished by using the false color image together.

As there is a characteristic that alteration zones containing alunite and kaolinite are expressed as bright white on the band ratioing composite (BGR = 4/5, 4/6, 4/7) and as light green on the false color image (BGR = 147), alteration zones were discriminated by eye together with the results of mineral identification. In most of the regions identified as alteration zones on the band ratioing composite and the false color image, alunite, kaolinite and sericite are identified from the result of mineral identification. Therefore, it is presumed that the results of analysis are good on the whole in this stage.

4-3-8 SiO₂ content map

One of characteristics of the ASTER sensor is that it has five bands in the thermal infrared region. METI (1998 - 2000) and Resource and Environment Observation and Analysis Center (1991, 1992) reported examples of study to estimate SiO₂ content in igneous rock from absorption characteristics resulting from Si-O-Si vibration in the TIR of the ASTER. Particularly, the METI (2000) suggested the following SiO₂ estimation expression from four bands of the ASTER, Bands 10 to 13:

$$\text{SiO}_2(\%) = 56.20 - 271.09 \times \text{Log}((\text{Ems}[10] + \text{Ems}[11] + \text{Ems}[12]) / 3 / \text{Ems}[13])$$

Ems [n] = Emissivity of ASTER Band n

However, at the same time, the METI (2000) showed that it was necessary to re-examine the accuracy of SiO₂, including the problem of influence of desert burnish upon emissivity characteristics (Ogawa et. al., 1999), because the 95% confidence interval of the estimated volume given by the calculation expression shown above reaches as high as $\pm 15\%$.

Here, we attempted mapping of SiO₂ content in the TIR of the ASTER using the SiO₂ calculation expression mentioned above.

(1) Atmospheric correction

In this study, atmospheric correction parameters (τ_λ , Rd_λ and Ru_λ) in Bands 10 to 14 were found by the use of MODTRAN 3, a program for calculation of radiation transmission. While

MODTRAN 3 has 6 kinds of air models and 12 kinds of aerosol models, the model of the 1976 US Standard was employed as an air model and the Desert Extinction Model was employed as an aerosol model. With consideration given to the fact that the climate of this area is dry to semi-dry, the value of vapor was determined to be that of the 1976 US Standard (average relative humidity: 19.36%).

Atmospheric correction parameters (τ_λ , Rd_λ and Ru_λ) were obtained from the following values by the use of the air model that had been established:

Air model: 1976 US Standard

Aerosol model: Desert Extinction Model

Height of the sensor: 100 km (which is the maximum value that can be set, actual height is 705 km.)

Height of ground surface: Set as 2 km

Direction of observation: Directly under (Zenith Angle = 18)

Angle of scanning in the ASTER TIR is $\pm 2.44^\circ$, and pointing angle is $\pm 8.55^\circ$. The difference of path length between observation with the sensor inclined most sharply and observation directly under the sensor is as small as around 2%.

Values of transmittance, sky radiance and optical path radiance in Bands 10 to 14 were weighted means, where a weight of 50% (wavelength at both ends) to 100% (central wavelength) was added to each wavelength.

In addition, elevation correction in atmospheric correction was carried out using DEM data of AST3A01 product in the analysis of this year.

2) Temperature-emissivity separation

Regarding temperature and emissivity separation in the thermal infrared region, as the number of unknown values is larger than that of observed values, temperature and emissivity are estimated by reducing the unknown number by various methods. ASTER data (Bands 10 to 14) has five observed values, while the number of unknown values is six in total: one value of temperature and five values of emissivity.

In this study, temperature and emissivity were segregated by the method combining the following three methods (Gillespie et al, 1996):

* Normalized emissivity method: NEM

* Ratio method: RAT

* Mean and max-min difference method: MMD

In this calculation, emissivity on the ground surface is simply estimated by the normalized emissivity method and the ratio method. Wavelength mean emissivity is found for the scatter of the estimated values in the direction of the wavelength by the use of the empirical formula (the mean and max-min difference method), and, using this value, the simply estimated values of emissivity on

the ground surface are modified.

3) Results of processing

The method described in the preceding section allows the emissivity image and the ground-surface temperature image to be prepared. The distinctive characteristic of the data used for this analysis is that scatter in the data is very large in comparison with that of the METI(2001). Especially, there are extremely small values, and, if such data is used as it is, there will be significant danger of arriving at wrong results of analysis when segregation of temperature and emissivity is calculated. Abnormally small values seem to be the result of the influence of clouds. Here, the mean value and the standard deviation were calculated for each band, and those that are beyond $\pm 3 \sigma$ in one or more bands of the five bands are excluded from processing.

4) Mapping of SiO₂ contents

A SiO₂ content map can be prepared by using emissivity data (Bands 10 to 13) and the SiO₂ conversion expression mentioned above. However, as the rock to which the conversion expression applies is silicate rock only, it is necessary to remove carbonate rock such as limestone. There are still many problems in the calculation of SiO₂ content, and examination is required including that of the problem of desert burnish.

3-1-8 DEM (Digital Elevation Model)

ERSDAC, the supplier of ASTER data, began to supply the advanced products of ASTER data as of present fiscal year. 3A01 data that is one of the advanced products was used in the analysis in this year. The 3A01 data consist of a data set of orthographic projection image and DEM. Before ERSDAC serves this product, users must obtain L1A data to convert the orthographic projection and to make DEM for themselves. After the service began, the users become to able to easily use DEM data. The consideration of the analyzed result was carried out by making three dimensional bird-eyes view by using DEM data, at the same time, the topographic map (contour map) of the field survey area was prepared previously to the survey, and was used for survey. In this analysis, using the thermal infrared data made the estimated SiO₂ content map. To make the above map, the elevation correction was carried out as a pre-processing by using DEM data.

3-1-9 Task for the future

In this analysis, the removal of vegetation data was tried by using PSAVI that had been calculated to obtain SAVI from pseudo-reflectance. The PSAVI has the following merits; 1) not influenced by the soil brightness, 2) not necessary to estimate the reflection spectrum from vegetation (possible to obtain the correction equation from statistic value corresponds to the vegetation of the target area). In this analysis, the accuracy of mineral identification could be improved in the area that is covered by vegetation up to 40%. However, at this time, there is no

counter-measure to change the correction equation in this PSVI method in case of the mixing existence of the plants with different reflection spectra. The popular vegetation consists of green plants and brown plants such as dry grass in the arid area. The correction equation change corresponds to the mixing ratio of the above two kind of plants remains as the subjects. But, since the characteristics of the reflection spectrum from dry grass is the similar to that of the iron oxide minerals such as hematite, the correction is considered to be difficult.

The mineral identification and the zoning of the alteration zone was carried out in the scenes (B11 & C05) including El pago region and Pancho Arias region in the survey area of porphyry type deposit. The target minerals of the mineral identification are 12 minerals of ordinary 10 minerals, and epidote and jarosite. As the result of the zoning of the alteration zone, the zonal structure including propiritic zone was confirmed. The detection of potassic zone becomes possible to add biotite for mineral identification target in the future, this method is considered to be more useful to prospect the deposit.

The data C 06 ~ 12 had been taken in the winter of this area within the data that were used in this analysis. The scenes that were taken in winter are suitable to topographic interpretation, because the slanting ray of light due to the low sun angle emphasizes the topographic characteristics. On the other hand, since the southern slope of mountain becomes the shadow side, the brightness becomes low, and the possibility of mis-interpretation becomes higher in mineral identification because of the relatively high noise level. The data that had taken in the west of C06 ~ C12 data had not been obtained as the high quality data. Therefore these data were not used in this analysis. The analysis of the area is necessary to use the proper (cloudless) data that are taken in summer of this area.

3-2 Interpretation and analysis of images

3-2-1 Method of interpretation and analysis

This section provides a summary of discriminated alteration zones for each scene. Results of ground truth survey are also described where it was carried out. Outline of the 22 scenes of ASTER data used for analysis, see Table II-3-1-1.

False color images, ratio images and alteration mineral identification images were mainly used to discriminate alteration zones. These were comprehensively examined by visual observation. The prepared images are described below.

- ①BGR=147 (False color image) Fig.II-3-2-1-1
- ②BGR=4/5, 4/6, 4/7 (Ratio image) Fig.II-3-2-1-2
- ③BGR=Sericite, Kaolinite, Alunite (Mineral identification) Fig.II-3-2-1-3
- ④BGR=Chlorite, Sericite, Alunite+Kaolinite (Mineral identification) Fig.II-3-2-1-4
- ⑤BGR=Chlorite, Sericite, Calcite (Mineral identification) Fig.II-3-2-1-5
- ⑥BGR=Hematite, Goethite, Jarosite (Mineral identification) Fig.II-3-2-1-6
- ⑦SiO₂ content Fig.II-3-2-1-7

In addition, discriminated alteration zone for entire scene is shown in Fig.II-3-2-1-8.

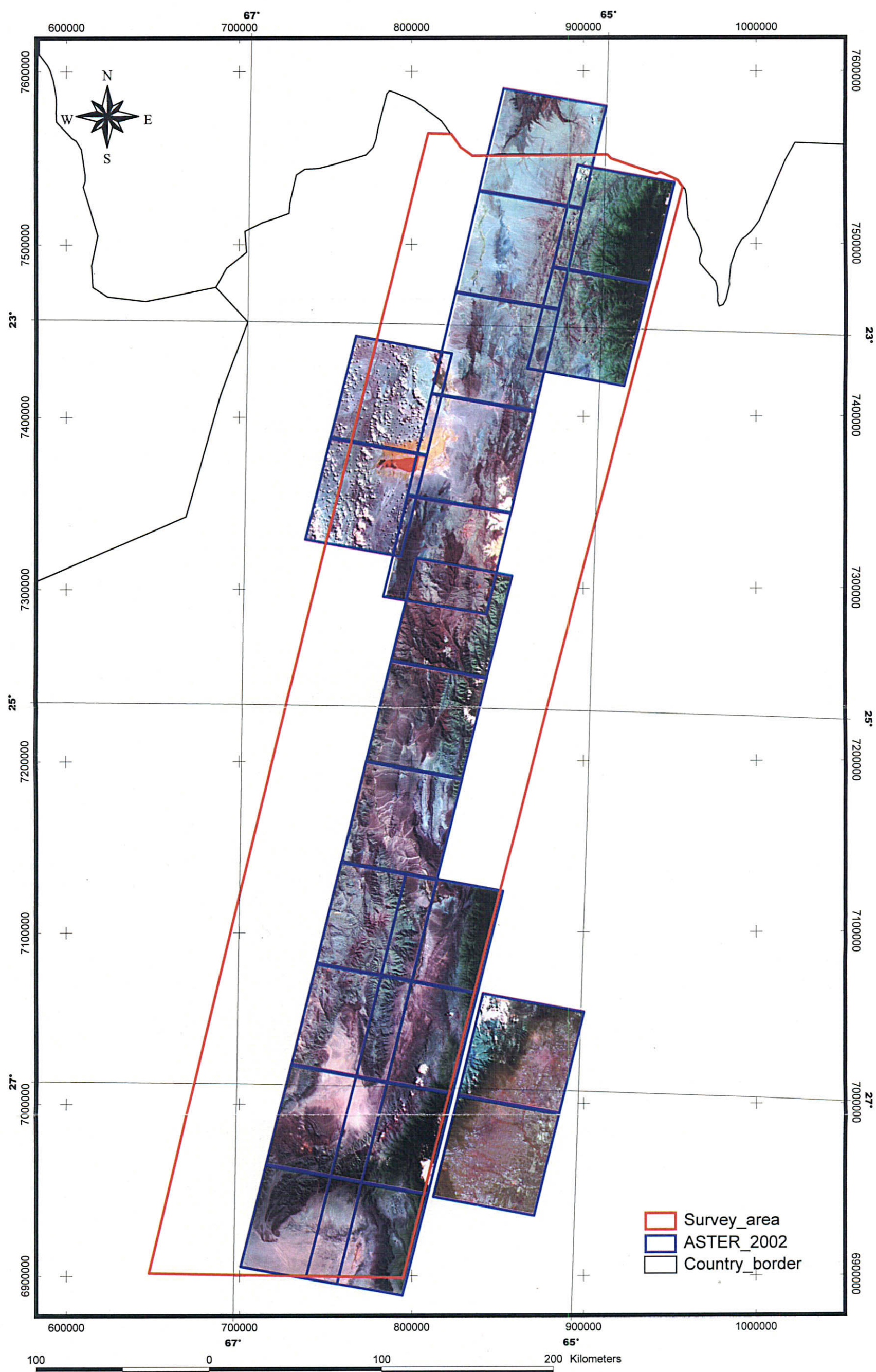


Fig.II-3-2-1-1 BGR=147 (False color image)

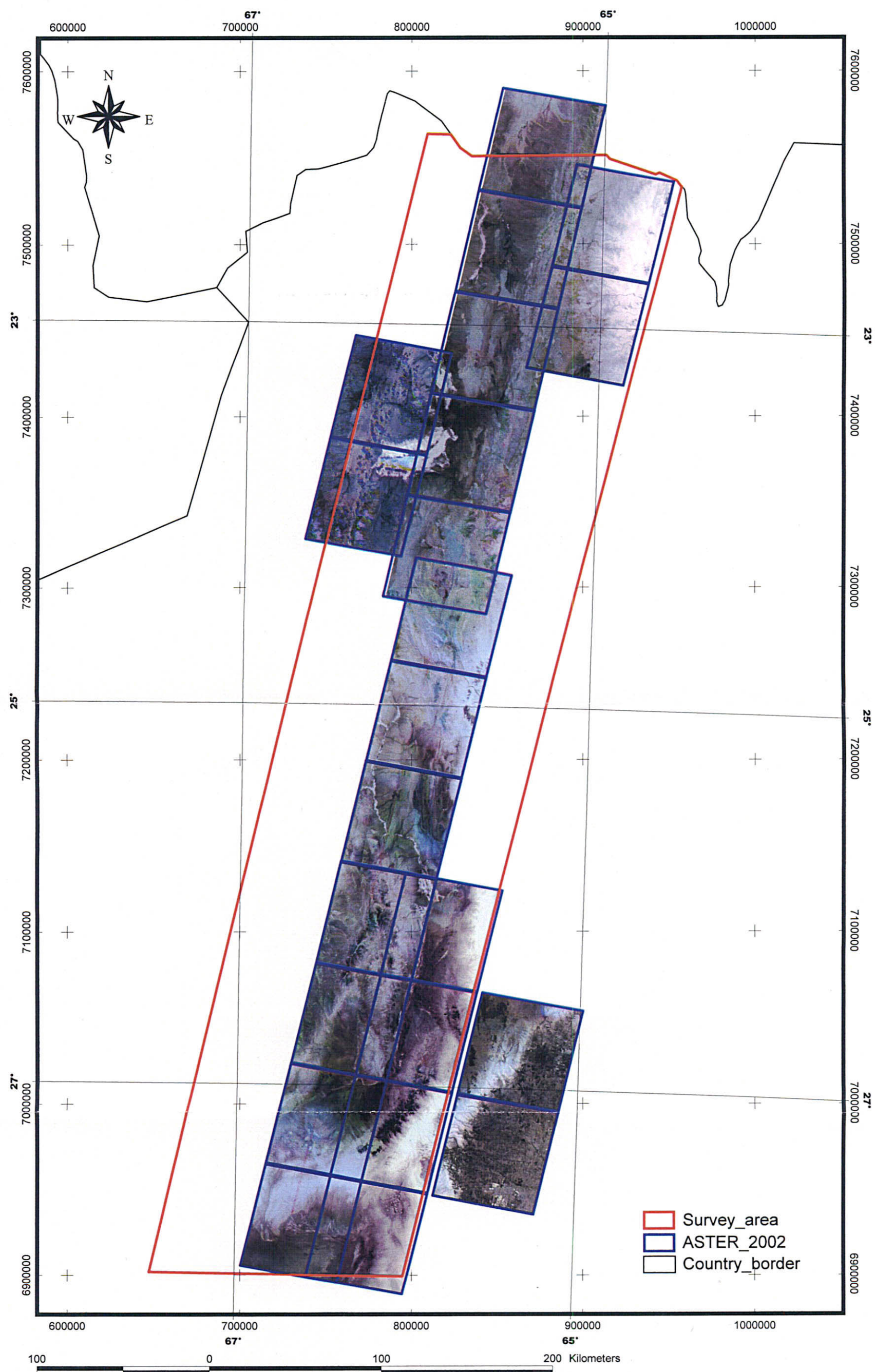


Fig.II-3-2-1-2a BGR=4/5, 4/6, 4/7 (Ratio image)

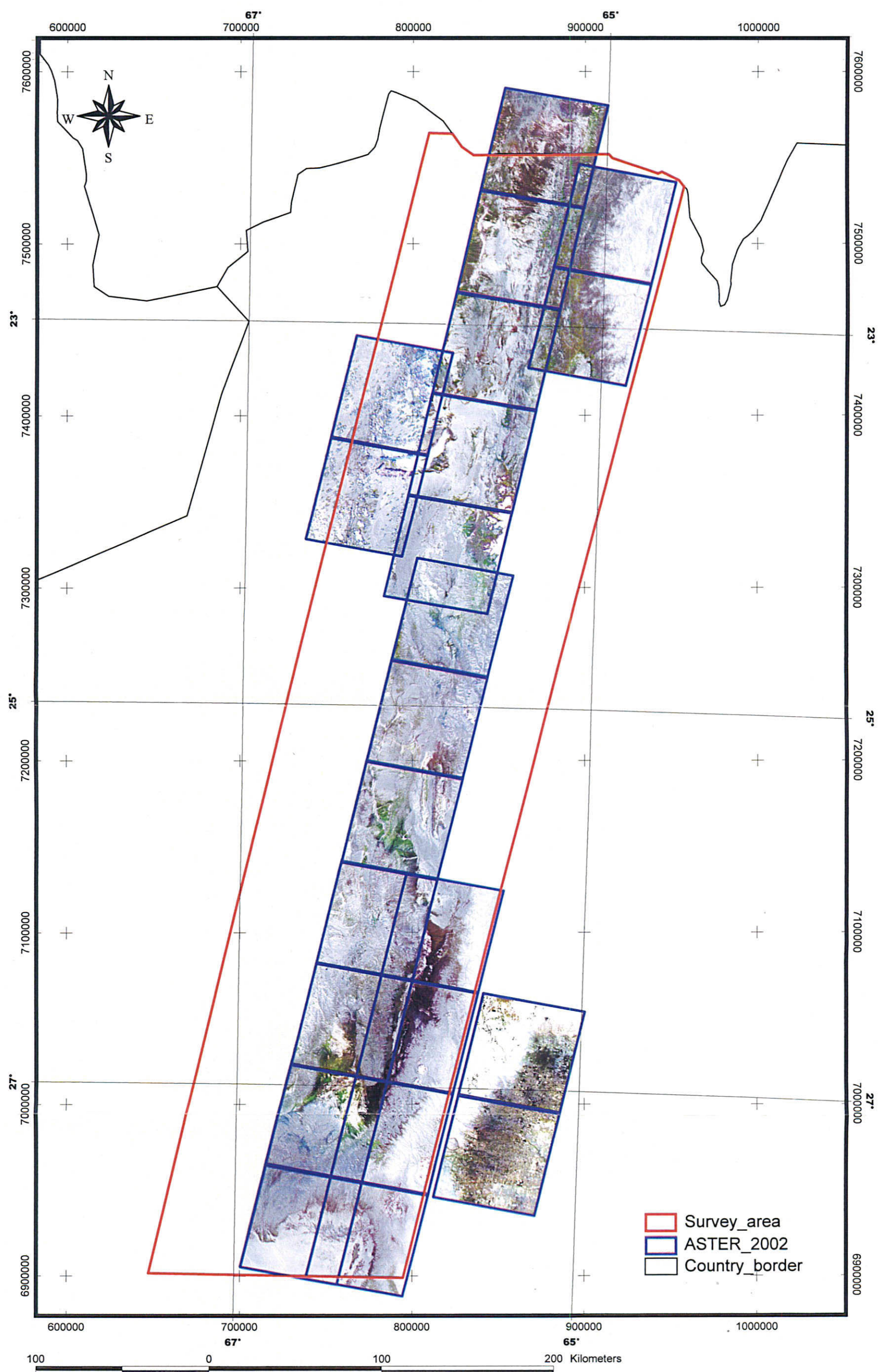


Fig.II-3-2-1-2b BGR=4/5, 4/6, 4/7 (Emphasized ratio image)

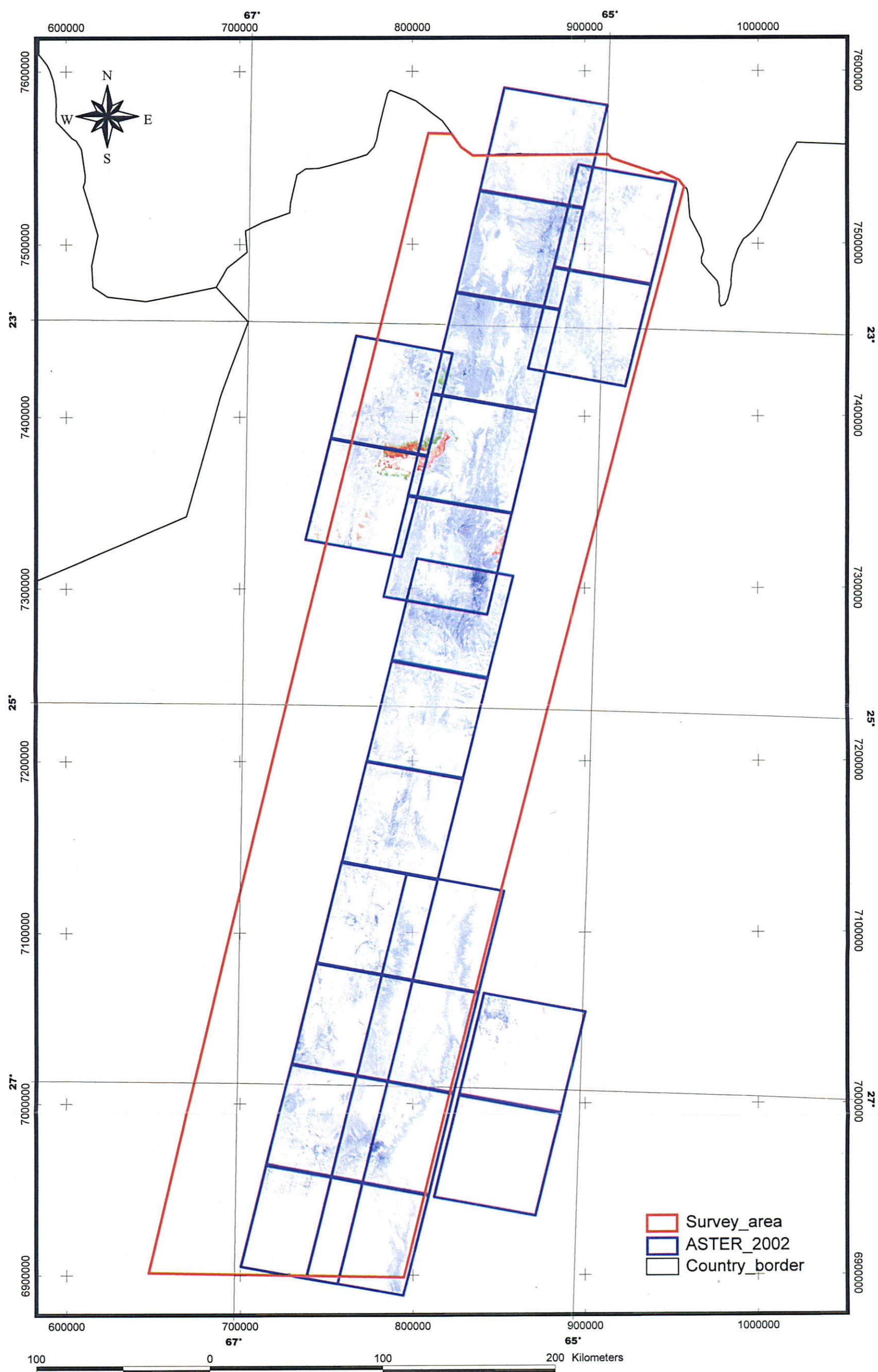


Fig.II-3-2-1-3 BGR=Sericite, Kaolinite, Alunite (Mineral identification)

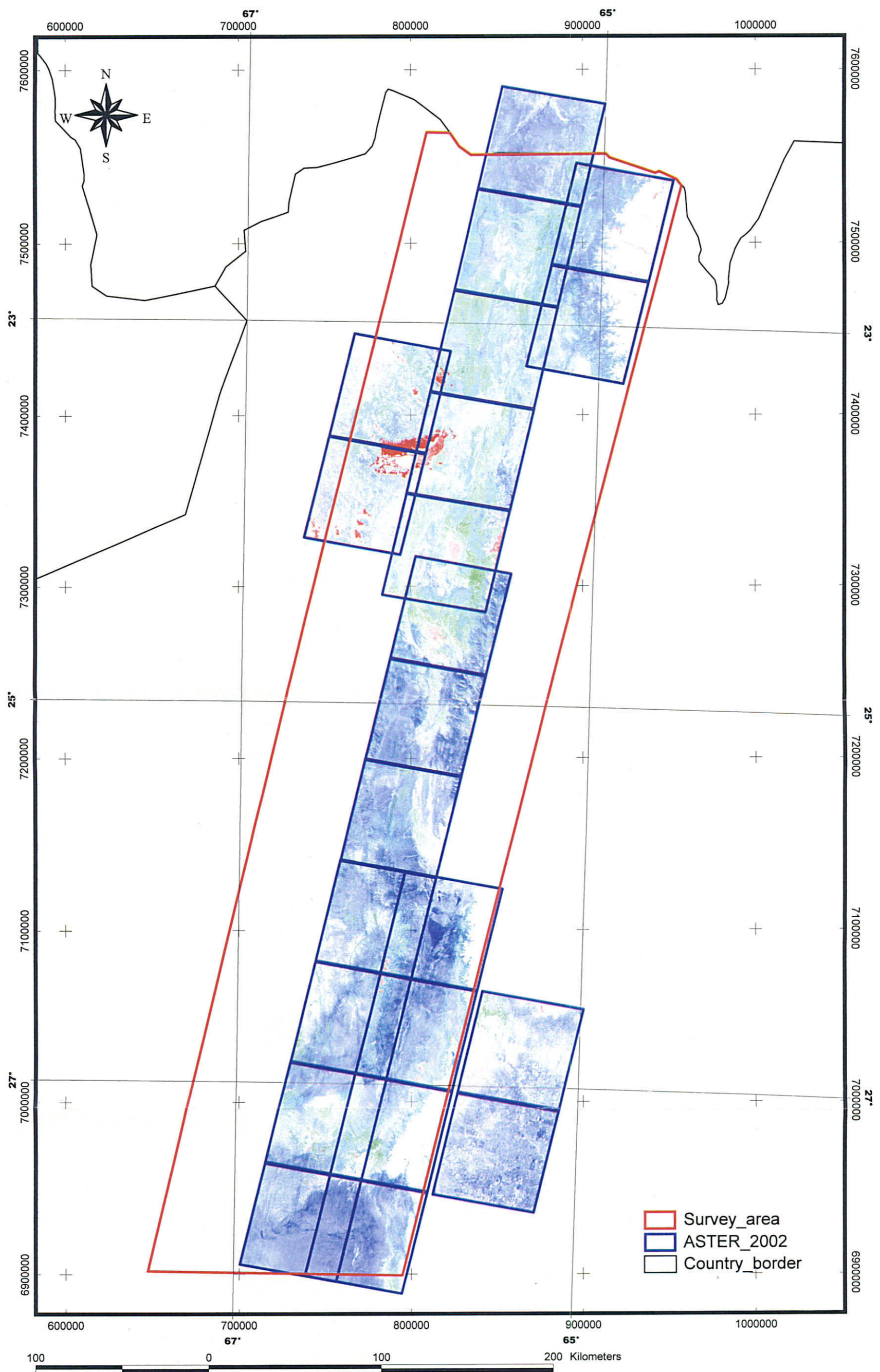


Fig.II-3-2-1-4 BGR=Chlorite, Sericite, Alunite+Kaolinite (Mineral identification)

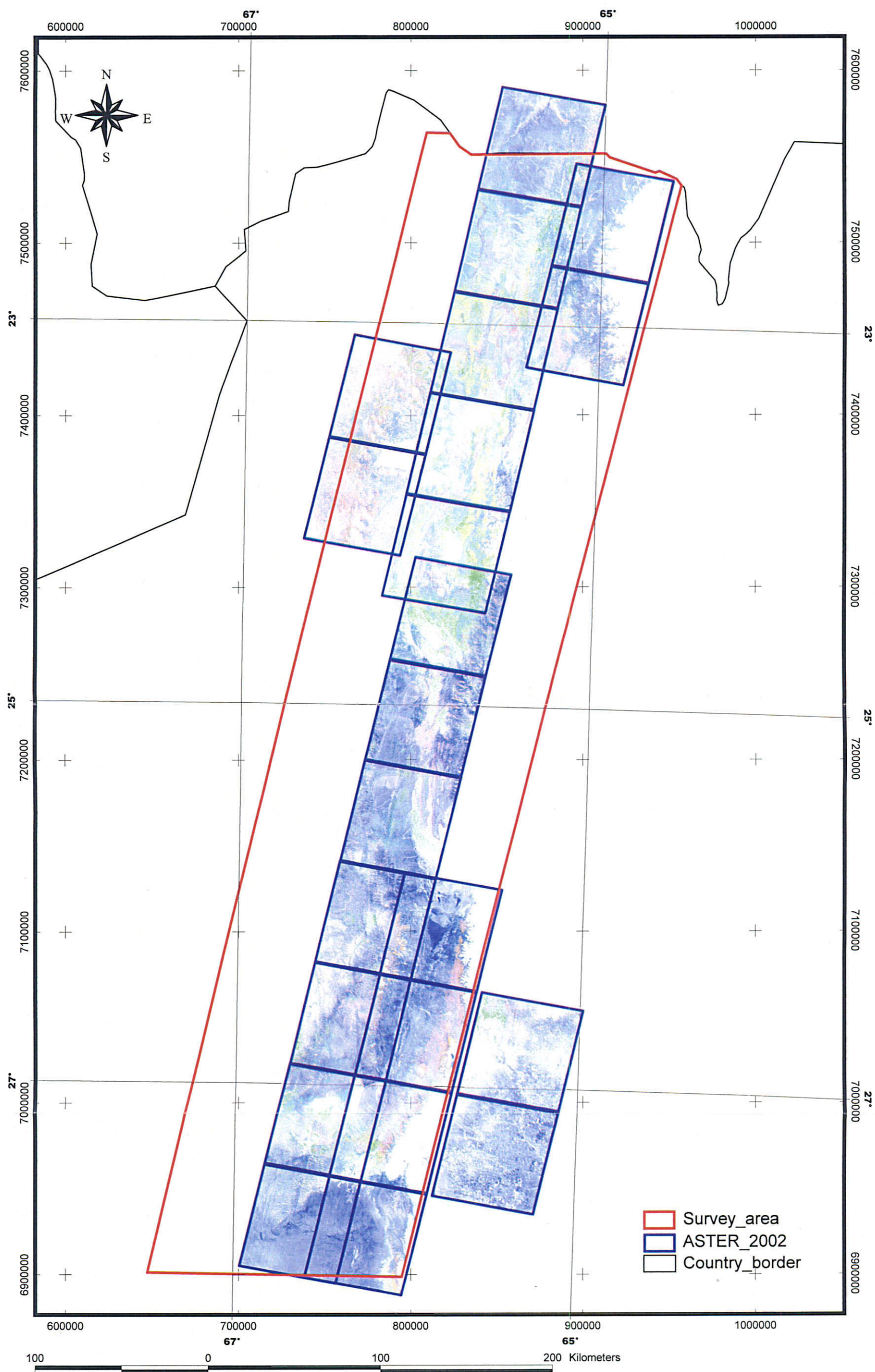


Fig.II-3-2-1-5 BGR=Chlorite, Sericite, Calcite (Mineral identification)

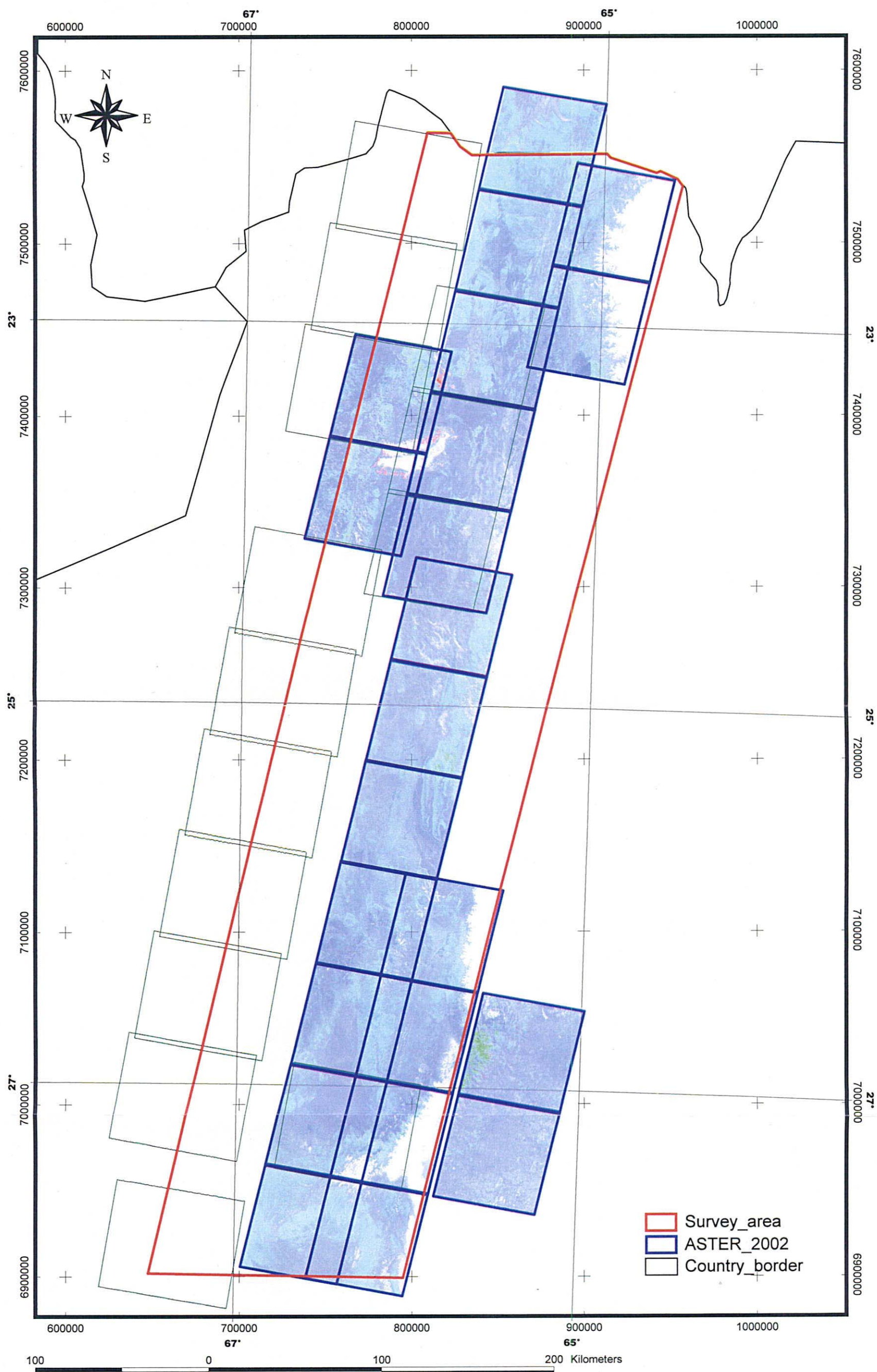


Fig.II-3-2-1-6 BGR=Hematite, Goethite, Jarosite (Mineral identification)

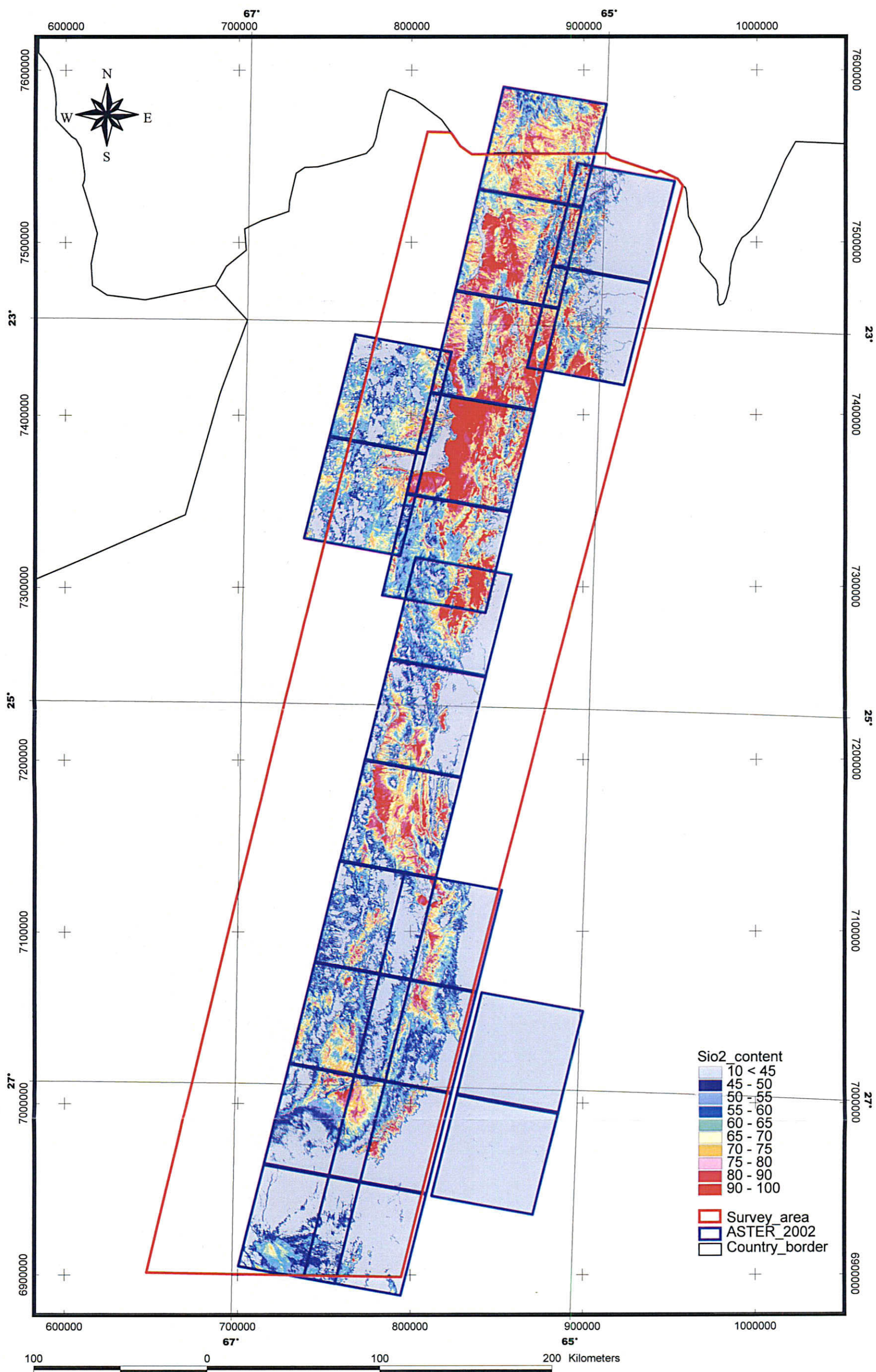


Fig.II-3-2-1-7 SiO₂ content

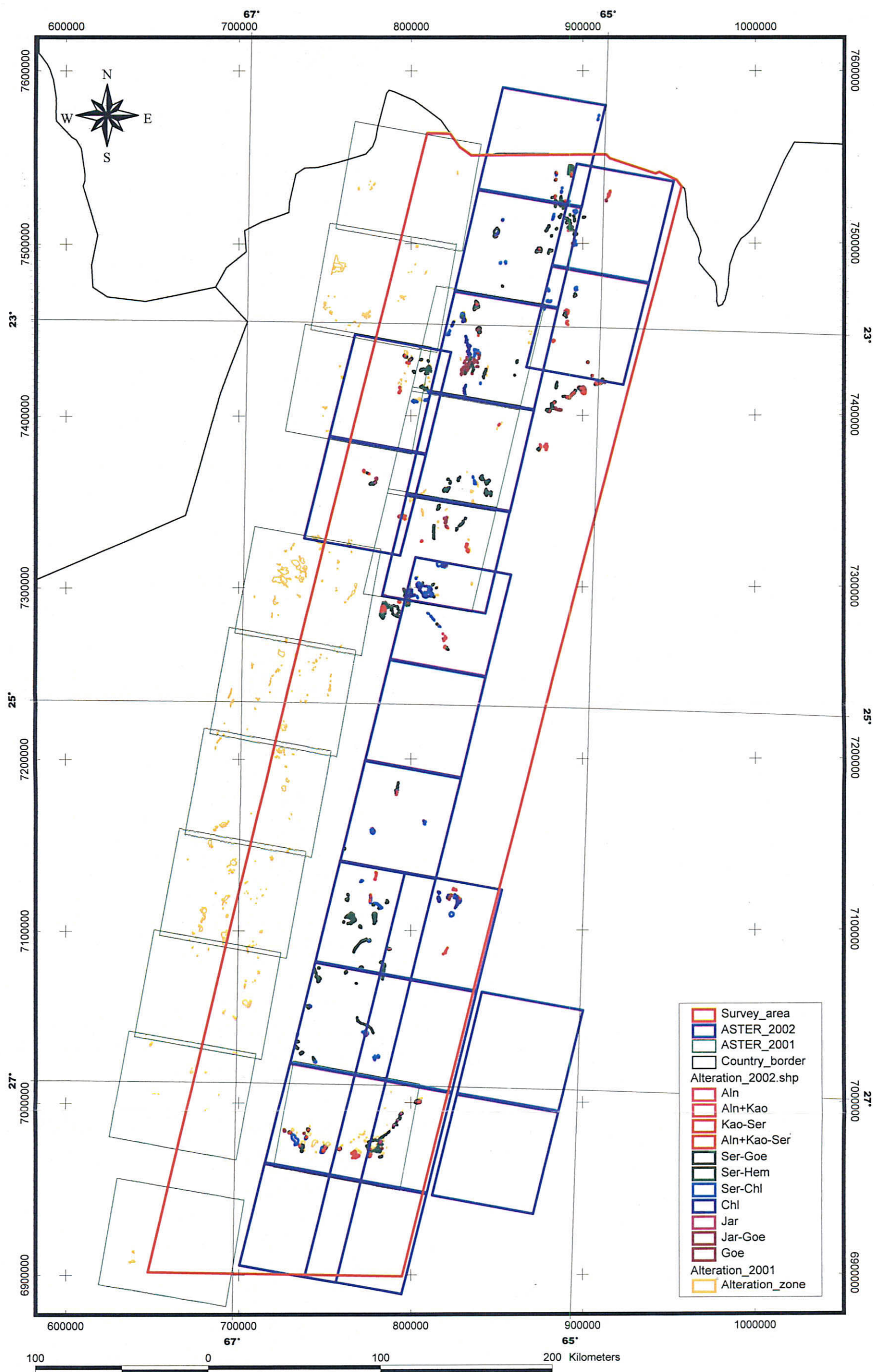
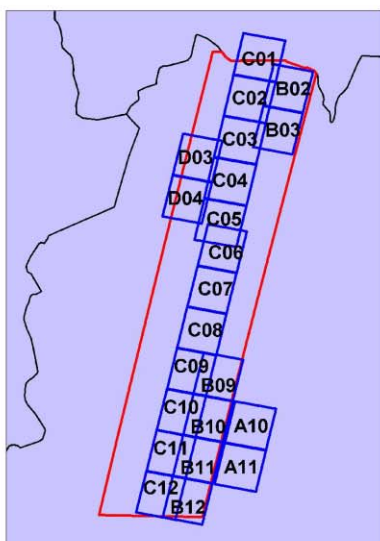
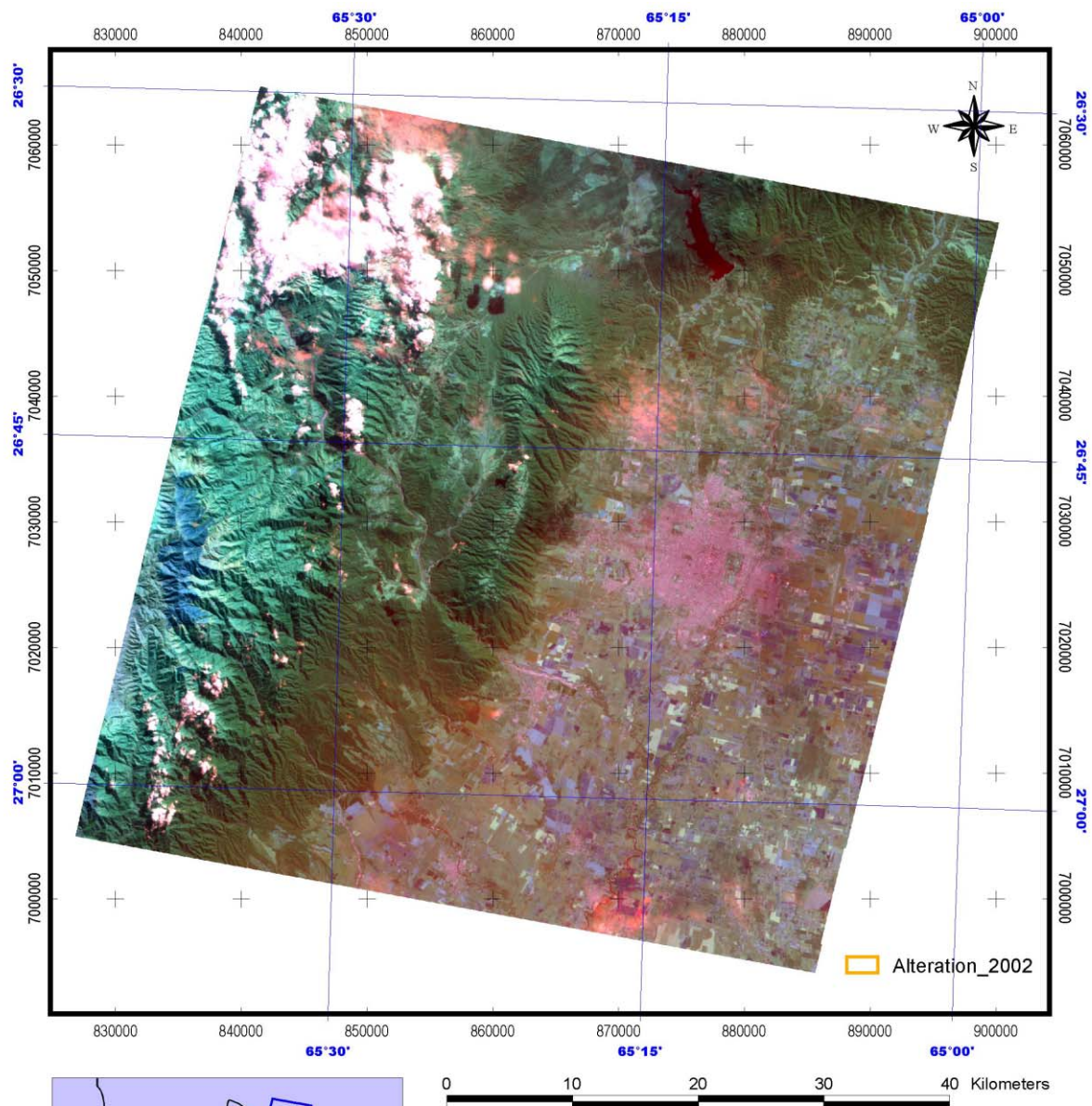


Fig.II-3-2-1-8 Alteration zone outlined by ASTER data analysis

3-2-2 Results of interpretation and analysis

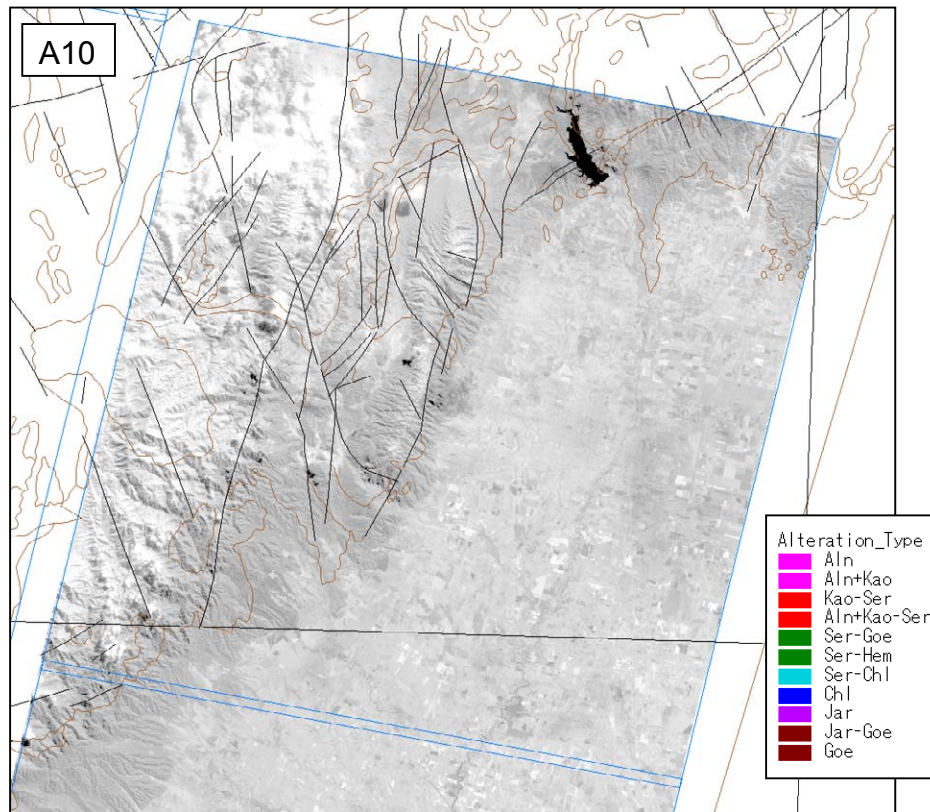
The results of interpretation of alteration zones in each scene are described below. The numerical values written in each interpretation map are the serial numbers of alteration zone groups in the whole analysis area. For alteration zones existing singly, A, B, C- - are used in each scene.



SCENE A10

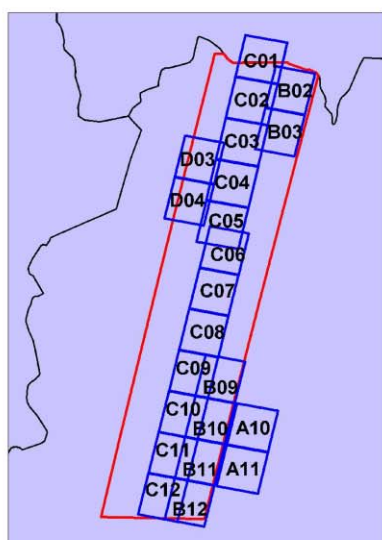
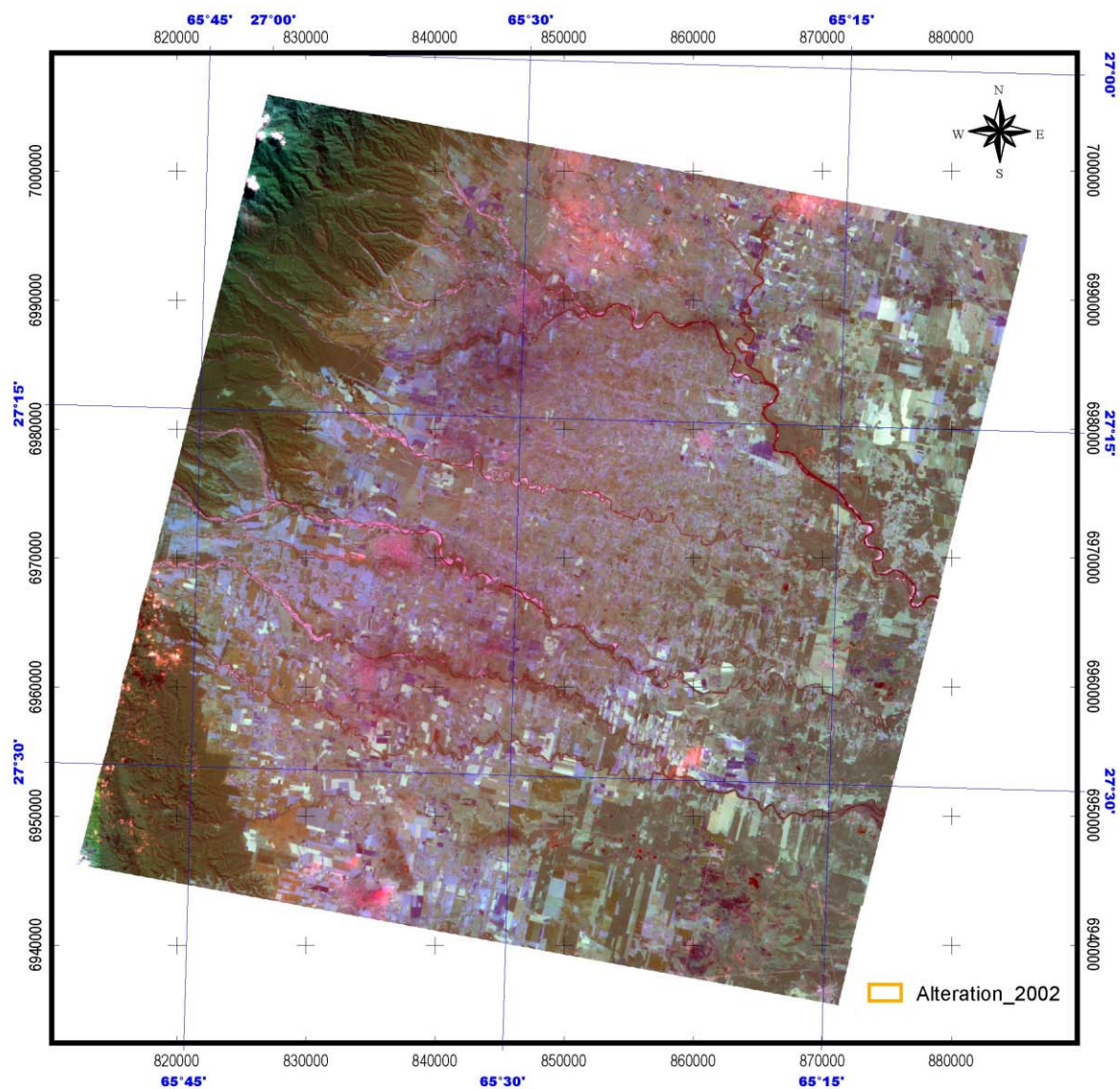
IMAGE : TERRA/ASTER BGR=147
PROJECTON : Universal Transverse Mercator
PROJECT : JICA/MMAJ/JMEC
DATA : ERSDAC/JAPAN

Fig.II-3-2-2-1 False color image of scene A10 (BGR=147)



[General]

Vegetated mountainous region distributes in the western part, and an urban area (Tucuman City) spread in the eastern part. El Alisar prospect, where field survey was carried out last year, locate at the western end of this scene. No alteration zones were discriminated in this scene

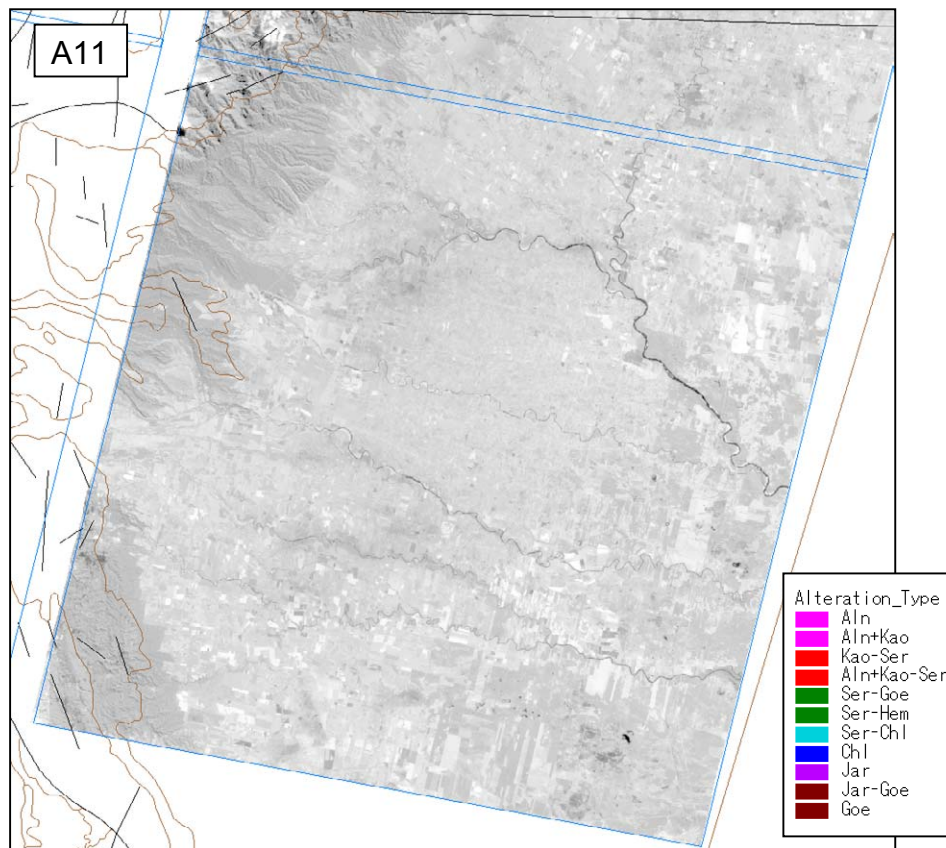


0 10 20 30 40 Kilometers

SCENE A11

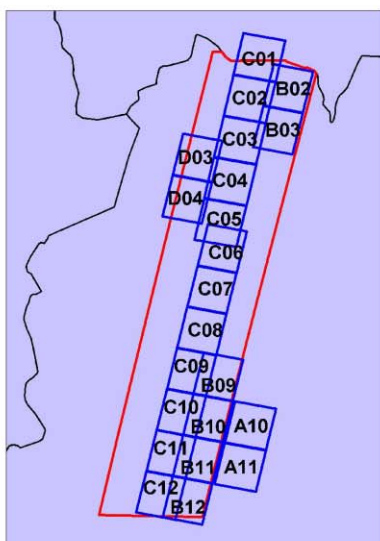
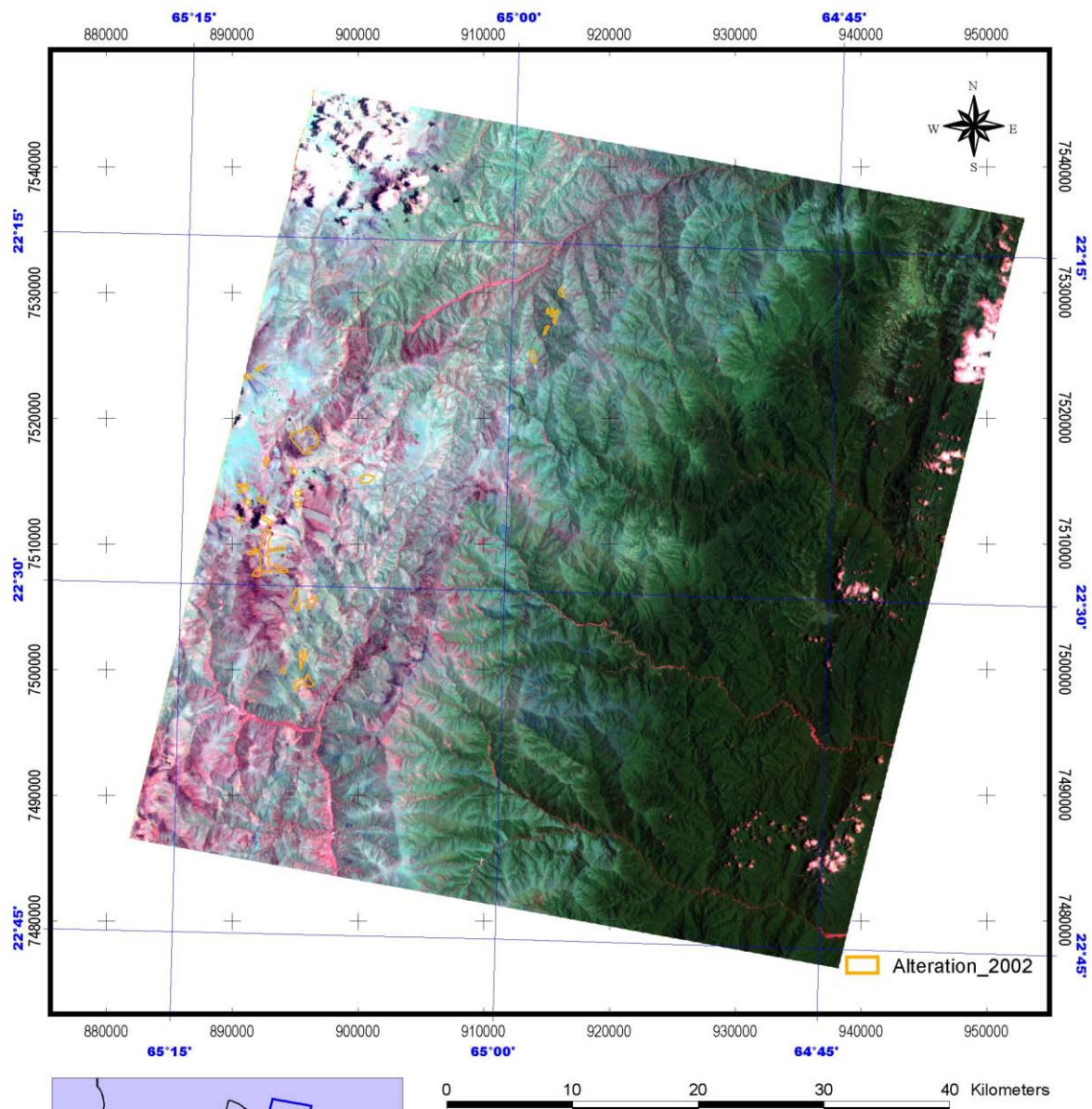
IMAGE : TERRA/ASTER BGR=147
 PROJECTON : Universal Transverse Mercator
 PROJECT : JICA/MMAJ/JMEC
 DATA : ERSDAC/JAPAN

Fig.II-3-2-2-2 False color image of scene A11 (BGR=147)



[General]

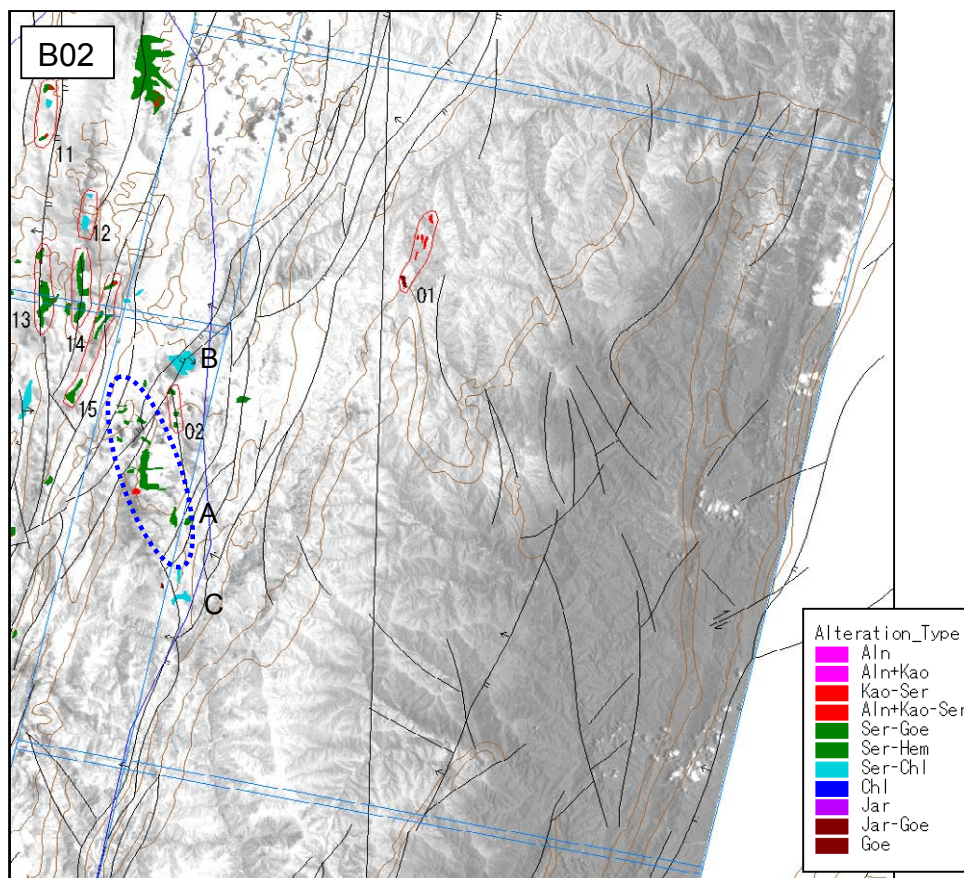
Vegetated mountainous region distributes at the western border, and an urban area (Concepcion City) is spread in the middle to eastern part. No alteration zones were discriminated in this scene.



SCENE B02

IMAGE : TERRA/ASTER BGR=147
PROJECTON : Universal Transverse Mercator
PROJECT : JICA/MMAJ/JMEC
DATA : ERSDAC/JAPAN

Fig.II-3-2-2-3 False color image of scene B02 (BGR=147)



[General]

The middle to eastern part is a vegetated area, and bare rocks are distributed in the western part. The western half of this scene corresponds to Santa Victoria area, where field survey was carried out. Several alteration zones are discriminated in the northwestern part.

[Alteration zones]

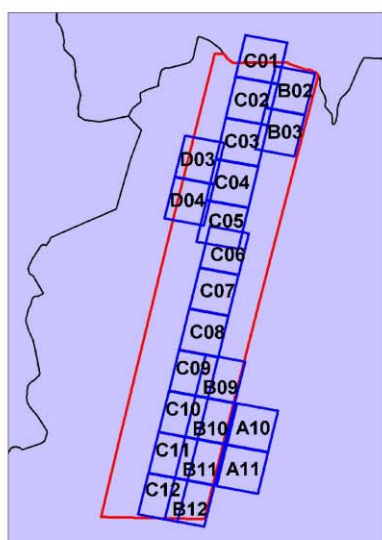
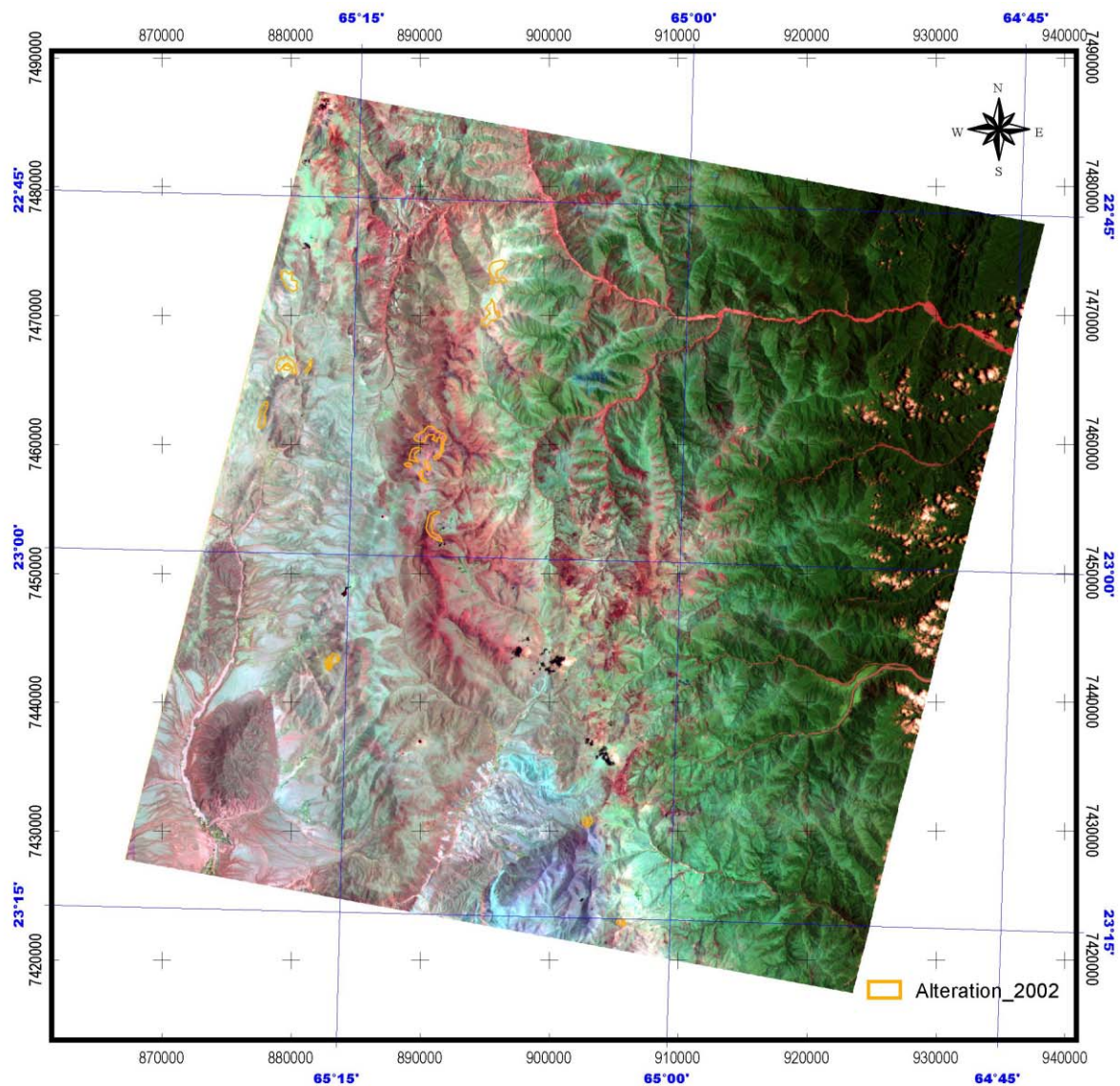
No.01: Alteration zone of *Ser* accompanied by some quantity of *Kao*. Their distribution is elongated in NNE-SSW direction. Geology is Ordovician sedimentary rocks, and distribution of the alteration zone is parallel to the main structures.

No.2: In the image of BGR=147 (hereinafter referred to as “in 147”), shown in right green. Alteration zone made up of *Ser-Goe* running in the NNW - SSE direction. Located on a fault.

A: Composed of *Ser* and *Hem*>*Goe*, and distributed near the ridgeline. Does not show the typical color of alteration zones (weak *Ser* alteration does not show the typical color in many cases). Mainly located in Cambrian sedimentary rocks.

B: Made up of *Ser-Chl* and *Hem*>*Goe*. Does not show the typical alteration color. Paleogene sedimentary rocks are distributed.

C: Composed of *Ser-Chl* and *Hem*>*Goe*. Shows dark brown in 147. Geology is Cambrian sedimentary rocks.

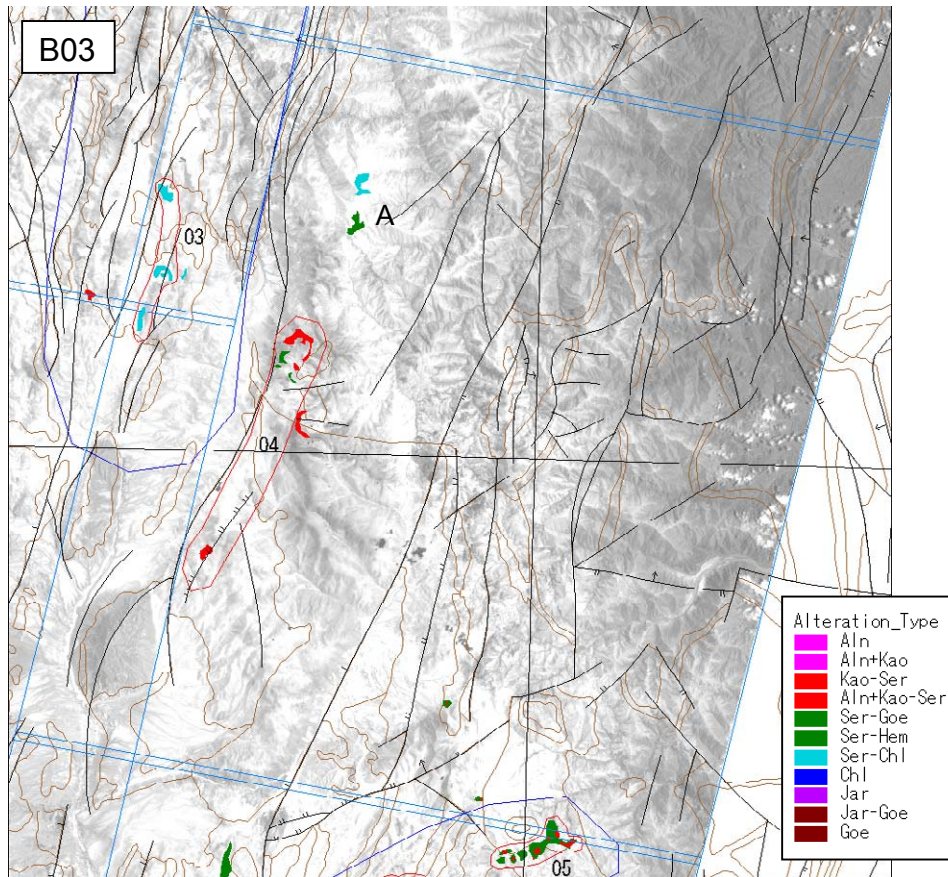


0 10 20 30 40 Kilometers

SCENE B03

IMAGE : TERRA/ASTER BGR=147
 PROJECTON : Universal Transverse Mercator
 PROJECT : JICA/MMAJ/JMEC
 DATA : ERSDAC/JAPAN

Fig.II-3-2-2-4 False color image of scene B03 (BGR=147)



[General]

The middle to eastern part is a vegetated area, and bare rocks are distributed in the western part. Two alteration zones discriminated and have the NNE-SSW oriented elongation harmonious with the main structure.

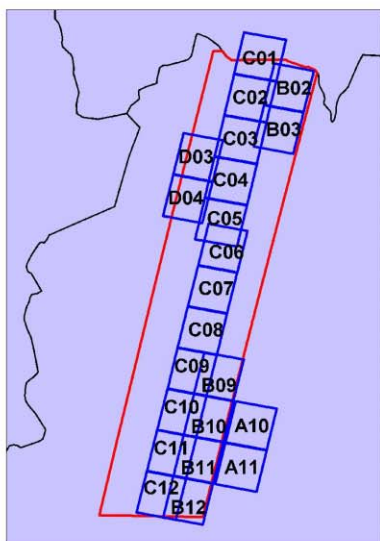
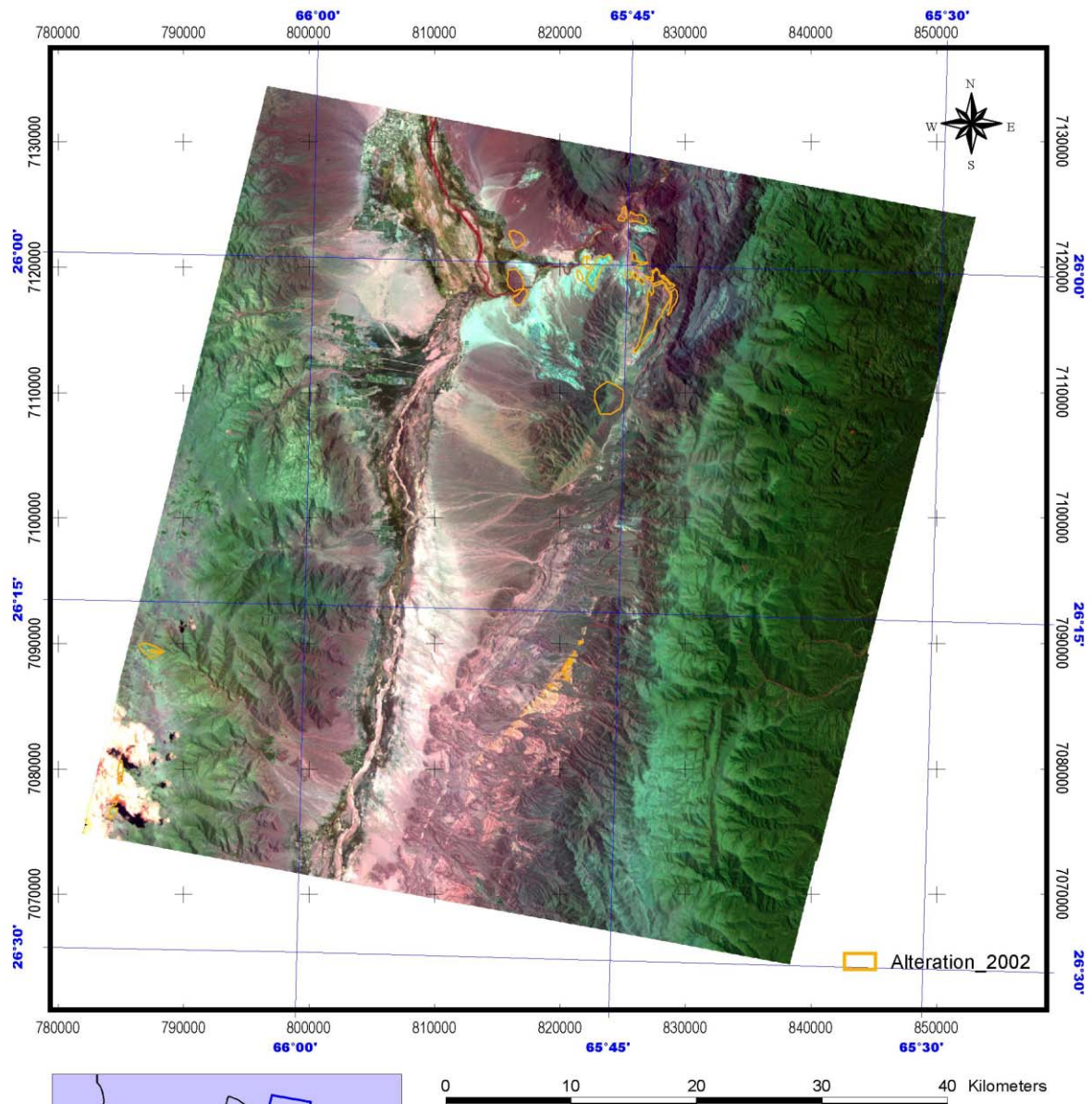
[Alteration zones]

No.03: Made up of *Ser-Chl* and *Hem-Goe*. Geology is Cambrian sedimentary rocks. There are faults on both sides of the alteration zones.

No.04: Shows brown in 147. Alteration zone of *Ser* accompanied by some quantity of *Kao*. Geology is Paleogene sedimentary rocks. Mainly located around the top of mountains, and shows circular structure in the northernmost part.

No.05: *Ser-Goe* zones are distributed around *Ser-Goe* with *Kao* zone. Geology is Silurian to Devonian sedimentary rocks.

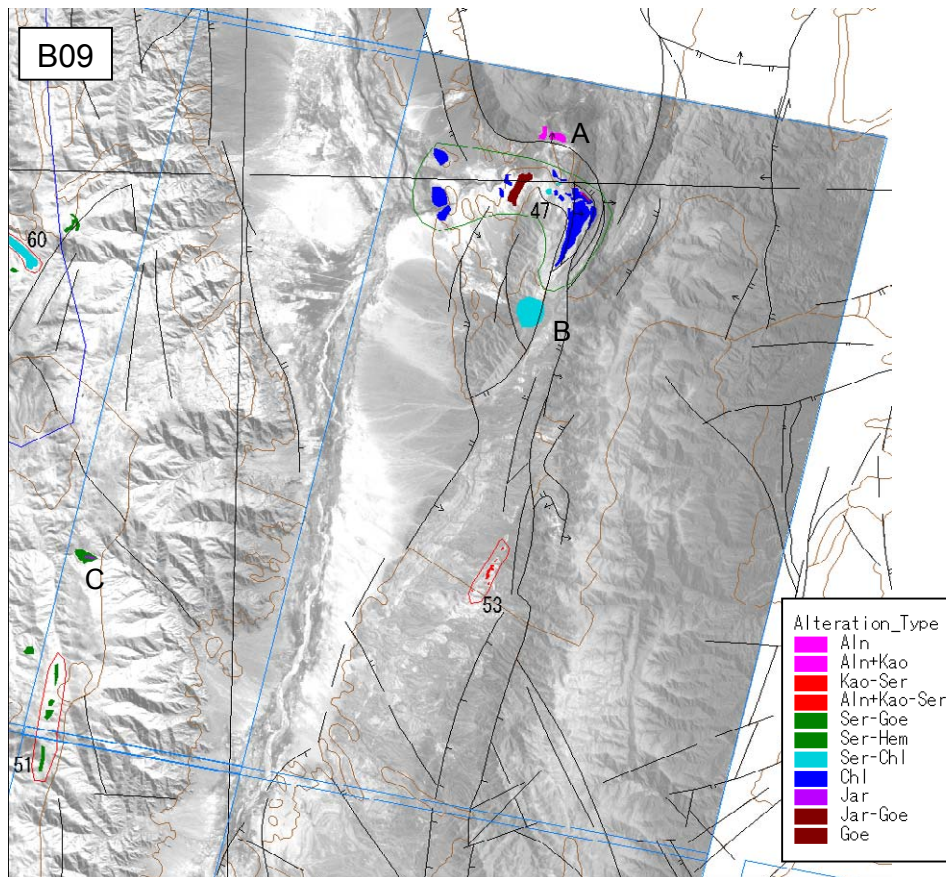
A: Shows dark brown in 147. Made up of *Chl-Ser-Goe* and *Ser-Goe* zones. Geology is Ordovician granites.



SCENE B09

IMAGE : TERRA/ASTER BGR=147
 PROJECTON : Universal Transverse Mercator
 PROJECT : JICA/MMAJ/JMEC
 DATA : ERSDAC/JAPAN

Fig.II-3-2-2-5 False color image of scene B09 (BGR=147)



[General]

The eastern part is a vegetated area, the middle part is a bare rock area, and the western part is a semi-vegetated area. Alteration zones have been discriminated in the north and middle parts.

[Alteration zones]

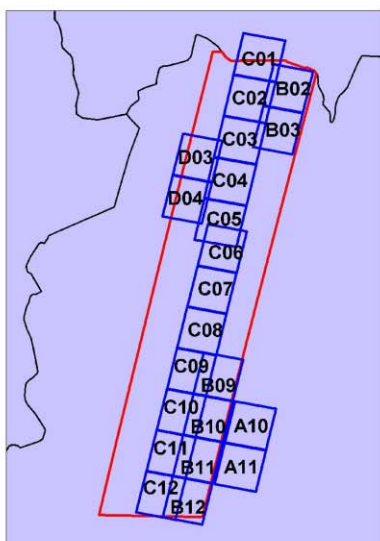
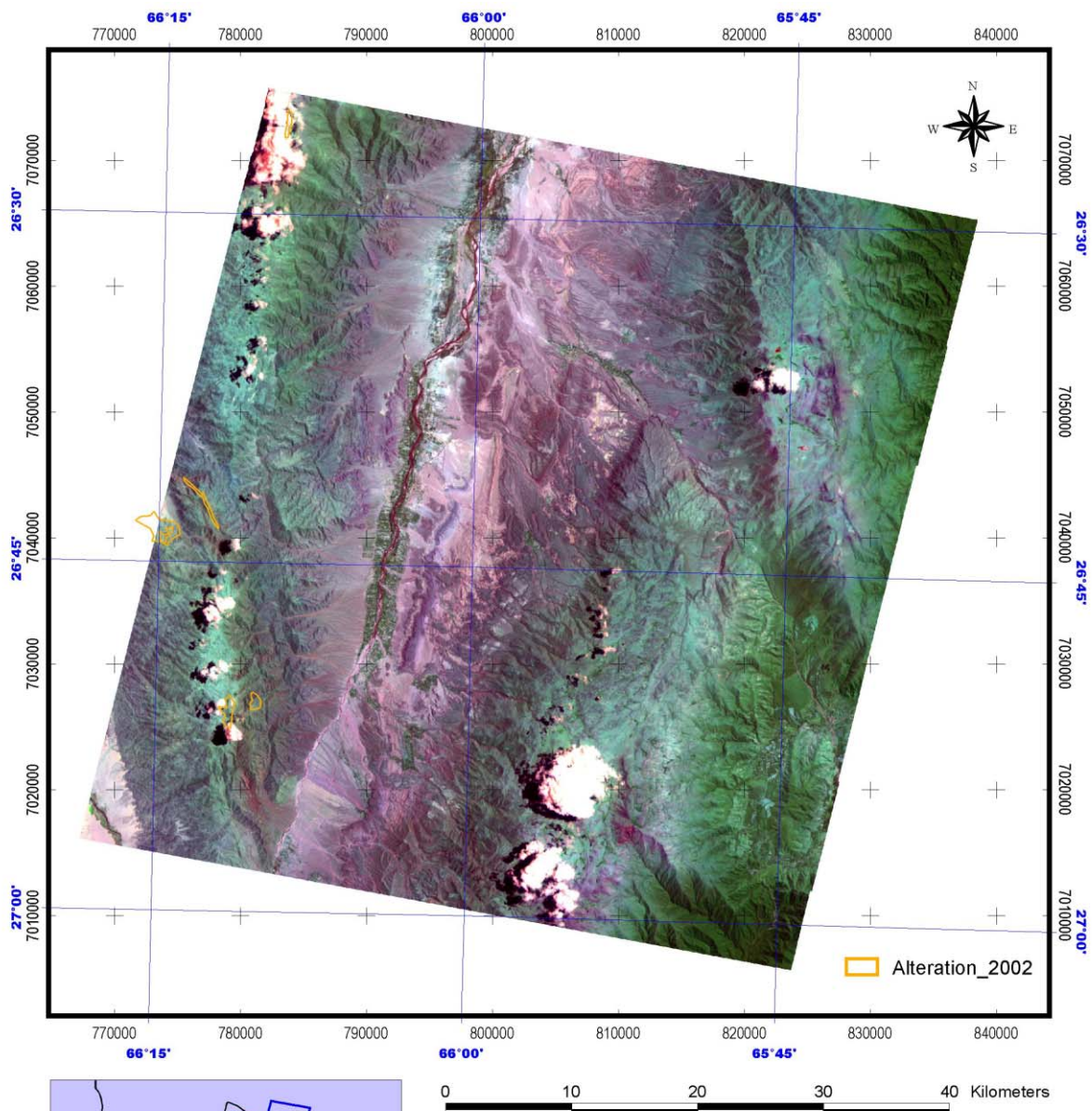
No.47: Shows light brown color in 147. *Chl* has been detected along a specific layer of Lower Cretaceous sedimentary rocks (andesite?). This could indicate tuff and/or propylitized andesite. Also *Goe* and *Hem* have been detected. A banded acid alteration zone (*Aln-Kao-Ser* and *Jar-Goe*) has been detected at the northeastern edge.

No.53: *Kao* and *Jar* are detected in sedimentary rocks, which shows dark brown in 147. Geology is Miocene sedimentary rocks. Some horizons of sedimentary rocks react to *Kao*.

A: *Aln-Ser* alteration zone, which shows reddish brown in 147. Geology is sedimentary rocks of the Lower Cretaceous.

B: Circularly discriminated *Ser-Chl*. Geology is Ordovician granites, and this could be an intrusive granites containing a large quantity of mica.

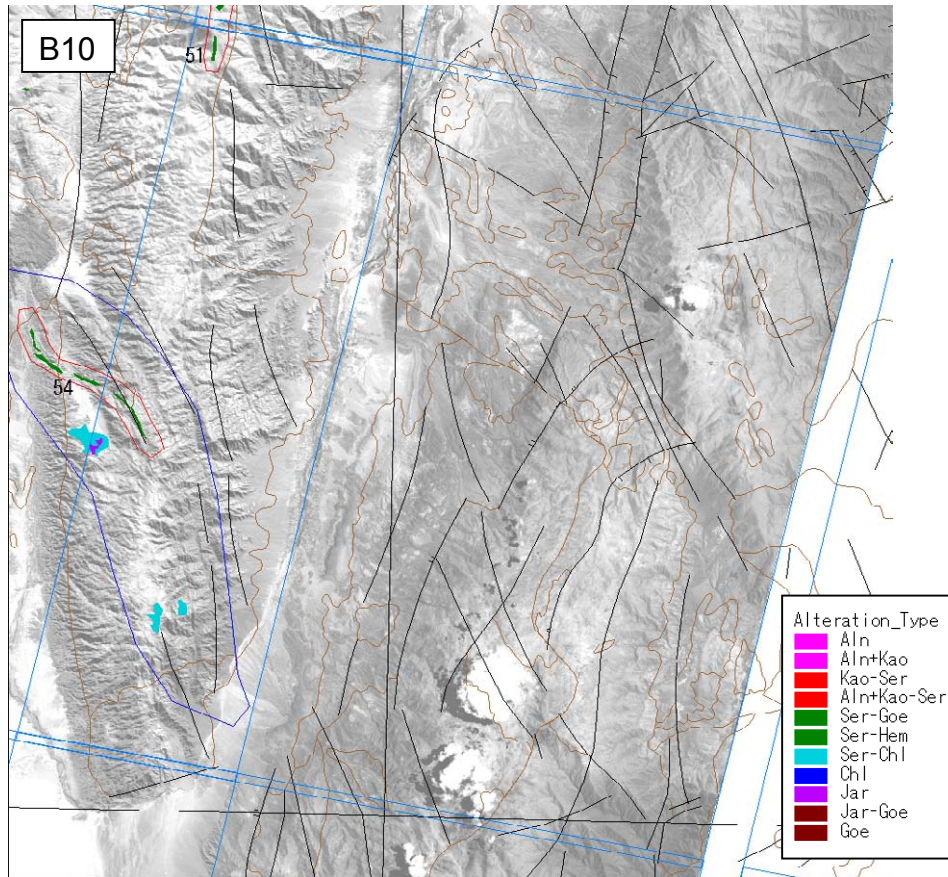
C: *Kao-Ser-Jar* zone discriminated along the valley line. Geology is Paleozoic sedimentary rocks.



SCENE B10

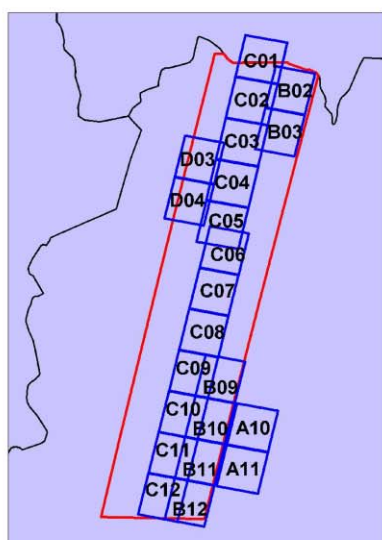
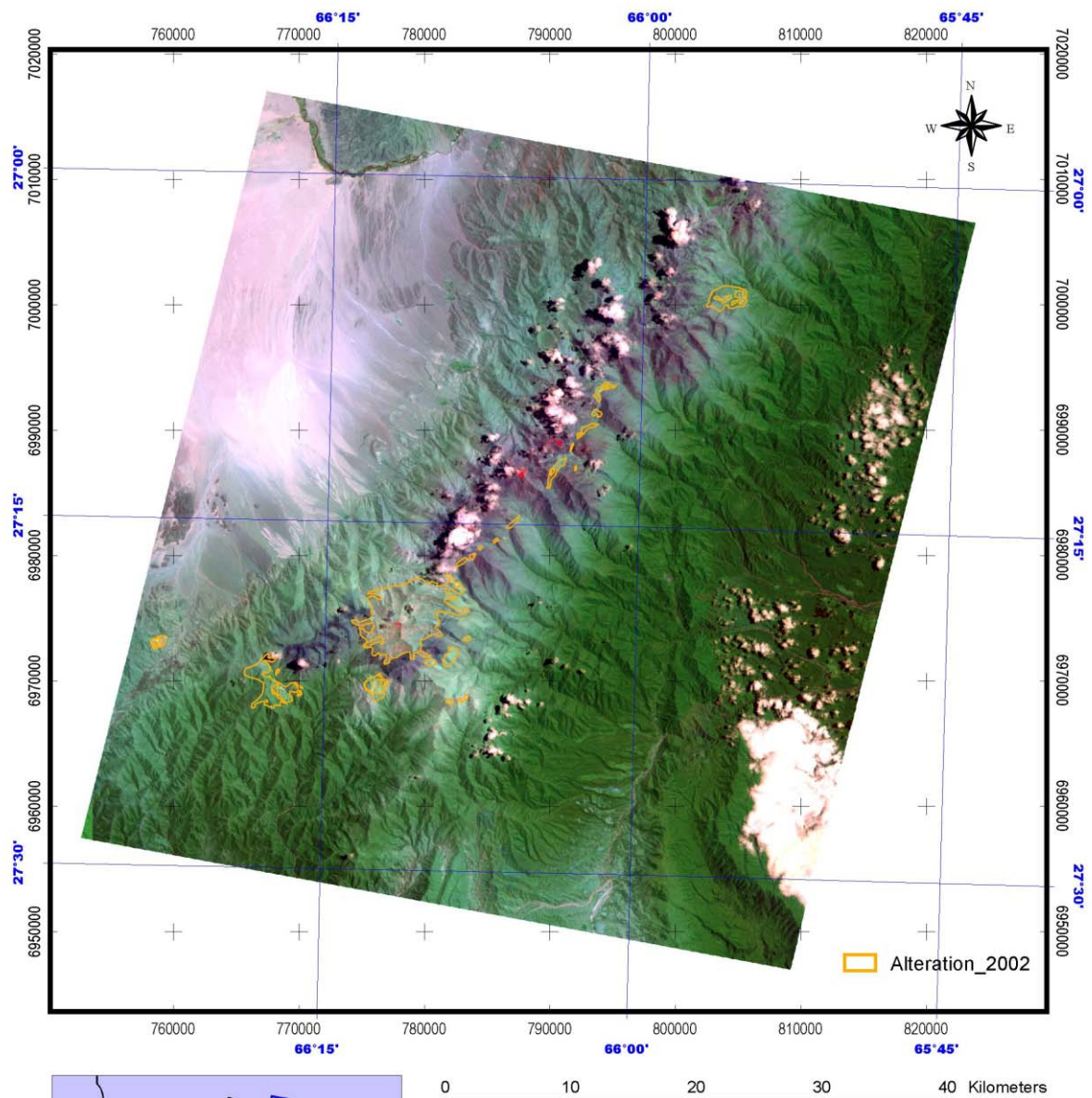
IMAGE : TERRA/ASTER BGR=147
 PROJECTION : Universal Transverse Mercator
 PROJECT : JICA/MMAJ/JMEC
 DATA : ERSDAC/JAPAN

Fig.II-3-2-2-6 False color image of scene B10 (BGR=147)



[General]

The eastern part is a vegetated area, the middle part is a bare rock area, and the western part consists of a semi-vegetation area. Most of the mountainous regions in the eastern and western parts are made up of Paleozoic sedimentary rocks and granites, and Tertiary sedimentary rocks are distributed around them. Alteration zones are discriminated in the western part, descriptions of which are presented in the explanation of C10.

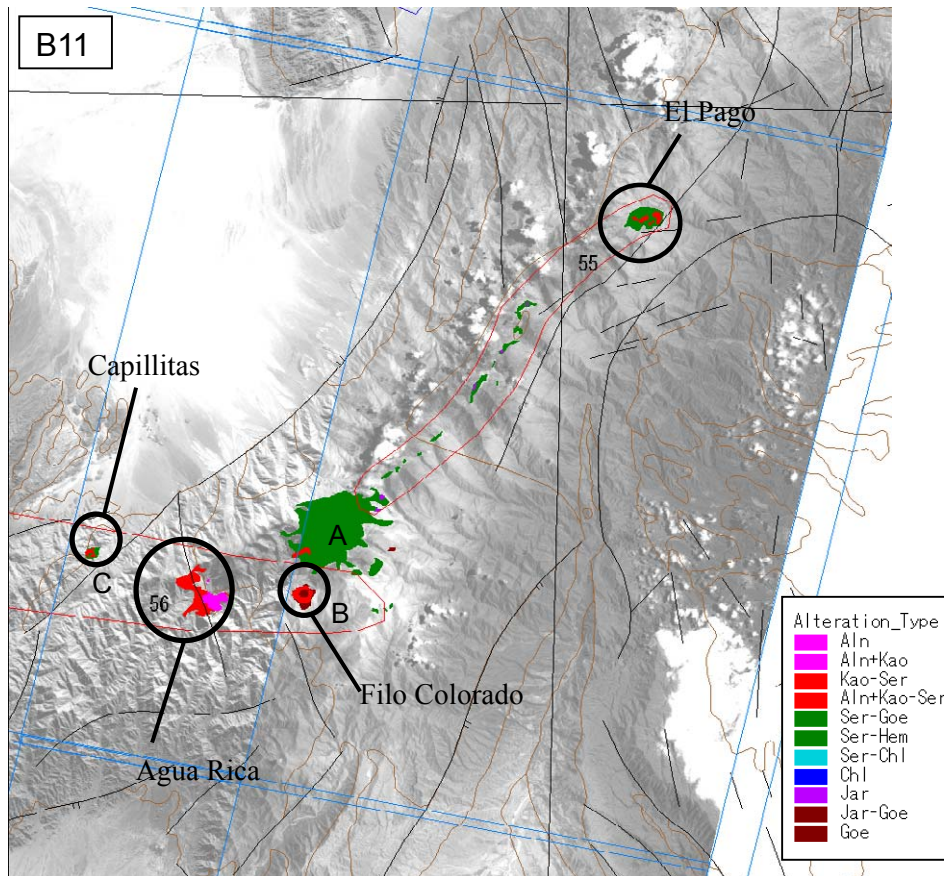


0 10 20 30 40 Kilometers

SCENE B11

IMAGE : TERRA/ASTER BGR=147
 PROJECTON : Universal Transverse Mercator
 PROJECT : JICA/MMAJ/JMEC
 DATA : ERSDAC/JAPAN

Fig.II-3-2-2-7 False color image of scene B11 (BGR=147)



[General]

This scene includes El Pago area where field survey was carried out (No. 55). The eastern part is heavily vegetated area, and the western part is covered with talus sediment. The middle part is a semi-vegetated area. Most of the mountainous region on the eastern part consists of sedimentary rocks and metamorphic rocks of the Proterozoic to Paleozoic, and partially granites are distributed. Alteration zones are distributed in parallel to the ridge in this mountainous region. Ground truth survey was conducted on No.55.

[Alteration zones]

No.55: A group of alteration zones running linearly with NE-SW orientation, including El Pago prospect at the northeastern edge. It shows light green in 147. Most zones are made up of *Ser-Goe*, and *Kao* accompanies at the center. El Pago prospect situated near the limit of analysis on the point of vegetation coverage. Geology is Precambrian metamorphic rocks.

No.56: Agua Rica prospect, where field survey was carried out last year. This is also a semi-vegetated area. Bare rocks appear along the valley and show dark brown. It is distributed on a fault. *Aln* and *Hem* are dominant in the eastern part, and *Kao* and *Goe* are dominant in the western part. Geology of the *Aln* dominant area is Miocene volcanic rocks.

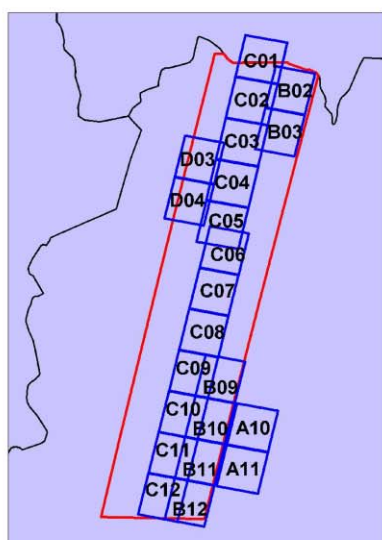
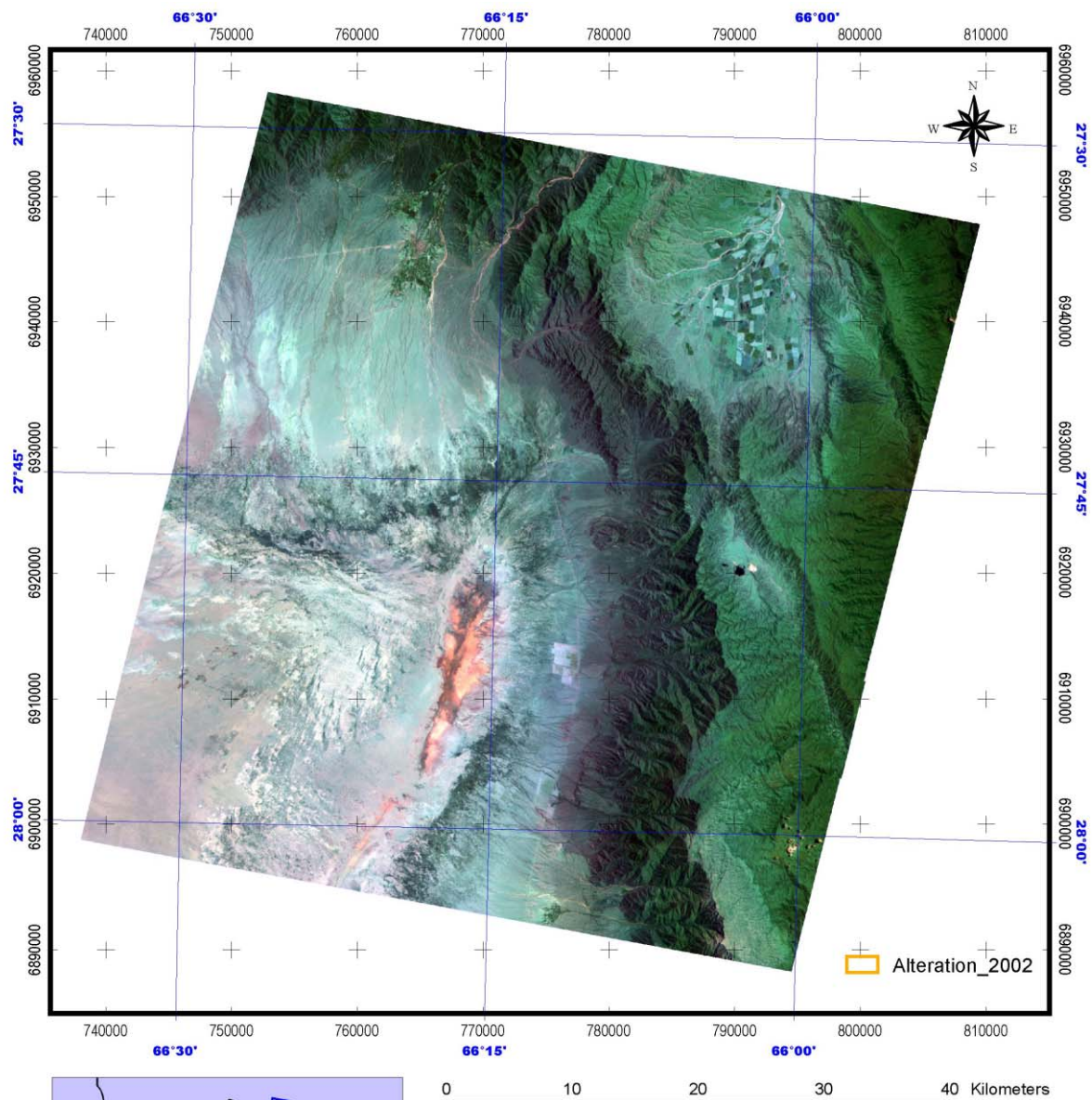
A: Made up of *Ser-Goe* and accompanied by *Kao* and *Jar*. Geology is Paleozoic metamorphic rocks. This is a very interesting area on the point of relation with No.55.

B: Filo Colorado prospect. Circular alteration zone made up of *Aln-Ser-Jar* discriminated in a semi-vegetated area. *Goe* zones accompanied by some quantity of *Ser* are distributed around it. Geology is Paleozoic metamorphic rocks.

C: Capillitas prospect, where field survey was carried out last year. It shows light green in the 147. Composed of *Kao*, *Ser*, *Jar* and *Goe*. Geology is Miocene basic volcanic rocks.

[Results of ground truth survey]

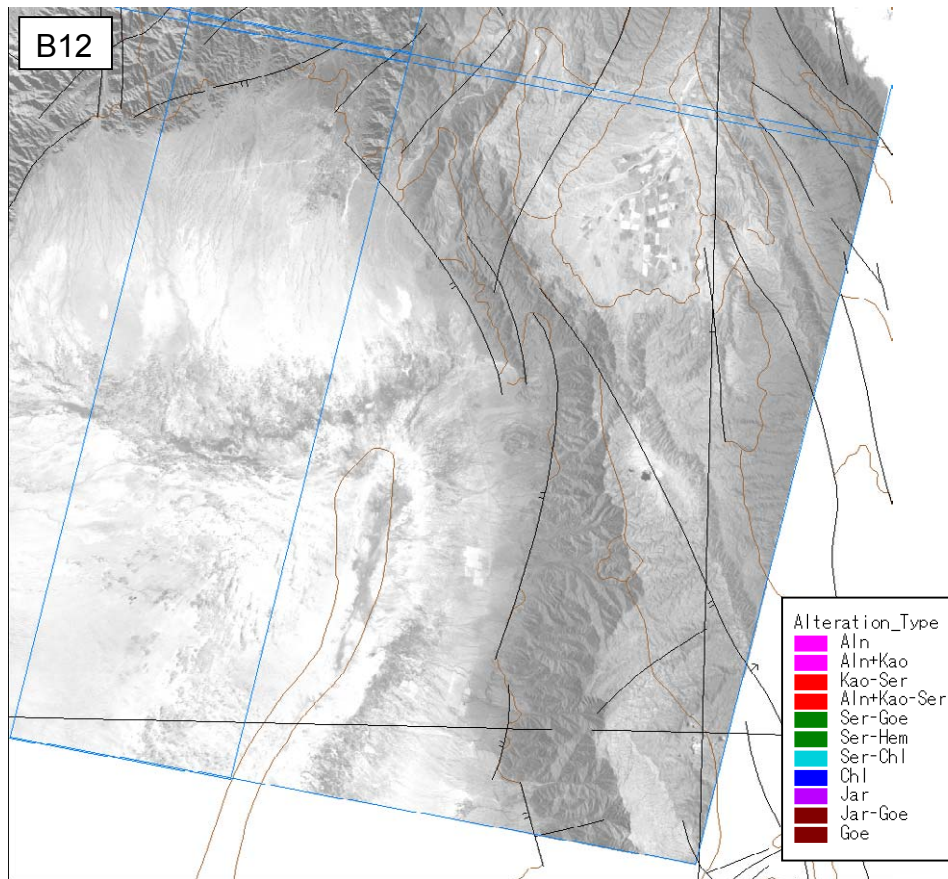
Ground truth survey was carried out for an alteration zone at the northeastern edge of No.55. This corresponds to El Pago area, which is one of the targeted areas for field survey this year. For results of the ground truth survey of this area, see Chapter 4.



SCENE B12

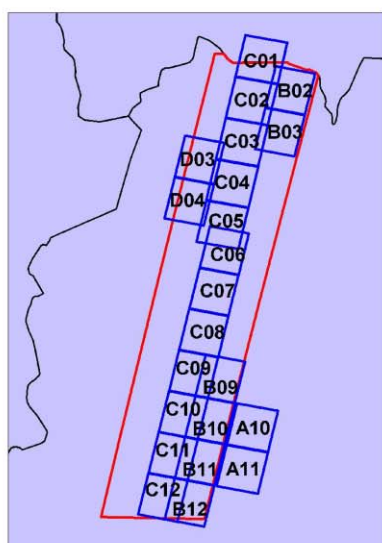
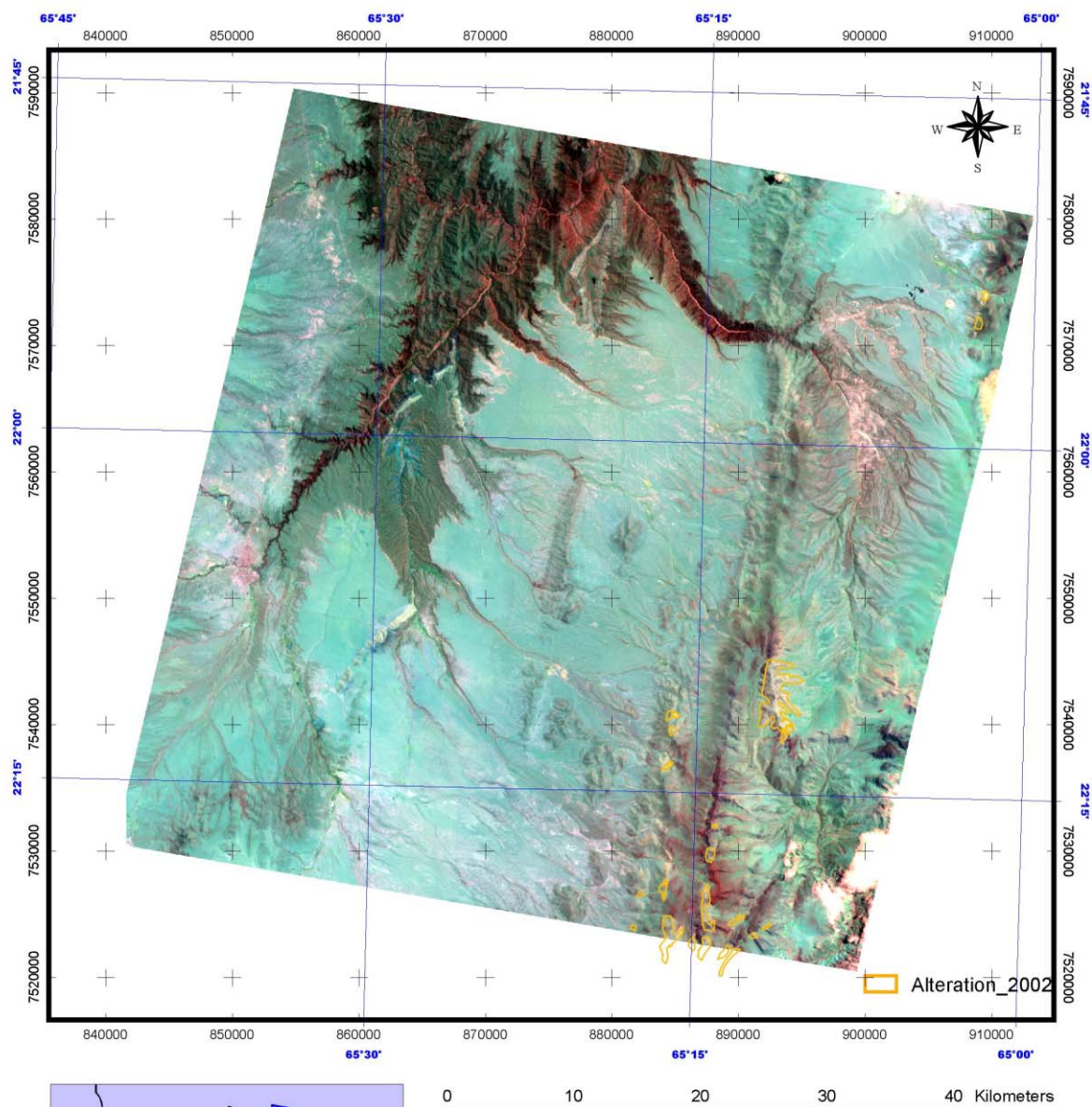
IMAGE : TERRA/ASTER BGR=147
 PROJECTON : Universal Transverse Mercator
 PROJECT : JICA/MMAJ/JMEC
 DATA : ERSDAC/JAPAN

Fig.II-3-2-2-8 False color image of scene B12 (BGR=147)



[General]

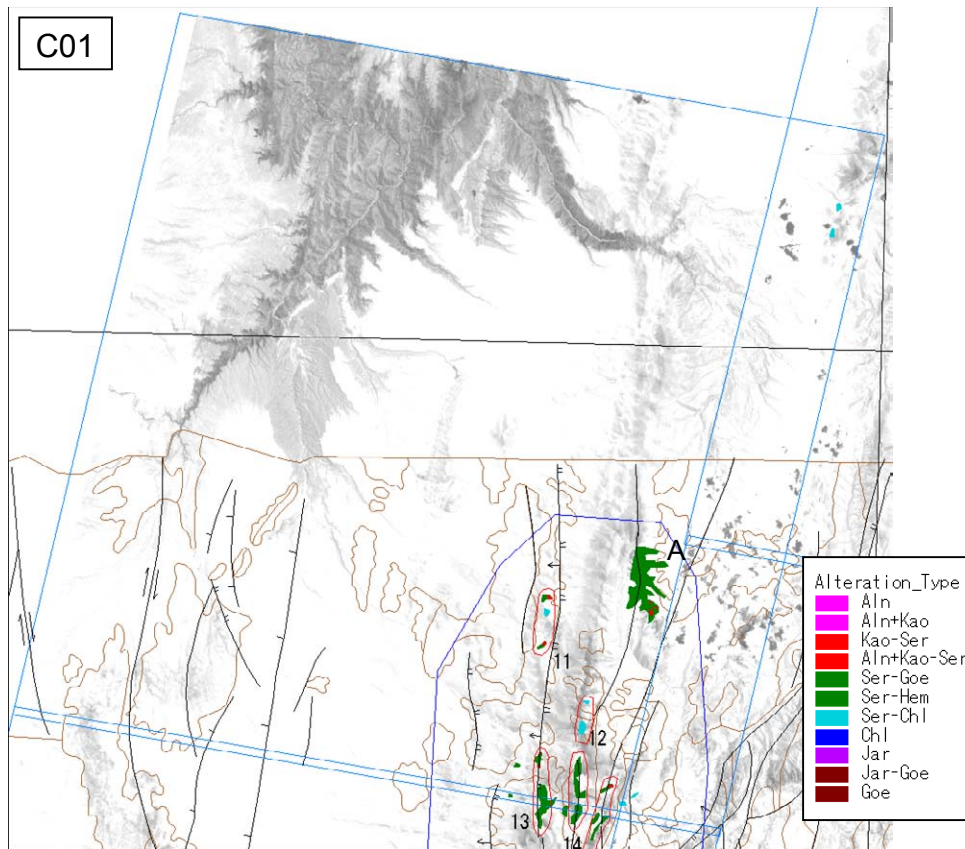
The eastern and northern parts are mainly composed of mountainous regions of Precambrian metamorphic rocks and Ordovician granites, and are covered with vegetation. The area from the center to the southwestern part is a basin between mountains. No alteration zones have been discriminated in this scene.



SCENE C01

IMAGE : TERRA/ASTER BGR=147
 PROJECTON : Universal Transverse Mercator
 PROJECT : JICA/MMAJ/JMEC
 DATA : ERSDAC/JAPAN

Fig.II-3-2-2-9 False color image of scene C01 (BGR=147)



[General]

Santa Victoria area and Pumahuasi area, carried out field survey this year, are included in this scene. This is almost non-vegetated area. Paleozoic sedimentary rocks are distributed in the eastern part, Ordovician sedimentary rocks are in southwestern part and the remaining area is widely covered with Quaternary sediments. Alteration zones are distributed in N-S orientation in the southeastern part. Ground truth survey was conducted for No.11, No.13 and No.14.

[Alteration zones]

No.11: Shows yellowish white color in 147. Composed of *Ser-Geo* and accompanied by *Kao* in some parts. The zones show N-S elongated distribution harmonious with the structure. Geology is Cambrian sedimentary rocks.

No.12: Shows grayish white in 147. Composed of *Ser-Chl-Goe*. Geology is Ordovician sedimentary rocks.

No.13: Similar to No.11. Made up of *Ser-Goe* and showing N-S oriented distribution. *Kao* has been detected in a small area in the northern part. Geology is Cambrian sedimentary rocks.

No.14: Shows grayish white to yellowish white in 147, and has characteristics of both No.11 and No.12. Made up of *Ser-Goe* with some quantity of *Chl* accompanying. Geology is Ordovician sedimentary rocks.

A: Shows yellowish gray in 147. *Ser-Goe* has been widely detected. In the southern part, an acid alteration zone made up of *Kao-Ser-Goe* has been detected. Geology is Cambrian sedimentary rocks.

[Results of ground truth survey]

Ground truth survey was carried out for *Kao-Ser* zone in the southern part of No.11, *Kao-Ser* zone in the northern part of No.13, and *Ser-Goe* zone in the southern part of No.14.

Those alteration zones are located in the northeastern part of Santa Victoria area where field survey was conducted this year. They are *Ser-Goe* and *Kao-Ser* zones discriminated from Precambrian, Cambrian or Ordovician sedimentary rocks and metamorphic rocks. They show yellowish to grayish white in 147, and don't show the typical color of alteration zones. In the SiO₂ content map (the figure shown below, c), a red colored area, indicating particularly high values, extends from north to south. Most of the discriminated alteration zones are distributed overlapping this red colored area. From these points, it was considered that alteration zones discriminated from this area were not typical ones.

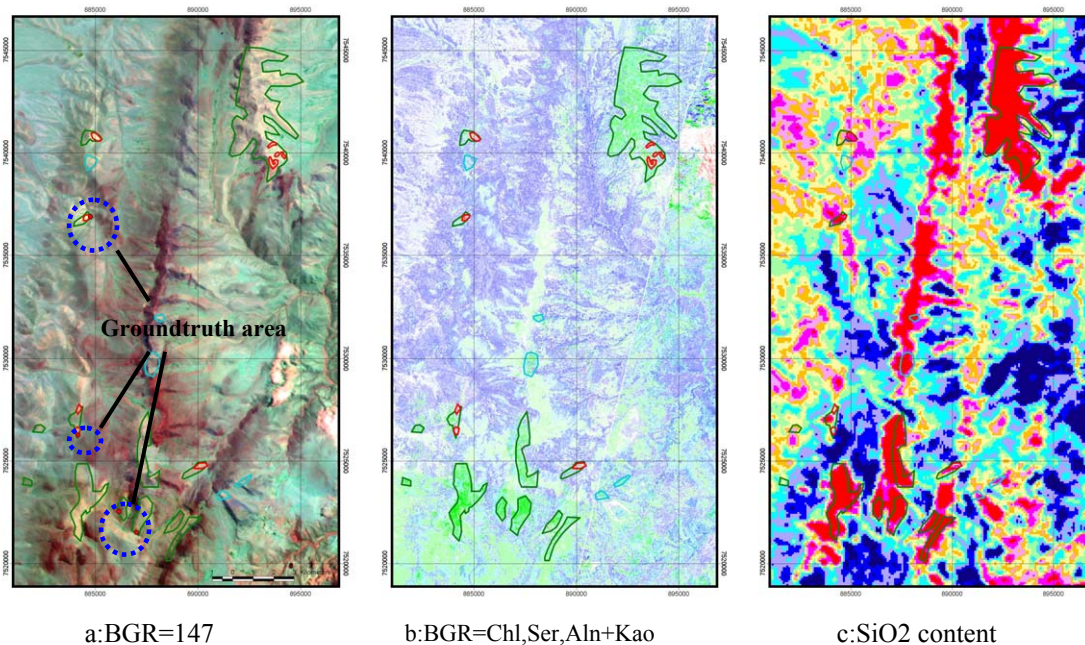
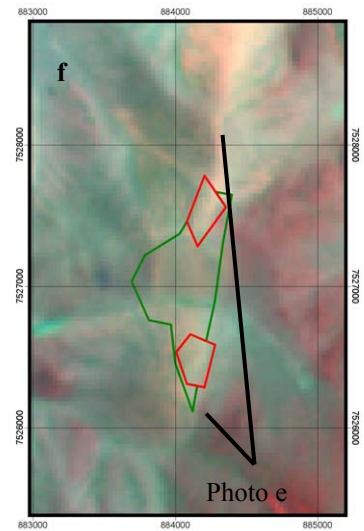
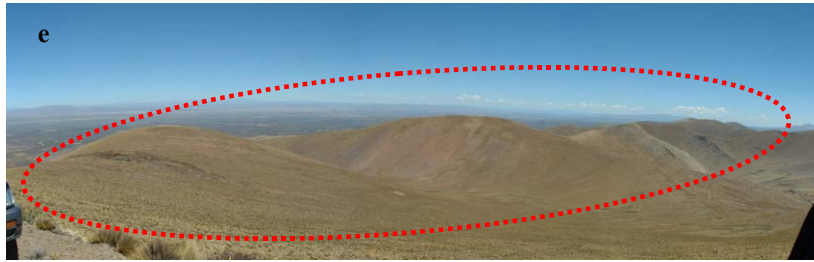
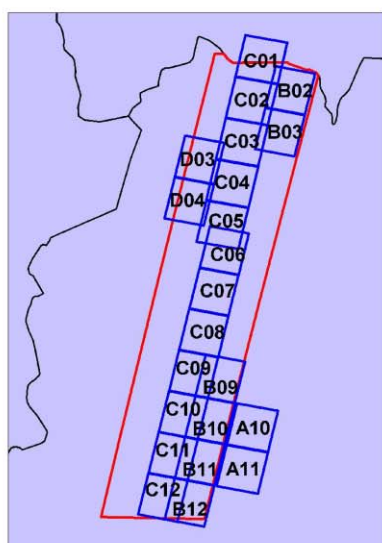
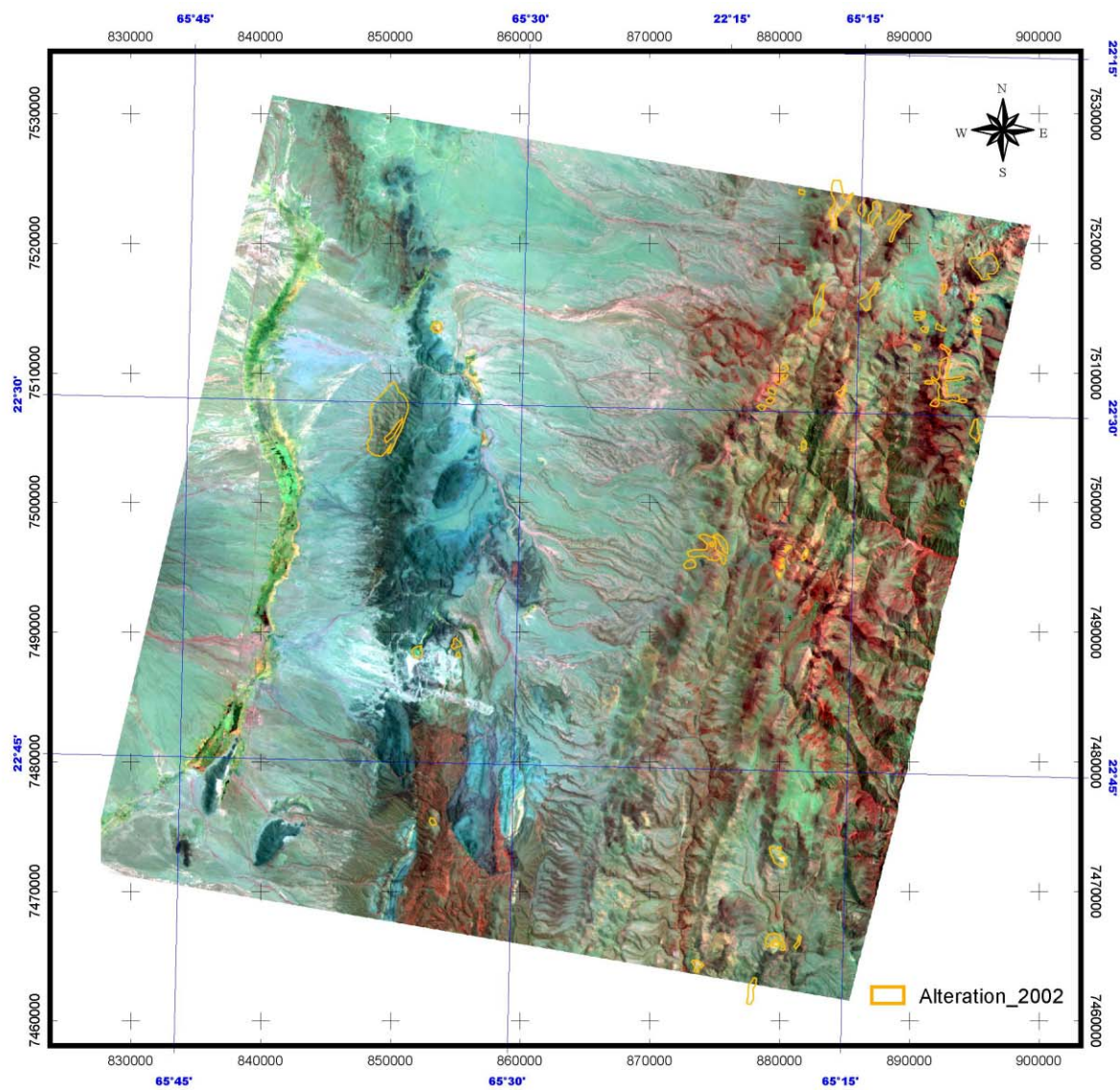


Photo d is a distant view of a survey point of No.11. Although this area was detected as a *Kao-Ser* zone, it was confirmed through field survey that almost non-altered quartzite was distributed. From the X-ray diffractive analysis for the samples taken, a trace quantity of sericite was detected.



Photo e is a distant view of a survey point of No.13. In this area, similarly to No.11, almost non-altered quartzite was distributed, and a trace quantity of sericite was detected in the X-ray diffractive analysis for the samples taken. This quartzite forms a ridge extending in the N-S direction (a red circle on Photo e), and detected alteration zones (f; *Ser-Goe* and *Kao-Ser*) seem to have reacted with this quartzite.

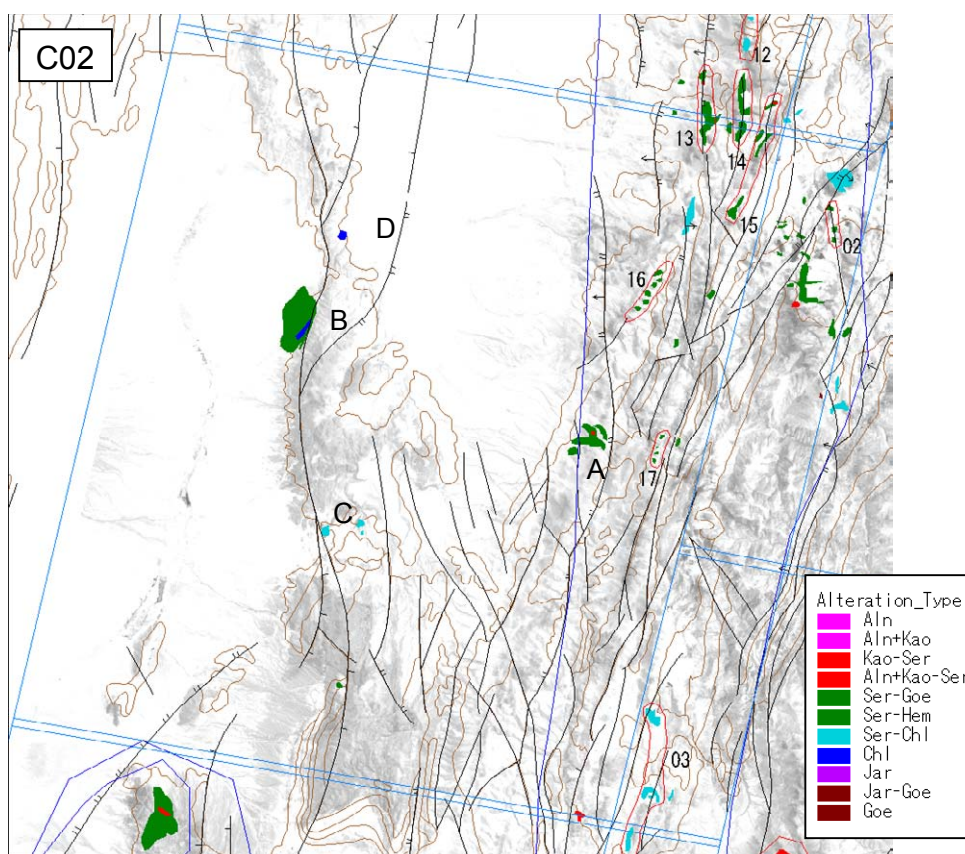




SCENE C02

IMAGE : TERRA/ASTER BGR=147
 PROJECTON : Universal Transverse Mercator
 PROJECT : JICA/MMAJ/JMEC
 DATA : ERSDAC/JAPAN

Fig.II-3-2-2-10 False color image of scene C02 (BGR=147)



[General]

This scene also includes Santa Victoria area and Pumahuasi area. Paleozoic sedimentary rocks are distributed in the eastern part, Paleozoic to Mesozoic sedimentary rocks are in the middle part, and the remaining area is widely covered with Quaternary sediments. Alteration zones are mainly discriminated in the northeastern part and show N-S elongated distribution. Ground truth survey was conducted for B and D.

[Alteration zones]

No.15: Shows grayish white to yellowish-grayish white in 147 and made up of *Ser-Goe*. *Kao* accompanies and *Jar* is detected in some parts. They show N-S elongated distribution. Geology is Ordovician sedimentary rocks.

No.16: Shows reddish brown in 147. It is consisting of *Ser-Goe* and showing NNE-SSW elongated distribution. Geology is Cambrian sedimentary rocks.

No.17: Shows yellowish gray in 147. *Hem* is dominant as iron oxide minerals. Geology is Cambrian sedimentary rocks.

A: Shows yellowish gray in 147. A small quantity of *Kao* is detected at the center, and the surrounding area is made up of *Ser-Goe-Hem* while the quantity of *Goe* is not so much. Geology is Cambrian sedimentary rocks.

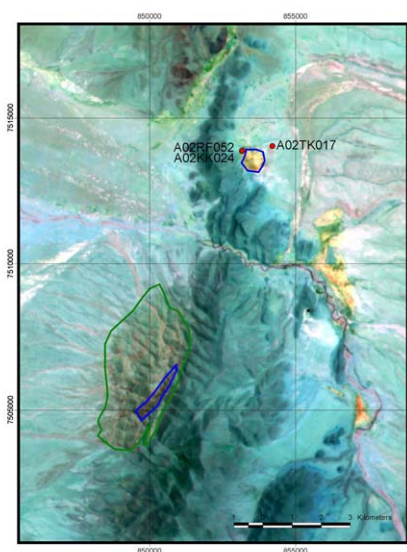
B: Shows gray in 147. Mainly composed of *Ser* and accompanied by *Chl* in the northern side. *Goe-Hem* has been detected as iron oxide minerals. Geology is Paleogene to Mesozoic sedimentary rocks.

C: Shows light green in 147. Made up of *Ser-Goe* with some quantity of *Jar* accompanying. Geology is Cretaceous sedimentary rocks.

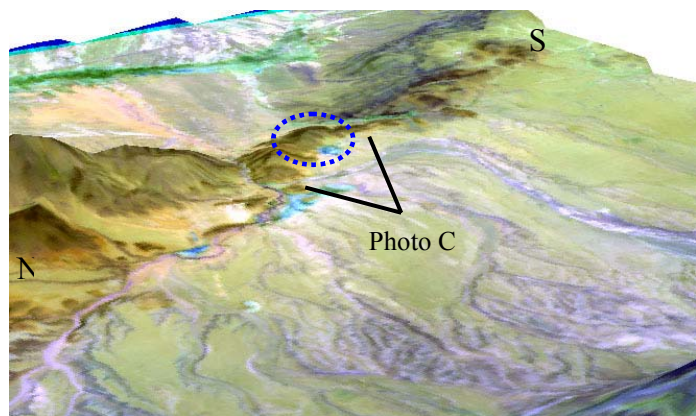
D: Shows yellowish gray in 147. *Chl* has been detected. Geology is Ordovician sedimentary rocks.

[Results of ground truth survey]

Alteration Zone D for which ground truth survey was carried out corresponds to the southern end of Pumahuasi area. In this area, Mesozoic sedimentary rocks distribute from north to south and a circular *Chl* alteration zone has been detected on the eastern side of them. In the bird's eye view prepared using DEM of ASTER (the figure shown below, b), it can be seen that this area detected as an alteration zone forms a depression.



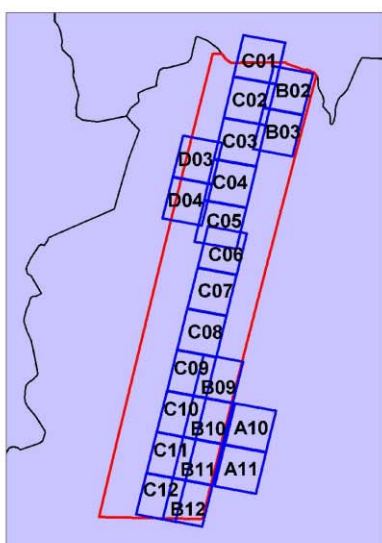
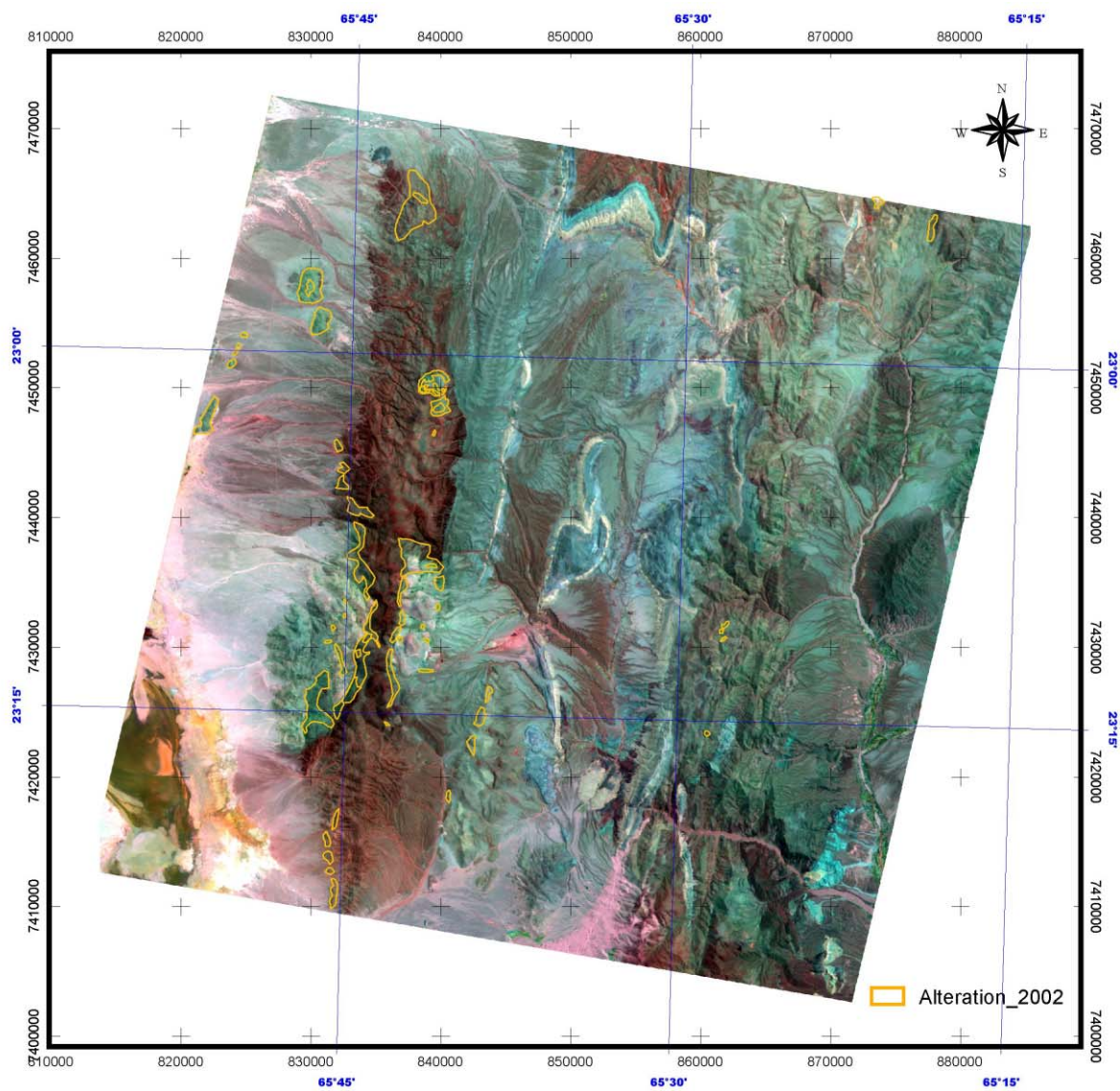
a:BGR=147



b: Bird-eye-view of the alteration zone

Photo c is a distant view of Alteration Zone D. A red sandstone of the Lower Cretaceous traverses from south to north, and a part of its eastern side forms depression. White to light green clay were widely distributed in this area, and smectite, sericite, chlorite and kaolinite were detected in the X-ray diffractive analysis. A yellowish-white sandstone formed by alteration of red sandstone was confirmed at the field survey, it is considered that the Alteration Zone D resulted from detection of alteration minerals within salt lake sediments.

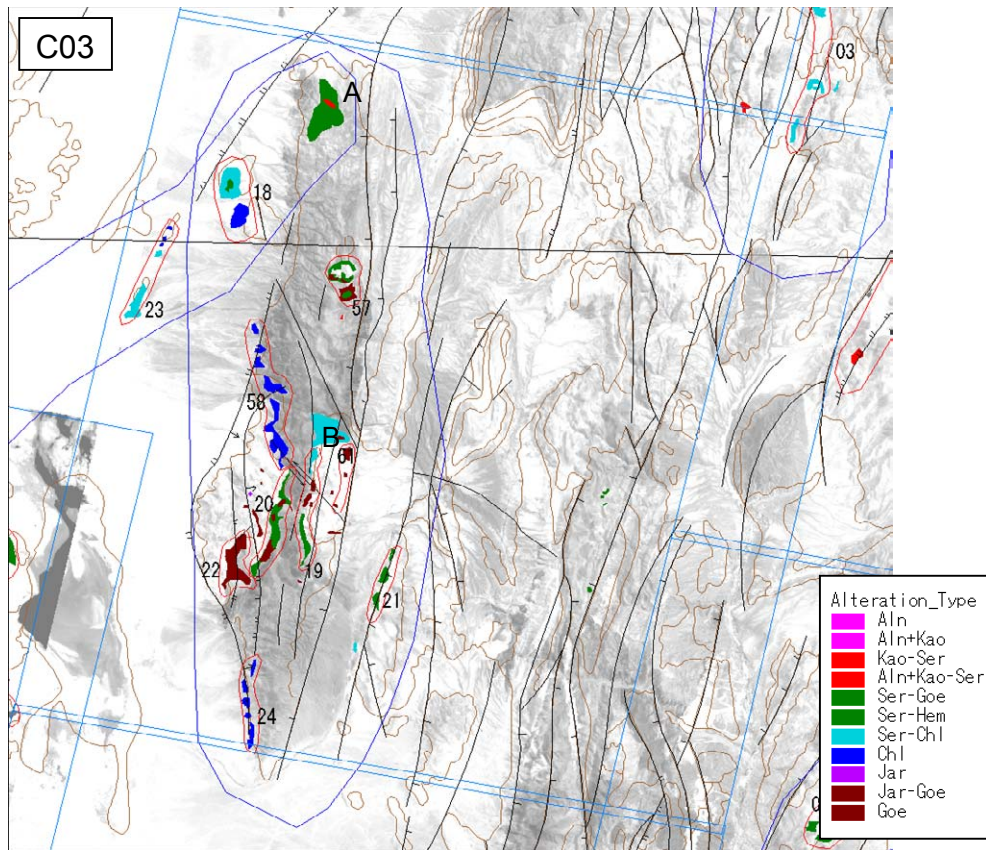




SCENE C03

IMAGE : TERRA/ASTER BGR=147
 PROJECTION : Universal Transverse Mercator
 PROJECT : JICA/MMAJ/JMEC
 DATA : ERSDAC/JAPAN

Fig.II-3-2-11 False color image of scene C03 (BGR=147)



[General]

This scene includes Aguilar area where field survey was conducted this year. This is almost non-vegetated area. Units of Paleozoic to Tertiary are distributed and controlled by N-S oriented structure. Alteration zones are recognized in Paleozoic sedimentary rocks and Mesozoic granites in the middle western part, and present N-S elongated distribution. Ground truth survey was carried out for No.19, No.20 and No.21.

[Explanation of alteration zones]

No.18: Shows light green in 147. Because *Ser-Chl* and *Goe* were detected and geology is Ordovician volcanic rocks, this could be propylitized.

No.19: Shows greenish color in 147. The main alteration mineral is *Ser-Goe*. Geology is Ordovician sedimentary rocks. Alteration zones are formed on the border with granite on the eastern side.

No.20: Similar to No.19. The alteration mineral is composed of *Ser-Goe* with *Jar* accompanying in some parts. This parts show greenish color in 147.

No.21: A group of alteration zones composed of *Ser-Goe* distribute in parallel with NNE-SSW oriented fault structure. Geology is considered as Cambrian sedimentary rocks.

No.22: Shows dark bluish green in 147. Composed of *Ser-Goe* and *Jar*. Geology is Ordovician sedimentary rocks.

No.23: Shows light green in 147. Similar to No.18. Geology is Ordovician sedimentary rocks.

No.24: Same as No.58.

No.57: Alteration zones that accompany granite which intrude Ordovician sedimentary rocks. At the outside edge of granite (on the granite side), strong *Ser* is detected and *Goe-Jar* is detected as iron oxide mineral. A small quantity of *Kao* is distributed accompanying *Jar*. The central part of the alteration zone on the northern side has weak alteration that presents a ring shape.

No.58: Mainly made up of *Chl-Hem* discriminated at the western border of Ordovician sedimentary rocks. Because it is harmonious with the structures, it could be reaction from tuff.

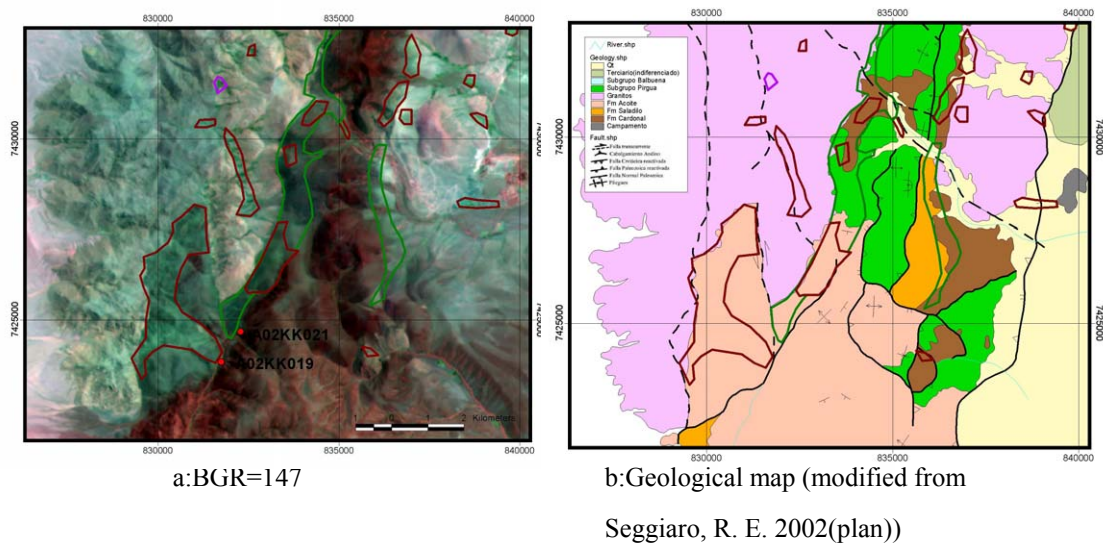
No.61: Strongly *Jar* detected area in granites. However, it shows deep green in 147, there is a possibility that vegetation was mis-identified for an alteration zone.

A: Shows grayish blue in 147. Composed of *Ser-Chl* and *Goe>Hem*. Geology is Ordovician sedimentary rocks.

B: *Chl* is detected in neighboring granite and Ordovician sedimentary rock. As iron oxide minerals, *Goe* is abundant on the granite and *Hem* is abundant on the sedimentary rock.

[Results of ground truth survey]

Ground truth survey was carried out for *Ser-Goe* zone in the southernmost part of No.20, and No.22 (*Jar-Goe* zone).



Both alteration zones No.20 and No.22 are located in the Lower Ordovician sedimentary rocks. The rock body containing these alteration zones is in contact with granite in the northwest side, and bordered by fault. It also cut by fault in the southwest side from the same unit. Moreover, the rock masses containing No.22 and No.20 are cut by fault.

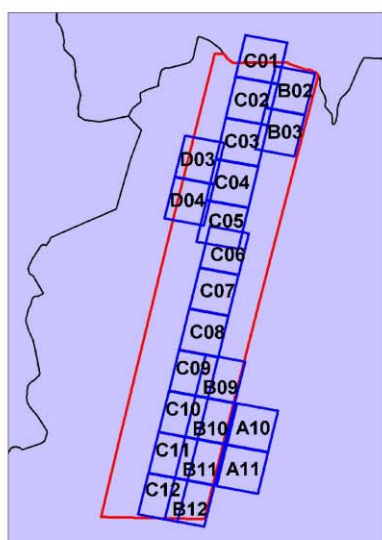
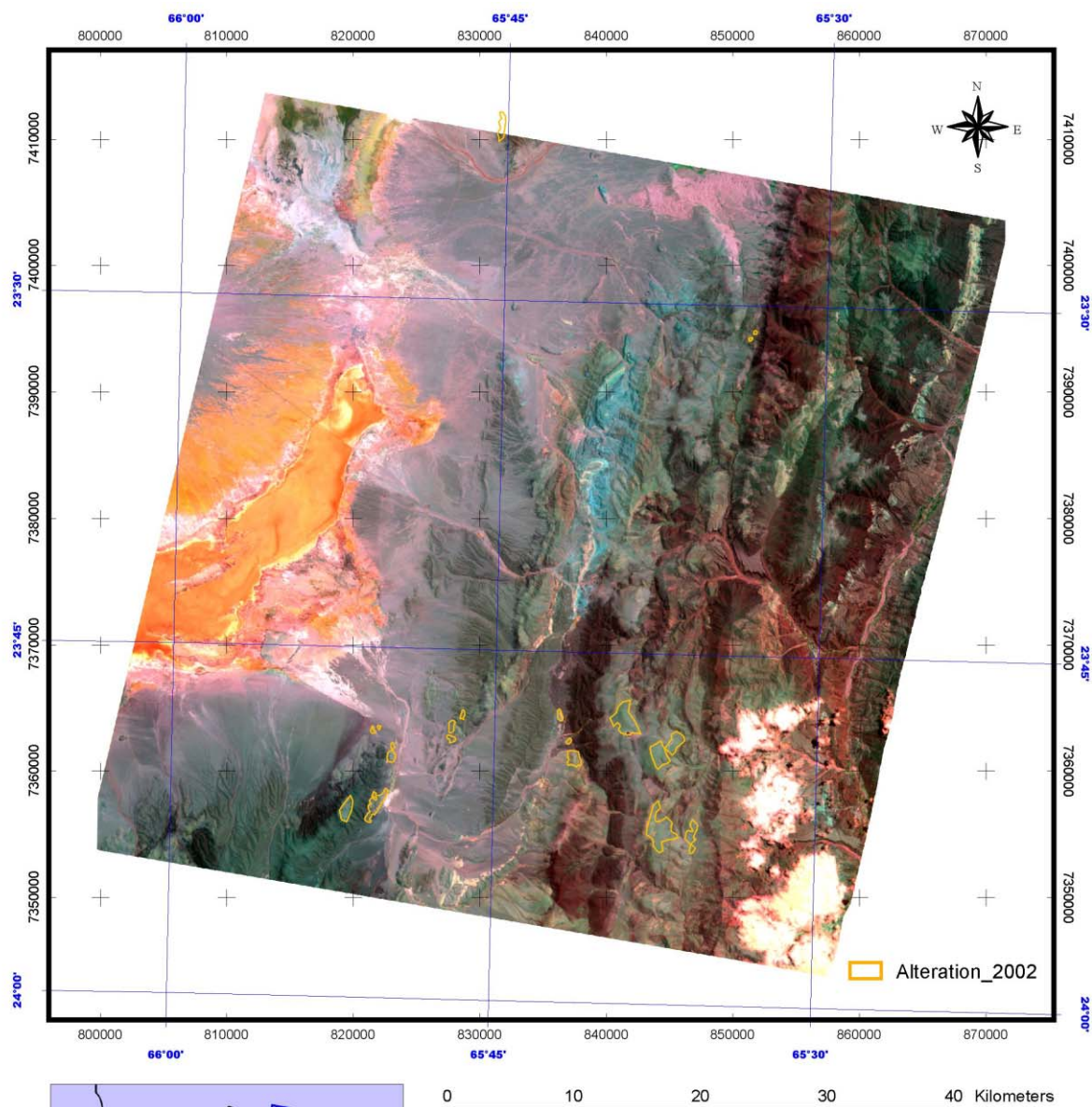
Outcrop of No.20 is shown in Photo c. As a result of ground truth survey, it was confirmed that Lower Ordovician sedimentary rocks are distributed in this area, and fault clay (gouge) have developed partially. From X-ray diffractive analysis for samples taken here, small

quantity of sericite and trace quantity of chlorite were detected. It is considered that those minerals were detected by mineral identification process.



Distant view of No.22 is shown in Photo d. This alteration zone is very similar to No.20. From X-ray diffractive analysis for samples taken here, small quantity of sericite and trace quantity of chlorite were detected. It is considered that those minerals were detected in mineral identification process.

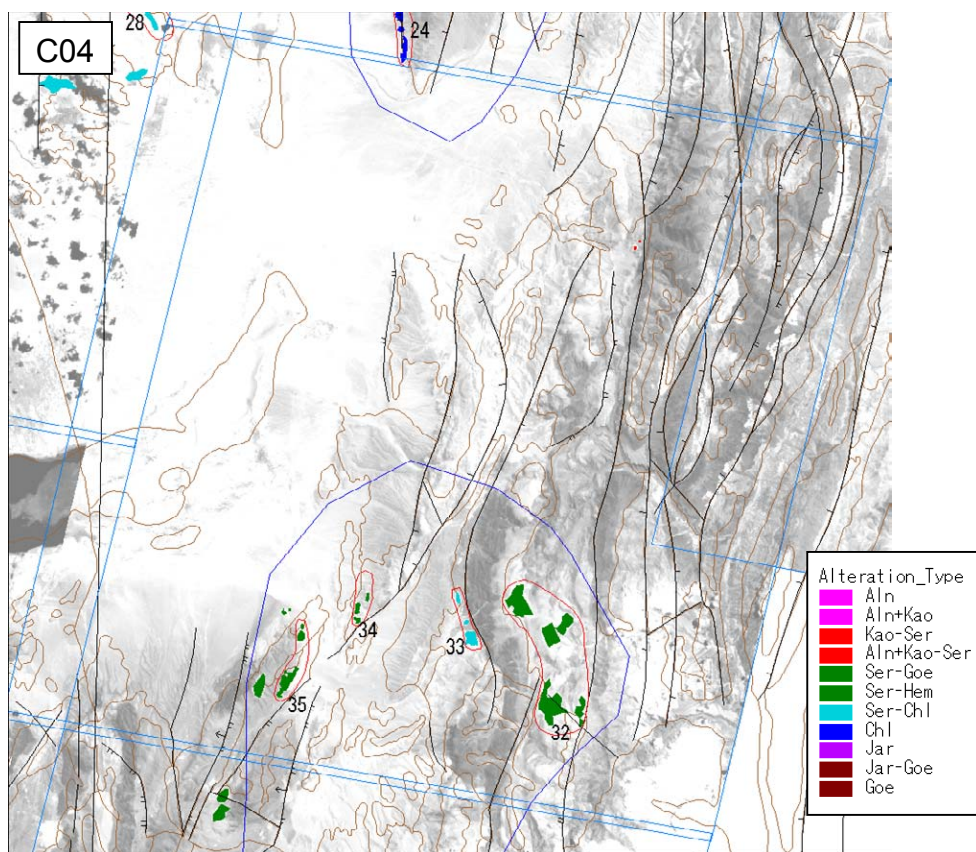




SCENE C04

IMAGE : TERRA/ASTER BGR=147
 PROJECTION : Universal Transverse Mercator
 PROJECT : JICA/MMAJ/JMEC
 DATA : ERSDAC/JAPAN

Fig.II-3-2-12 False color image of scene C04 (BGR=147)



[General]

The eastern part consists of a mountainous region mainly made up of Paleozoic sedimentary rocks, and the western part is widely covered with the Quaternary sediment. In low land in the western part, salt lake sediments are distributed. Alteration zones are discriminated more in the central south part.

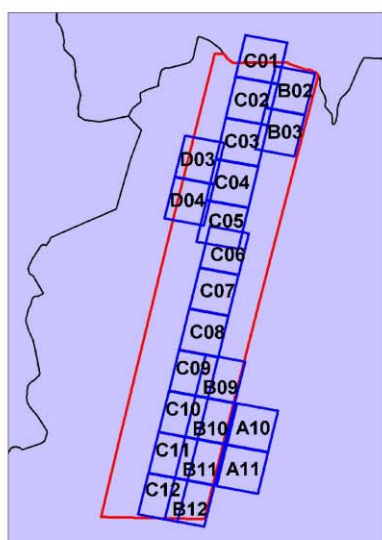
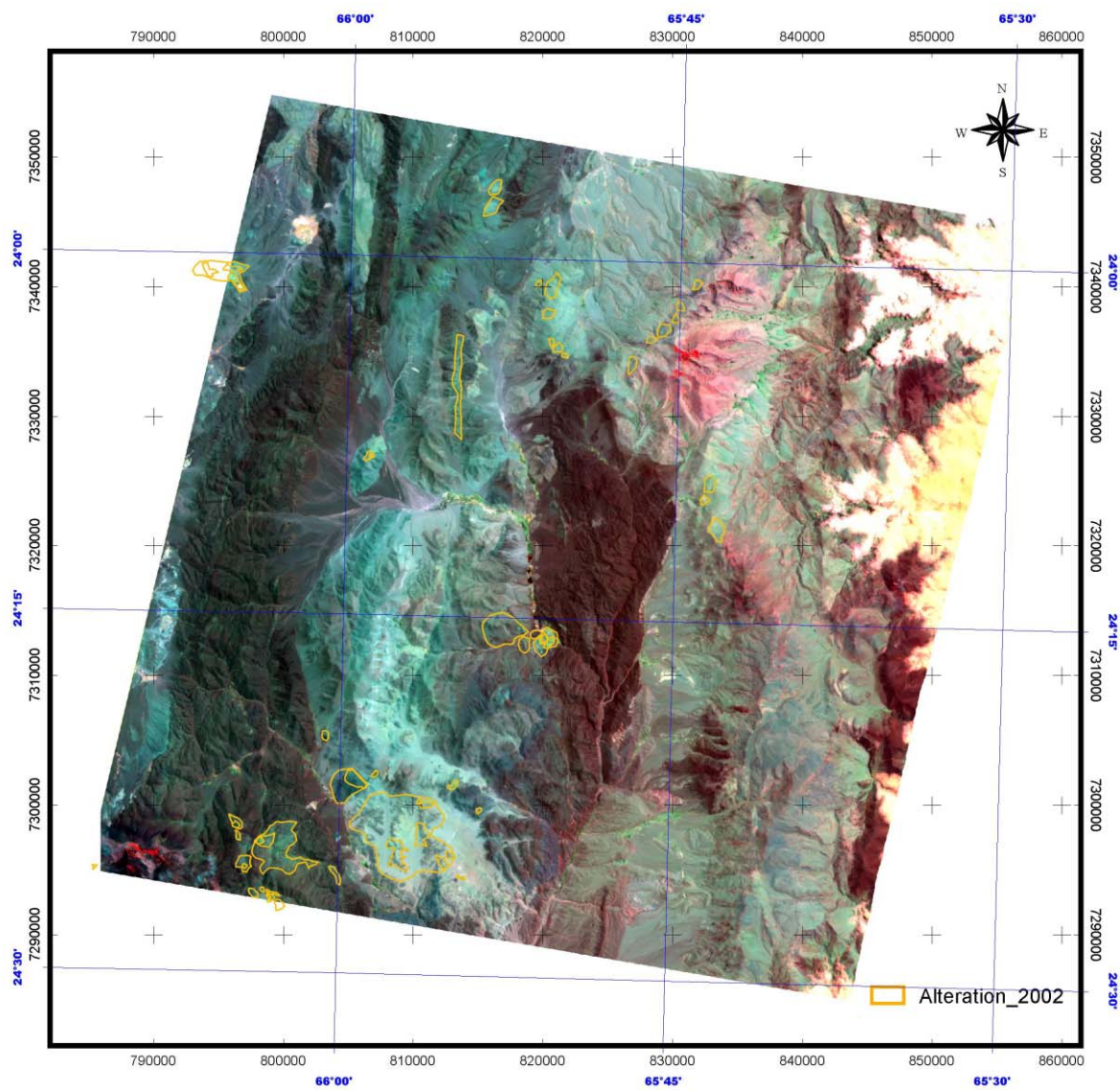
[Alteration zones]

No.32: Shows light green in 147. *Ser-Goe* has been detected. Geology is Cambrian sedimentary rocks.

No.33: Shows light green in 147. Composed of *Ser-Chl* and *Goe*. Geology is Precambrian sedimentary rocks.

No.34: Similar to No.32. The kind of detected minerals are also the same. Geology is Ordovician sedimentary rocks.

No.35: Similar to No.32. The kind of detected minerals are also the same. Geology is Precambrian and Cambrian sedimentary rocks.

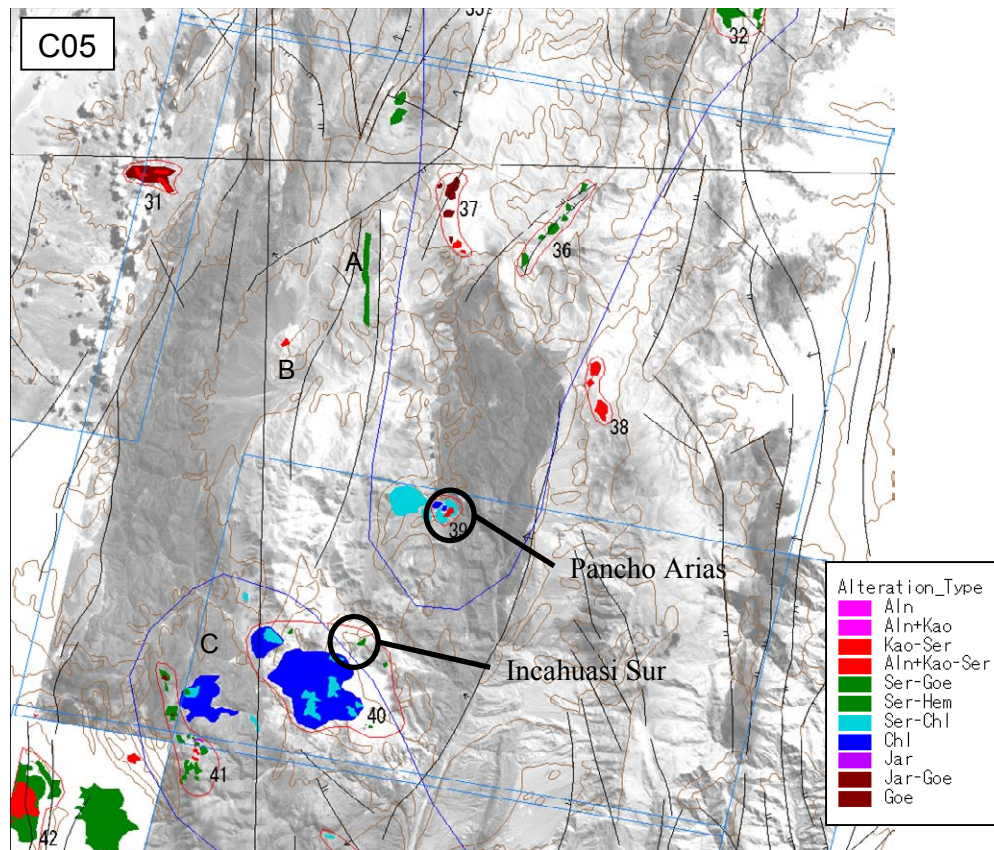


0 10 20 30 40 Kilometers

SCENE C05

IMAGE : TERRA/ASTER BGR=147
 PROJECTON : Universal Transverse Mercator
 PROJECT : JICA/MMAJ/JMEC
 DATA : ERSDAC/JAPAN

Fig.II-3-2-2-13 False color image of scene C05 (BGR=147)



[General]

This scene includes Pancho Arias area (No.39 and No.40) where field survey was conducted. Most of the area is made up of Paleozoic sedimentary rocks and granites, while some parts consist of Miocene sedimentary rocks. Alteration zones have been discriminated in the mid-axis part. Several acid alteration zones are also recognized. Ground truth survey was carried out for No.39 and No.40.

[Alteration zones]

No.31: Advanced argillic part consisting of *Aln-Kao* and *Jar*, accompanied by small quantities of *Ser* and *Goe* around it. Though advanced argillic part shows green in 147. Geology is Miocene volcanic rocks.

No.36: Shows light greenish gray in 147, and composed of *Ser-Goe*. Zones present NE-SW oriented distribution and are harmonious with the fault structure. Geology is Cambrian and Miocene sedimentary rocks.

No.37: Shows bluish green in 147. *Jar* is detected strongly and small quantities of *Kao* and *Ser* are also detected. N-S oriented distribution is shown. Geology is Cambrian sedimentary rocks.

No.38: Shows light green in 147. *Kao-Ser* and *Jar* are dominant, and indicate the existence of advanced argillic alteration. Geology is Cambrian sedimentary rocks.

No.39: Alteration zones of Pancho Arias prospect. The central part shows green clearly. This part is an advanced argillic alteration zone made up of *Kao-Ser* and *Jar-Goe*. Around it, a halo of *Ser-Goe* spreads, forming the circular alteration zone. Geology is Miocene volcanic rocks. In Cambrian

sedimentary rocks in the western and northwestern parts, two circular alteration zones consisting of *Chl-Ser-Hem* are recognized.

No.40: Includes Incahuasi Sur prospect in the northern part. Shows bluish and grayish white in 147 for the most part, while shows bluish green very partly. Mainly *Ser-Chl* has been detected. Since the geology is Cambrian granites, it could be a reaction of mica in granites, although the part shows bluish green in 147 is considered to be an alteration zone.

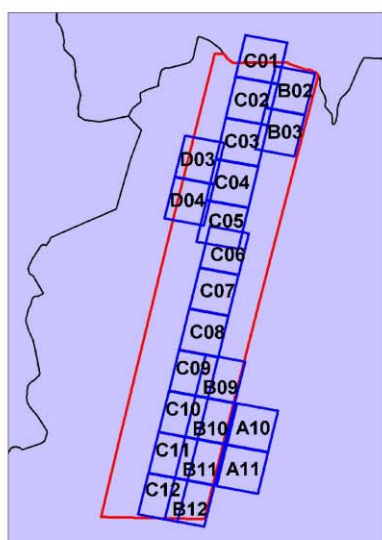
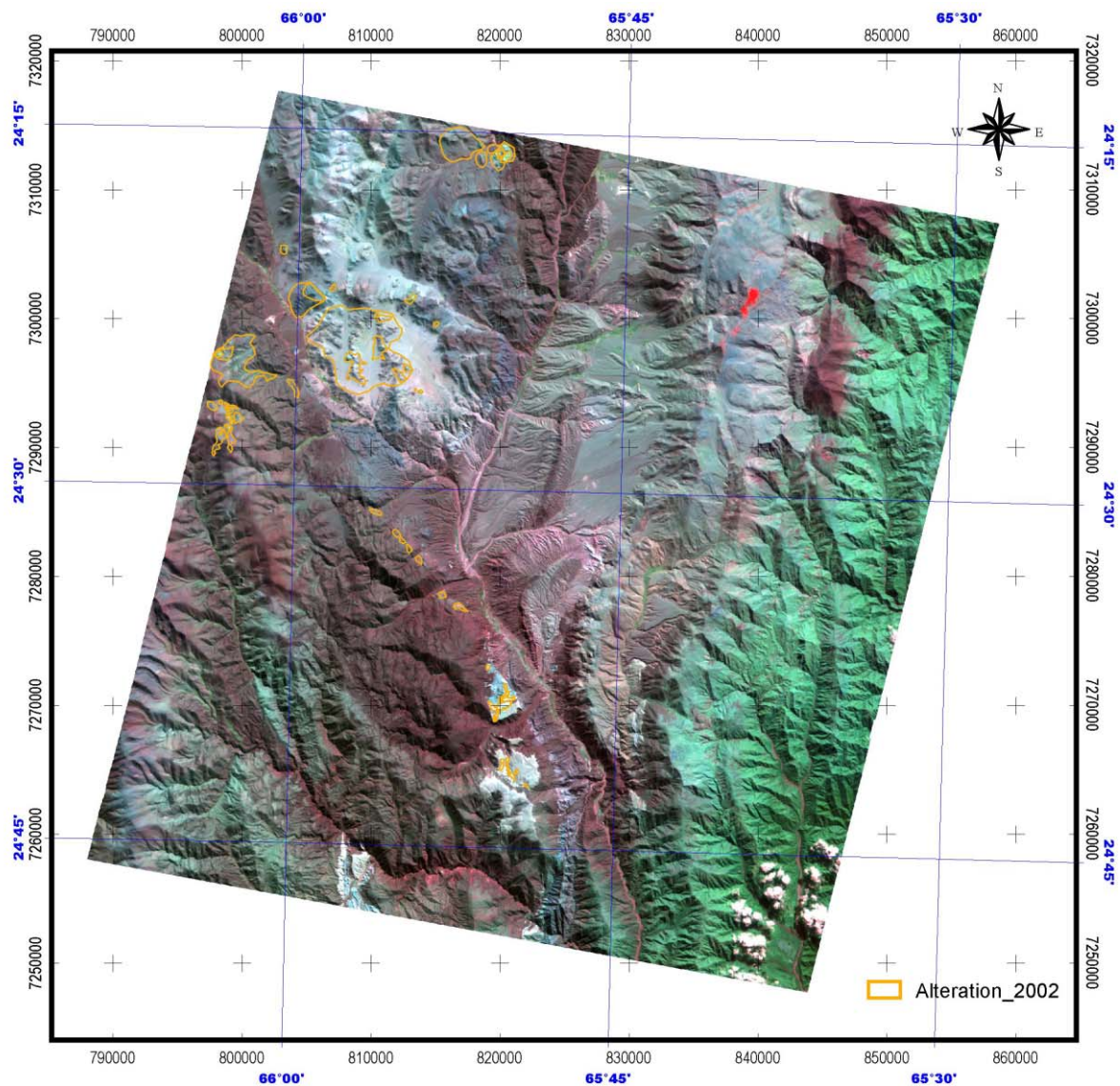
A: Shows bluish green in 147, and consists of *Chl>Ser* with *Goe* accompanying. Since it shows clear rectangular shape, it could be tuff of the same horizon. Geology is Cambrian granites.

B: Shows light green in 147. The central part is composed of *Kao-Ser* and *Goe-Jar*, and has advanced argillic characteristics. A halo made up of *Ser-Goe* is distributed around it. Geology is Cambrian sedimentary rocks.

C: Some part shows green in reddish brown surroundings in 147. Strongly altered part distributes at the northwestern edge, which consists of *Ser-Goe*. The remaining area is mainly made up of *Chl-Ser*, and *Hem* is also dominant. Therefore, it is assumed to be a phyllic to propylitic alteration zone. Geology is Ordovician granite rocks.

[Results of ground truth survey]

Ground truth survey was carried out for alteration zones in the eastern part of No.39, and for the northeastern end of No.40. These correspond to Pancho Arias prospect and Incahuasi Sur prospect in Pancho Arias area, where field survey was carried out this year. For results of the ground truth survey of this area, see Chapter 4.

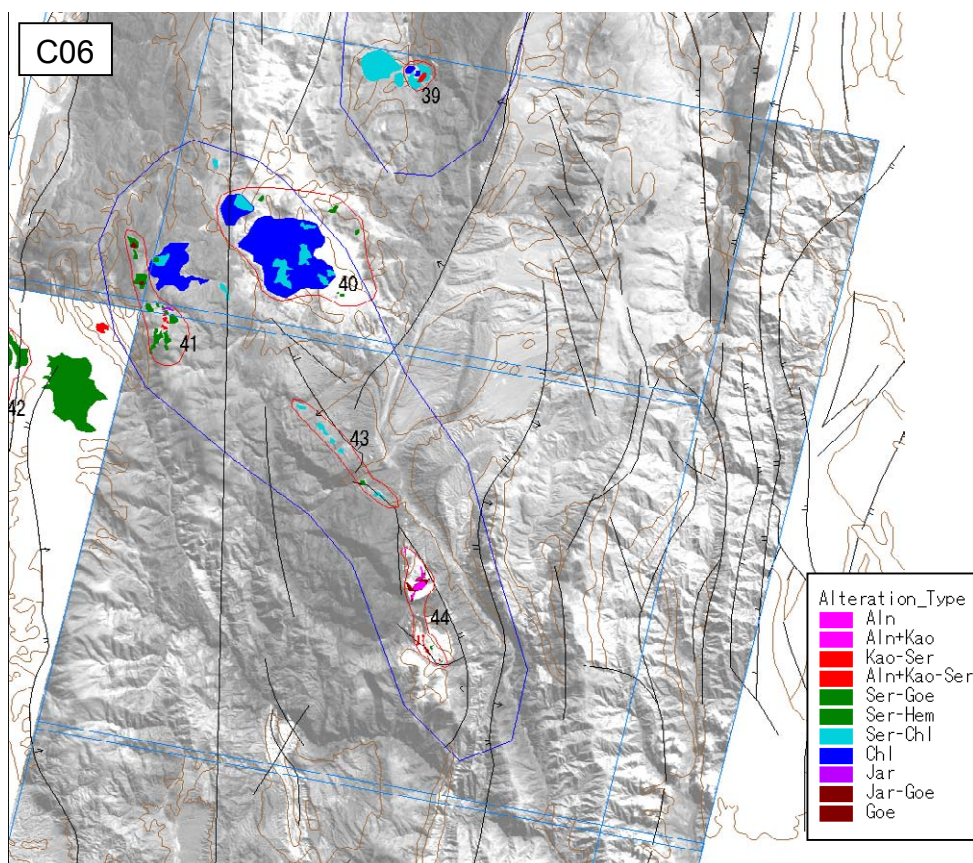


0 10 20 30 40 Kilometers

SCENE C06

IMAGE : TERRA/ASTER BGR=147
 PROJECTON : Universal Transverse Mercator
 PROJECT : JICA/MMAJ/JMEC
 DATA : ERSDAC/JAPAN

Fig.II-3-2-2-14 False color image of scene C06 (BGR=147)



[General]

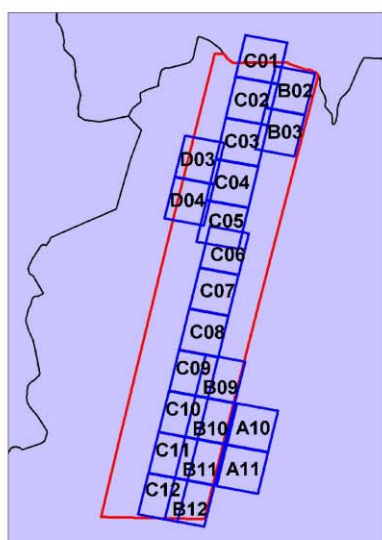
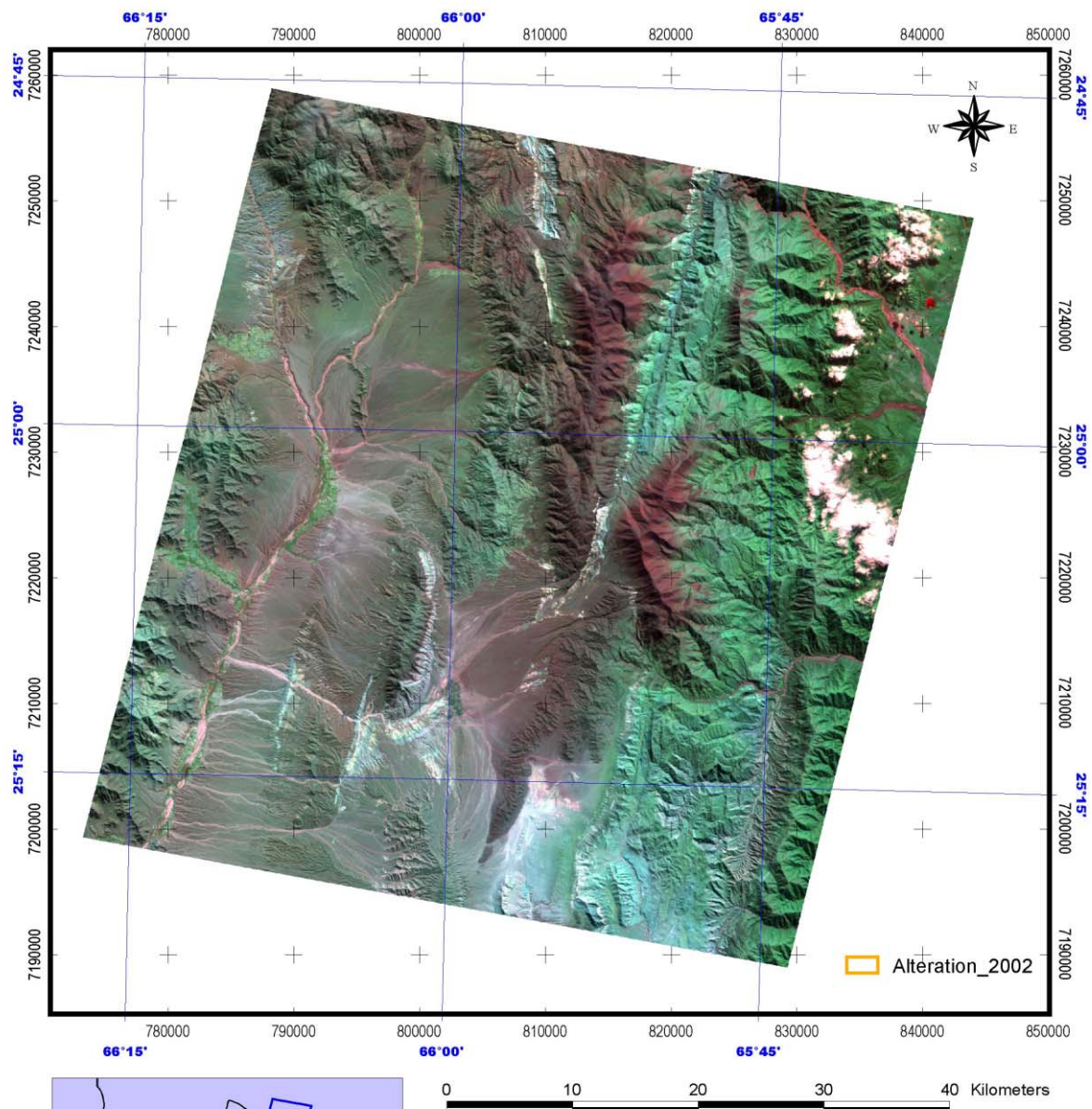
Paleozoic sedimentary rocks are distributed in the eastern and western part. In central part, Miocene sedimentary rocks are distributed in N-S direction. Alteration zones are discriminated in the western part. Meanwhile, following C-row images (C06-12) are taken in winter, radiance values are lower because of the sun elevation. Therefore, the error of identification could be larger.

[Alteration zones]

No.41: Made up of *Ser-Goe-Jar* in the northwestern part, and of *Ser-Chl-Goe* in the southeastern part. *Kao-Ser* is detected in some areas, and which show light green in 147. Geology is Ordovician granite rocks.

No.43: Distributed as a slightly greenish small area in the dark brown part in 147. *Chl* is dominant and is accompanied by *Ser*. A small quantity of *Goe* has been also detected. Located on a NW-SE oriented fault dividing Miocene sedimentary rocks and Ordovician granites.

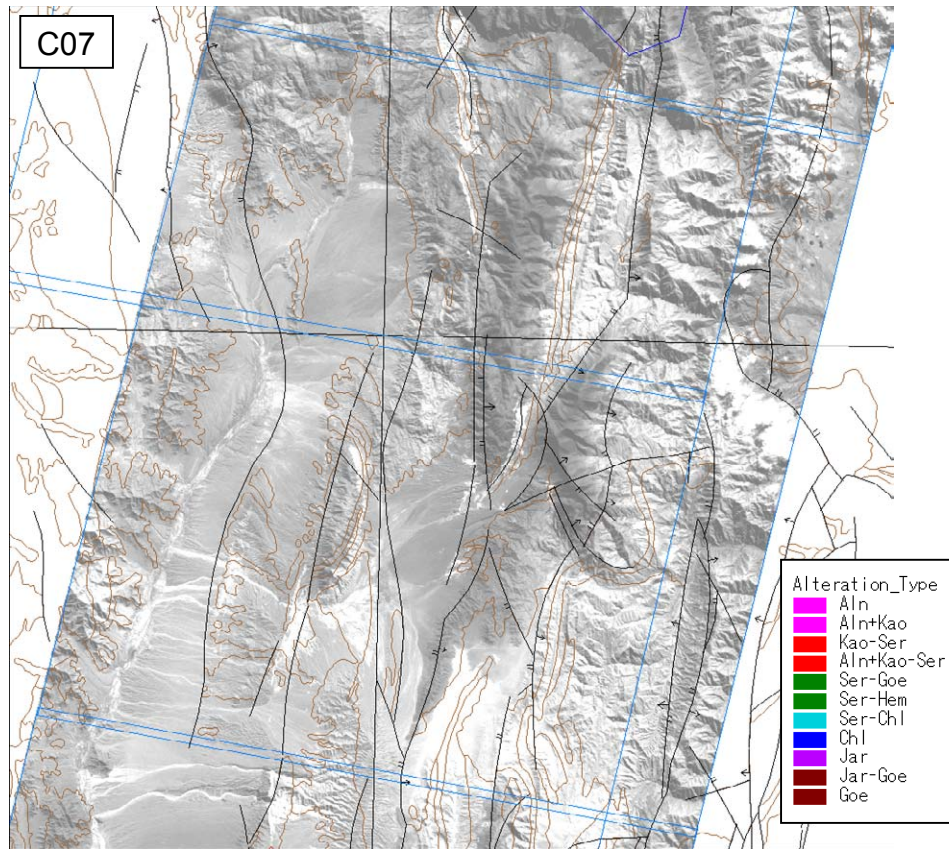
No.44: *Aln-Kao* is dominant, and *Goe* is also detected. On the point of mineral assemblage it is an apparent alteration zone, while it shows bright white in 147. Geology is Cretaceous and Paleogene sedimentary rocks.



SCENE C07

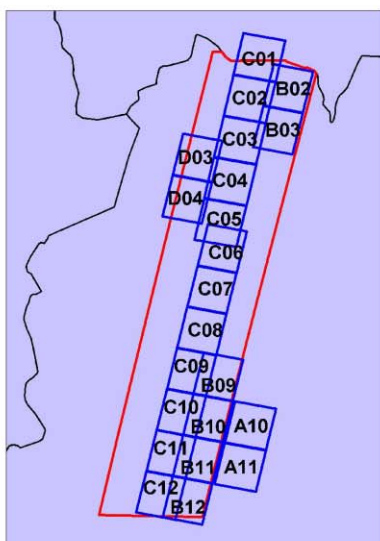
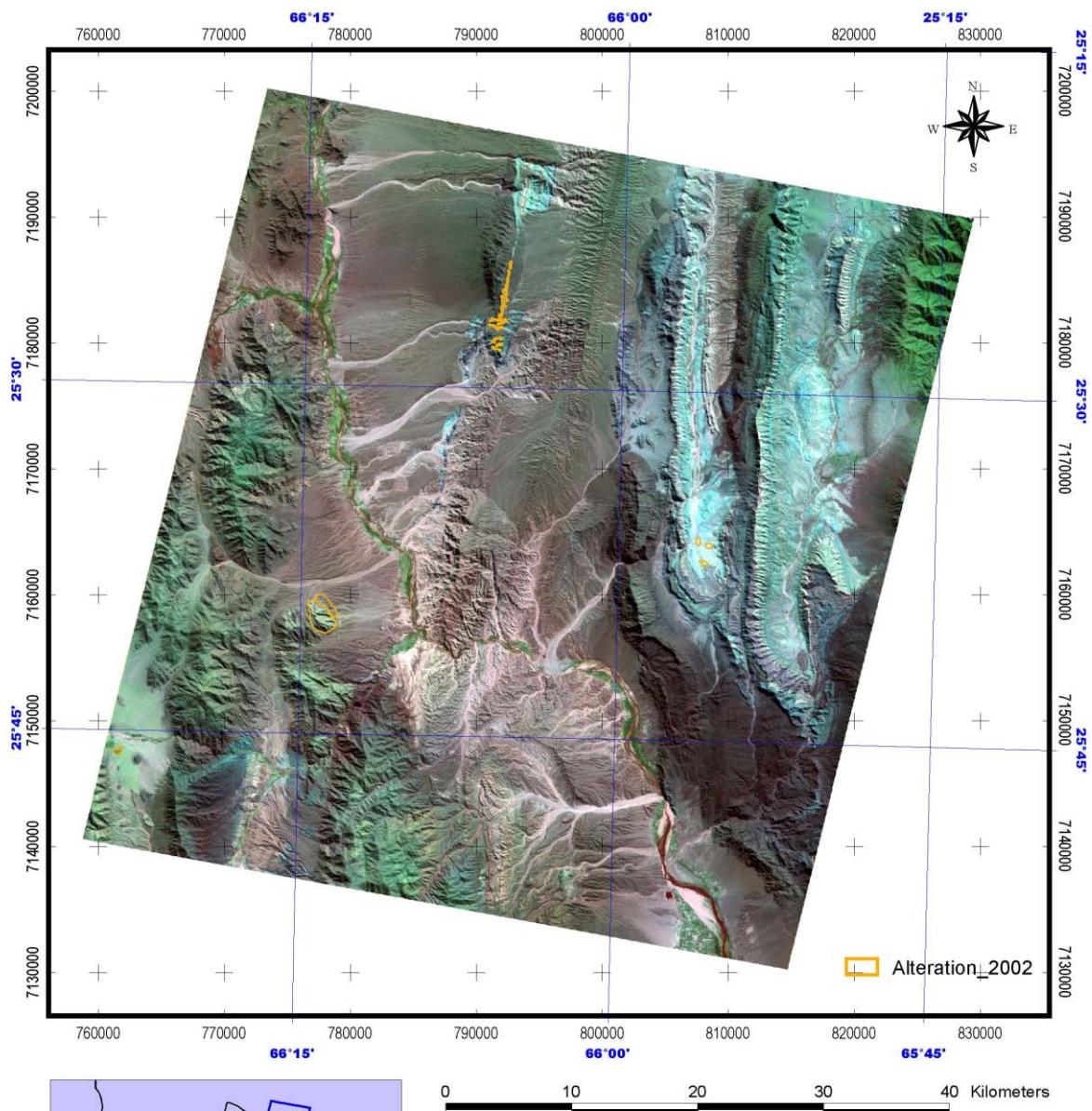
IMAGE : TERRA/ASTER BGR=147
 PROJECTON : Universal Transverse Mercator
 PROJECT : JICA/MMAJ/JMEC
 DATA : ERSDAC/JAPAN

Fig.II-3-2-2-15 False color image of scene C07 (BGR=147)



[General]

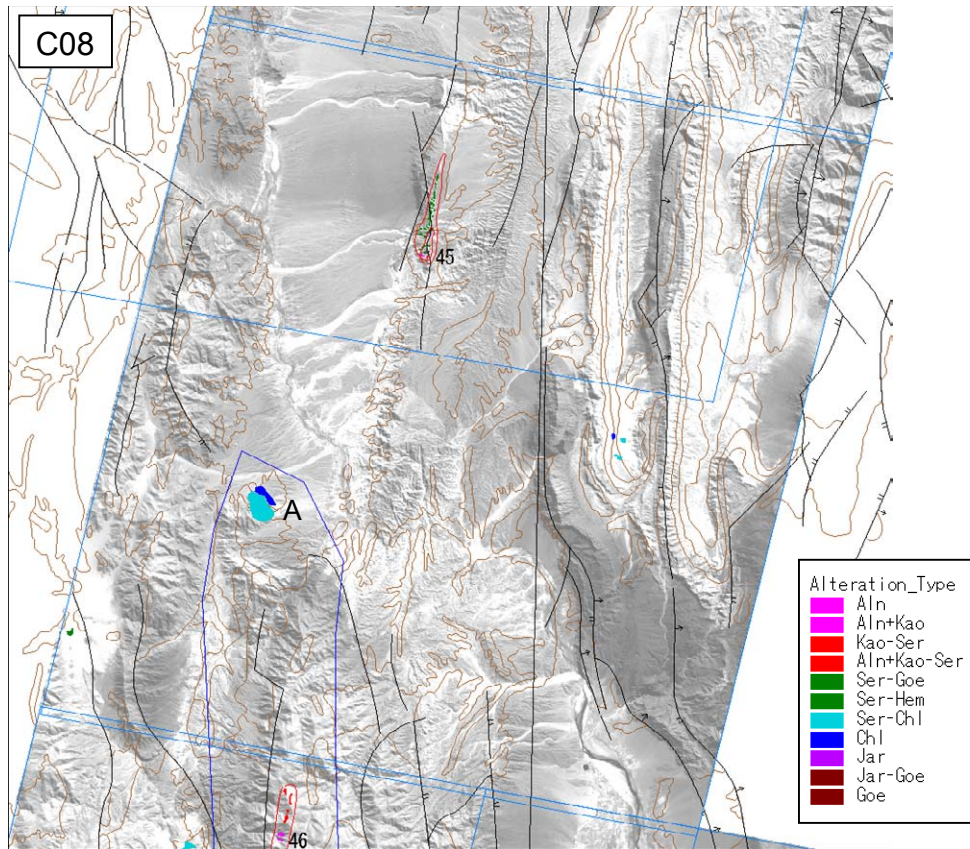
In the eastern part, Paleozoic to Tertiary units are distributed. In the western part, Paleozoic granites and sedimentary rocks are dominant. No alteration zones were discriminated.



SCENE C08

IMAGE : TERRA/ASTER BGR=147
 PROJECTON : Universal Transverse Mercator
 PROJECT : JICA/MMAJ/JMEC
 DATA : ERSDAC/JAPAN

Fig.II-3-2-2-16 False color image of scene C08 (BGR=147)



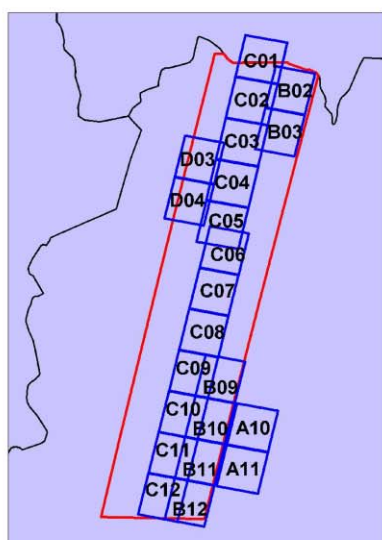
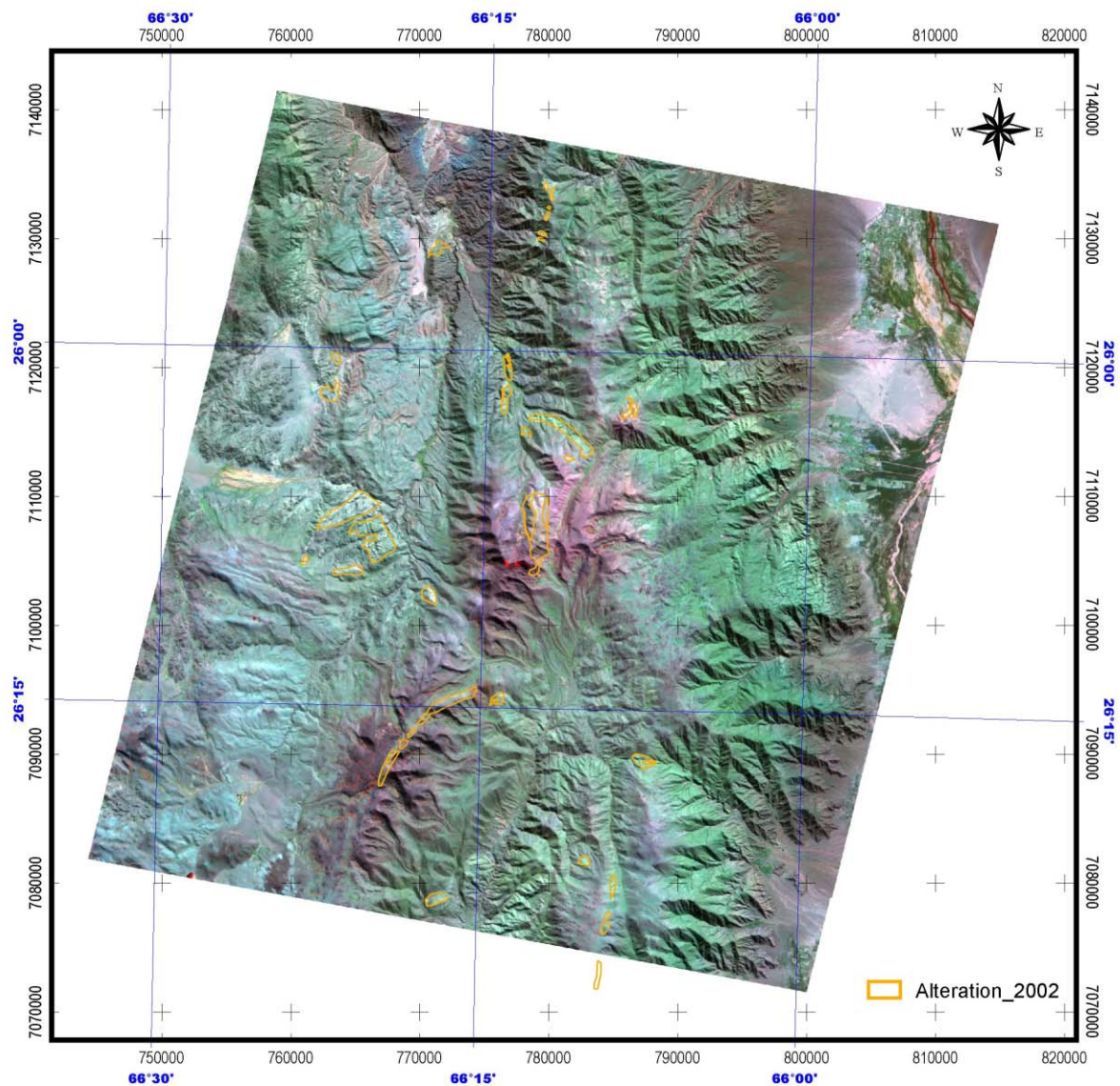
[General]

Sedimentary rocks of the Cretaceous to Neogene are distributed in the middle to eastern part, and Paleozoic metamorphic rocks and Miocene sedimentary rocks are in the western part. N-S oriented structure is developed in totality. Alteration zones have been discriminated from the middle and the western part.

[Alteration zones]

No.45: Shows watery blue in 147. Since geology is Cretaceous sedimentary rocks it is assumed to be tuff of the same horizon, although *Ser-Goe* is detected.

A: Shows light green in 147, and *Ser-Chl-Goe* has been detected. As the geology is Ordovician granites, there is a possibility that weathering surface of granites were detected. *Chl* has been detected strongly also in talus sediments contacting the base of a mountain in the northeast of granites.

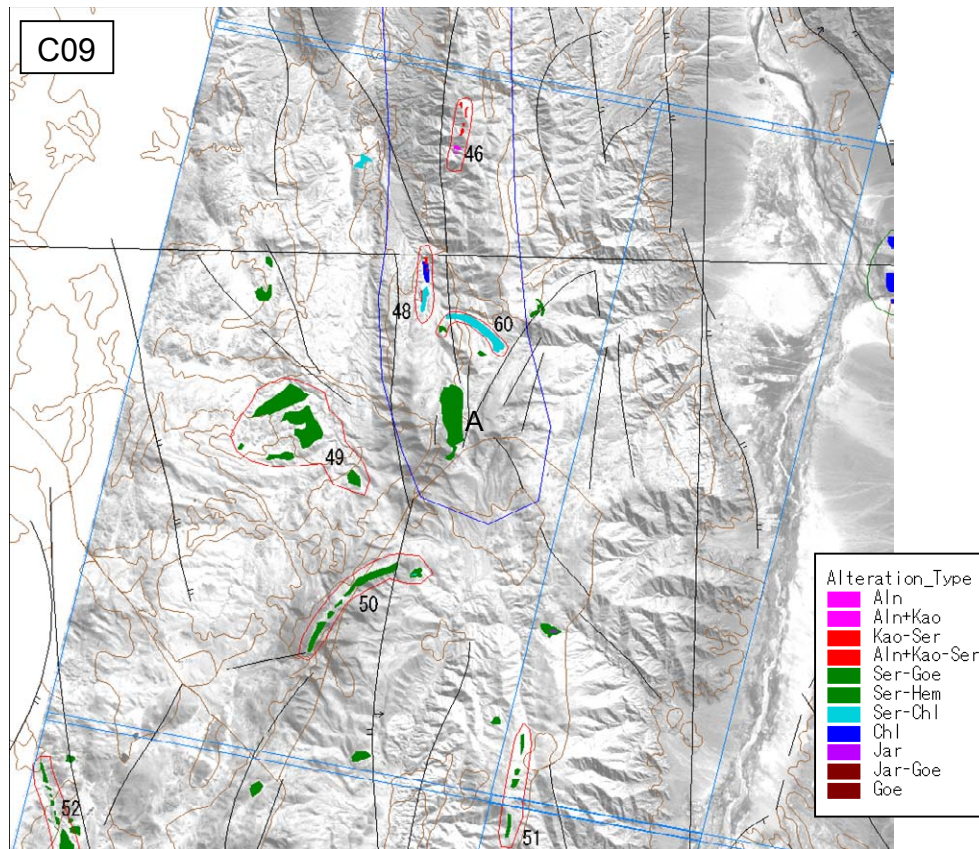


0 10 20 30 40 Kilometers

SCENE C09

IMAGE : TERRA/ASTER BGR=147
 PROJECTON : Universal Transverse Mercator
 PROJECT : JICA/MMAJ/JMEC
 DATA : ERSDAC/JAPAN

Fig.II-3-2-2-17 False color image of scene C09 (BGR=147)



[General]

Precambrian metamorphic rocks are dominant in the mid-axis part, Paleozoic granites and Miocene volcanic rocks extending in N-S in the western part. The eastern part is covered with Quaternary sediments. Alteration zones are mainly discriminated around the mid-axis part.

[Alteration zones]

No.46: Shows light green in 147 and *Aln-Goe* is detected. In the analyzed image, a strip in the N - S direction overlapping this part is recognized, and there is a possibility that location error between bands were detected.

No.48: Shows green in 147. Small quantities of *Kao-Ser* and *Goe* have been detected. Geology is Precambrian metamorphic rocks.

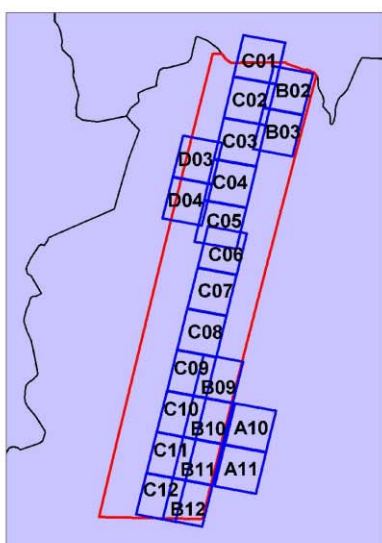
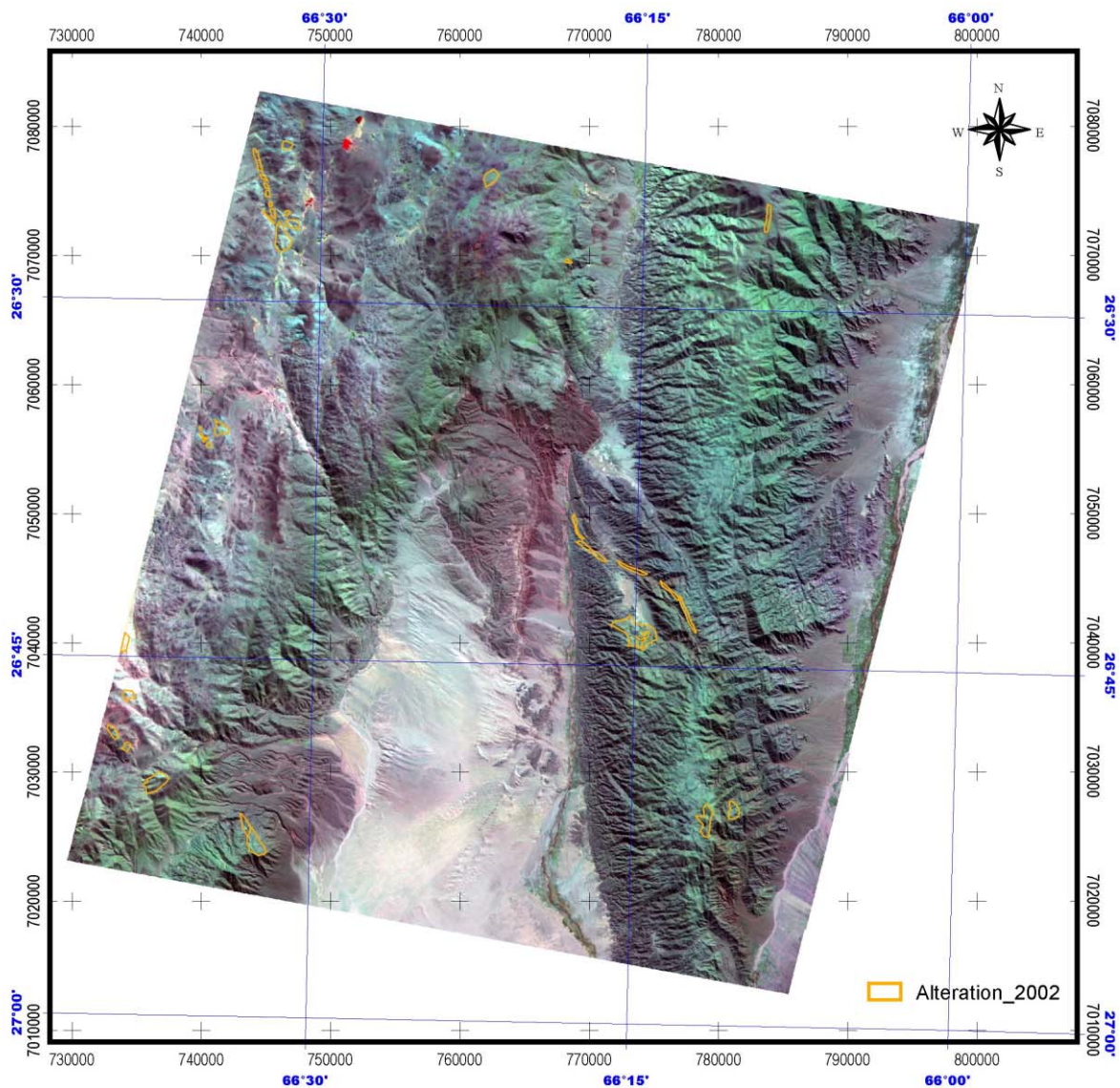
No.49: Shows grayish white in 147. *Ser-Goe* has been detected in a circular shape. Because the geology is Ordovician granites, there is a possibility that mica in granite was detected.

No.50: Shows reddish and grayish white in 147. *Ser-Goe* has been detected in an arc shape. Geology is Precambrian metamorphic rocks.

No.51: *Ser-Goe* has been detected. Since some vegetation is recognized, its certainty may be low.

No.60: Shows green along the base of the mountain in 147, and *Ser-Chl* and *Goe* have been detected there. Geology is Paleozoic metamorphic rocks.

A: Shows light green in the northern part and brown in other parts in 147. *Ser-Hem* is dominant in the axis part, and *Ser-Goe* is dominant on both sides. Geology is Precambrian metamorphic rocks.

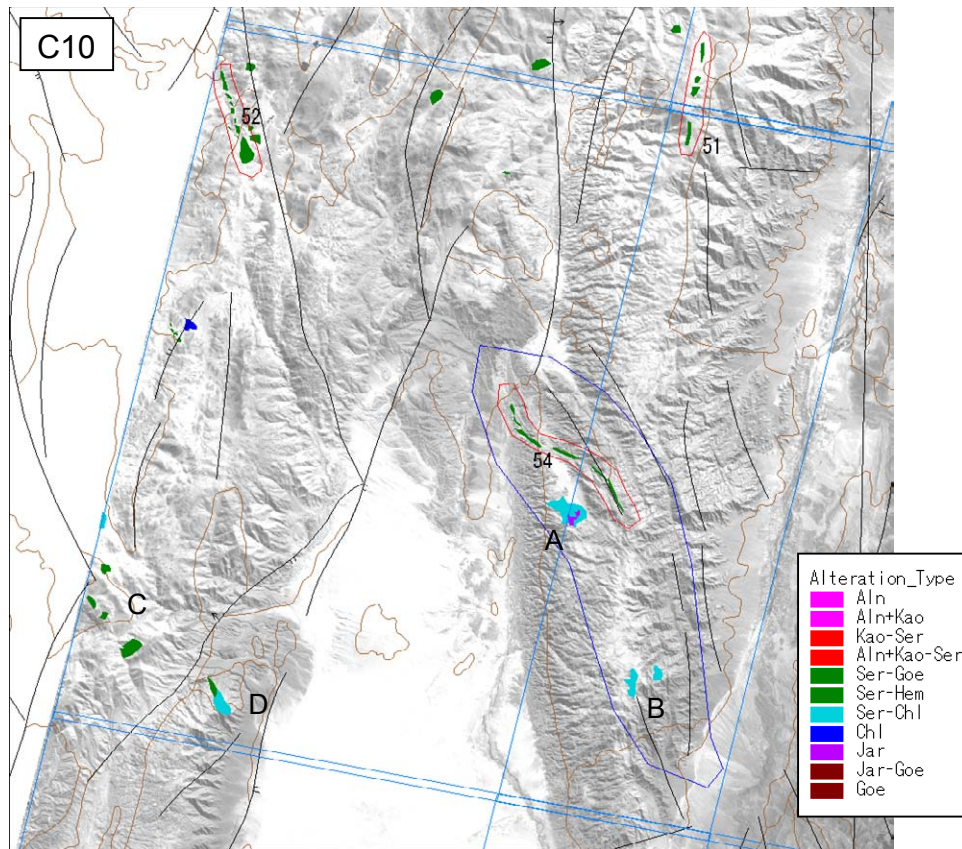


0 10 20 30 40 Kilometers

SCENE C10

IMAGE : TERRA/ASTER BGR=147
 PROJECTON : Universal Transverse Mercator
 PROJECT : JICA/MMAJ/JMEC
 DATA : ERSDAC/JAPAN

Fig.II-3-2-2-18 False color image of scene C10 (BGR=147)



[General]

The mountainous region in the eastern part is composed of Precambrian and Cambrian metamorphic rocks, and the mountainous region in the western part is Ordovician granites. The central basin consists of Miocene sedimentary rocks and has synclinal structure.

[Alteration zones]

No.52: Shows bluish green in 147, it is similar to Cretaceous tuff. *Ser-Goe* is accompanied by a small quantity of *Chl*. Geology is Ordovician granites and Tertiary volcanic rocks.

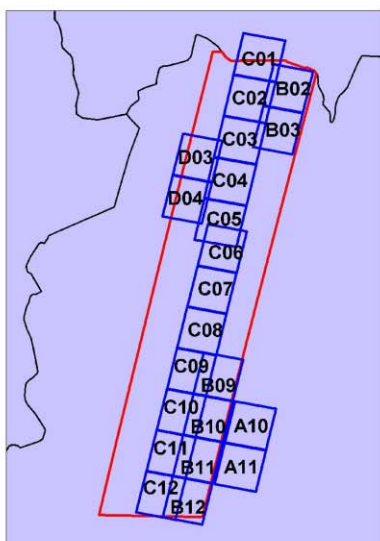
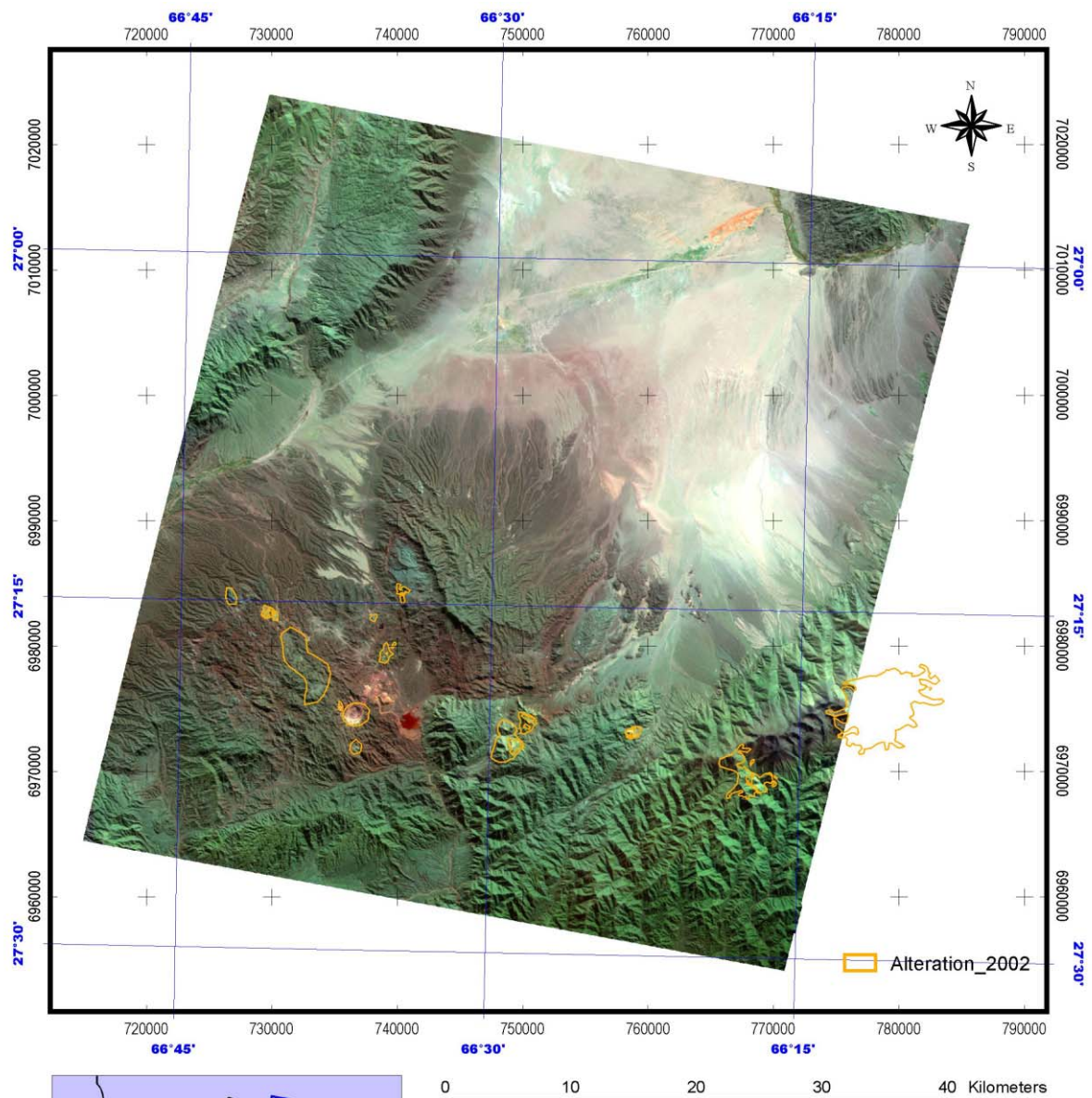
No.54: Alteration zone accompanying fault structure, similarly to No.52. It shows brown in 147. *Ser-Chl* and *Goe* have been detected. There is the possibility of fault clay.

A: Shows a slightly greenish color in 147. *Ser-Goe* is accompanied by some quantity of *Chl*. Geology is Precambrian and Cambrian metamorphic rocks.

B: Shows a slightly greenish color in 147. *Ser-Chl* has been detected. Geology is Precambrian and Cambrian metamorphic rocks.

C: Shows light green in 147. *Ser-Goe* is accompanied by some quantity of *Chl*. Geology is Ordovician granites.

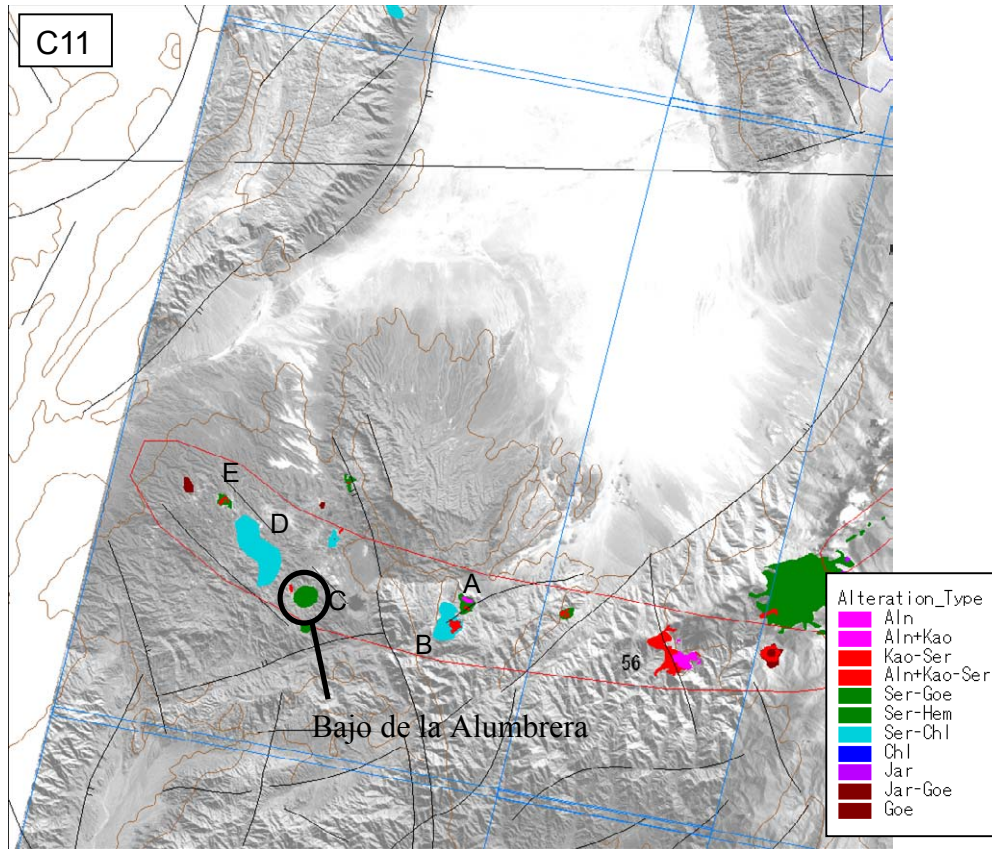
D: Shows bluish green in 147. A large quantity of *Ser* has been detected as a block in the discriminated area. Since geology is Paleozoic granites, there is a possibility that mica in granites was detected.



SCENE C11

IMAGE : TERRA/ASTER BGR=147
 PROJECTON : Universal Transverse Mercator
 PROJECT : JICA/MMAJ/JMEC
 DATA : ERSDAC/JAPAN

Fig.II-3-2-2-19 False color image of scene C11 (BGR=147)



[General]

The mountainous region in the southeastern part mainly consists of Paleozoic granites, and the middle western part is composed of basic volcanic rocks and sedimentary rocks of the Miocene. Alteration zones are distributed in E-W direction in this scene, although distributed in N-S direction in neighboring scene B11.

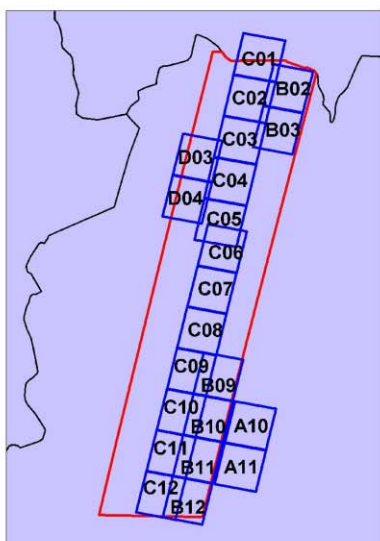
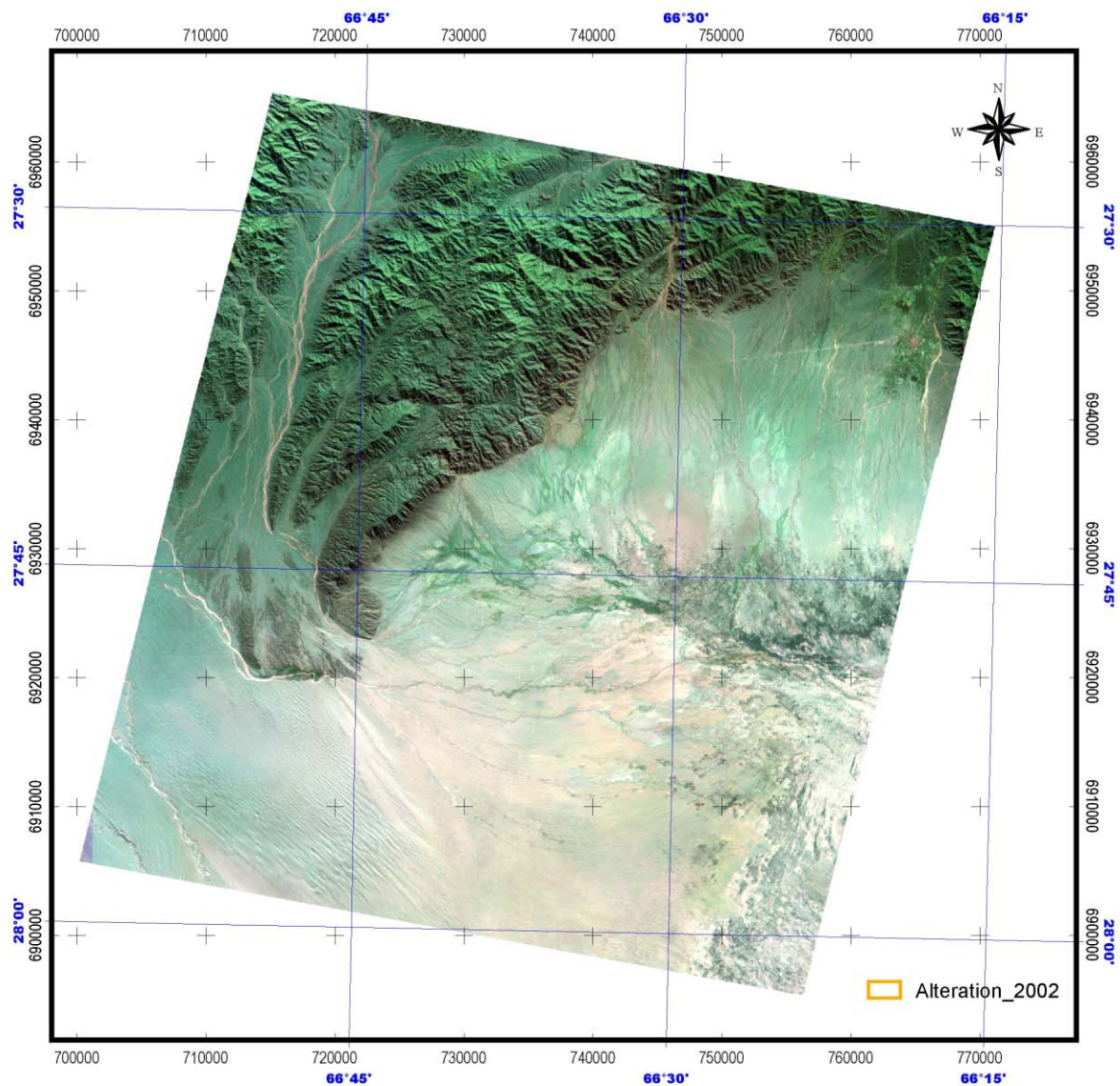
[Alteration zones]

A: Shows light green in 147. *Aln* is dominant in the northern part, *kao* is dominant in the southern part, and halo made up of *Ser-Goe* exists around them. Geology is Miocene basic volcanic rocks

B: Shows light green in 147. *Aln-Kao-Ser* and strong *Jar* have been detected at the center, and has advanced argillic features. *Ser* and some quantity of *Chl* accompanied by *Goe* have been recognized as a halo.

C: Alteration zone of Bajo de la Alumbreira mine. Shows reddish brown in 147. *Ser-Hem* has been detected in a pit, and some quantity of *Kao* at the south border of the pit. Annular-shape intrusive rocks are recognized in the south of the pit, and alteration made up of *Ser-Goe* with *Chl* is discriminated.

D: Alteration zone adjoining Farallon Negro mine. Shows dark reddish brown in 147. *Chl-Ser* is detected more than in the surrounding area, and makes outline of the alteration zone unclear.

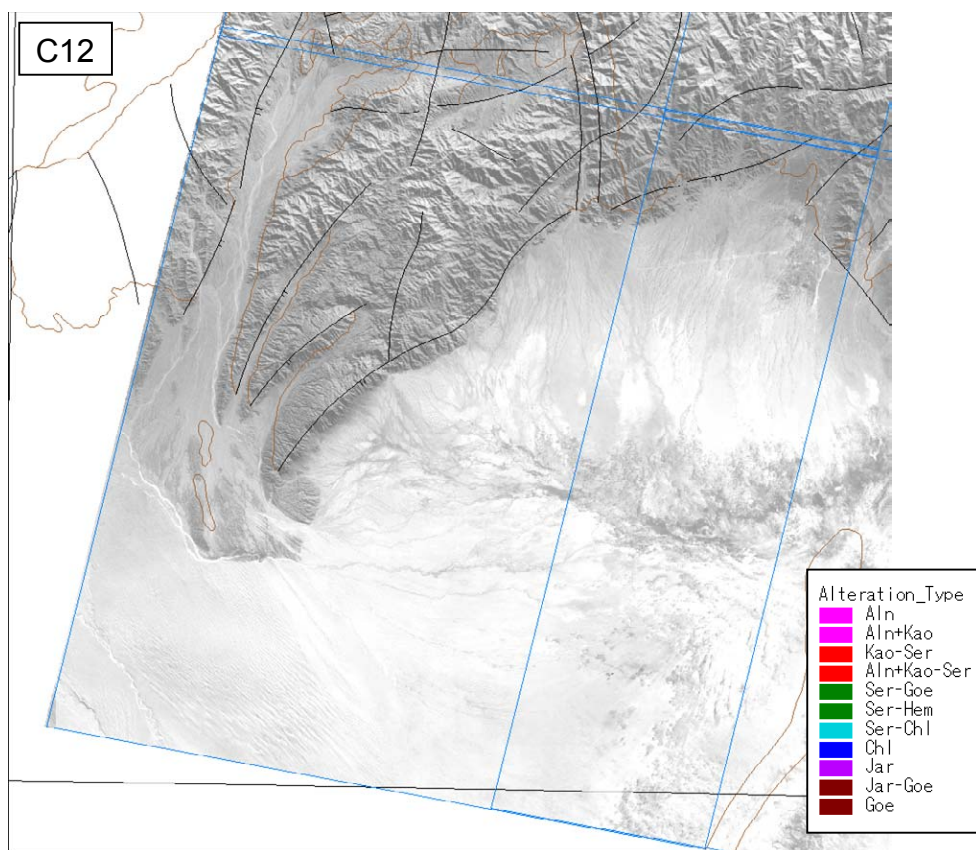


0 10 20 30 40 Kilometers

SCENE C12

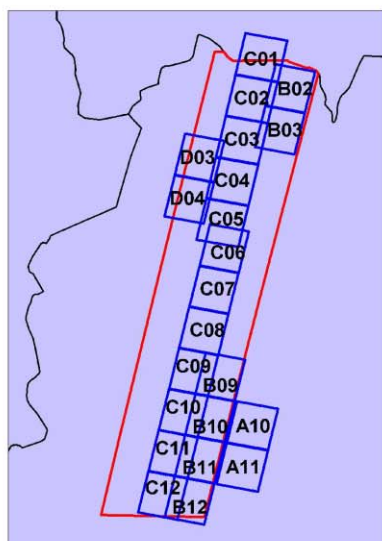
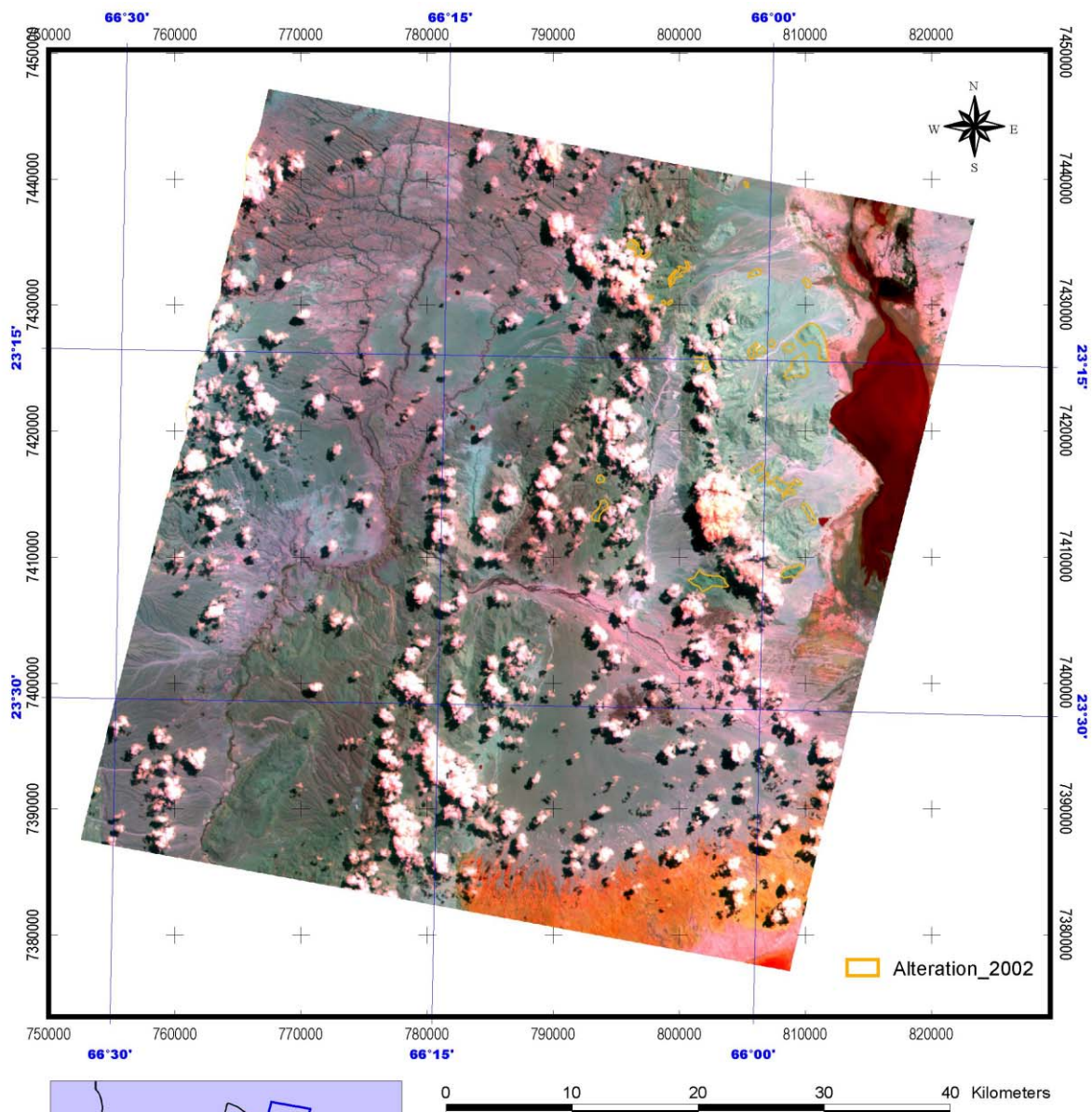
IMAGE : TERRA/ASTER BGR=147
 PROJECTON : Universal Transverse Mercator
 PROJECT : JICA/MMAJ/JMEC
 DATA : ERSDAC/JAPAN

Fig.II-3-2-2-20 False color image of scene C12 (BGR=147)



[General]

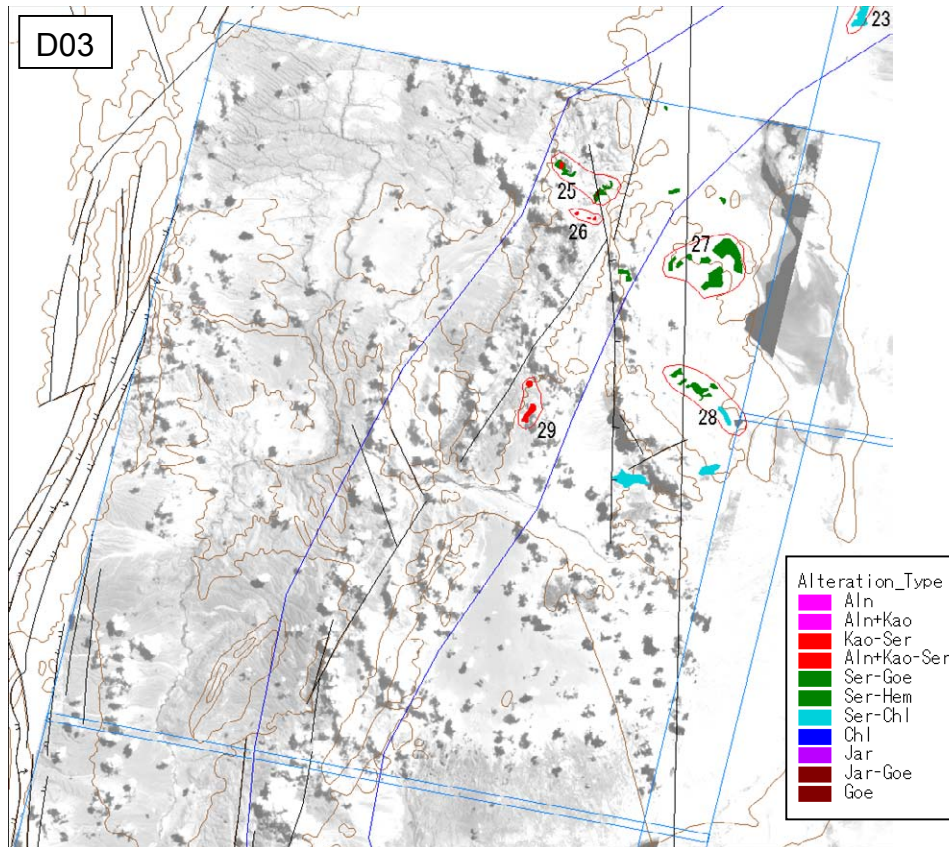
The mountainous region in the northwestern part is composed of Paleozoic granites, and the remaining area is covered with Quaternary sediments. No alteration zones were detected.



SCENE D03

IMAGE : TERRA/ASTER BGR=147
 PROJECTION : Universal Transverse Mercator
 PROJECT : JICA/MMAJ/JMEC
 DATA : ERSDAC/JAPAN

Fig.II-3-2-2-21 False color image of scene D03 (BGR=147)



[General]

This scene includes La Colorada area, where field survey was conducted this year. In the central part, Ordovician sedimentary rocks and granites are distributed in N-S orientation. The northeastern part consists of Paleozoic granites. Alteration zones are mainly detected in granites and sedimentary rocks in the northern part. Ground truth survey was carried out for No.27.

[Alteration zones]

No.25: Shows light green in 147. *Kao-Ser* is dominant with *Jar* and *Goe* accompanying in the eastern part. *Ser-Goe* is distributed around *Kao-Ser-Jar* in the western part. Geology is Ordovician sedimentary rocks.

No.26: Similar to No.25.

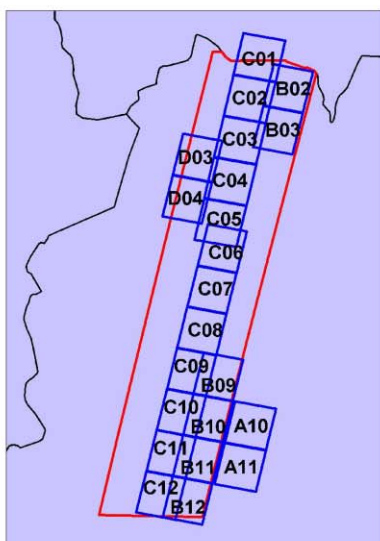
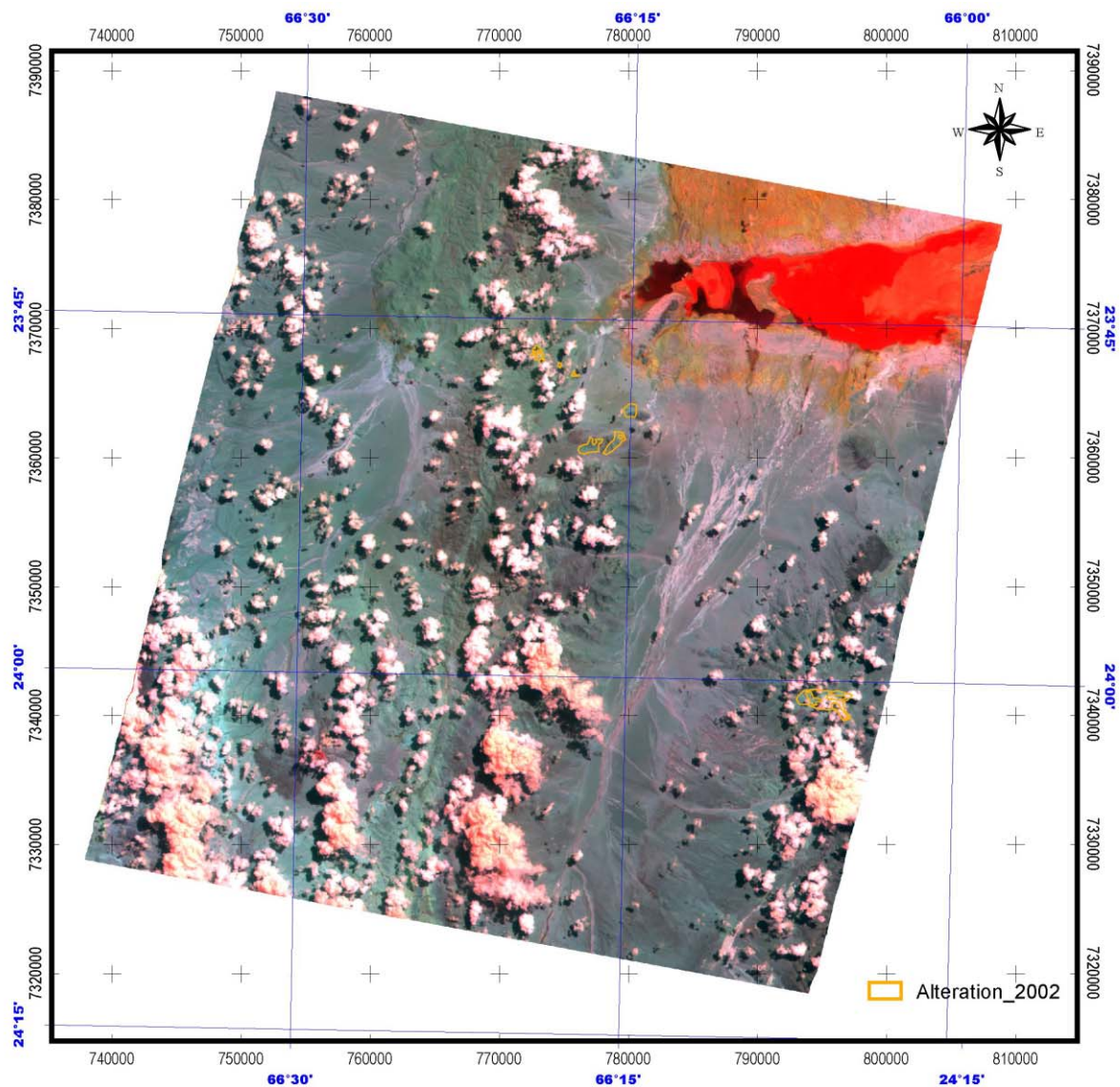
No.27: Shows bluish green in 147. *Ser* was detected in this whole bluish green area. Because the geology is Paleozoic granites, it is considered that mica in granite was detected.

No.28: Similar to No.27.

No.29: Shows light green in 147. *Kao-Ser* is dominant with *Goe* and *Jar* accompanying.

[Results of ground truth survey]

Ground truth survey was carried out for No.27. It is confirmed that granites are distributed in this area. From X-ray diffractive analysis for samples taken here (A02TK029), small quantity of sericite was detected. It is considered that this sericite was detected in mineral identification process.

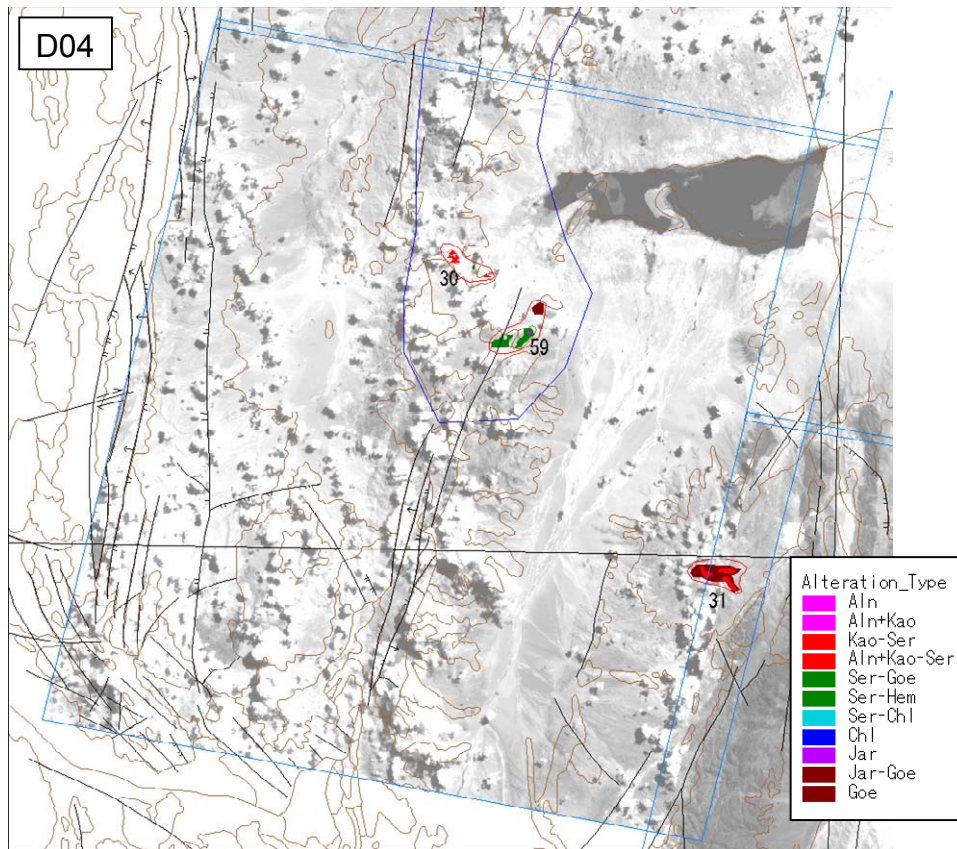


SCENE D04

IMAGE : TERRA/ASTER BGR=147
 PROJECTON : Universal Transverse Mercator
 PROJECT : JICA/MMAJ/JMEC
 DATA : ERSDAC/JAPAN

Fig.II-3-2-2-22

False color image of scene D04 (BGR=147)



[General]

This scene includes La Colorada area, where field survey was made. In the central part, Ordovician sedimentary rocks and granites are distributed in N-S direction. Tertiary sedimentary rocks and volcanoclastics area distributed in other area. Alteration zones are discriminated in Ordovician sedimentary rocks and granites. Ground truth survey was carried out for No.59.

[Alteration zones]

No.30: Shows light green in 147. Made up of *Kao-Ser* and *Jar-Goe*, particularly dominant in *Jar*. Geology is Ordovician sedimentary rocks.

No.59: Shows light green in 147. Geology is Ordovician granites for southeastern part, and Ordovician sedimentary rocks for southwestern part. Both are mainly composed of *Ser-Goe* with some quantities of *Kao* and *Jar* accompanying.

[Results of ground truth survey]

Ground truth survey was carried out for southeastern part of No.59. *Jar* is dominant at the center. The area where *Jar* is detected is an area where Cambrian quartzite is distributed. A trace quantity of sericite was detected in the X-ray diffractive analysis for the sample taken here (A02KK035). It is considered that this sericite was detected in mineral identification process.

3-3 Discussion

Using 22 scenes ASTER images in this survey, image analysis was carried out. In addition to the analyzed area in the survey of the previous year, the analysis by ASTER data were finished in the greater part of the survey target area except the plain.

The advanced vegetation removal as the pre-processing was carried out to improve the accuracy of altered mineral identification in the analysis of this year. SAVI is generally used to calculate the vegetation index in the spectral analysis of the semi-arid zone like the survey area. SAVI was used in the analysis of the previous year as the index of vegetation coverage to try to remove the vegetation information in the analysis of last year. However, since the removal of vegetation information by using SAVI without the specification of the soil brightness includes the errors, the removal by using PSAVI was carried out in the analysis of this year. Since PSAVI is obtained by the calculation SAVI by using pseudo-reflectivity, the removal by this method includes the soil brightness information. Therefore, the removal of vegetation by using PSAVI can offset the effect of the soil brightness. By using this method, the accuracy of mineral identification could be made improve in the area with vegetation coverage of less than 40% (analytical limit in the present).

In this analysis, we made estimated SiO₂ contents map using the thermal infrared data that is one of the characteristics of ASTER, and carried out the consideration about the usability of the map. In the analysis result of last year, although the difference of rock strata were reflected as the difference of silica contents in some parts of the area, the reverse tendency that the low SiO₂ contents in acid rock as granite was also obtained. To avoid this kind of mis-interpretation, the necessity of the elevation correction by using DEM was pointed out. In this year, since ERSDAC began to distribute the advanced products of ASTER data, the 3A01 product that is a data set of orthographic projection transformed image and DEM was obtained, the elevation correction was carried out for atmospheric correction by using DEM data to estimate the SiO₂ contents. In the estimation using estimated SiO₂ contents map, estimated high SiO₂ content area is observed in the sedimentary rocks dominant area (B02 ~ 03, C01 ~ 03) in the north of the survey area. Quartzite in this area was confirmed by the field survey, the usability of the estimation was shown. However, since the further field verification is necessary, the estimation of SiO₂ content remains as the future subject.

541 places were detected as the alteration zones by the analysis of this year. The verification for a part of the alteration zones was carried out in the field survey. As the result, the alteration was confirmed in many points that were detected as the alteration zones by the analysis. Almost all the shallow hydrothermal ore deposit with alteration zone, and the known porphyry type ore deposit and ore-bearing area were detected in this analysis. However, some mis-detection also occurred. In the above estimated high SiO₂ contents area, in spite of the quartzite area without alteration, many alteration zones with sericite – goethite or kaolinite – sericite were detected by the analysis. The

consideration of the above mis-detection has not been carried out, because of no spectral data of quartzite in the field. Although this is also the subject for the future, the correct classification of processed image is considered to be possible by the total interpretation including the estimated SiO₂ content map.

541 alteration zones were detected by using images of 22 scenes in the analysis of this year. The following areas are worth the attention as the prospective ore-bearing area from the results of satellite image analysis based on the comprehensive study including site verification.

①The area that the alteration relatively developed (alunite and kaolinite were detected)

: B11 – No.55, C11 – No.56

②The area that the alteration relatively low (chlorite was detected)

: C05 – D and No.40

Location of those interested area are shown in Fig.II-3-3-1. In the type ①, the highly altered minerals are distributed on the surface. Although these areas are the extremely interesting area, the possibilities as the areas that are already known are high. There are some prospecting in the alteration zone in spite of the remote locality and the inconvenient access. In the type ②, chlorite and other clay minerals are distributed in this alteration zone that means the alteration is comparatively weak. However, chlorite is one of the minerals that is difficult to identify by LANDSAT TM, so, the areas of this type are worth to pay attention as the future prospecting target area.

Alteration zone discriminated by ASTER in Phase I, Phase II and alteration by Landsat TM (Regional survey 1997) are shown in Fig.II-3-3-2. Based on this figure, it is clear that alterations are distributed mainly on four Tertiary volcanic rock zone extending NE-SW direction and on its extension. The distribution of alterations is also match the location of major tectonic line, which is concordantly located with Tertiary volcanic rock zone.

3-4 Summary

This analysis was carried out to identify the altered minerals in the alteration zones that are accompanied by ore deposit by using actual ASTER data that is able to use satellite data effectively for the metal deposit survey. The target area is located in rock exposing area and the climate of this area is semi-arid.

The following pre-processing was carried out before the analysis.

- Conversion to pseudo-reflectance by using pseudo-reflectance conversion coefficients (Ministry of Economy, Trade and Industry, 2002)
- Removal of reflection spectrum from vegetation by using PSAVI (Pseudo Soil Adjust Vegetation Index)

The iso-grain Model that is considered the reflection and absorption among the particles of minerals were used in the identification of alteration minerals and the semi-quantitative analysis. In this analysis, using the iso-grain Model made the database of spectral reflectivity. Mixing of the selected 10 popular minerals made the Model. Then mineral identification on the surface and the semi-quantitative analysis were carried out to make the mineral mapping.

The atmospheric correction, and the separation of the temperature and emissivity of the data of thermal band that is one of the characteristics of ASTER. Then, the mapping of SiO₂ contents was carried out. The mapping was carried out by using the conversion equation that had been proposed in the data analysis of Earth Resources Satellite (Ministry of Economy, Trade and Industry, 2000).

541 alteration zones were detected by using the visible and short wavelength of infrared Bands, and iso-grain model. Within the detected zone, there are the places that have no relation to ore showing. Based on the analysis, the establishment of recognition method (or standard) of alteration zone with mineral showing is the subject for the future.

Based on the field verification, the areas that are desirable to make further prospecting from the result of satellite image analysis are as follows:

- ① The area where the alteration developed and acid altered minerals such as alunite and kaolinite were sampled
: B11 – No.55, C11 – No.56
- ② The area where the alteration is weak, and chlorite was (ring-shaped) detected
: C05 – C, No.40

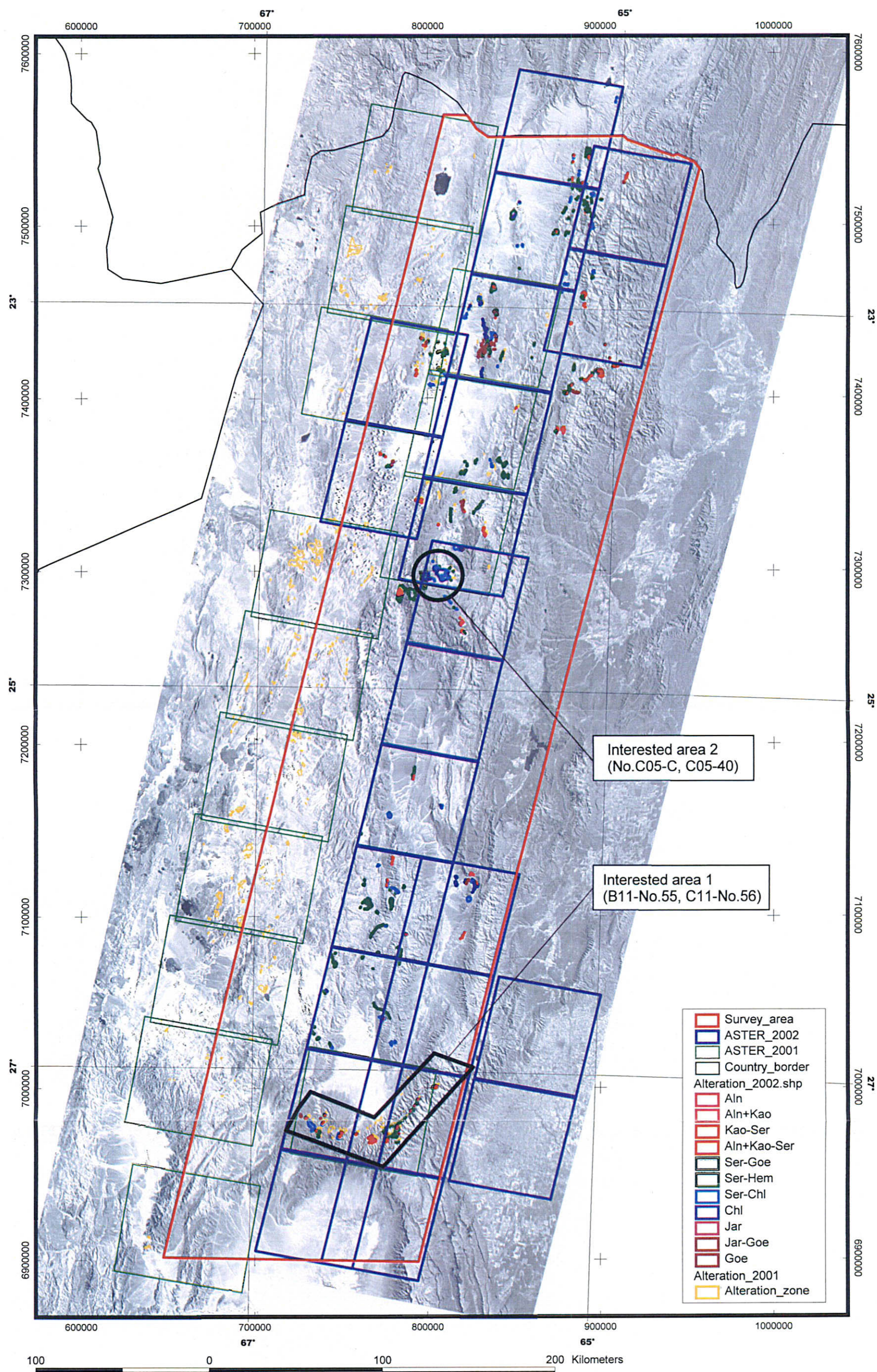


Fig.II-3-3-1 Interested area extracted from satellite data analysis

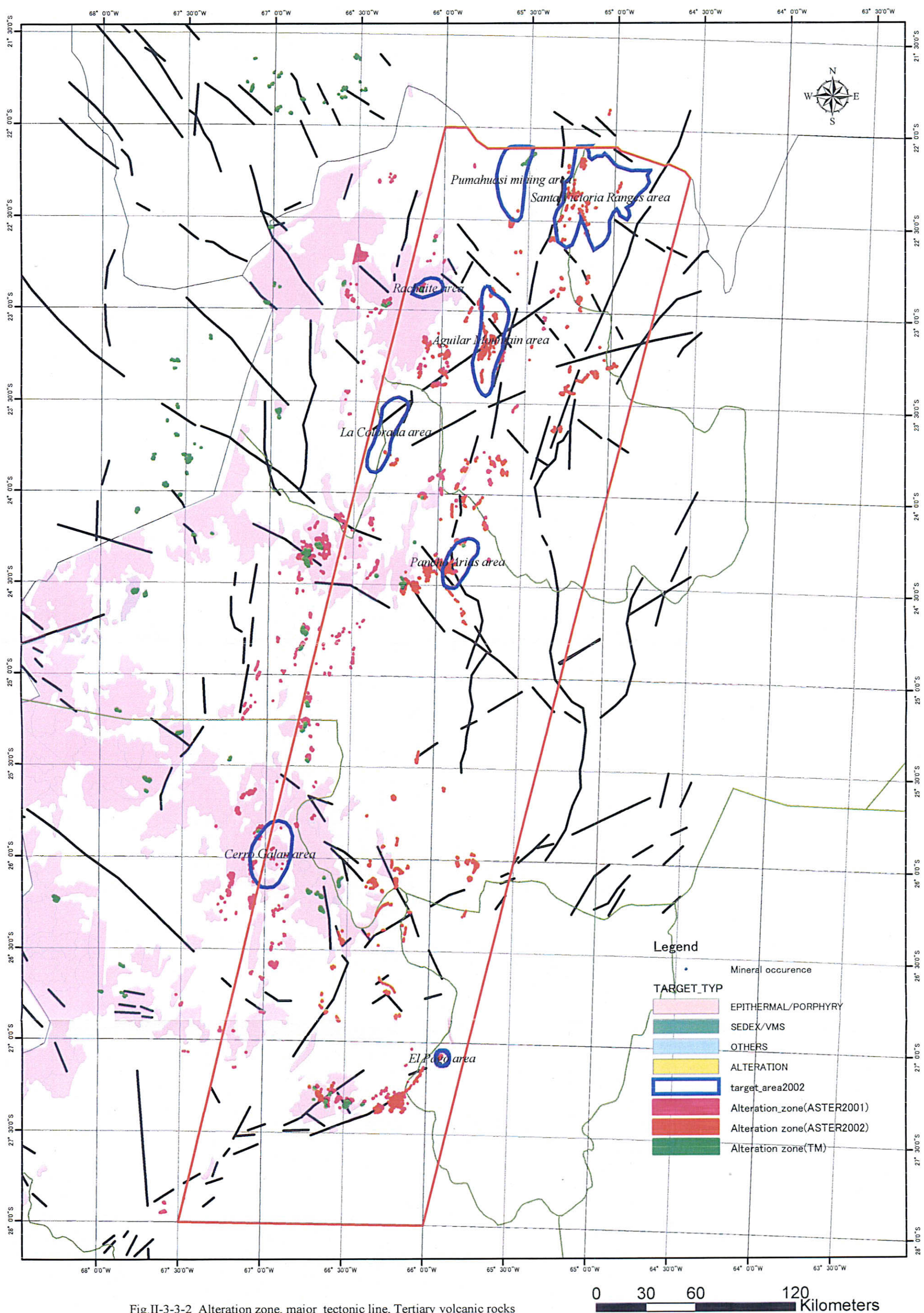


Fig.II-3-3-2 Alteration zone, major tectonic line, Tertiary volcanic rocks